Universitat Autònoma de Barcelona

MODULATION OF THE INFLAMMATORY RESPONSE AFTER SPINAL CORD INJURY

Jesús Amo Aparicio

MODULATION OF THE INFLAMMATORY RESPONSE AFTER SPINAL CORD INJURY

Presented by Jesús Amo Aparicio

ACADEMIC DISSERTATION

To obtain the degree of PhD in Neuroscience

by the Universitat Autònoma de Barcelona

2019

Directed by Dr. Rubèn López Vales

Tutorized by Dr. Xavier Navarro Acebes

NeuroPlasticity & Regeneration

INc Institut de Neurociències

BCFI

UAB Universitat Autònoma de Barcelona

MINISTERIO DE ECONOMÍA Y COMPETITIVIDAD

INDEX

SUMMARY

MODULATION OF INFLAMMATORY RESPONSE AFTER SPINAL CORD INJURY

Spinal cord injury (SCI) consists in the disruption of the ascending and/or descending information pathways due to the death of nervous tissue. Since axons from the central nervous system do not regenerate, injury results in a permanent lack of communication between the brain and the regions of the body below the lesion site. This lack of communication translates into loss of movement, loss of sensation, autonomic deficits, and pain. The final magnitude of these dysfunctions is defined by the level, the severity, and the type of injury. However, there are many secondary degenerative processes that take place in the spinal cord after primary injury and that contribute to the final dysfunctions. Among these processes, inflammatory response is one of the most important.

Spinal cord injury elicits an inflammatory response produced mainly by macrophages and microglia. All the process is orchestrated by cytokines. These cells and mediators are fundamental for the clearance of cellular debris and the healing of damaged tissue. However, in contrast to other tissues, inflammatory response in the central nervous system is not properly resolved. Exacerbated and uncontrolled inflammatory response produces damage to healthy neighboring tissue, increasing the lesion size and worsening the final deficits. The main objective of this thesis is the modulation of the inflammatory response after SCI, maintaining the essential benefits of an immune response but avoiding dangers of exacerbated immunity. We hypothesize that this modulation will result in improvement of tissue preservation and functional recovery in a murine model of SCI.

First two strategies of this thesis are based on the suppression of pro-inflammatory environment targeting IL-1α and IL-1β, main cytokines in the first stages of the inflammatory response. Targeting of IL-1α was performed by MABp1, a monoclonal antibody recently approved for clinical use. This antibody neutralizes the soluble form of IL-1α and inhibits its binding to receptors. Besides promising findings in other inflammatory-mediated diseases, MABp1 failed to promote protection after SCI. Targeting of IL-1β was performed by OLT1177, an inhibitor of the NLRP3 inflammasome needed for the processing and release of IL-1β and IL-18. OLT1177 successfully promoted tissue protection and locomotor improvement when injected intraperitoneally after SCI. Since OLT1177 is safe in humans, it is a promising candidate for the treatment of SCI.

Last two strategies of this thesis are based on the potentiation of the anti-inflammatory environment by IL-37 and IL-13. Previous result from our group showed that increasing IL-37 levels promoted a protective effect after SCI. Here we studied the contribution of the nuclear and extracellular pathways to the role of IL-37. We demonstrated that, although both pathways promote protective effects, benefits after SCI were attributed mainly to extracellular signaling.

Increasing levels of IL-13 promoted anti-inflammatory environment after SCI, as previously reported by our group with IL-4. However, in contrast to IL-4, IL-13 failed to confer functional

improvement. To determine differences between these two cytokines, we performed the first cell-specific RNA sequencing of macrophages and microglia after SCI. We observed that, although both cytokines have the same effect on the modulation of the injury environment, they induce differences in the metabolism of macrophages and microglia. Metabolism induced by IL-4 was more oxidative whereas metabolism induced by IL-13 was more glycolytic. Since inflammatory response is a very demanding process, how cell obtain energy may be crucial for the development of the immune response and may explain differences observed at functional level.

Future of SCI is multidisciplinary. Through this thesis we provide evidences to support that trophic modulation of the injury environment is a fundamental component of novel therapeutic approaches to treat SCI.

MODULACIÓN DE LA RESPUESTA INFLAMATORIA DESPUÉS DE UNA LESIÓN DE MÉDULA ESPINAL

La lesión de médula espinal (LME) consiste en la disrupción de la vías ascendentes y/o descendentes de información debido a un daño del tejido nervioso. Puesto que los axones del sistema nervioso central no regeneran, el daño conduce a una falta de comunicación permanente entre el cerebro y las regiones del cuerpo que están por debajo de la zona de lesión. Esta falta de comunicación se traduce en pérdida de movimiento, pérdida de sensación, déficits autonómicos y dolor. La magnitud final de estos déficits se define en base al nivel, la severidad y el tipo de lesión. Sin embargo, hay muchos procesos secundarios degenerativos que ocurren en la médula espinal después del daño primario y que contribuyen a los déficits finales. Entre estos procesos, la respuesta inflamatoria es uno de los más importantes.

La LME activa una respuesta inflamatoria producida principalmente por macrófagos y microglía. Todo el proceso está dirigido por citoquinas. Estas células y mediadores son fundamentales para la limpieza de los restos celulares y la recuperación del tejido dañado. Sin embargo, a diferencia de otros tejidos, la respuesta inflamatoria del sistema nervioso central no se resuelve adecuadamente. Una respuesta inflamatoria exacerbada puede producir daños en el tejido vecino sano, incrementando el tamaño de la lesión y empeorando los déficits finales. El objetivo principal de esta tesis es la modulación de la respuesta inflamatoria después de la LME, manteniendo los beneficios esenciales de la respuesta inflamatoria pero evitando los daños atribuidos a una respuesta exacerbada. Según nuestra hipótesis, esta modulación resultará en una mejora de la preservación del tejido y de la recuperación funcional en un modelo murino de LME.

Las primeras dos estrategias de esta tesis están basadas en la supresión del ambiente proinflamatorio actuando sobre IL-1α e IL-1β, citoquinas principales en las primeras fases de la respuesta inflamatoria. La actuación sobre IL-1α se realizó mediante MABp1, un anticuerpo monoclonal recientemente aprobado para su uso clínico. Este anticuerpo neutraliza la forma soluble de la IL-1α e inhibe su unión a los receptores. A pesar de los hallazgos prometedores en otras enfermedades mediadas por la respuesta inflamatoria, MABp1 no promovió protección después de una LME. La actuación sobre IL-1β se realizó mediante OLT1177, un inhibidor del inflamasoma NLRP3 necesario para el procesamiento y la liberación de IL-1β e IL-18. OLT1177 promovió de manera exitosa la preservación del tejido y la mejora funcional cuando se inyectó intraperitonealmente después de una LME. Puesto que OLT1177 es seguro en humanos, es un candidato prometedor para el tratamiento de la LME.

Las últimas dos estrategias de esta tesis están basadas en la potenciación del ambiente antiinflamatorio mediante IL-37 en IL-13. Resultados previos de nuestro grupo mostraron que incrementar los niveles de IL-37 promovía un efecto protector después de una LME. En esta tesis estudiamos la contribución de la rutas nucleares y extracelulares en el papel de la IL-37. Demostramos que, aunque las dos rutas promueven efectos protectores, los efectos beneficios después de una LME eran atribuidos principalmente a una señalización extracelular.

Incrementar los niveles de IL-13 promovió un ambiente antiinflamatorio después de una LME, como había sido previamente demostrado por nuestro grupo con IL-4. Sin embargo, a diferencia de IL-4, IL-13 no proporcionó mejora funcional. Para determinar las diferencias

entre estas dos citoquinas, realizamos la primera secuenciación de ARN de las poblaciones de macrófagos y microglía después de una LME. Observamos que, aunque ambas citoquinas tienen el mismo efecto en la modulación del ambiente inflamatorio, inducen diferencias en el metabolismo de macrófagos y microglía. El metabolismo inducido por IL-4 era más oxidativo mientras que el metabolismo inducido por IL-13 era más glucolítico. Puesto que la respuesta inflamatoria es un proceso muy exigente, la forma en la que las células obtienen energía puede ser crucial para el desarrollo de la respuesta inmune y podría explicar las diferencias observadas a nivel funcional.

El futuro de la LME es multidisciplinar. A través de esta tesis, proporcionamos evidencias para apoyar que la modulación trófica del ambiente inflamatoria es un componente fundamental de las nuevas estrategias terapéuticas para tratar la LME.

INTRODUCTION

Spinal cord

The spinal cord is a complex organ of the nervous system. Together with the brain, they compose the central nervous (CNS). Contrary, the peripheral nervous system (PNS) is composed of all the peripheral nerves.

The spinal cord connects the brain with the peripheral nerves acting as a pathway where information travels bidirectionally. It plays a role in movement, sensation, and autonomy. More precisely, the spinal cord transmits motor signals from the brain motor cortex to the muscles and glands in order to execute actions. It also returns sensory signals from body parts to the brain sensory cortex in order to be processed. Finally, the spinal cord coordinates many reflex responses (Conta and Stelzner, 2008).

The organization of the spinal cord is extremely complex. Anatomically, it can be separated into external and internal structures. A detailed description of these structures is explained below.

External structure of the spinal cord

The spinal cord begins in the occipital bone and extends throw the dorsal part of the body. In humans, the average length of the spinal cord is 45 cm in males and 42.5 cm in females (Frostell et al., 2016). The width varies from 13.5 mm thick in cervical regions to 8.3 mm thick in thoracic regions (Frostell et al., 2016). Its shape is ovoid and has a deep longitudinal fissure, named the ventral (or anterior) median fissure, on the surface (Conta and Stelzner, 2008).

The entire spinal cord is protected by the vertebral column which is composed of individual segments or vertebrae. The human spinal cord is composed by 31 segments: 8 cervical (named C1 – C8), 12 thoracic (T1 – T12), 5 lumbar (L1 – L5), 5 sacral (S1 – S5) and 1 coccygeal (Co1) (Fig. 1A). Most of the mammals have a regional segment pattern like this one, except those animals with substantial tails that have more coccygeal segments. Vertebrae are separated from each other by discs of cartilage. By the narrow spaces between them, spinal nerves pass through and connect with the rest of the body. From each side of these segments, two nerve roots emerge containing efferent motor fibers and afferent sensory fibers (Conta and Stelzner, 2008).

Cervical spinal nerves control signals to the back of the head, neck, shoulders, arms and the diaphragm. Thoracic spinal nerves control signals to the chest muscles, some muscles of the back and the abdomen partially. Lumbar spinal nerves control signals to the lower part of the abdomen and the back, the buttocks, part of the external genital organs and parts of the legs. Sacral spinal nerves control signals to the thighs and lower parts of the legs, the feet, most of the external genital organs and the area around the anus. The single coccygeal nerve controls the lower back (Conta and Stelzner, 2008).

The spinal cord is enclosed in a tube of spinal meninges that protects it. These meninges are pia mater, arachnoid mater, and dura mater (Fig. 1B). Each membrane is separated from each other by subdural and subarachnoid space. The cerebrospinal fluid lies in the subarachnoid

space, between the arachnoid and pia. Between the dura and the periosteum of the vertebral column the epidural space is filled with fat tissue, lymphatic tissue, small arteries, and venous plexus (Conta and Stelzner, 2008).

Regarding arteries, the entire spinal cord is supplied by a single ventral spinal artery and two dorsal spinal arteries. The ventral spinal artery originates from the central artery and descends within the ventral median fissure of the spinal cord. The dorsal spinal arteries originate either from the vertebral artery or its inferior posterior cerebellar branch and descend in the dorsolateral sulcus of the spinal cord (Conta and Stelzner, 2008).

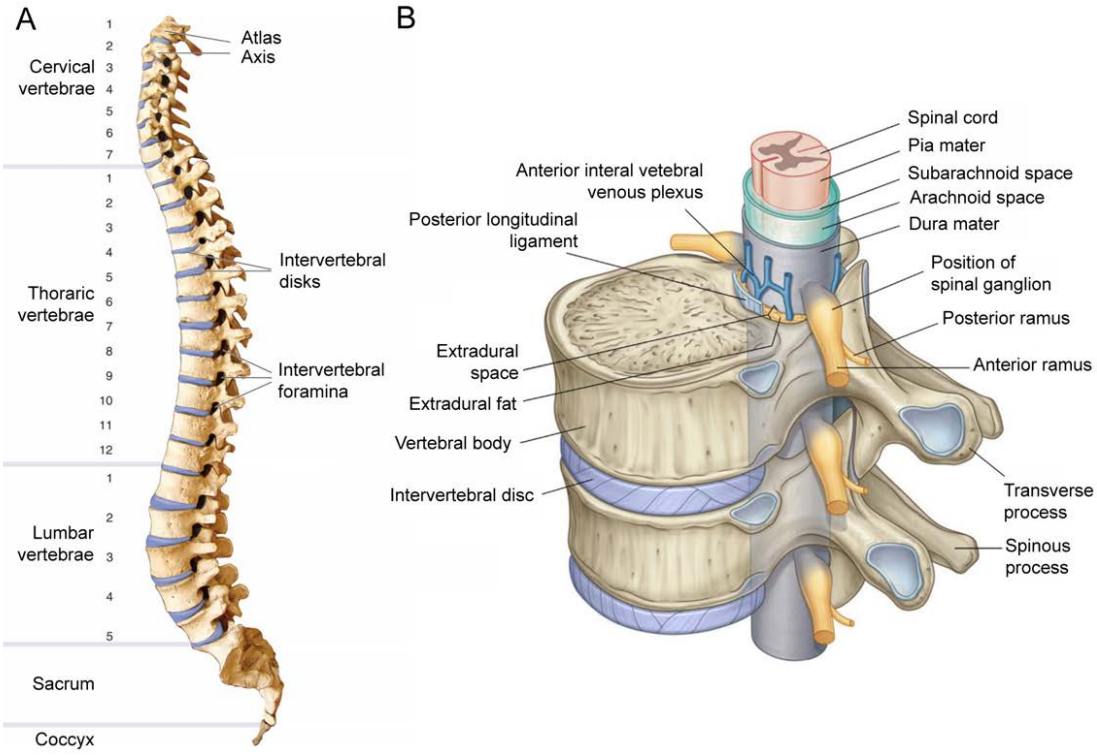

Figure 1: Anatomy of the spinal column. (A) Lateral view of the adult vertebral column. Vertebral patter is indicated. Image adapted from *Nysora*®. (B) Spinal cord inside the vertebral column showing the three meninges. Image adapted from (Drake et al., 2015).

Internal structure of the spinal cord

When a transverse section of spinal cord is observed, two parts can be easily identified. These parts are the gray and the white matters (Fig. 2).

The gray matter has the shape of a butterfly or a capital letter H, although it changes depending on the level (Conta and Stelzner, 2008). This part contains neural bodies, dendrites, axons, and glial cells and it can be macroscopically divided into dorsal and ventral parts. The dorsally projecting arms of the gray matter are called the dorsal horns and the ventrally projecting arms are called the ventral horns. The intermediate regions, which connect the dorsal and the ventral horns, are called the intermediate gray matter. In the thoracic spinal

cord and in the upper lumbar segments, there are two small lateral projections of the gray matter called the intermediolateral horns. Microscopically, the gray matter can be divided in ten successive layers of cells called the Laminae of Rexed each of one is composed by different kind of neurons (Fig. 2) (Rexed, 1952). Central canal is in the middle of the gray matter and it's filled with cerebrospinal fluid (Conta and Stelzner, 2008).

Except in those points where the dorsal horn touches the margin of the spinal cord, they gray matter is surrounded by a layer of white matter (Fig. 2). The white matter consists mostly of longitudinally running axons and also glial cells. A large group of axons located in a given area is called funiculus. Smaller bundles of axons, which share common features within a funiculus, are called fasciculus. Tract and pathways reference bundles of fasciculus that have a functional connotation. More precisely, a tract is a groups of nerve fibers with the same origin, course, termination, and function. The term pathway applied to a group of tracts with a related function (Conta and Stelzner, 2008).

Based on the direction of the information they carry on, tracts can be divided in ascending or descending. Ascending tracts arise from primary neurons and carry sensory information up. Descending tract carry motor information down (Conta and Stelzner, 2008).

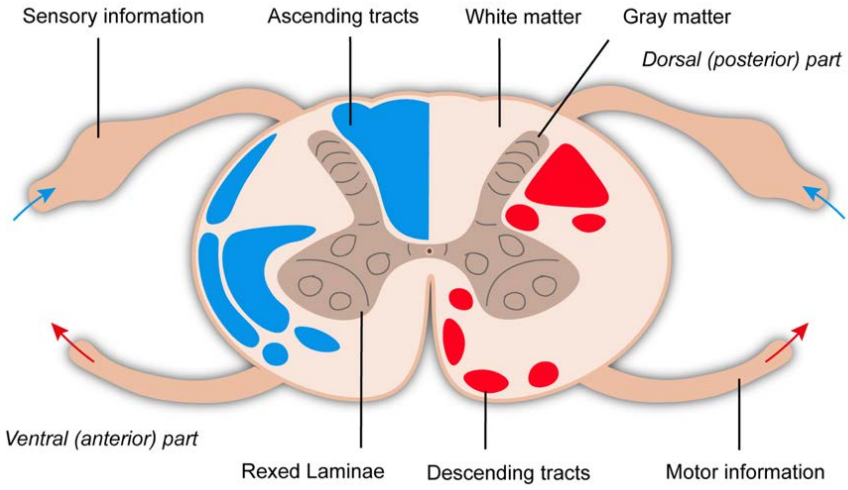

Figure 2: Internal structure of the spinal cord showing the distribution of the gray and white matters.

Spinal cord injury

Although the spinal cord is protected by the vertebral column, it can be damaged. Spinal cord injury (SCI) consists in the disruption of the ascending and/or descending information pathways of the spinal cord and the death of neurons and glial cells due to a damage of its nervous tissue. Since axons from the central nervous system do not regenerate, injury results in a permanent loss of communication between the brain and the regions below the lesion site. This loss of communication produces loss of movement, loss of sensation, autonomic deficits, and pain. The final magnitude of these dysfunctions is defined by the level, the severity, and the type of injury (Burns et al., 2012).

Incidence and causes

The incidence of SCI varies worldwide. Usually, data of SCI is reported by provincial or national databases. In addition, these databases follow different codes making generalizations between countries very difficult (Kang et al., 2017). Among developed countries, the incidence is higher in North America (39 cases per million individuals) than in Australia (16 cases per million individuals) or western Europe (15 cases per million individuals) (Kang et al., 2017). In Spain, the incidence of SCI is 16 cases per million individuals (Jazayeri et al., 2015). Although the survival of patients with SCI has improved over the last decades, patients continue to have high mortality rates. In fact, between 4% – 17% of patients die during hospital internalization. After hospital discharge, 3.8% of patients die in the first year and 1.6% in the second year (Ahuja et al., 2017).

For all the cases of SCI, mechanical damage injury is the most common. Automobile accident are the leading cause of traumatic SCI, accounting for 39.2% of all cases. This is followed by falls (26.6%), sport accidents (14.9%), violence (11.5%), medical/surgical complications (4.3%), and other remaining causes (3.5%) (statistics from the U.S. from 2005 to 2011) (Chen et al., 2013). High-energy impacts such as traffic accidents and sport-related injuries are more common in younger individuals, whereas low-energy impacts, such as falls, occurs in older individuals (Ahuja et al., 2017). SCI other than trauma include tumors, spinal vascular diseases, inflammatory diseases, spinal stenosis, radiation myelopathy, neural tube defects, among others (Yılmaz et al., 2014).

Types of SCI

The most general way to classify the spinal cord injury is **based on the level** of the spinal cord where the damage is produced. According to this, spinal cord injuries can be differentiated into the following types (Fig. 3).

Cervical injuries

They are the most severe type of injury because they lead to tetraplegia. This is the full disconnection of all the four extremities of the body. Patients with high-cervical injury (C1-C4) may have problem breathing by their own, controlling bladder or doing digestion. Speaking can be also impaired. These patients will require assistance in all their life activities (Nas, 2015). Patients with low-cervical injury (C5-C8) may be able to breathe and speak by their own. They may have limited control of shoulder, arms or wrists. Assistance is also required in all their life activities, although they can move from one place to another independently in power wheelchair (Nas, 2015).

Thoracic injuries

They result in paraplegia that is the affection of trunk and legs while arm and hand functions are usually normal. These patients can use manual wheelchairs. Patients with high-thoracic injuries (T1 – T5) may not be able to control abdominal muscles and trunk balance (Nas, 2015).

Patients with low-thoracic injuries (T6 – T12) may be able to control trunk balance and have little control of bowel and bladder (Nas, 2015).

Lumbosacral injuries

They result in some loss of function in the hips and the legs. Patients may be ambulatory with leg walking devices for short distances. They may be independent in bowel and bladder care (Nas, 2015).

In addition to the level, spinal cord injuries can be defined **based on their severity**. In the case of complete injuries, there is a full disconnection of the spinal fibers and therefore the complete loss of sensory and motor functions below the lesion site. In the case of incomplete injuries, a percentage of preserved fibers allows some remaining sensory or motor function below the lesion site (Burns et al., 2012).

In an attempt to develop a universal system to classify the spinal cord injury, the American Spinal Cord Injury Association (ASIA) elaborated the ASIA Impairment Scale (AIS) (Burns et al., 2012). This classification is **based on the examination of the neurological function** and is the most used nowadays (Burns et al., 2012).

A = Complete

No sensory or motor function is preserved in the sacral segments S4-S5 (Burns et al., 2012).

B = Sensory incomplete

Sensory but not motor function is preserved below the neurological level of injury and includes the sacral segments S4-S5 AND no motor function is preserved more than three levels below the motor level on either side of the body (Burns et al., 2012).

C = Motor incomplete

Motor function is preserved at the most caudal sacral segments for voluntary anal contraction OR the patient meets the criteria for sensory incomplete status, previously described, with some sparing of motor function more than three levels below the ipsilateral motor level on either side of the body. Less than half of key muscle functions below the single neurological level of injury having a muscle grade ≥ 3 (active movement, full range of motion against gravity) (Burns et al., 2012).

D = Motor incomplete

Motor incomplete status as defined above, with at least half of key muscle functions below the neurological level of injury having a muscle grade ≥ 3 (Burns et al., 2012).

E = Normal

If sensation and motor function are normal in all segments and the patient had prior deficits. Someone without an initial SCI does not receive an AIS grade (Burns et al., 2012).

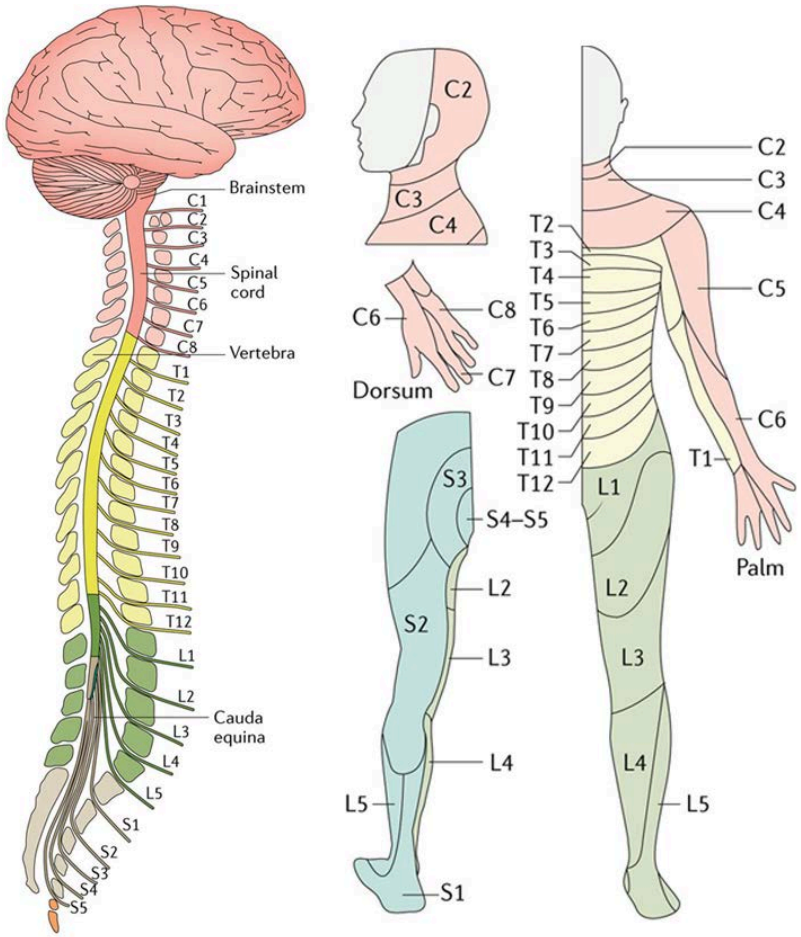

Figure 3: Spinal cord innervation of specific parts of the body showing the affected areas after injury. Image extracted from (Ahuja et al., 2017).

Biological events after SCI

In 1911, Allen was the first in providing an exhaustive description of the changes after SCI (Allen, 1911). He reported a progressive softening in the gray matter even 2 cm far from the impact area in animals with spinal cord injury. This progressive loss of neural tissue days after injury is now known as secondary damage and it is separated from the primary damage caused by the trauma itself.

Primary damage

The primary damage begins within seconds after the injury and it is restricted to the lesion area. The injury produces an immediate hemorrhage and the interruption of the blood supply in the lesion site. This leads to cell death, ischemia, edema, derangement of ionic homeostasis, accumulation of neurotransmitters, and alterations of the plasma membrane (Oyinbo, 2011). The disruption of ionic potentials limits the generation of action potentials abolishing all the spinal function and reflexes for a certain period of time. This is called spinal shock (Ditunno et al., 2004).

Primary injury is unexpected and immediate. Therefore, the therapeutic window in the primary phase of injury is very limited, and consequently, inaccessible for specialized intervention (Oyinbo, 2011). For these reasons, although both primary and secondary injuries are involved in the neurological dysfunction after SCI, most research has been focused on understanding the pathophysiology of the secondary damage.

Secondary damage

The secondary damage starts in minutes after the injury and lasts from weeks to months. In contrast to primary injury, secondary damage is not restricted to the lesion area and includes all the events that happen after the initial trauma. Some of these events are the extension of processes from the primary damage but also novel ones here described. By these events, the degenerative processes of the initial zone expand through healthy neighboring tissue and increase the original lesion size (Fig. 4) (Oyinbo, 2011).

Glutamate excitotoxicity

Glutamate is the principal excitatory neurotransmitter of the CNS. It binds to a variety of excitatory receptors leading to depolarization and neural excitation. In normal synaptic function, the activation of these receptors is transitory, but SCI produces the disruption of cell membranes and the release of glutamate. Soon after trauma, the extracellular levels of glutamate in the injury site and in the surroundings rise (Liu et al., 1999). The increased extracellular glutamate levels lead to excessive stimulation of glutamate receptors. The resultant influx of Ca^{+2} into neurons causes persistent depolarization and neural death by necrosis or apoptosis through a process known as excitotoxic cell death. Oligodendrocytes and microglia, that express glutamate receptors, are also vulnerable to glutamate excitotoxicity (Liu et al., 2016). Thus, glutamate excitotoxicity results in demyelination of axons, loss of neurons and astrocytes around the injury site, and changes in microglia (Doble, 1999). Furthermore, glutamate binds to receptor proteins that act as potassium and calcium gates. This produces the dysregulation in the ionic homeostasis leading to osmotic cell lysis and the consequent release of cell contents into the extracellular medium (Doble, 1999).

Lipid peroxidation

A well-characterized process occurring after SCI is the formation of reactive oxygen species (ROS) and reactive nitrogen species (RNS). This is the consequence of increased intracellular calcium levels, mitochondrial dysfunction, arachidonic acid breakdown, and activation of inducible nitric oxide synthase (iNOS). The central nervous system is particularly vulnerable to oxidative stress due to its high oxygen consumption rate, the weakly antioxidative systems, and the terminal-differentiation characteristic of neurons (Li et al., 2013). ROS and RNS absorb an electron from lipid molecules, turning them into less stable and launching a chain reaction that leads to cell membrane lysis and cell death by necrosis. Apart from lipid peroxidation, free radical species produce damage to proteins and nucleic acids (Profyris et al., 2004).

Local vascular derangements

Hemorrhage after SCI is initially localized in the highly vascularized central gray matter. The release of blood produces damage to cell membranes and DNA of the neural tissue (Fig. 4)

(Sadrzadeh et al., 1987). Damage of the blood vessels also induces the accumulation of interstitial fluids and the lack of drainage promotes compression of nervous tissue (Oudega et al., 2012). Ischemia drives to a decrease in oxygen and glucose required for cell metabolism. This leads to the production of lactic acid and the acidification of the environment (Chu and Xiong, 2013). The restoration of blood supply to ischemic tissue can also produce additional damage known as reperfusion injury. The return of oxygen to the tissue causes an increase in free radicals and reactive oxygen species that contribute to the destruction of cells, accumulation of calcium in tissues, and increased inflammation (Oudega et al., 2012).

Blood-spinal cord barrier breakdown

SCI is covered by the blood-spinal cord barrier (BSCB). This is a monolayer of endothelial cells that regulates the traffic of molecules and cells between the CNS and the blood. Trauma of the spinal cord produces a prominent disruption of this barrier and alters its normal permeability (Fig. 4). The permeability of the BSCB reaches a maximum within a few hours after trauma and usually turns to normal within days or weeks after SCI. As happened with the vascular derangements, all these changes can lead to metabolic disturbances, astrocytic dysfunction and compromise the spinal cord functionality (Shlosberg et al., 2010; Whetstone et al., 2003).

Cell death

Excitotoxicity and hypoxia induce the death of cell from the lesion zone. After spinal cord injury, two cell death mechanisms can be found: necrosis and apoptosis. Necrosis is characterized by passive cell swelling, rupture of plasma membrane, mitochondrial damage with rapid energy loss, and disruption of internal homeostasis (Kroemer et al., 2009). The membrane disruption during necrosis produces the release of all the internal components of the cell activating a rapid inflammatory response. In contrast, apoptosis is characterized by initial rounding-up of the cells, surface bleeding, chromatin aggregation with genomic fragmentation (*karyorrhexis*) and reduction of cellular and nuclear volume (pyknosis) (Kroemer et al., 2009). Necrosis is found immediately after SCI at the lesion site and can spread up to two vertebral levels (Profyris et al., 2004). Apoptotic occurs in two cascades. The first one coexists with necrosis, starting at 6 hours after injury in the lesion site. It lasts for several days and affects multiple cell types. After one week, the number of apoptotic cells in the lesion site decreases and increases away from the lesion site. This new wave is predominantly localized in the white matter and can arise large distances from the lesion site (Hausmann, 2003; Profyris et al., 2004).

Demyelination of intact axons

Demyelination is due to loss of oligodendrocytes. Although some oligodendrocytes can survive the initial trauma, they are vulnerable to all the processes of the secondary damage (Fig. 4). The loss of myelin produces conduction delay and/or conduction blockade. With the loss of myelin, axons are directly exposed to the damaging effects of free radicals and inflammatory cytokines (Oyinbo, 2011).

Glial scar

SCI initiates reactive gliosis leading by microglia, macrophages, oligodendrocytes, meningeal cells, and precursor cells. By invading the injury site, these cells clear up debris but also establish a burden of massive deposition of molecules called glial scar (Fig. 4). The glial scar is an evolving structure, with different cells arriving and participating at different stages. Al first stages, the glial scar is formed by macrophages and microglia. However, the final structure is formed mainly by astrocytes (Fawcett and Asher, 1999). Although the glial scar delimitates the injury site, it also produces an inhibitory environment where axons fail to regenerate. Characterization of CNS myelin led to the identification of several components that exert a potent inhibitory action on neurite outgrowth. These molecules include Nogo, myelin-associated glycoprotein (MAG), oligodendrocyte myelin glycoprotein (OMgp), and chondroitin sulfate proteoglycans (CSPGs) (Fawcett and Asher, 1999).

Neuroinflammation

The inflammatory response triggered after spinal cord injury is the most important event that contributes to secondary injury (Fig. 4). Immune cells are required for effective clearance of damaged cell and myelin debris and for the release of bioactive molecules that lead to tissue healing and repair (Yong et al., 2019). However, immune cells also secrete several factors that mediate cytotoxicity to neurons, glia, axons, and myelin (David and Kroner, 2011; Francos-Quijorna et al., 2017). The inflammatory response must be precisely regulated and finished when is no longer needed as happens in the peripheral nervous system. However, after damage to the central nervous system, inflammation fails to be resolved leading to chronic inflammation (David and Kroner, 2011; López-Vales and David, 2019). Further details of the inflammatory response after spinal cord are discussed in the following sections.

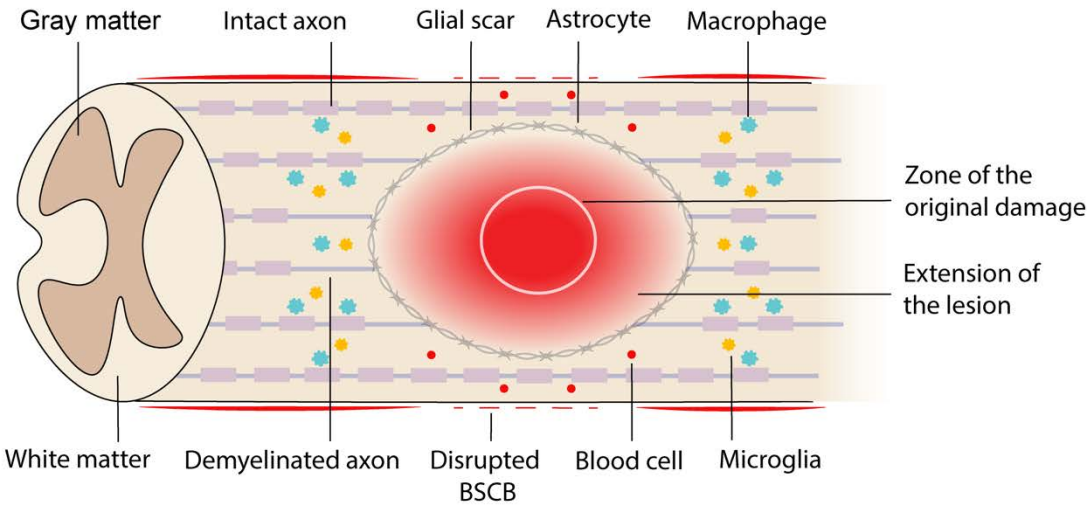

Figure 4: Expansion of the lesion size due to secondary damage. Representation of some of the biological process that contribute to secondary damage after SCI.

Studying SCI

Contrary to was it though, endogenous restorative mechanisms allow at least partial regeneration of the injured spinal cord. CNS neurons have both anatomic and synaptic plasticity which contribute to functional recovery (Raineteau and Schwab, 2001). Furthermore, neural precursor cells from the ependymal layers of the central canal, as well as, oligodendrocyte precursor cells, can generate neurons, oligodendrocytes, and astrocytes (Meletis et al., 2008). These endogenous mechanisms can lead to some gain of lost function during the following years after SCI, but they are far away to produce a complete recovery. Studying of SCI is essential to overcome this challenge.

Animal models

Animals models are useful for the preclinical testing of new therapeutics, but also for the better understanding of the pathophysiology of SCI. Ideally, animal models should have low generation rates, low requirements, and low cost. Moreover, animal models should be anatomical and pathophysiological similar to spinal cord injured humans (Jones et al., 2017).

Rat and mice are the most commonly used for SCI research (92% of studies) as they are well established and inexpensive (Sharif-Alhoseini et al., 2017). Their response to SCI is very resembled to the response found in humans. Rat response to SCI includes the production of cystic cavities as happened in humans. In mice, these cavities are rapidly occupied by fibroblasts, meningeal cells and pericytes, and therefore, they are not observed (Byrnes et al., 2010). Rats add another challenge since genetic modifications are much more limited than in mice. Large animal models, such as non-human primates, are also used for studying of SCI. Due to their expensive care, housing and ethical consideration, they are normally used only as intermediaries before clinic to confirm results from rodents (Cheriyan et al., 2014).

Lesion models

Lesion models aim to recreate features of human SCI. Although models have evolved significantly in the last years, due to the development of new injury mechanisms, five basic types of traumatic lesion models can be identified.

Contusion

Contusion models are the most extensively studied since they are the most common on traffic accidents (Jazayeri et al., 2015). This model inflicts a transient and acute force to the spinal cord through weight-drop, impactor or air gun device. For this model, the spinal cord needs to be previously exposed by surgical laminectomy. Weight-drop contusion model was the first developed in 1911 and it was based on a defined mass dropped to the spinal cord from a precise height (Allen, 1911). Nowadays, the Infinite horizon (IH) impactor device is the most claimed since allows a monitorization of the actual force and displacement of the spinal cord (Amo-Aparicio et al., 2018; Cheriyan et al., 2014)

Compression

Compression models inflict prolonged compaction of the spinal cord during a certain period of time. Some of these models are contusion-compression models since involve an acute contusion followed by persistent compression. The compression can be produced through a clip, calibrated forceps or balloon. In the case of the balloon, for example, a catheter with a small inflatable balloon is inserted into epidural or subdural space. Injury is controlled by the inflation volume. Although this model is less expensive, parameters are harder to monitor (Cheriyan et al., 2014).

Distraction

Distraction models involve a controlled stretching of the cord aimed to simulate the tension forces experienced in SCI. Injuries of this type have been investigated in cats, dogs, monkeys, and pigs. Although some devices have been developed, reproducible modeling of this type of injury in under active research. Harrington distractor is one of the most used (Cheriyan et al., 2014).

Dislocation

Dislocation models use a vertebral displacement mechanism to replicate column dislocations commonly seen in traumatic SCI. In this model, beams are attached adjacently to the vertebrae. One of them is fixed meanwhile the other one is laterally displaced to a specified distance. This model is advantageous since laminectomy is not required (Cheriyan et al., 2014).

Transection

Transection models involve a cut of the spinal cord producing a disconnection between the caudal and rostral segments. Cut can be full or partial. Although this type of injury is not very often in patients, this model is highly reproducible and especially useful to study axonal regeneration. (Cheriyan et al., 2014).

Current therapies for SCI

The therapeutic complications for severe SCI were first described in 1700BC in an Egyptian papyrus translated by Edwin Smith. This papyrus reveals the frustration caused by SCI and describes it has a “disease that should not be treated” (Feldman and Goodrich, 1999). Nowadays, treatment for SCI includes prevention but also different therapies to restore the lost function. Prevention measures include awareness campaigns to reduce traffic accident, dangerous praxis in sport, falls in the elderly, enhance vehicle safety, etc. In the case of restorative therapies, current approaches can be categorized in the following strategies. Selected clinal trials these procedures are summarized in Table 1.

Procedural

These strategies include several interventions to be applied following diagnosis and aimed to avoid complications that could aggravate the injury. Some of these strategies are cerebrospinal fluid drainage or hypothermia. Hypothermia (33°C) decreases the basal metabolic rate after SCI providing an anti-inflammatory effect and improving behavioral outcomes recovery in rats (Dietrich et al., 2011). Cerebrospinal fluid drainage avoid the compression of nervous tissue due to vascular derangements (Oudega et al., 2012).

Cell transplants

Extensive loss of tissue caused by SCI cannot be replaced by endogenous mechanisms. Transplantation of cells into the injured spinal cord can replace lost cells, but also can modulate the injury environment and stimulate regenerative programs. Neural stem or precursor cells, mesenchymal stem cells, oligodendrocytes precursor cells, olfactory ensheathing cells, and Schwann cells, among others, have been extensively used in the preclinical phase for the treatment of SCI (Ahuja et al., 2017). Besides promising outcomes, safety and efficacy of these treatments are still under research.

Bioengineering

The use of bioengineering for SCI is starting to have a substantive role as technology improves. In 2014, the first robotic exoskeleton four use in patients with paraplegia was approved. This exoskeleton fits around the legs and back and aims to facilitate sitting, standing and walking (Miller et al., 2016).

Neuromodulation

These approaches involve a focused electrical stimulation of the brain or spinal cord. Electrical stimulation using surgically implanted electrodes into the spinal cord has recently demonstrated to enable voluntary control of walking in individuals with SCI even years after injury (Wagner et al., 2018).

Pharmacological

Pharmacological strategies are based on the use of the drugs to modulates some procedures of the secondary damage. For example, the use of minocycline after SCI have demonstrated to improve functional recovery probably through reduction of oligodendrocyte apoptosis and local inflammation (Wells, 2003). Riluzole has shown a beneficial effect through reduction of excitotoxicity and cell death (Wilson and Fehlings, 2014). Despite several compounds are being tested in clinical trials (Table 1), currently there is no effective drug to treat acute and chronic SCI.

Treatment	Stage	ClinicalTrials.gov identifier
Pharmacological		
Minocycline	Phase III	NCT01828203
Riluzole	Phase II/III	NCT01597518
Cethrin	Phase II/III	NCT02669849
Procedural		
Systemic hypothermia	N/A	NCT02991690
Cerebrospinal fluid drainage	Phase II	NCT02495545
Neuromodulation		
Spinal cord stimulation	N/A	NCT02592668
Deep brain stimulation	N/A	NCT03053791
Cell-based strategies		
Oligodendrocytes precursor cells	Phase I/II	NCT02302157
Schwann cells	Phase I	NCT01739023
Umbilical cord-derived stem cells	Phase I/II	NCT02481440
Bone marrow-derived mesenchymal stem cells	Phase II	NCT02570932
Bioengineering		
Robotic exoskeletons	N/A	NCT02322125
Implantable bioengineered scaffolds or matrices	N/A	NCT02138110

Table 1: Selection of clinical trials for spinal cord injury. N/A: Not applicable. Adapted from (Ahuja et al., 2017).

Basic principles of the immune system

The immune system is in charge of the defense of the body against external pathogens, surveillance of the cell's identity, and the maintenance of tissue homeostasis. As a key step in all these duties, the immune system has to be able to differentiate between self and foreign antigens. Based on its speed and specificity, the immune system can be divided into innate and adaptive.

Innate immune system

Innate immunity refers to all the nonspecific mechanisms of the immune system that identify and remove foreign substances presented in the body. They take place immediately or within the first hours after pathogen is detected. Before that, pathogens have to challenge mechanical and chemical barriers such as skin, saliva, stomach acids, etc. that establish the first defense line of the body. If pathogens overcome these barriers, they are recognized by pattern recognition receptors (PRRs) such as the toll-like receptor (TLR). These receptors can detect pathogen-associated molecular patterns (PAMPs) or damage-associated molecular patterns (DAMPs) from pathogens or damaged cells, respectively. Activation of PRRs activates downstream signaling pathways, such as nuclear factor kappa-light-chain-enhancer of activated B cells (NF-κB) or mitogen-activated protein kinase (MAPK), that result in the

upregulation of pro-inflammatory cytokines and chemokines (Allan et al., 2005). These receptors have low specificity and sometimes their activation may result in damage of normal tissue (Charles A Janeway et al., 2001; Parkin and Cohen, 2001).

The most important innate immune cells are polymorphonuclear leukocytes and monocytes. Polymorphonuclear leukocytes are crucial for the removal of bacteria and parasites. Among polymorphonuclear leucocytes, neutrophils are the main responders. Their removal mechanism consists on the engulfment of foreign bodies that are then degraded by lytic enzymes. Monocytes are rapidly recruited to the tissue after infection or damage. They differentiate into macrophages or dendritic cells and phagocyte pathogens to destroy them. Apart from destroying pathogens, these cells can act as antigen-presenting cell (APC) as they can process pathogens large molecules into "readable" fragments or antigens. These antigens can be now recognized by the adaptive immune system for more specific actions (Charles A Janeway et al., 2001; Parkin and Cohen, 2001).

All these responses of the innate immunity are controlled by cytokines, opsonins, and proteins of the complement cascade. Cytokines are small pleiotropic molecules secreted by a broad range of cells that control several processes on the immune system and act as supporting actors in every single step. They include members such as colony-stimulating factors (CSFs), interferons (IFNs), interleukins (ILs), chemokines (CC, CXC, C, and CX3C), and tumor necrosis factors (TNFs), among others. Opsonins are molecules involved in the coating of pathogens or damaged cells in order to be recognized and destroyed by the immune system. The complement cascade is composed of lytic proteins that support pathogen destruction by direct lysis or by the promotion of phagocytosis (Charles A Janeway et al., 2001; Parkin and Cohen, 2001).

In summary, innate immunity is a rapid and nonspecific reaction to eradicate infections or damage before they invade healthy areas. However, many pathogens resist innate immunity and require more powerful and specialized mechanisms to be removed. These mechanisms are included in adaptive immunity.

Adaptive immune system

The adaptive immunity refers to all the antigen-specific mechanisms of the immune system carried on by lymphocytes. Whereas the innate response is rapid, the adaptive response takes several days or weeks to develop. Adaptive immunity also leads to "memory" mechanisms since a fraction of activated lymphocytes persist as memory cells. These memory cells provide long-term protection with augmented and more rapid responses on secondary challenge. There are two types of adaptive immune responses: humoral immunity and cell-mediated. Humoral immunity is produced by B lymphocytes whereas cell-mediated immunity is produced by T lymphocytes (Charles A Janeway et al., 2001; Parkin and Cohen, 2001; Wherry and Masopust, 2016).

B lymphocytes, or B cells, receive that name because they were first discovered in the *Bursa of Fabricius* of birds. In mammals, they mature in hematopoietic tissues. They produce antibodies in response to antigens from bacteria, viruses, and tumor cells. Each antigen, presented to B cells through APCs from the innate immunity, is recognized by a unique B-cell

receptor. Upon this recognition, the selective B lymphocytes become activated and transform into plasma B lymphocytes. These cells secrete a large number of antibodies against the specific antigen that coats the surface of pathogens. This coating can produce neutralization, affecting the binding of pathogens to other host cells; opsonization, creating a destroy-me signal in the pathogens to be phagocytized by immune cells such as neutrophils; and complement activation, inducing a complement cascade to destroy pathogens. In addition to all these functions, B lymphocytes can also act as APCs to T lymphocytes (Charles A Janeway et al., 2001; Parkin and Cohen, 2001; Wherry and Masopust, 2016).

T lymphocytes, or T cells, receive that name because they mature in the thymus from thymocytes. They are characterized by the expression of T-cell receptors that recognize antigens when presented as peptides bound to major histocompatibility complex (MHC) together with a co-stimulatory molecule. MHC molecules are divided into class I and class II. MHC class I are expressed on all nucleated cells and platelets whereas MHC class II are only expressed on certain cells such as dendritic cells, macrophages and B lymphocytes. T lymphocytes stimulation triggers a complex cascade of intracellular signaling driving the maturation, proliferation, and production of immune mediators. T lymphocytes mediate different functions depending on the T lymphocyte subtype. For example, CD4 T lymphocytes, also called helper T cells (Th), recognize antigens via their T-cell receptor that are presented by MHC class II. Once activated, they play important roles in orchestrating multiple immune actions. In contrast, CD8 T lymphocytes, also called cytotoxic T cells (Tc), recognize antigens that are present by MHC class I. They are crucial controlling and destroying intracellular pathogens. According to their cytokine secretion profile, three main subsets of Th and Tc lymphocytes have been described: Th1/Tc1 (IFNγ), Th2/Tc2 (IL-4) and Th17/Tc17 (IL-17) (Charles A Janeway et al., 2001; Parkin and Cohen, 2001; Wherry and Masopust, 2016).

Inflammatory response

The inflammatory response involves those processes of the innate and adaptive immune system aimed to establish a physical barrier to isolate the damaged area from healthy tissue, remove the dangerous stimuli, and promote the healing of damaged tissue (Libby, 2007). This response compromises immune cells, blood vessels, and molecular mediators. The inflammatory response often causes temporary discomfort such as pain, heat, redness, swelling, and loss of function. Depending on its duration, the inflammatory response can be classified in chronic and acute (Libby, 2007).

Acute inflammation

Acute inflammation is a short-term response developed from the first minutes or hours to days after challenge. After recognition of infection or damage, PRRs induce inflammatory transcription factors that promote the expression of pro-inflammatory cytokines such as interleukin 1 alpha (IL-1α) and beta (IL-1β), interleukin 6 (IL-6), and tumor necrosis factor alpha (TNFα), among others. Together with chemokines and co-stimulatory molecules, these soluble proteins facilitate the recruitment of effector cells such as monocytes and neutrophils to the site of disturbance. Mast cells and tissue-resident macrophages, presented in the insulted

tissue, facilitate the migration of cells by releasing histamine, leukotrienes, and prostaglandins that produce vasodilatation and increase the vascular permeability. Once in the infected or damaged area, macrophages and neutrophils create a cytotoxic environment by releasing ROS and proteases that destroy the source of inflammation. In addition, macrophages and dendritic cells also act as antigen presenting cells inducing the adaptive immune response. To do that, T and B lymphocytes are recruited from the vascular system to the site of infection (Libby, 2007).

The final phase of the acute inflammation is called resolution. Resolution is also a finely orchestrated process that includes limiting further leukocyte influx, clearance of inflammatory cells, reduction of pro-inflammatory factors, and release of pro-resolving factors (Serhan and Savill, 2005). During this phase, there is an influx of macrophages known as *nonphlogistic* (not-inflammatory). These macrophages promote the clearance of apoptosis cells without induce pro-inflammatory signaling cascade or tissue damage (Ren et al., 2001). Complete resolution should eventually lead to restoration of tissue homeostasis.

Chronic inflammation

All the events of the acute inflammation must be tightly regulated avoiding damage of healthy host tissue and finishing in a proper way. However, under certain circumstances, acute inflammation is hampered, and immune cells remain for several weeks and months in the disturbed tissue. Chronic inflammation refers to a prolonged inflammatory response that involves a progressive change in the type of cells present at the site of inflammation. It is characterized by the simultaneous destruction and repair of host tissue (David et al., 2018; Libby, 2007).

Inflammatory response after SCI

SCI leads to ischemia and extravasation of red blood cells and plasma components that can induce the activation of cell-resident immune cells. Moreover, although the spinal cord is protected by the blood-spinal cord barrier that limits the entrance of immune cells and mediators, trauma produces a breakdown of this barrier allowing the invasion of immune cells to the spinal cord parenchyma (Muldoon et al., 2013). In parallel, trauma produces direct damage to neurons, glia, vascular and meningeal cells leading to cell death. During necrosis, the plasma membrane is altered allowing the release of intracellular material as proteins and nucleic acids to the extracellular milieu. This material is recognized as DAMPs, triggering the immune response and the recruitment of immune cells from circulation (Muldoon et al., 2013). All these processes make the inflammatory response after SCI very complex.

The whole inflammatory response after SCI is orchestrated by **cytokines** (Fig. 5A). Among all the cytokines that participate in the inflammatory response after SCI, TNFα and IL-1β are considered the most important (Dinarello, 2007). The expression of these pro-inflammatory cytokines increases rapidly after injury at the RNA level. Specifically, the expression of TNFα reaches a peak at 1 hour after injury and decreases at 24 hours. This first peak of TNFα comes from microglia, astrocytes, oligodendrocytes, and neurons. In mice, there is a second peak of

expression from microglia starting at 3 weeks after injury. The expression pattern of IL-1β is similar to TNFα showing also two peaks (in mice) at the same time points (Donnelly and Popovich, 2008). Microglia, astrocytes, and neutrophils are the sources of the first peak while endothelial cells are the source of the second one. IL-6 and leukemia inhibitor factor (LIF) are also expressed in the first hours after injury showing a peak around 4 – 8 hours after injury. LIF shows a second peak at 4 days after injury. Astrocytes and microglia are major cellular sources of these two cytokines (Donnelly and Popovich, 2008; Pineau and Lacroix, 2007).

Among cytokines, **chemokines** are the ones specialized in the recruitment of leukocytes from the blood to the damaged area. They act through G-proteins coupled to transmembrane receptors. In most of the cases, chemokines mRNA levels peaks rapidly in the first hour after injury (Rice et al., 2007). Chemokines are classified into the subfamilies CXC, CC, CX3C, and C according to the presence and number of amino acids between N-terminal cysteine residues. In normal conditions, there is low but constitutive expression of chemokines in astrocytes, microglia, neurons, and endothelial cells (Glabinski et al., 1996; Nhong et al., 2002). However, after SCI the expression of chemokines and their receptors is induced. When expressed, chemokines produce local vasodilatation and expression of adhesion molecules in endothelial cells allowing the binding and diapedesis of circulating leukocytes. Finally, chemokines force leukocytes to move along a chemotactic gradient towards the source of inflammation. By these mechanisms, the recruitment of leukocytes is done sequentially being neutrophils the first in respond, followed by monocytes, eosinophils, basophils, and lymphocytes (Ley et al., 2007).

Microglial cells are the macrophage resident cells of the central nervous system and they are the first cells responding to SCI (David et al., 2018; Popovich and Hickey, 2001). In contrast to macrophages, microglial cells are not derived from the bone marrow but from the yolk sac and they migrate to the CNS during development (Ginhoux et al., 2010). In normal conditions, microglia display numerous cytoplasmic process with PRRs on their surface that extend and retract to monitor tissue homeostasis. When damage is recognized, microglial cells became activated reorienting and extending rapidly their process towards the injury site. This happens within minutes to hours after lesion (Davalos et al., 2005). Over the following hours and days, microglia retract their process and adopt an amoeboid morphology. Cytokines, chemokines, prostaglandins, and lysophosphatidic acids participates in the activation and process extension of microglia (David et al., 2012a). Specifically, macrophages colony-stimulating factor (M-CSF) allows the proliferation of microglial cells reaching a peak at day 7 after injury (Fig. 5B) and facilitating the expansion of these cells within the injured spinal cord (David et al., 2012b; Francos-Quijorna et al., 2017; Gómez-Nicola et al., 2013). Recent studies suggest that nitric oxide (NO) and adenosine triphosphate (ATP) play a pivotal role in regulating these morphological changes (Dibaj et al., 2010). Once microglia became fully activated, they participates in the phagocytosis of cellular debris (Greenhalgh and David, 2014).

Neutrophils migrate rapidly into the injured spinal cord reaching a peak at 24 hours after trauma (Fig. 5B) (Donnelly and Popovich, 2008; Francos-Quijorna et al., 2017). They phagocytose damaged cells and send instructions to all the cells that participate in the inflammatory response after injury. Neutrophils can further increase the extent of inflammatory response since they produce inflammatory cytokines such as TNFα, IL-1β, and

IL-6 that promotes the recruitment of more neutrophils via adhesion factors and chemoattractant upregulation. Neutrophils also release other signaling mediators that enhances vasodilatation, vascular permeability, leukocyte attraction, and cytokine production (David et al., 2018). Moreover, neutrophils can secrete matrix metallopeptidase 9 (MMP-9) that degrades the collagen matrix of the BSCB increasing leukocyte infiltration and creating positive feedback (Noble et al., 2002).

Higher levels of chemokines and cytokines and increased expression of MMPs at the site leads to the entry of monocytes from the peripheral blood. Integrins play an important role in the migration of monocytes out of the circulation. When monocytes infiltrate into the injured spinal cord, they differentiate into activated **macrophages**. First macrophages are detected in the spinal cord at 18 hours after injury and reach a peak at 3 days (Fig. 5B) (Francos-Quijorna et al., 2017). These macrophages can be found in the spinal cord months, and even years, after injury (Fleming et al., 2006). As microglia cells, they participate in the clearance of cellular debris (Prüss et al., 2011).

SCI also elicits the activation of the adaptive immune system. Although the brain and the spinal cord do not have defined lymphatic channels, APC from the spinal cord can travel through the cerebrospinal fluid to the lymph nodes where they activate lymphocytes (Laman and Weller, 2013). Within the first 24 hours after injury, **T and B lymphocytes** are recruited and start to infiltrate into the spinal cord. Activated lymphocytes increase in number reaching a peak at day 3 and lasting until several months after injury (Fig 5B) (Donnelly and Popovich, 2008; Francos-Quijorna et al., 2017). Since SCI leads to the release of many self-antigens, it has been reported that lymphocytes can cause autoimmune reactions that exacerbate the injury (Davies et al., 2007).

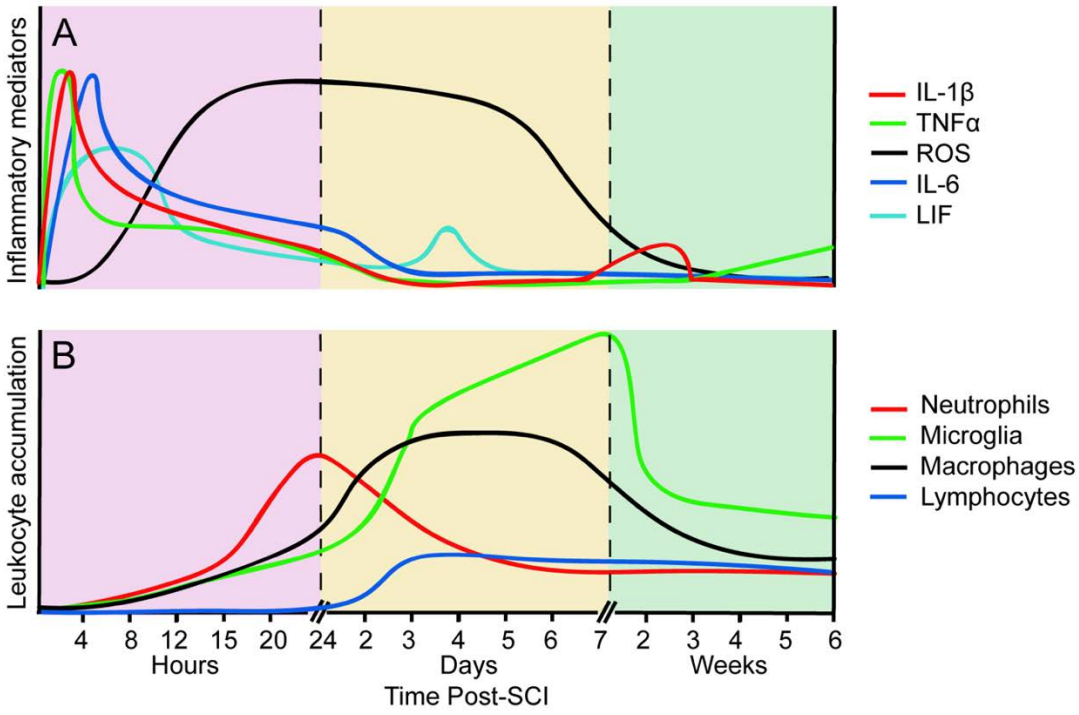

Figure 5: Dynamics of the inflammatory response in the mouse spinal cord after injury. Inflammatory mediators (A) and immune cells (B) from hours to weeks after SCI. Values on the vertical axis

represent relative changes and are not to scale. Adapted from (Donnelly and Popovich, 2008) with data from (Francos-Quijorna et al., 2017).

Definition of macrophages and microglia

For decades, microglia and infiltrated macrophages were thought to be homogenous populations. Both populations display similar morphology making impossible to be distinguished using the state-of-the-art techniques. Over the years, collecting data allow us to make a clearer distinction between both populations.

Macrophages and microglia have distinct origins. Macrophages derive from classical hematopoietic stem cells from the bone marrow or even the spleen (Yona et al., 2013). They reach the target organs via the bloodstream following insult. In contrast, microglia cells derive from the primitive ectoderm and reach the CNS early in embryonic development (Ginhoux et al., 2010). They are a tissue-specific macrophage population, maintained by self-renewal. After injury, they both activate and become amoeboid being impossible to distinguish them morphologically. Moreover, they express the same markers such as CD45, CD11b, Iba1, CSF1R and F4/80 (David et al., 2018)

Different **wide-analysis** studies have been done to compare microglia from yolk sac or from adult brains to macrophages from the peripheral blood or the spleen. Looking at their transcriptome, some extracellular markers were proposed as microglia-specific: P2ry12, Fcrls, Tmem119, Olfml3 Siglec-H and, Sall1, among other (Bedard et al., 2007; Gautiar et al., 2012; Hickman et al., 2013). Moreover, some miRNAs such as miR-99, miR-342-3p, and miR-125-5p have also been proposed as highly expressed in microglia but not in circulating blood monocytes or bone-marrow derived macrophages (Butovsky et al., 2014). Although these genes could indicate several unique differences between macrophages and microglia, these studies were performed in homeostatic conditions and it is not known whether expression pattern changes under inflammatory conditions (Haynes et al., 2006). Nowadays, none of these markers have demonstrated to be enough to distinguish microglial cells from infiltrated macrophages in the context of SCI.

Genetic engineering allowed the creation of **genetic reporter mice** to study microglia and macrophages. One example is the LysM-EGFP mice. In these mice, enhanced green fluorescent protein (EGFP) is used as reported gene and inserted into the lysozyme M locus that is expressed in mature myeloid cells such as macrophages and neutrophils (Faust et al., 2000). Besides that, some laboratories reported LysM expression partially and at low levels in the population of microglia (Lein et al., 2007), making necessary bone marrow transplantation to separate both populations (Zhu et al., 2017). However, LysM-EGFP expression in microglial cells is not observed in all the laboratories (David et al., 2018) and the reasons to explain such differences are currently unknown.

Currently, the most widely used tool to distinguish macrophages from microglial cells is **flow cytometry**. Separation of both populations through this technique is based on the differential expression of superficial markers. Characterization of microglia and macrophages based on the expression of CD45, CD11b and F4/80 allows a rapid and reproducible gating of macrophages and microglia (Amo-Aparicio et al., 2018; Campanella et al., 2002). Caution is

needed when defining the populations since the expression of these markers in microglia and macrophages may change under inflammatory conditions. However, this technique correctly gates more than 95% of cell the immune cells, even after CNS injury (Greenhalgh and David, 2014; Zhou et al., 2017).

Detrimental and beneficial states

A lot has been discussed about the contribution of macrophages and microglia after injury. Several studies showed that abolition of macrophages through different approaches could reduce the damage after SCI. These approaches include the use of anti-inflammatory drugs such as minocycline and FK506 to inhibit macrophage activation (López-Vales et al., 2005; Stirling, 2004); clodronate liposomes to deplete macrophages (Popovich et al., 1999); and genetic modifications to block macrophage infiltration (Letellier et al., 2010). However, there are also several lines of evidence showing that macrophages and microglia, under certain conditions, are protective and pro-regenerative (Yong et al., 2019). For example, it has also been reported that when macrophages are depleted, the number of oligodendrocytes is reduced and the remyelination is impaired (Kotter et al., 2005). Blocking of microglial processes extension towards lesions makes the lesion bigger (Hines et al., 2009). Furthermore, inducing activation of macrophages promotes greater axonal regeneration of retinal neurons after optic nerve injury (Yin et al., 2003). These opposite effects of macrophages and microglia seem to reflex a dual function.

Since macrophages and microglia have remarkable plasticity, they can change their phenotype. The term polarization was used to refer the process by through macrophages and microglia acquire different and, even opposite, phenotypes. Traditionally, two distinct polarization states have been described. These states were termed as M1 and M2, based on the Th1 and Th2 polarization of T lymphocytes (Gordon and Martinez, 2010). Stimulation of macrophages and microglia with the prototypical Th1 cytokines IFNγ or LPS induces **M1 (classic)** polarization in which cells express pro-inflammatory cytokines (IL-12, IL-23, IL-1β, and TNF), cytotoxic mediators (iNOS and NO), extracellular matrix-degrading enzymes (MMPs), lipid mediators, and glutamate. On their surface, they express phagocytic receptors (CD16/32), and costimulatory molecules (CD86) (David and Kroner, 2011). They are therefore often referred to as **pro-inflammatory** cells. In contrast, stimulation with the Th2 cytokines IL-4 or IL-13 as well as other factors (IL-10, glucocorticoids, immunoglobulin complexes/TLR ligands) induces **M2 (alternative)** polarization. This M2 phenotype is characterized by inhibition of production of pro-inflammatory cytokines (TNF, IL-1β, IL-2, IL-8, IL-12, and CXCL10), expression of high levels of anti-inflammatory cytokines such as IL-10 and TGFβ, defective NF-κB activation, upregulation of arginase 1 (Arg1), and increased expression of receptors CD204 and CD206 (David and Kroner, 2011; Martinez et al., 2009). They are therefore referred to as **anti-inflammatory** cells.

M2 phenotype is more complex than M1 and, for some authors, it should be broken down into M2a, M2b, and M2c profiles based on works on tumors (Figure 6). M2a (alternative state) is induced by IL-4 or IL-13 and results in the upregulation of Arg1 and CD206. These cells are involved in tissue repair and clearance of parasites. M2b (homeostatic state) is induced by TLR ligands and produces high levels of both pro-inflammatory cytokines (IL-1β) and anti-

inflammatory cytokines (IL-10) They are involved in inflammation and homoeostasis. Finally, M2c (deactivation state) is induced by IL-10 and TGF-β and is characterized by the lack of IL-1β expression and high IL-10 expression. Therefore, these cells are involved in anti-inflammatory responses (David, 2015; Mantovani et al., 2002).

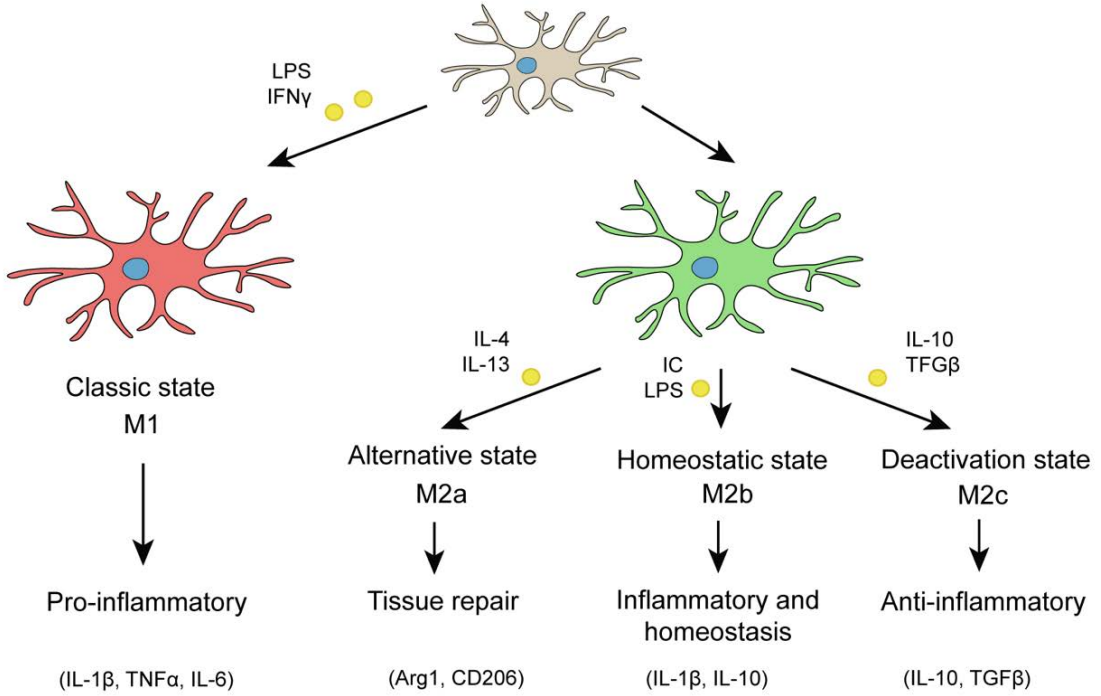

Figure 6: Polarization of macrophages and microglia towards M1 and M2 phenotypes. M2 phenotype can be divided into M2a, M2b, and M2c profiles. Stimuli that induce polarization, general roles of these profiles and factors they produce are indicated. Image adapted from (David, 2015).

M1 macrophages help fight bacterial infections by phagocytosing microorganisms and killing them intracellularly. M2 macrophages help fight infections by generating a fibrous capsule around them and thus helping to sequester the parasites. They have also phagocytic capacity (David and Kroner, 2011). Traditionally, M1 macrophages and microglia have been related with the detrimental effects of the inflammatory response since they secrete cytotoxic factors that could induce damage in healthy tissue when inflammation is not properly resolved (David et al., 2012b). In contrast, M2 macrophages and microglia have been related with beneficial effects since they are implicated in the healing process (David and Kroner, 2011). In the context of tumors, M2 macrophages are associated with immunosuppressive characteristics because they allow tumor cells to evade immune attack (Mantovani et al., 2002).

In the context of SCI, it has been demonstrated that although both phenotypes are in the spinal cord after injury, most of the macrophages and microglia show a predominant pro-inflammatory phenotype (Francos-Quijorna et al., 2016; Kroner et al., 2014). These cells were reported to express high levels of pro-inflammatory markers CD14, CD32, CD86, CD64, and iNOS and low levels of anti-inflammatory markers Arg1, CD163, CD206, CD14, and CD23 during the first two weeks after SCI (Kigerl et al., 2009). Interestingly, when bone marrow-derived macrophages (BMDMs) were polarized *in vitro* towards an anti-inflammatory phenotype and transplanted into a naïve spinal cord, they stayed as anti-inflammatory. In contrast, when they

were transplanted into an injured spinal cord, they switched to pro-inflammatory (Kigerl et al., 2009). These findings revealed that the polarization of macrophages and microglia depends on the injury environment and therefore can be modulated. They also showed that modulation rather than suppression of immune cells may be a promising approach for the treatment of SCI.

It is necessary to have in mind that the M1/M2 classification of macrophages and microglia is an experimental construct that was originally described using *in vitro* systems (Martinez et al., 2009). *In vivo*, cells are influenced my multiple additional factors leading to a wide spectrum of intermediate phenotypes where cells can express opposite signals. For this reason, the terms M1 and M2 became obsolete (Murray et al., 2014). In the present manuscript the terms **detrimental/pro-inflammatory** and **beneficial/anti-inflammatory** will be used to refer these archetypical states of macrophages and microglia. We hope this puts in light the need of a consensus between researches to refer macrophages and microglia plasticity.

Modulation of injury environment

Since in 2009 Kigler demonstrated that the injury environment can compromise the phenotype of macrophages and therefore the secondary damage after SCI, different approaches have been aimed to remodel it (Kigerl et al., 2009).

Knocking out *Tnf* gene resulted in a greater number of anti-inflammatory macrophages after SCI as compared to wild-type (WT) controls (Kroner et al., 2014). *Tnf* null mice also demonstrated to have an improved locomotor performance after injury (Kroner et al., 2014). Injection of recombinant human granulocyte-colony stimulating factor (G-CSF) after spinal cord hemisection reduced the expression of pro-inflammatory factors while increased the expression of anti-inflammatory factors (Guo et al., 2013). Blockade of IL-6 with a monoclonal antibody against IL-6 receptor led to a significant increase of anti-inflammatory markers (Arg1 and CD206) and reduction of M1 markers (iNOS and CD16/32) after SCI (Guerrero et al., 2012). These results correlated with an improvement of the locomotor recovery and tissue preservation. Results from our group showed that increasing levels of IL-37 or IL-4 by recombinant proteins leads to a more anti-inflammatory environment after SCI. This correlated with improved myelin preservation and functional outcomes (Coll-Miro et al., 2016; Francos-Quijorna et al., 2016).

These results demonstrate that targeting of key cytokines can be used for the modulation of the inflammatory response after SCI. Based on this, in the following section of this manuscript, novel therapeutic approaches for the treatment of SCI will be discussed.

Interleukin 1 family

Interleukin 1 (IL-1) was the first interleukin to be identified (Mizel and Farrar, 1979). This cytokine plays a role in mediating the activation of innate immunity, the first line of defense against pathogens and damage (Dinarello, 2015). There are 11 proteins related with IL-1 and they all compose the interleukin-1 family (IL-1F) (Table 2). The family is composed by seven

ligands with agonist activity (IL-1α, IL-1β, IL-18, IL-33, IL-36α, IL-36β, and IL-36γ), three receptor antagonist (IL-1Ra, IL-36Ra, and IL-38), and an anti-inflammatory cytokine (IL-37). All of the proteins share a similar β-barrel structure and bind to Ig-like receptors (Garlanda et al., 2013).

Stimulation of innate system through TLR induces the production of some cytokines from the IL-1F. Some of these cytokines activate target cells through a group of receptors and amplify the immune response. Other cytokines from the IL-1F are involved in homeostatic cell-cell communication. Finally, some of the cytokines of the IL-1F are not inflammatory. They can inhibit the inflammation or trigger anti-inflammatory reactions (Boraschi et al., 2011).

Cytokine	Aliases	Receptor	Coreceptor	Activity
IL-1α	IL-1F1	IL-1R1, IL-1R2	IL-1RAcP	Alarmin, inflammation, Th17
IL-1β	IL-1F2	IL-1R1, IL-1R2	IL-1RAcP	Inflammation, Th17 cell responses
IL-1Ra	IL-1F3	IL-1R1		Inhibition of inflammation
IL-18	IL-1F4	IL-18Ra	IL-18Rb	Inflammation, Th1 cell responses
IL-33	IL-1F11	ST2	IL-1RAcP	Inflammation, Th1 cell responses
IL-36α	IL-1F6	IL-1Rrp2 (IL-36R)	IL-1RAcP	Skin and lung inflammation
IL-36β	IL-1F9	IL-1Rrp2 (IL-36R)	IL-1RAcP	Skin and lung inflammation
IL-36γ	IL-1F8	IL-1Rrp2 (IL-36R)	IL-1RAcP	Skin and lung inflammation
IL-36Ra	IL-1F5	IL-1Rrp2 (IL-36R)		Inhibition of inflammation
IL-37	IL-1F7	IL-18Ra	IL-1R8 (SIGIRR)	Inhibition of inflammation
IL-38	IL-1F10	IL-1Rrp2 (IL-36R)		Inhibition of inflammation
		IL-1R8 (SIGIRR)		Inhibition of inflammation
		TIGIRR-1 (IL1RAPL2)		Not known
		TIGIRR-2		Not known
		IL-1R1(?)	IL-1RAcPb	Inhibition of inflammation

Table 2. Classification of the cytokines and receptors of the IL-1 family. Brief explanation of the activity of these cytokines is indicated. Adapted from (Garlanda et al., 2013).

IL-1α

IL-1α and IL-1β affects all cells and organs and are major pathogenic mediators of the immune response. They are encoded by distinct genes but bind to the same IL-1 receptor and exert similar biological properties (Garlanda et al., 2013). However, there are some distinctions that change their effect on immunity, inflammation, and cancer.

The IL-1α cytokine is constitutively present in epithelial layers of the entire gastrointestinal tract, lung, liver, kidney, endothelial cells, and astrocytes. More specifically, the IL-1α precursor is located into the cell nucleus since it expresses a string of basic amino acid termed the nuclear localization sequence (NLS) that binds to DNA. Upon a signal to initiate necrosis, the IL-1α precursor leaves the nucleus and resides in the cytosolic compartment. After cell death, the IL-1 precursor is released to the extracellular space and functions as an “alarmin” initiating rapidly a cascade of inflammatory cytokines and chemokines by binding to its target cells (Chen et al., 2007). In contrast, upon a signal to initiate apoptosis, IL-1α remains tightly

bound to chromatin and is unavailable for initiation inflammation (Dinarello et al., 2011; White et al., 2010). Thus, this IL-1α mediates the early phases of inflammation. The IL-1α precursor is rarely detected into the circulation since it is contained in cell death bodies released from dead endothelial cells (Berda-Haddad et al., 2011).

IL-1β

The IL-1β cytokine is produced by hematopoietic cells such as blood monocytes, tissue macrophages, skin dendritic cells, and microglia. It is produced in response to TLR, activated complement components, other cytokines or IL-1 itself (Dinarello, 2011). Unlike the IL-1α, IL-1β precursor is not active. It needs the processing by caspase-1 and the releasing of active cytokine to the extracellular space. Although caspase-1 is abundant in hematopoietic cells, the proenzyme (procaspase-1) first requires cleavage by inflammasomes. In some cases, IL-1β can also be secreted as a precursor, without cleavage by caspase-1. In this case, in order to be active, extracellular cleavage of the IL-1β precursor is performed by neutrophil enzymes such as proteinase-3 and elastase. The cleavage site of these enzymes is very close to the cleavage site of caspase-1 (Dinarello, 2011).

IL-18

IL-18 was first described in 1989 as "interferon-γ-(IFN-γ)-inducing factor" (Nakamura et al., 1989). IL-18 is a pro-inflammatory cytokine that facilitates the production of IFN-γ by Th1 cells together with IL-12. It also acts on non-polarized T cells, natural killer cells, B cell, dendritic cells, and macrophages (Yasuda et al., 2019). IL-18 is found in the same cells as IL-1α (Puren et al., 2002). Similar to IL-1β, IL-18 is firstly synthesized as an inactive precursor and requires caspase-1 (or proteinase-3) to be processed (Yasuda et al., 2019). Besides, upregulation of IL-1β is produced within 4 h after focal ischemia in rats whereas IL-18 is upregulated much later, at time points associates with infiltration of peripheral immune cells (Jander et al., 2002). The tertiary structure of IL-18 precursor is closely related to IL-37 and the intron-exon borders of the *IL18* and *IL37* genes suggest a close relationship. Indeed, IL-37 binds to the IL-18 receptor (Nold-Petry et al., 2015).

Inflammasomes

Both IL-1β and IL-18 requires caspase-1 processing. The activation of caspase-1 is produced by inflammasomes. Inflammasomes are macromolecular complexed in the cytoplasm of stimulated immune cell that mediates the activation of inflammatory caspases (Franchi et al., 2009; Martinon et al., 2002). Inflammasomes are composed by three different elements: a pathogen recognition receptor (PRR); an adaptor protein known as ASC, and a procaspase-1 protein. To date, five different inflammasomes has been identified each one being dictated by the unique PRR they are composed by. These inflammasomes are the nucleotide-binding oligomerization domain (NOD) leucine-rich repeat (LRR)-containing protein family members NLRP1, NLRP3 and NLRC4; as well as the proteins absent in melanoma 2 (AIM2), and pyrin (Broz and Dixit, 2016).

The NLRP3 inflammasome

The NOD-like receptor pyrin domain-containing protein 3 (NLRP3) inflammasome is one of the best characterized. This inflammasome is composed by the sensor molecule NLRP3, the adaptor protein ASC, and the procaspase-1. ASC adaptor protein harbors the pyrin domain (PYD) from the NLRP3 protein and the caspase recruitment domain (CARD) from procaspase-1 protein. Assembly of NLRP3 inflammasome requires two steps: priming and activation. The priming step (signal 1) is provided by inflammatory stimuli such as TLR4 agonist that induce the NF-κB-mediated *NLRP3* and *IL1B* expression. The activation step (signal 2) starts with the recognition of inflammatory ligands by NLRP3 sensor protein. This results in interaction with ASC via PYD and the recruitment of procaspase-1 via CARD forming a NLRP3-ASC-procaspase-1 complex, also named NLRP3 inflammasome. Proximity-induced auto-processing results in the formation of the catalytically active caspase-1, which initiates downstream responses, including the release of IL-1β and IL-18 but also the induction pyroptosis, which is a lytic form of cell death by forming pores in the plasma membrane (Fig. 7) (Broz and Dixit, 2016; Yang et al., 2019).

NLRP3 respond to a wide variety of stimuli including bacterial toxins, particulate matter or extracellular ATP. All these stimuli share a reduction in intracellular potassium levels as common denominator (Muñoz-Planillo et al., 2013). Although specific activation mechanism is not fully understood, it may involve a newly identified component of NLRPR3 inflammasome, known as NEK7 (NIMA-related kinase 7), which binds to NLRP3 protein and requires potassium efflux (Shi et al., 2016).

The classic way of maturation and release of IL-1β and IL-18 is known as **canonical pathway**. However, occasionally both cytokines can mature following a **non-canonical pathway** (Fig. 7). Non-canonical pathway is produced in response to LPS from Gram-negative bacteria. LPS is directly recognized by the CARD domain of caspase-11 in mice and caspase 4 and/or caspase 5 in human leading to its oligomerization. Active caspases cleavage gasdermin D, a pore-forming protein that induce pyroptotic cell death. Pyroptosis leads to potassium efflux and, therefore, to the activation of NLRP3 inflammasome and IL-1β and IL-18 processing (Yang et al., 2019).

In 1997, Fantuzzi demonstrated that there is also an inflammasome-independent processing of IL-1 cytokines (Fantuzzi et al., 1997). In this case, mice lacking the caspase-1 gene show the same severity inflammation than wild-type demonstrating that IL-1β could be processed independently of caspase-1 (Fantuzzi et al., 1997). Subsequent studies identified neutrophil- and macrophage-derived neutral serine proteases such as proteinase 3, elastase, cathepsin-G as enzyme that can process pro-IL-1β into a 17 kDa bioactive fragment (Coeshott et al., 2002; Sugawara et al., 2014). Similar to IL-1β, pro-IL-18 can also be processed by metalloproteinase Meprin β or proteinase 3 (Bae et al., 2012; Banerjee and Bond, 2008). These inflammasome-independent processing occurs mainly in inflammatory circumstances when neutrophils are the major cell population (Mencacci et al., 2000).

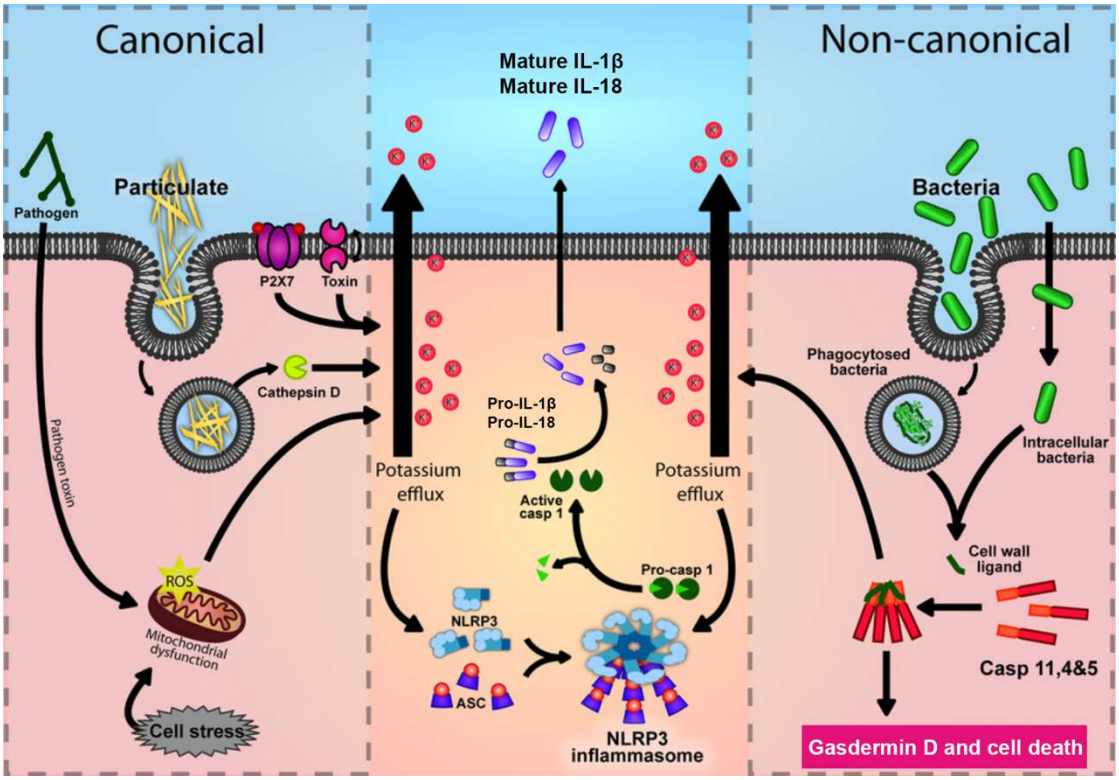

Figure 7: Canonical and non-canonical pathways of NLRP3 activation. The canonical pathway (left) involves a diverse range of stimuli. The non-canonical pathway (right) requires LPS and involves caspases 4/5/11. Assembly of NLRP3 inflammasome (middle) results in caspase-1 activation and the processing of IL-1β and IL-18. Image adapted from (Rivers-Auty and Brough, 2015).

Interleukin 37

Interleukin 37 (IL-37 or IL1F7) is an anti-inflammatory cytokine of the IL-1 family that was discovered in the year 2000 by computational cloning (Dunn et al., 2001).

Gene organization and expression

In humans, nine of the IL-1 family members are located in chromosome 2. The two other members, IL-18 and IL-33, are located in chromosome 11 and chromosome 9, respectively. Unlike other members of the IL-1 family, the open read frame for the *IL37* homolog is lacking in the mouse and chimpanzee, and thus, they do not have this cytokine (Taylor et al., 2002).

Human *IL37* gene is located between *IL1B* and *IL36G* genes at chromosome 2. The gene size is 3617 base pairs (bp) and undergoes five forms of alternative splicing (Figure 8). From all of them, *IL37b* (isoform 1) is the best characterized and largest isoform (but not protein) containing five of the six available exons (Boraschi et al., 2011). *IL37* is expressed in a variety of normal tissues and tumors. Some isoforms of *IL37* seem to be enriched in some tissues against others. For example, *IL37a* is the only isoform expressed in the brain while *IL37b* is the only expressed in the kidney (Boraschi et al., 2011).

In normal conditions, levels of *IL37* mRNA are very low. This is the result of untranslated region-independent control elements, such an A-rich homology box, found in *IL37* gene (Bufler

et al., 2004). These instability elements seem to be present in exon 5, as exon 5 deletion significantly increases mRNA stability. Since all the *IL-37* isoforms contain exon 5, these instability elements are present in all the forms, and thus, they are not expressed. However, under inflammatory conditions, the *IL37* mRNA is stabilized, and the protein can be synthetized (Boraschi et al., 2011). The mechanisms involved in the stabilization of *IL37* mRNA are not known yet.

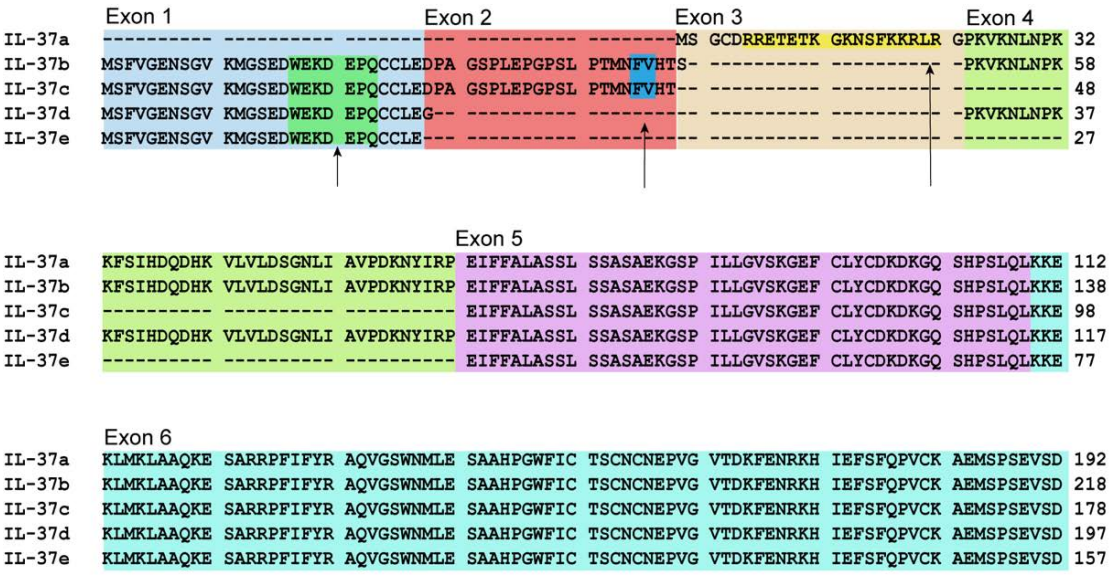

Figure 8: Human *IL37* gene organization and protein processing. Alignment of the five splice variants. Exons 1 containing the caspase-1 cleavage site (arrow). Exon 2 containing the second cleavage site (arrow). Exon 3 containing the putative elastase cleavage site (arrow) and NLS (yellow). Number of amino acids of each isoform before processing is indicated. Image adapted from (Boraschi et al., 2011).

Protein processing

IL-37 protein is synthesized as a precursor molecule composed of 12 β-barrel strands. Maturation is produced through cleavage in specific sites. In total, IL-37 has three possible cleavage sites (Figure 7). The first one is located in exon 1, between residues D20 and E21, and is present in isoforms b, c, d, and e. This cleavage site is recognized by caspase-1, the major enzyme responsible for the maturation of IL-37 precursors. The second cleavage site is located in exon 2, between residues F45 and V46, and is presented in isoforms b and c. Because isoform a does not contain exons 1 and 2, an alternative elastase cleavage site is predicted in exon 3, between residues L21 and R22. This cleavage site is downstream of a NLS (Figure 7), suggesting that the protein precursor, in addition to the mature protein, can translocate to the nucleus (Boraschi et al., 2011; de Castro et al., 2006). According to cleavages sites, isoform d produces the largest mature protein that starts at 46 and contains 177 amino acids (Boraschi et al., 2011) (Figure 7).

Once IL-37 is fully activated, it can exacerbate a double-function through intracellular and extracellular pathways. However, only the isoforms a, b, and d are fully functional because,

contrary to the isoforms c and e, they contain the 12 putative β-strands necessary for the forming of the IL-1-like β-trefoil secondary structure and binding to IL-18Rα receptor (Murzin et al., 1992; Wang et al., 2018).

Extracellular role

Members of the IL-1 family have a family of receptors (IL-1Rs) that shares structural properties including extracellular immunoglobulin-like domains and intracellular Toll-IL-1R (TIR) domains. The canonical signaling pathways involve the binding of a ligand from the IL-1 family to an IL-1R chain followed by the recruitment of a second IL-1R chain (co-receptor chain). This complex then attracts the intracellular adaptor MyD88 to the TIR domain of the IL-1R co-receptor, triggering a signaling cascade. In the case of IL-37, this protein binds to the α-chain of the IL-18 receptor (IL-18Rα) and recruits the IL-1R8 co-receptor, also known as SIGIRR, forming a tripartite ligand-receptor complex (Nold-Petry et al., 2015).

The formation of IL-37-IL-18Rα-IL-1R8 complex results in a variety of different effects, but one that may be pivotal for the role of IL-37 in the suppression of the innate immune response is the inhibition of Fyn and TAK1 kinases. Fyn kinase promotes inflammation and skews macrophage polarization away from the anti-inflammatory phenotype. TAK1 is an adaptor kinase with the ability to relay the pro-inflammatory signals of TLRs, IL-1R1, IL-18R, TNFR, and the antigen receptors on T cells and B cells to a variety of downstream effector pathways, including NF-κB, MKK3-p38, and Akt (Li et al., 2015; Nold-Petry et al., 2015). Other effects described include the inhibition of the insulin receptor-mTOR-kinase S6K and the increasing activity of the AMP-activated kinase (AMPK), signal transducer and activator of transcription (STAT) 6, and transcription factors of the Foxo family. All these process result in an anti-inflammatory activation (Li et al., 2015; Nold-Petry et al., 2015).

The discovery of the extracellular pathway of IL-37 was due to IL-18. Although both proteins share part of their amino acids sequence, they have opposite functions. IL-18 is a pro-inflammatory cytokine considered the major inducer of IFNγ. IL-18 binds to the IL-18Rα and recruits the accessory protein IL-18Rβ to initiate a cell activation (Garlanda et al., 2013). Soluble IL-18 binding protein (IL-18BP) binds to active IL-18, preventing its binding to the IL-18R chains and reducing the production of IFNγ. This reduction was effective with low doses of IL-18BP. However, the anti-inflammatory effects of the IL-18BP were lost by increasing its concentrations. This suggests that IL-18BP also binds to another ligand that has anti-inflammatory effects but with lower affinity than IL-18. This ligand is IL-37 (Boraschi et al., 2011).

Nuclear role

Similar to IL-1α and IL-33, IL-37 can be translocate dto the nucleus. To be translocated, IL-37 is proceeded by caspase-1 since specific inhibition of caspase-1 reduces the presence of this protein in the nucleus (Bulau et al., 2014; Sharma et al., 2008). After cytoplasmic processing, IL-37 binds to the Smad3 kinase generating a complex that translocates to the nucleus, through the nuclear pore. In the nucleus, IL-37 regulates gene expression to suppress inflammatory response (Sharma et al., 2008).

Studying IL-37 in mouse models

Unlike other members of the IL-1 family, the open read frame for the IL-37 homolog is lacking in the mouse (Taylor et al., 2002). To investigate the role of this interleukin in mouse models, a transgenic mouse expressing the full-length of *IL37b* cDNA was generated (Nold et al., 2010). In this transgenic mouse, the expression of the human *IL37* gene is driven by a constitutive cytomegalovirus (CMV) promoter. However, due to the instability elements of exons 5, synthesis of IL-37 is very low in normal conditions and elevated after inflammatory challenge such as LPS (Boraschi et al., 2011; Bufler et al., 2004).

In normal conditions, the IL-37 transgenic mice (hIL-37Tg) bred normally, do not differ from negative or wild-type mice in growth, reproduction, and male-to-female ration over many generations. However, compared to WT mice, hIL-37Tg mice are protected against LPS challenge exhibiting less hypothermia, acidosis, hyperkalemia, hepatitis, dehydration and inflammatory cytokines (Nold et al., 2010).

IL-37 and diseases

IL-37 has been used as a therapeutic target in a wide variety of diseases, some of them lately explained. As a common feature of these studies, IL-37 protection is associated with decreased concentrations of inflammatory cytokines and chemokines. A complete list of IL-37 related-models is listed on Table 3.

Disease model	Effect	Reference
Endotoxemia	↓Inflammation, ↓cytokines	(Nold-Petry et al., 2015)
Acute lung injury	↓Neutrophils, ↓IL-1β, ↓NLRP3 mRNA	(Moretti et al., 2014)
Acute lung injury	↑IL-10 production	(Moretti et al., 2014)
Spinal cord injury	↑Mobility, ↓cytokines	(Coll-Miro et al., 2016)
Hepatic ischemia	↓Inflammation, ↓cytokines	(Sakai et al., 2012)
Metabolic syndrome	↓Insulin resistance, ↓cytokines	(Ballak et al., 2014)
Inflammatory arthritis	↓Neutrophils, ↓cytokines	(Cavalli et al., 2016)
Asthma	↓Airway response, ↓cytokines	(Lunding et al., 2015)
Myocardial infarction	↓Infarct size, ↓MPO, ↑function	(Wu et al., 2014)
Renal ischemic	↑Function, ↓cytokines, ↓inflammation	(Yang et al., 2015)
ConA hepatitis	↓Serum IL-1α, IL-6, IL-5 and IL-9	(Bulau et al., 2011)
Atherosclerosis	↓Plaque in APO E deficient mice	(Chai et al., 2015)
Myopathy	↓Inflammation, ↓cytokines	(Yan et al., 2018)

Table 3: Selected therapies with rIL-37 in different disease-models. Effects observed are indicated. Adapted from (Dinarello et al., 2016).

In the case of colitis, transgenic mice expressing human *IL37* subjected to dextran sulfate sodium-induced colitis showed reduction of the clinical disease scores and in the histological markers compared to their WT counterparts. Transgenic animals also shown reduced inflammation associated with decreased leukocyte recruitment into the colonic lamina propria (McNamee et al., 2011). Transgenic mice subjected to concanavalin A-induced hepatitis and LPS-induced sepsis showed significant reduction in the levels of pro-inflammatory cytokines

such as IL-1α, IL-6, IL-5, and IL-9 (Bulau et al., 2011). In the case of myocardial infarction, the injection of recombinant IL-37 protein, immediately before myocardial ischemia/reperfusion injury in mice, resulted in reduction of the infarct size. Cardiac vascular endothelial cells also showed reduced NF-κB activation when stimulated with TLR2 and TLR4 agonists (Wu et al., 2014). In metabolic syndrome, mice expressing the human *IL37* gene fed with high-fat diet had reduced numbers of adipose tissue macrophages, less lipid accumulation in the liver, improved response to insulin, and increased glucose tolerance compared with WT mice on the same diet (Ballak et al., 2014). Importantly, in 2016 results from our group showed that IL-37 exerts beneficial effects after SCI improving the locomotor skills and myelin sparing (Coll-Miro et al., 2016).

Interleukin 13

Interleukin 13 (IL-13) is a highly pleiotropic anti-inflammatory cytokine. IL-13 has a molecular weight of about 10 kDa and its gene is located in the human chromosome 5q23/31 (Minty et al., 1993). Despite intensive study since their discovery more than 30 years ago, their full range of functions has not been elucidated yet.

Function

IL-13 derives from T cells (mainly Th2 cells) but it can also be produced by a variety of other cells including granulocytes and macrophages (M. et al., 2015). This interleukin has a main role in the immune response. It induces the expression of surface antigens in B lymphocytes including MHC class II and CD23, the synthesis of immune proteins especially immunoglobulin E (IgE), and it promotes the proliferation and differentiation of B lymphocytes, leading to the formation of a large number of antibodies (May and Fung, 2015). IL-13 activates macrophages promoting their anti-inflammatory properties and the expression of anti-inflammatory cytokines through the activation of STAT6 in an IL-13Rα1-dependent pathway (Sheikh et al., 2015). IL-13 also induces eosinophil aggregation and promotes its activation and survival (Horie et al., 1997).

Signaling pathways

IL-13 receptors are widely expressed on almost every cell in the body and change during disease. Generally, two types of receptors can be found. The first type can be found in cells of the myeloid hemopoietic lineage and is composed of the subunits IL-4Rα and IL-13Rα1. To form this complex, IL-13 binds to IL-13Rα1 with low affinity leading to dimerization with the IL-4Rα chain. This heterodimer can now induce cytoplasmic signaling cascade. The second type of receptor for IL-13 is composed of a single specific chain named IL-13Rα2 that binds to IL-13 with high affinity (Fig. 8) (Suzuki et al., 2015). This receptor type has been reported on a variety of solid human tumors such as glioma, pancreatic cancer, and ovarian cancer (Martinez et al., 2009; Suzuki et al., 2015). There is controversy around IL-13Rα2 receptor since it lacks the intracellular tail and it also exists as a soluble form. For these reasons, some authors consider IL-13Rα2 as a decoy receptor (Chandriani et al., 2014).

Signaling transduction of IL-13 through IL-4Rα and IL-13Rα1 involves JAK/STAT pathways. IL-13 phosphorylates and activates Janus kinase (JAK) 1 in hematopoietic cells while it phosphorylates JAK1 and JAK2 tyrosine kinases in non-hematopoietic cells such as colon carcinoma and fibroblast cells. Although the proximal signaling pathways in hematopoietic and non-hematopoietic cells are different, signaling produces the phosphorylation and activation of STAT6 (Fig. 8). Once phosphorylated, pSTAT6 translocates to the nucleus where it binds DNA promoter elements to regulate gene transcription (Suzuki et al., 2015). Besides controversy reported above about the second receptor for IL-13, a previous study indicated that IL-13 signaling through IL-13Rα2 led to the activation of the transcription factor AP-1 and the TGF-β1 promoter (Fichtner-Feigl et al., 2006).

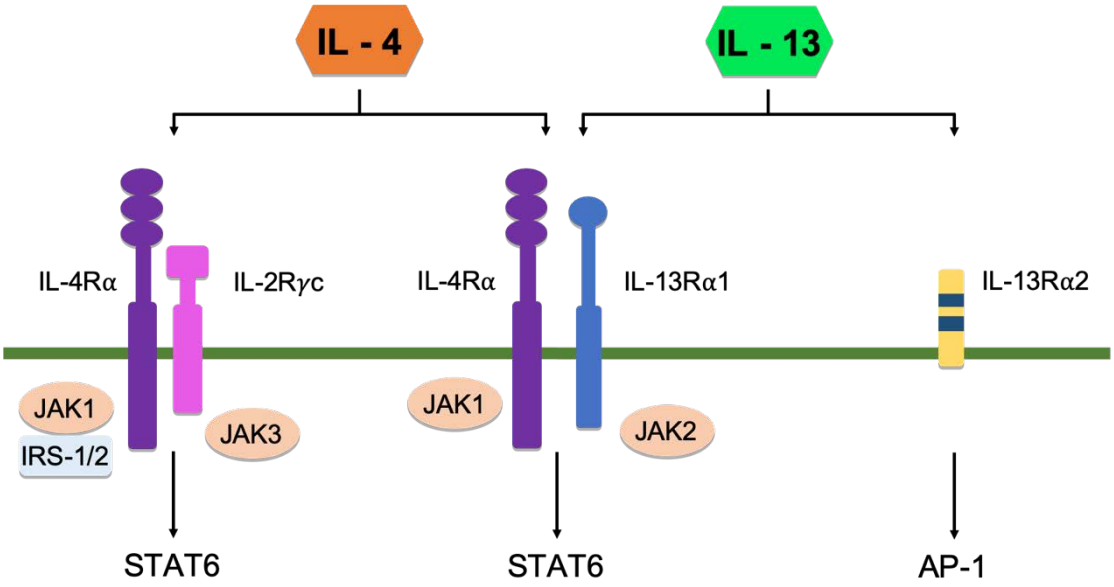

Figure 9: IL-4 and IL-13 signaling pathways through IL-4Rα, IL-13Rα1, and IL-13Rα2 receptor subunits.

IL-13 and diseases

IL-13 has been used for the treatment of a wide range of inflammatory diseases especially in those related with autoimmunity.

Naïve CD4 cells can differentiate into multiple effector subsets, such as T helper Th1, Th2, and Th17. The unbalance between these cells is the common characteristic of autoimmune diseases such as systemic lupus erythematous, rheumatoid arthritis, ulcerative colitis, type 1 diabetes, Sjogren's syndrome, etc. IL-13 can alter this balance since it has been demonstrated to interfere in the apoptosis pathway of T cell (Yang et al., 2016) and in the development of Th17 cells (Newcomb et al., 2012). For this reason, targeting IL-13 by different approaches is a promising therapy for these diseases (Mao et al., 2018). For example, monoclonal antibodies against IL-13 have been shown to be effective in the treatment of asthma (Brightling et al., 2015; Hanania et al., 2016; Tripp et al., 2017). Blockade of IL-4Rα with monoclonal antibodies has been proven to be effective in controlling asthma symptoms and improving lung function signaling (Castro et al., 2018). Finally, a selective inhibitor for JAK1 and JAK3 has demonstrated

to produce higher rate of mucosal healing and remission in the treatment of ulcerative colitis (Motoya et al., 2018), systemic lupus erythematous, and rheumatoid arthritis (Y. et al., 2017). In the case of CNS diseases, in a multiple sclerosis model by cuprizone, lentiviral mediates expression of IL-13 forced macrophages and microglia towards an anti-inflammatory phenotype during the course of the disease. This was correlated with subsequent protective effects on oligodendrocyte survival and, subsequently, with less severe demyelination due to cuprizone (Guglielmetti et al., 2016).

IL-13 and IL-4

IL-13 is closely related to interleukin-4 (IL-4), sharing about 20% of their amino acid sequence (Paul, 2015). Both interleukins are expressed by the same cells and share the first type of receptor, composed by IL-4Rα and IL-13Rα1. In the case of IL-4, it binds to the IL-4Rα chain with high affinity and then recruits the IL-13Rα1 subunit initiating the signal transduction. Similar to IL-13, IL-4 can also act through another receptor composed of IL-4Rα and IL-2RγC chains (Fig. 8) (Suzuki et al., 2015). Once IL-4 binds to any of its receptors, it activates the same JAK/STAT pathways previously described. IL-4 could also phosphorylate JAK3 in hematopoietic cells but not in any solid cancer cell type (Suzuki et al., 2015). Although both interleukins were considered to be redundant for a long time, it has been demonstrated that they differ in many important features. For example, it has been found that IL-13 negatively regulates the differentiation and secretion of cytokines such as IL-17α by Th17 cells. This was produced in cells without the IL-13Rα2 specific receptor indicating a specific pathway not related to IL-4 (Wilson et al., 2011).

OBJECTIVES

The general objective of the present thesis is to investigate whether the modulation of the inflammatory response confers protection after SCI. Our hypothesis is that exacerbated inflammation exerts deleterious effects. Therefore, modulation of the bioavailability of pro-inflammatory and anti-inflammatory cytokines will improve functional deficits and histopathological outcomes after SCI.

This thesis has been divided in 4 chapters according to the following specific aims.

Chapter 1: Neuroinflammation quantification for spinal cord injury

- To stablish a protocol to induce reproducible spinal cord contusion injury in mice.
- To determine whether quantification of different immune cell subsets can be performed in the injured spinal cord by flow cytometry.
- To evaluate whether Luminex assay is a useful tool to quantify multiple cytokines in the spinal cord after injury.

Chapter 2: Modulation of the inflammatory response after spinal cord injury by MABp1 and OLT1177

- To characterize the dynamics changes in protein levels of IL-1α, IL-1β, and IL-18 in the spinal cord after injury.
- To determine the effects of the IL-1α blocking antibody MABp1 on locomotor recovery and tissue preservation after SCI.
- To study the effects of the inflammasome inhibitor OLT1177 on functional outcomes and tissue sparing after SCI.

Chapter 3: Extracellular and nuclear roles of IL-37 after spinal cord injury

- To assess the contribution of nuclear IL-37 to inflammation in cell cultures.
- To study the what degree nuclear and extracellular IL-37 contributes to beneficial effects of this cytokine after SCI.
- To determine whether IL-37 exerts therapeutic actions after SCI by acting peripherally or centrally.

Chapter 4: Modulation of the inflammatory response after spinal cord injury by IL-13

- To characterize the dynamic changes in IL-13 protein levels in the spinal cord after injury.
- To study whether IL-13Rα and IL-4Rα are expressed in microglia and macrophages in the spinal cord after lesion.
- To evaluate whether administration of rIL-13 into the lesioned spinal cord modulates the counts and polarization of macrophages and microglia.
- To compare the effects of rIL-13 on microglia and macrophages after SCI to those exerted by rIL-4.
- To determine the therapeutic potential of rIL-13 after SCI.
- To analyze the transcriptomic differences mediated by rIL-13 and rIL-4 in macrophages and microglia after SCI
- To determine the metabolic state of myeloid cells in the contused spinal cord after treatment with rIL-13 and rIL-4.

MATERIALS AND METHODS

Approvals

All the experiments described in this manuscript were approved by the Ethics Committee on Animal and Human Experimentation from the Universitat Autònoma de Barcelona (CEEAH: 4057) and followed the European Communities Council Directive 2010/63/EU. Methods from each procedure were carried out in accordance with approved guidelines.

Mice

C57BL/6J

Wild-type (WT) C57BL/6J mice were purchased from Charles Rivers (originally from The Jackson Laboratory). Mice were obtained prior experiment and maintained in our facilities until need in a 12 hours light/dark cycle.

IL-37 knock-in mice (hIL-37Tg)

Transgenic mice expressing the human form of *IL37* gene (hIL-37Tg) were kindly donated by Dr. Dinarello (University of Colorado, USA). To generate these mice, fertilized zygotes from C57BL/6J mice were injected with an expression plasmid containing the isoform b of the *IL37* cDNA (pIRES *IL37b*). In this plasmid, the expression of the human *IL37* gene is under a constitute cytomegalovirus (CMV) promoter. Zygotes were then implanted into C57BL/6 females (Nold et al., 2010). Mice were crossed until homozygous knock-in line was obtained. Continuous crossing was maintained in our facilities to certify a constant supply.

IL-1R8 knock-out mice (IL-1R8KO)

Mice lacking the *Il1r8* gene were kindly donated by Dr. Garlanda (Humanitas Clinical and Research Center, Italy). To generate these mice, embryonic stem cells were electroporated with a targeting vector containing the LacZ gene and a PGK-neomycin resistance reporter. Targeting vector was inserted at the exon 2 of the *Il1r8* gene. Knock-out cells were injected into C57BL/6J blastocysts and implanted into C57BL/6J females generating chimeric mice (Garlanda et al., 2004). Mice were crossed until a homozygotic knock-out line was obtained. Continuous crossing was maintained in our facilities to certify a constant supply.

Double homozygous transgenic mice hIL-37TgxIL-1R8KO

Double transgenic mice expressing the human *IL37* gene (hIL-37Tg) but lacking the *Il1r8* gene (IL-1R8KO) were generated in our animal facility by crossing both previous lines. Heterozygotic offspring were crossed between them or with hIL-37Tg mice until the generation of double homozygotic transgenic mice. These mice receive the name of hIL-37TgxIL-1R8KO. Continuous crossing was maintained in our facilities to certify a constant supply.

IL-37 D20A knock-in mice (hIL-37D20ATg)

Transgenic mice expressing a mutated version of the human *IL37* gene were kindly provided by Dr. Dinarello (University of Colorado, USA). These mice were generated using the same the same protocol as hIL-37Tg mice. In this case, human *IL37* cDNA was generated with a D (aspartic acid) to A (alanine) mutation at position 20 and inserted into a pIRES vector. This

mutation prevents the IL-37 processing by caspase-1 and the nuclear internalization. Fertilized zygotes were injected with the vector and implanted into C57BL/6J females. Offspring was crossed until homozygotic line was obtained. Crossing and genotyping was performed by the Animal Care Service of the University of Colorado.

Genotyping

At 3 weeks after birth, small pieces of the tails were cut. Tail tissue was digested using a combination of lysis buffer and proteinase K (DANAGEN) following protocol stablished by the manufacturer. Proteins were removed using a protein precipitation buffer (DANAGEN). DNA was precipitated and washed using 2-propanol and 70% ethanol, respectively. After ethanol removal, DNA was solubilized with hydration buffer (DNAGEN).

IL-1R8KO mice were genotyped by PCR reaction with Taq DNA polymerase (Invitrogen). List of primers used for this genotype are listed at Table 1. Cycle conditions were set as follow: activation of polymerase at 95°C for 5 min; 32 cycles of denaturalization at 95°C for 30 sec, annealing at 54.5°C for 30 sec, and extension at 72°C for 30 secs; and final elongation at 72°C for 15 min. Since annealing temperature for these primers is very low, *touchdown* program was used in order to increase the specificity. In this program, the annealing temperature was gradually reduced from 65 to 54.5 °C during the first 8 cycles.

IL37 and *IL37D20A* genes were genotypes by qPCR reaction with SYBR Green Master Mix (Agilent). List of primers used for these genotypes are listed at Table 1. *Il2* gene was used as a loading control to normalize results. Cycle conditions were set as follow: polymerase activation for 3 min at 95°C; 40 cycles of denaturalization for 10 sec at 95°C plus annealing/extension for 30 sec at 60°C (capture). Expression levels were normalized with the loading control by the ΔCT method. Final fold-change values were obtained by normalization with positive controls.

Gene	Primer	Sequence
IL37 **(for qPCR)**	IL-37f:	5'- CTT AGA CCC GGC TGG AAG -3'
	IL-37r:	5'- TGT GAT CCT CAT GAA TGC T -3'
Il2 **(loading control for qPCR)**	IL-2f:	5'- CTA GGC CAC AGA ATT GAA AGA TCT -3'
	IL-2r:	5'- GTA GGT GGA AAT TCT AGC ATC ATC C -3'
Il1r8	25/10N:	5'- ATC TTT CAG CCA CTG CAC TGA -3'
	5mAcp:	5'- GTC TGT GAC ATG GCC CCT AAT -3'
	PGK:	5'- CTG CTC TTT ACT GAA GGC TC -3'

Table 1: List of primers used for the genotyping of hIL-37Tg, IL-1R8KO and hIL-37TgxIL-1R8KO mice. Standard PCR was used for *Il1r8* whereas qPCR was used for *IL37* gene.

Spinal cord injury surgery

Adult (8 – 10 weeks old) female were anesthetized by intramuscular injection with a mixture of ketamine (90 mg/kg) and xylazine (10 mg/kg). After skin and muscle incision, laminectomy at 11th thoracic vertebrae and the spinal cord was exposed. To perform the injury, a contusion was applied to the exposed spinal cord using the Infinite Horizon Impactor device (Precision Scientific Instrumentation). This device is based on a computer-controlled piston mounted on a stereotaxic apparatus capable of inflicting a consistent and measurable contusion to the spinal cord. For most of the experiments described in this manuscript, a force of 60 kdynes and a tissue displacement of 450 – 550 µm were applied. In those experiments where cytokines were administered directly into the spinal cord, a force of 50 kdynes and tissue displacement of 400 – 500 µm was applied since direct injection produces damage itself and worsens the lesion. Detailed explanation of spinal cord injury surgery can be found at published protocol (Amo-Aparicio et al., 2018).

Treatment injections

In the case of intraspinal injections, interleukins were administered directly into the spinal cord at the lesion center. Administration were performed at different time points after injury, depending on the experiment. Administrations were carried out using a glass micropipette (30 µm internal diameter, Eppendorf) coupled to a 10 µL Hamilton syringe (Hamilton #701, Hamilton Co). Injections were controlled by an automatic injector (KDS 310 Plus, KD Scientific) with a 2 µL/min rate. 1 µL per mouse was injected. After injection, the tip of the micropipette was maintained inside the cord tissue for 3 min to avoid liquid reflux.

In the case of intraperitoneal injections, compounds were administered with a 500 µl syringe coupled to a 29G needle. Injections were performed at the lower right quadrant of the abdomen to minimize the risk of causing damage to the urinary bladder, cecum and other abdominal organs. 200 µl per animal were injected.

Flow cytometry

Flow cytometry from spinal cord was performed according to described protocol (Amo-Aparicio et al., 2018). Animals received an intraperitoneal injection of sodium pentobarbital (Dolethal). Blood was removed by perfusion with 60 mL of 0.9% NaCl in distillated water. 0.6 cm of the spinal cord, centered into the injury site, were taken from each mouse. Cell suspension was obtained by enzymatic disaggregation with a mixture of collagenase (Sigma-Aldrich) and DNase (Roche) and mechanic disaggregation through 70-µm cell strainers (Fisherbrand). Cells were labelled with antibodies listed in Table 2. For intracellular labelling, cells were previously permeabilized with permeabilization buffer (Life Technologies). Proper isotypes for each antibody were used. At the end, cells were fixed with 1% paraformaldehyde (Sigma-Aldrich) in 0.1 M of phosphate buffer and maintained at 4°C until analysis.

Cells were analyzed using the FACSCanto flow cytometer (BD Bioscience). Gating and quantification were performed using a FlowJo® software. Microglia cells were defined as

$CD45^{low}$, $CD11b^{+}$, and $F4/80^{+}$ whereas macrophages were defined as $CD45^{high}$, $CD11b^{+}$, and $F4/80^{+}$. Granulocytes, mainly neutrophils, were defined ad $CD45^{high}$, $CD11b^{+}$, and $F4/80^{-}$ (Amo-Aparicio et al., 2018; Francos-Quijorna et al., 2016). Number of cells over the total $CD45^{+}$ cells or percentage of cells expressing certain markers within a specific population were measured.

Antibody	Fluorophore	Brand	Dilution
CD45	PerCP	BioLegend	1:200
CD11b	PE-Cy7	BioLegend	1:200
F4/80	PE	eBioscience	1:200
F4/80	APC	eBioscience	1:200
F4/80	FITC	Miltenyi	1:200
CD16/32	PE	eBioscience	1:200
CD206	FITC	BioLegend	1:200
Arg1	-	SantaCruz	1:200
iNOS	-	Abcam	1:200
-	Alexa 488	ThermoFisher Scientific	1:500
-	Alexa 647	Abcam	1:500
IL-4Rα	APC	Miltenyi	1:200
IL-13Rα1	PE	eBioscience	1:200

Table 2: List of antibodies used for flow cytometry. Dilution for each antibody is indicated. References can be found at Product's References section.

Gene expression (qPCR)

At different time points after SCI, mice received an intraperitoneal injection of sodium pentobarbital (Dolethal). Blood was removed by perfusion with 60 mL of 0.9 % NaCl in distillated water. 0.6 cm of the spinal cord, centered into the injury site, were taken from each animal and freeze in liquid nitrogen. Samples were homogenized with QIAzol lysis reagent and TissueRuptor (Qiagen). RNA was purified using a RNeasy Lipid Tissue kit (Qiagen) following users guide protocol. Additional step with DNase I was included to avoid genomic DNA contamination. 1 µg of RNA from each sample was reversely transcribed using the Omniscript RT kit (Qiagen) and random primers (Promega). RNase inhibitor (Roche) was added to avoid RNA degradation.

Quantitative pCR (qPCR) was performed using a MyiQ Single-color Real-time PCR Detection System (BIO-RAD). Taqman primers were purchased from ThermoFisher Scientist. *Gapgh* was used as a housekeeping gene. Components for qPCR reaction were supplied as Universal Master Mix II with UNG (ThermoFisher Scientific) and recommended thermal cycling parameters were used: UNG incubation for 2 min at 50°C; polymerase activation for 10 min at 95°C; and 40 cycles of denaturalization for 15 sec at 95°C plus annealing/extension for 1 min at 60°C (capture). Expression levels of targets mRNAs were normalized to the relative ration of expression of the *Gapdh* gene following the ΔCT method. Final fold-change values were obtained by normalization with naïve condition.

LUMINEX (bead-based multiplex assay)

At different time points after injury, mice were euthanized with an overdose intraperitoneal injection of sodium pentobarbital. Blood was removed by perfusion with 60 mL of 0.9 % NaCl in distillated water. 0.6. cm of the spinal cord, centered at the lesion site, were taken and frozen in liquid nitrogen. Samples were homogenized in protein extraction buffer using a TissueRuptor (Qiagen) and a Ultrasonic Homogenizer (Biologics Inc.). Extraction buffer was prepared as previously described (Amo-Aparicio et al., 2018). After centrifugation and removal of non-soluble fragments, samples were quantified and diluted to 2 µg/µl. Luminex plates were prepared following specific commercial protocol. Plates were washed with specific buffer and magnetic beads were attached. Finally, samples and standards were added and incubated overnight at 4°C. At the next day, plates were washed and secondary (PE-streptavidin) and detection antibody were added. Finally, plates were read in a Luminex Analyzer (MAGPIX Luminex, ThermoFisher Scientific). Median Fluorescent Intensity (MFI) of each specific bead were measured and translated into to protein concentrations. Final values were normalized by the amount of protein added in each well.

Functional Assessment

Locomotor recovery was measured through the widely used Basso Mouse Scale (BMS) (Basso et al., 2006). Following this guide, animals were allowed to move in an open field for 5 minutes and then evaluation is performed. Analysis of hindlimb movements and coordination was performed following a blind method. Consensus score between two researchers was taken. Scores equivalencies are listed in Table 3. Locomotor recovery was evaluated at prior to surgery and at 1, 3, 5,7, 10, 14, 21, and 28 days post-injury (dpi).

A

Score	Meaning
0	No ankle movement
1	Slight ankle movement
2	Extensive ankle movement
3	Plantar placing of the paw with or without weight support -OR- Occasional, frequent or consistent dorsal stepping but no plantar stepping
4	Occasional plantar stepping
5	Frequent or consistent plantar stepping, no coordination -OR- Frequent or consistent plantar stepping, *some* coordination, paws *rotated* at initial contact and lift off (R/R)
6	Frequent or consistent plantar stepping, *some* coordination, paws *parallel* at initial contact (P/R, P/P) -OR- Frequent or consistent plantar stepping, *mostly* coordinated, paws *rotated* at initial contact and lift off (R/R)
7	Frequent or consistent plantar stepping, *mostly* coordinated, paws *parallel* at initial contact and *rotated* at lift off (P/R) -OR-

	Frequent or consistent plantar stepping, *mostly* coordinated, paws *parallel* at initial contact and lift off (P/P), and *severe* trunk instability
8	Frequent or consistent plantar stepping, *mostly* coordinated, paws *parallel* at initial contact and lift off (P/P), and *mild* trunk instability -OR- Frequent or consistent plantar stepping, *mostly* coordinated, paws *parallel* at initial contact and lift off (P/P), and *normal* trunk stability and tail *down or up & down*
9	Frequent or consistent plantar stepping, *mostly* coordinated, paws *parallel* at initial contact and lift off (P/P), and *normal* trunk stability and tail *always* up.

B

Subscore	Frequency	Type
0	Frequent	Plantar stepping (score both paws)
1	Consistent	
0	None	Coordination
1	Some	
2	Most	
0	Rotated thru out	Paw position (score both paws)
1	Parallel and rotated	
2	Parallel thru out	
0	Severe	Trunk instability
1	Mild	
2	Normal	
0	Down	Tail
0	Up and down	
1	Up	

Table 3: Basso Mouse Scale (BMS) used for the evaluation of the locomotor recovery. Meaning of main scores (A) and subscores (B) are indicated. Subscore is only applicable after the mouse achieves a threshold of frequent stepping. Taken from (Basso et al., 2006).

Histology

At 28 dpi, animals receive an intraperitoneal injection of sodium pentobarbital (Dolethal) and were perfused with 4% paraformaldehyde in 0.1 M of phosphate buffer. A 0.6 cm of spinal cord centered into the lesion site was removed and cryoprotected with 30% sucrose in 0.1 M of phosphate buffer saline (PBS) at 4°C. Samples were embedded in Tissue-Tek (Sakura), cut with 10-15 µm thick in the cryostat, and picked up with a glass slide. Samples were arranged following a serial distribution. Adjacent sections in the same slide were 100-150 µm apart. After graded dehydration, sections were placed in a 1 mg/ml Luxol Fast Blue (LFB) (Sigma) solution in 95% ethanol and 0.05% acetic acid and left overnight at 37°C. Sections were then washed in 95% ethanol and distilled water before clearing with 0.5 mg/ml of Li_2CO_3 in distilled water for 1.5 min. After several washes, sections were dehydrated, embedded in xylene, and mounted with DPX mounting media (Sigma-Aldrich). After fixation, the epicenter of the

contusion was localized by determining the tissue section with the lowest LFB stained area. NIH ImageJ software was used to perform the quantifications.

Cell sorting and RNA extraction

The flow cytometry protocol with slight modifications, was used for cell sorting. Before staining, myelin was removed using Miltenyi myelin removal beads following manufacturer's recommendations. After labelling with previous described antibodies, cells were kept in PBS with 5% of FBS (Sigma) and then sorted using FACSJazz (BD Bioscience). 1 drop pure method was used. A drop frequency of 39.05 kHz and a sheath pressure of 27 psi were established. Sort rate varied between 100-150 cells/sec depending on the sample since treatments can alter cells distribution. Population were gated as previously described using basis of FSC and SSC and CD45-PerCP, CD11b-PE-Cy7 and F4/80-PE antibodies. From 9000 to 73000 events of macrophages or microglia were obtained from each mouse. The purity after sorting was of 99%.

Cells from sorting were collected in Eppendorf tubes with 350 µL of ice-cold RLT buffer. To prevent changes, collection tubes were maintained on ice during the sorting time. Volumes were corrected with water to maintain a ration of 350 µL of RLT buffer for every 100 µL of sorted cells. RNA extraction was performed using the Qiagen RNeasy Micro Kit following the manufacturer's recommendations. RNA was stored at -80°C until processing.

Low-input RNA-seq

RNA sequencing libraries were prepared following the SMARTseq2 protocol (Picelli et al., 2013) with some modifications. Briefly, RNA was quantified using the Qubit RNA HS Assay Kit (ThermoFisher Scientific) and the input material used for the initial cDNA synthesis varied in function of the available sample concentration (0.12 ng-10 ng). Reverse transcription was performed using SuperScrpit II (Invitrogen) in the presence of oligo-dT30VN (1 µM; 5'-AAGCAGTGGTATCAACGCAGAGTACT30VN-3'), template-switching oligonucleotides (1 µM) and betaine (1 M). The cDNA was amplified using the KAPA Hifi Hotstart ReadyMix (Kappa Biosystems), 100 nM ISPCR primer (5'-AAGCAGTGGTATCAACGCAGAGT-3') and 15 cycles of amplification. Following purification with Agencourt Ampure XP beads (1:1 ratio; Beckmann Coulter), product size distribution and quantity were assessed on a Bioanalyzer High Sensitvity DNA Kit (Agilent). The amplified cDNA (200 ng) was fragmented for 10 min at 55°C using Nextera® XT (Illumina) and amplified for 10-12 cycles with indexed Nextera® PCR primers. The Nextera® library was purified twice with Agencourt Ampure XP beads (0.8:1 ratio) and quantified again on a Bioanalyzer using a High Sensitvity DNA Kit.

The libraries were sequenced on HiSeq2500 (Illumina, Inc) in paired-end mode with a read length of 2x76bp using TruSeq SBS Kit v4 and Nextera XT Index Kit of 8bp+8bp. We generated a mean 45 million paired-end reads for each sample in a fraction of a sequencing v4 flow cell lane, following the manufacturer's protocol. Image analysis, base calling and quality scoring of the run were processed using the manufacturer's software Real Time Analysis (RTA 1.18.66.3) and followed by generation of FASTQ sequence files by CASAVA.

RNA-seq processing and data analysis

RNA-seq paired-end reads were mapped against the mouse reference genome (GRCm38) using STAR version 2.5.3a (Dobin et al., 2013) with ENCODE parameters for long RNA. Annotated genes (gencode version M16) were quantified using RSEM version 1.3.0 with default parameters (Li and Dewey, 2014). Differential expression analysis was performed with DESeq2 version 1.18.1 (Love et al., 2014) for the microglia and macrophages experiments separately. Principal component analysis was done using the top 500 most variable genes with the 'prcomp' R function and 'ggplot2' R library. Heatmap with the top 50 differentially expressed genes for each comparison was performed with the 'pheatmap' R package with the 'rlog' transformed counts from DESeq2 and scaling by row. Functional enrichment analysis of the differentially expressed genes was done with Gprofiler (Reimand et al., 2007).

Cell culture

Bone marrow cells were obtained from femurs and tibias of mice after euthanasia. Cells were flushed out using a 21G needle-syringe with 5 ml of RPMI medium (ThermoFisher Scientific) with Penicillin/Streptomycin (P/S) (Sigma-Aldrich). Cells were passed through a 70 µm-cell strainer and quantified by Neubauer chamber. 4 millions of cells in 2 ml of RPMI + P/S were seeded in each well of a 24-well plate. After 2 hours, the medium was aspirated, and non-adherent cells were removed. Adherent cells were washed twice gently with RPMI + P/S. Cells were then cultured with RPMI + P/S and 10% of FBS (Sigma) in a humidified atmosphere with 5% CO_2 and 37°C. Cells were stimulated with LPS (Sigma) at 1 µg/ml at different time points. Finally, supernatant was removed and stored until cytokines measurement.

ELISA

ELISA DuoSet kits for TNFα, IL-6, and KC (R&D Systems) were used following the manufacturer's protocol. 96-well plates (ThermoFisher Scientific) were coated with respective capture antibodies the day before. Samples were incubated for 2 hours at room temperature. Detection antibodies and streptavidin-HRP were added. TMB ELISA (eBioscience) was used as substrate solution. Results were measured in a microplate reader (Bio-Tek).

Gene expression (cytokine array)

At 6 hours after LPS stimulation, RNA from bone marrow macrophages in culture was extracted as has been previously described. Reverse transcription was performed using the RT2 first strand kit (Qiagen) following the recommended protocol. Samples from the hIL-37Tg group were polled and added to the RT2 profiler cytokine array (Qiagen). Same procedure was applied to the samples from the hIL-37D20ATg group. At least 1500 ng of cDNA were added to each plate. Recommended thermal cycling parameters were used: polymerase activation for 10 min at 95°C; and 40 cycles of denaturalization for 15 sec at 95°C plus annealing/extension for 1 min at 60°C (capture). Array results were analyzed using the

software tools provided by the manufacturer. Only gene with at least 2-fold up- or down-regulated were selected.

Cell metabolism

24 hours after treatment, mice were deeply anesthetized with sodium pentobarbital and perfused with 60 ml of saline solution to remove blood. A piece of 0.6 cm of the spinal cord, centered into the injury site, were taken from each mice and maintained in DMEM (ThermoFisher Scientific) at 4°C. Cell suspension was obtained by enzymatic disaggregation with a mixture of collagenase (Sigma-Aldrich) and DNase (Roche) and mechanic disaggregation through 70-µm cell strainers (Fisherbrand). Cells were then magnetically labeled with CD11b microbeads (MACS Miltenyi) and loaded onto LS MACS columns (Miltenyi Biotec) following the manufacturer's protocol. Negative cells were depleted, and positive-myeloid cells were flushed and collected. Cells were quantified in the Neubauer Chamber. 200,000 cells per mice were plated in a XFp cell culture miniplate (Agilent) following protocol for cell suspension. Seahorse XF Base Medium (Agilent) supplemented with 1 mM pyruvate (Sigma-Aldrich), 2 mM glutamine (Sigma-Aldrich), and 25 mM glucose (Sigma-Aldrich) was used. A Mixture of oligomycin (1 µM) and FCCP (1,5 µM) were loaded into the proper cartridge (Agilent). Measurements of extracellular acidification rate (ECR) and oxygen consumption rate (OCR) from live cells were performed using the Seahorse XFp Cell Energy Phenotype protocol in a XFp Analyzer (Agilent). 3 measures were taken under basal conditions and 5 measures after exposition to oligomycin and FCCP.

Statistics

BMS, OCR, and ECAR scores were analyzed using two-way ANOVA with repeated measures (RM) with Bonferroni's post hoc correction. Gene expression and Luminex were analyzed using one-way ANOVA with Dunnett's post hoc correction. Flow cytometry and ELISA were analyzed using two-way ANOVA with Tukey's post hoc correction. Myelin sparing was analyzed using multiple t-test comparisons with Holm-Sidak's post hoc correction. Results were expressed as mean ± SEM and differences were considered significant at $p < 0.05$.

PRODUCTS' REFERENCES

REAGENT	SOURCE	IDENTIFIER
Antibodies		
Anti-CD45 PerCP	BioLegend	103130
Anti-CD11b PE-Cy7	BioLegend	101216
Anti-F4/80 PE	eBioscience	12-4801-80
Anti-F4/80 APC	eBioscience	17-4801-82
Anti-F4/80 FITC	Miltenyi	130-102-988
Anti-CD16/32 PE	BioLegend	101308
Anti-CD206 FITC	BioLegend	141704
Anti-Arg1 (goat, unconjugated)	SantaCruz	SC-18354
Anti-iNOS (rabbit, unconjugated)	Abcam	ab15323
AlexaFluor 488 anti-goat	ThermoFisher Scientific	A1105
AlexaFluor 647 anti-rabbit	Abcam	ab150075
Anti-IL-4Rα APC	Miltenyi	130-103-348
Anti-IL-13Rα1 PE	eBioscience	12-2130-80
CD11b microbeads	Miltenyi	130-049-601
Myelin removal microbeads	Miltenyi	130-096-731
Organisms		
Mouse: C57BL/6J	The Jackson Laboratory	000664
Mouse: hIL-37Tg	Dinarello's Laboratory	N/A
Mouse: IL-1R8KO	Garlanda's Laboratory	N/A
Mouse: hIL-37TgxIL-1R8KO	N/A	N/A
Treatments		
Anti-IL1a antibody (MABp1)	Xbiotech	N/A
OLT1177	Olatec Therapeutics LLC	N/A
Recombinant interleukin-37	Dinarello's Laboratory	N/A
Recombinant interleukin-4	BioLegend	574302
Recombinant interleukin-13	BD Biosciences	554599
Media and buffers		
DPBS	ThermoFisher Scientific	14190094
HBSS without Ca^{+2} and Mg^{+2}	ThermoFisher Scientific	14170088
DMEM	ThermoFisher Scientific	41966052
Permeabilization Buffer	Life Technologies66	PB001
RPMI 1640	Corning	10-040-CV
Chemicals		
Ketamine (Imalgene 1000)	Centauro (Boehringer-Ingelheim)	1006141
Xylazine hidroclorure (Rompu)	Centauro (Bayer)	1000558

Sodium Pentobarbital (Dolethal)	Centauro (Vetoquinol)	1002198
Collagenase	Sigma-Aldrich	C-2674
DNase	Roche	11284932001
Fetal Bovine Serum (FBS)	Sigma-Aldrich	F7524
Glucose	Sigma-Aldrich	G-7021
L-Glutamine	Sigma-Aldrich	G-7513
Sodium Pyruvate	Sigma-Aldrich	S8636
Tissue-Tek	Sakura	4583
Paraformaldehyde	Sigma-Aldrich	158127
Solvent Blue 38	Sigma-Aldrich	S3382-25G
Lithium Carbonate	Sigma-Aldricjh	255823
Xylene	Panreac	141769
DPX Mountant	Sigma-Aldrich	44581
Lipopolysaccharide (LPS)	Sigma-Aldrich	L2880
Universal Master Mix II	ThermoFisher Scientific	4440042
Taqman: *Il1r8*	ThermoFisher Scientific	Mm01275624_g1
Taqman: *Il18ra*	ThermoFisher Scientific	Mm00515178_m1
Taqman: *Gapdh*	ThermoFisher Scientific	Mm99999915_g1
Qiazol Lysis Reagent	Qiagen	79306
Penicillin/Streptomycin	Sigma-Aldrich	P-0781

Instruments and kits		
LS columns	Miltenyi Biotec	130-042-401
Seahorse XFp Cell Culture Miniplate	Agilent	103025-100
Seahorse XFp FluxPak	Agilent	103022-100
Seahorse XF Calibrant Solution	Agilent	103059-000
Seahorse XF base medium, without phenol red	Agilent	103335-100
Seahorse XFp Cell Energy Phenotype Test Kit	Agilent	103275-100
RNeasy Mini kit	Qiagen	74104
RNeasy Micro kit	Qiagen	74004
Omniscript RT kit	Qiagen	20511
SYBR Green qPCR Master Mix	Qiagen	600882
Taq DNA polymerase	Invitrogen	10342-020
RT2 First Strand Kit	Qiagen	330401
RT2 profiler cytokine array	Qiagen	PAMM-150Z
Genomic DNA Mouse Tail Kit	DANAGEN	0603
Mouse TNF-alpha DuoSet ELISA	R&D System	DY410
Mouse IL-6 DuoSet ELISA	R&D System	DY406
Mouse IFN-gamma DuoSet ELISA	R&D System	DY485
Mouse KC DuoSet ELISA	R&D System	DY453
TMB ELISA Substrate Solution	eBioscience	00420156
ProcartaPlex Immunoassays	Invitrogen	N/A

Equipment		
Infinite Horizon Impactor	Precision Systems and Instrumentation, LLC	IH-0400
Mouse Impactor Tip	Precision Systems and Instrumentation, LLC	1067–150
Hamilton Syringe	Sigma-Aldrich	24530
Infusion pump KDS310	KDS Scientific	789311
Glass Micropipette Tip	Fisher Scientific	50-821-968
TissueRuptor II	Qiagen	9002755
Untrasonic Homogenizer (Sonicator)	Biologics Inc.	Model 3000
FACS Canto	BDBioscience	N/A
FACS Jazz	BDBioscience	N/A
Seahorse XFp Analyzer	Agilent	N/A
ELx800 microplate reader	Bio-Tek	N/A
Real-time PCR Detection System	BIO-RAD	N/A
Luminex MAGPIX	ThermoFisher Scientific	N/A
Open field for BMS evaluation	N/A	N/A

Software		
FACS Diva	BDBioscience	N/A
FlowJo	FlowJo, LLC	N/A
Prism7	Graphpad	N/A
Seahorse Wave	Agilent	N/A
Fiji 2.0	ImageJ	N/A

RESULTS

Chapter 1

Neuroinflammation quantification for spinal cord injury

Jesus Amo-Aparicio[1], Anna Martinzez-Muriana[1], Alba Sanchez-Fernandez[1], and Ruben Lopez-Vales[1]

[1]Departament de Biologia Cel·lular, Fisiologia i Immunologia, Institut de Neurociències, Centro de Investigación Biomédica en Red sobre Enfermedades Neurodegenerativas (CIBERNED), Universitat Autònoma de Barcelona, Bellaterra, Catalonia 08193, Spain

Abstract

Spinal cord injury (SCI) leads to irreversible devastating neurological disabilities. Accumulated evidence in the literature indicates that the inflammatory response that occurs in the spinal cord following injury contributes importantly to spread tissue damage to healthy regions adjacent to the lesion site, and consequently, to increase neurological deficits. Therefore, targeting inflammation could lead to the development of new therapies to prevent tissue damage and neurological impairments after SCI.

Inflammation is regulated, in part, by the expression of pro-inflammatory and anti-inflammatory cytokines synthesized, mainly, by glial cells. Hence, methodologies that could ease the quantification of multiple cytokines and immune cells from spinal cord tissue samples are needed to assess the potential of new anti-inflammatory therapies. In the present chapter, we describe how to induce contusion injuries in the mouse spinal cord, as well as, two useful methodologies to assess neuroinflammation in lesioned spinal cord tissue samples.

Keywords: cytokines, immune cells, neuroinflammation, spinal cord injury

Introduction

In the present chapter, we show how to induce reproducible spinal cord contusion injuries at thoracic level in mice using a validated and computerized device (Basic Protocol 1). Moreover, we describe how inflammation in the injured spinal cord can be studied by assessing immune cells populations by flow cytometry (Basic Protocol 2), as well as, cytokine levels by Luminex Bead-based Multiplex Assay (Basic Protocol 3). The protocols described below can also be used to assess inflammation in other nervous system tissue samples from different neurological conditions, such as experimental autoimmune encephalomyelitis, amyotrophic lateral sclerosis or peripheral nerve injury.

Basic protocol 1: Spinal cord contusion injury

Introduction

Spinal cord injury (SCI) models are indispensable for the understanding the pathophysiology of SCI and to assess the efficacy of novel therapeutic approaches. Since most SCI in humans occur due to a blunt trauma, experimental models of traumatic SCI are the most commonly used in research to assess the efficacy of neuroprotective approaches (Ahuja et al., 2017). Models can be classified as contusion, compression, distraction, dislocation or transection (Cheriyan et al., 2014). Among them, contusion models are the most extensively studied since they are the most common on traffic accidents (Ghasemlou et al., 2005; Scheff et al., 2003).

The Infinite Horizon impactor (IH0400) developed by Precision Systems and Instrumentation is one of the most widely used devices for inducing contusion injury to the spinal cord (Ghasemlou et al., 2005; Scheff et al., 2003). This device is based on a computer-controlled piston mounted on a stereotaxic apparatus capable of inflicting a consistent contusion injury at the exposed spinal cord by applying a controlled force (Fig. 1A). The extent of damage can be gradually controlled by changing the diameter of the piston tip, the force applied and the dwell time. Here, we describe a protocol for performing spinal cord contusion at thoracic level in mice using this device.

All the experimental procedures here described were approved by the Universitat Autònoma de Barcelona Animal Experimentation Ethical Committee (CEEAH 1188R3-DMAH 6131) and followed the European Communities Council Directive 2010/63/EU. Methods for each procedure were carried out in accordance with the approved guidelines.

Materials

- Ketamine (Imalgene 100 mg/mL))
- Xylazine (Rompun 20 mg/mL)
- Povidone-iodine solution
- Ophthalmic ointment (THEA, 822635.1)
- Buprenorphine (Buprex 0.3 mg)
- Computer
- Infinite Horizon Device (Precision System and Instrumentation)
- Mouse Impactor tip (Precision System and Instrumentation, 1067-150)
- Scalpels (Swann-Morton, 0205)
- Surgical foam (Sugi, 30601)
- Surgical microscope
- Serrated grip forceps (Fine Science Tools, 11006-12)
- Fine tweezers (Fine Science Tools, 11223-20)

- Surgical Suture 6-0 (Laboratorios Aragó)
- Staples (Michel, 46-8570-08)
- Insulin syringes (Novico, 14107S)

Preparation

1. Attach the mouse tip to the force sensor and turn on the impactor device. Tip diameter will depend on the animal size and the injury extension desired.
2. Test the device function by impacting a piece of rubber material supplied with the IH device. Repeat the contusion at least three times for every force used to ensure that displacement and force values recorded are replicable.
3. Anesthetize the mouse by intramuscular injection with a mixture of ketamine (90 mg/kg) and xylazine (10 mg/kg). Confirm that the animal is under an acceptable plane of anesthesia by performing a toe pinch with forceps to the animal. If there is pedal reflex, wait for a deeper plain of anesthesia until the animal is unresponsive to this procedure.
4. Shave hairs of the back of the mice and disinfect the surgical area with a povidone-iodine solution.
5. Put the animal in a prone position on a conductive-material surface and attach the paws to the surface.
6. Apply ophthalmic ointment to the eyes to prevent eye drying.
7. Place the conductive-material surface with the animal on a heating pad to maintain the temperature during the process. Use a surgical microscope during the surgery.

Surgery

8. Perform a midline sagittal incision approximately 2 to 3 cm centered over the thoracic T11 vertebrae using a scalpel. Expose skin and adipose tissue.
9. Perform another sagittal incision in the internal skin to expose muscles and vertebral column.
10. Control bleeding during all these processes. Use surgical foam to clear the excess of blood.
11. Perform an axial incision across the muscular and connective tissue that involves the dorsal site of the vertebral column. Separate the external layer of this tissue from the vertebral column. Do not cut this layer completely and hide it under the adipose tissue of the upper spinal cord to avoid dryness. Expose vertebras for their correct identification.

12. Identify the T11 vertebra (Fig. 1D) and perform a laminectomy using fine tweezers. The laminectomy should be bigger than the impactor tip (Fig. 1B). Use serrated grip forceps to hold the vertebral column.
13. Remove the mouse from the conductive-material surface and put it on the middle of the base plate supplied with the IH impactor device.
14. Clamp T10 vertebra by using the Adson forceps attached to flexible armatures on the base plate (Fig. 1A).
15. Use the same protocol to clamp the T12 vertebra. Clamping the T10 and T12 vertebrae is a critical step to stabilize the spinal cord during the impact injury (Fig. 1C).
16. Test that both Adson forceps are securely clamped and hold the vertebral column. The spine should be straight and not curved. The vertebral column should be suspended without raising the abdomen more than 1 cm.
17. Move the base plate to the impactor device with gentle movements.
18. Centre the laminectomy site under the impactor tip using the X and Y axis wheels.
19. Lower the impactor tip with the Z axis wheel until touching the spinal cord.
20. Check the position of the tip from different angles. Avoid touch bones with the tip.
21. Raise the impactor tip 1.75 rotations (counter clockwise) with the Z axis wheel.
22. Define the applied force into the software. For a mild injury use 30 kdynes, for a moderate injury, 50 kdynes, and for a severe injury, 60-70 kdynes. Dwell time is recommended to be set at 0s. The remaining parameters (displacement and velocity) cannot be changed.
23. Press “Start Experiment” button. This will slightly move the impactor tip as a calibration check by the device.
24. In the new pop up window available press “Impact Now”. The impactor tip will perform a contusion on the exposed spinal cord.
25. Save the contusion recording generated in the appropriated folder.

Post injury

26. Remove the base plate from the IH impactor device and separate the animal from the armatures by loosening the stretching screws of the Adson forceps.
27. Clear the excess of blood.
28. Put the muscular tissue hidden under the exposed adipose tissue (point 11) on their natural position to protect the contusion zone.
29. Put together the muscles and the skin and suture them. Make at least one suture at both site of the lesion area using 6-0 braided silk suture. Avoid stretch the vertebral column.

30. Close the surface incision with surgical staples.
31. Disinfect the surgical area with a povidone-iodine solution.
32. Turn off the impactor device and clean it.

Post-operative care

33. After recovery from the anesthesia, inject buprenorphine at 0.1 mg/kg subcutaneously analgesic for relieving pain following this surgical procedure. Repeat the injection for the following two days every 12 hours. The use of analgesia is necessary to reduce the sensation of pain due to the surgery.
34. Express bladder by restraining the mouse in one hand and expressing the bladder with the fingertips of the other hand until emptiness. Repeat this procedure twice a day until total recovery of bladder function.
35. Remove staples after 10 days.

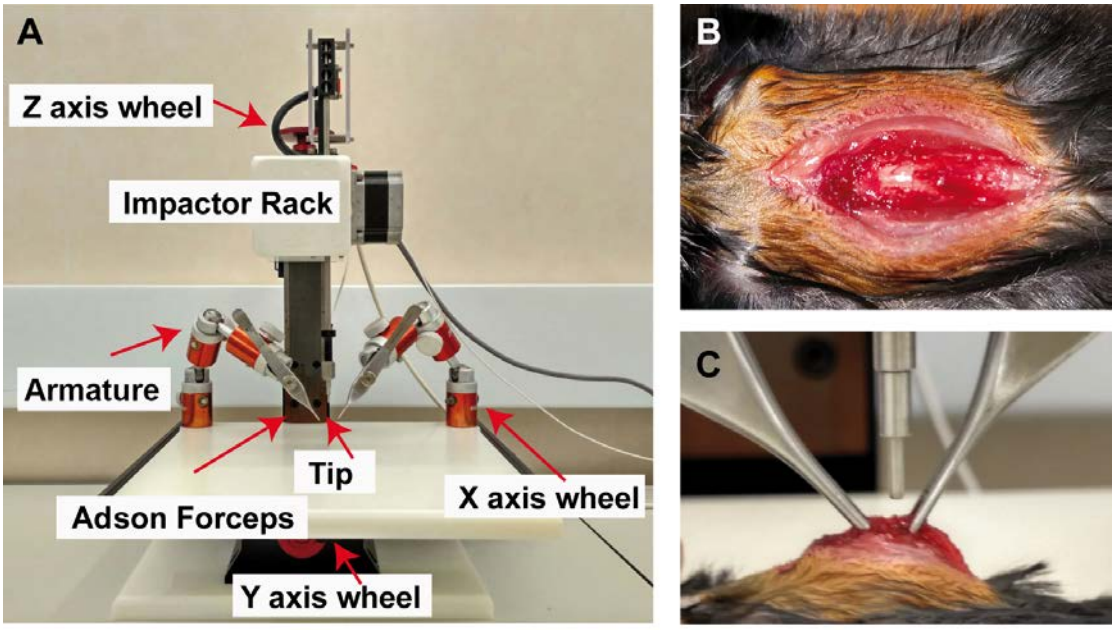

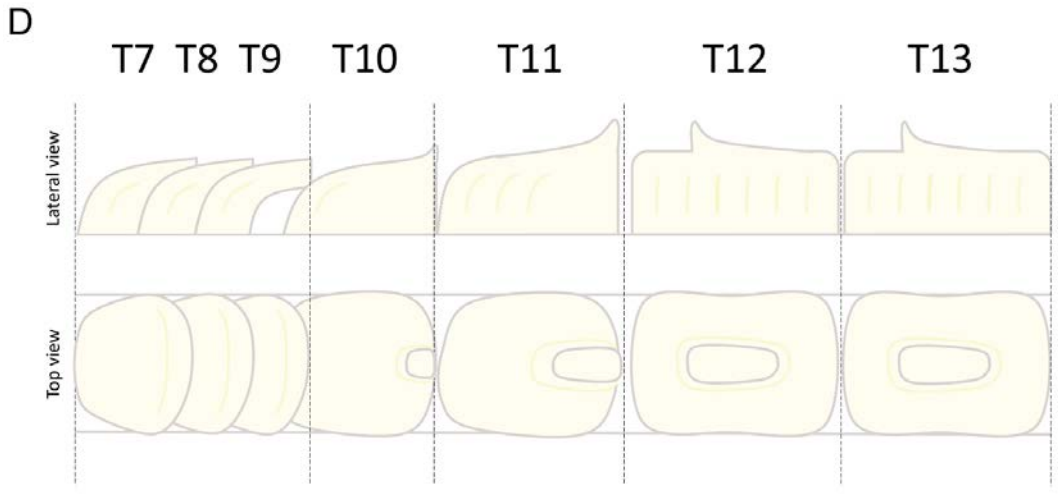

Figure 1: Figure 1 Spinal cord contusion injury in mice. (A) Image of the Infinite Horizon Device. (B) Image showing the exposed spinal cord after laminectomy. (C) Image showing how the vertebral column is clamped with the Adson forceps before impacting on the spinal cord. (D) Drawing of the lower thoracic vertebral column in the mouse. Note that the morphology of the spinous process from vertebra T11 is different than those observed in vertebrae T10 and T12.

Basic protocol 2: Fluorescent activated cell sorting (FACS) protocol

Introduction

The use of flow cytometry in the clinical laboratory has grown substantially in the past decade. This is attributable in part to the development of smaller, user-friendly, less-expensive instruments and a continuous increase in the number of clinical applications. Flow cytometry measures multiple characteristics of individual particles flowing in single file in a stream of fluid. Light scattering at different angles can distinguish differences in size and internal complexity. Moreover, light emitted from fluorescently labelled antibodies can identify a wide array of cell surface and cytoplasmic antigens. The advantage over other techniques, such as the immunohistochemistry, is that flow cytometry allows to simultaneously analyze several cellular markers at the time. This makes flow cytometry a powerful tool for detailed identification and quantification of immune populations, that are highly complex (Brown and Wittwer, 2000). Here we will combine CD45, CD11b, F4/80, Ly6G and CD3 to identify and quantify microglia, macrophages, neutrophils, and T cells (Roederer, 2004).

Materials

- Sodium Pentobarbital (Dolethal) (Vetoquinol, 07400060)
- Sodium chloride (NaCl) (Sigma, 71376)
- 60 mL Syringe (BD Biosciences, BD 309653)
- 23G needle (BD Biosciences, BD 300800)
- 70% Alcohol
- Centrifuge
- 1.5 mL Eppendorf tubes (Fisherbrand)
- 70 µm diameter Cell Strainer (ClearLine, 141379C)
- 60 mm Petri dishes (ThermoFisher, 122TS1)
- Collagenase (Sigma, C-2674)
- DNase (Roche, 11284932001)
- Paraformaldehyde (Sigma, 158127)
- Hank's Balanced Salt Solution (HBSS) w/o Ca^{2+} neither Mg^{2+} (Gibco,14170-088)
- Fetal Bovine Serum (FBS) (Sigma, F7524)

- Dulbecco's Modified Eagle Medium (DMEM) (Invitrogen,31330-035)
- Antibodies: CD45 PerCP.Cy5 (Biolegend, 103130); CD11b PE-Cy7 (Biolegend, 101216); F4/80 APC (eBioscience, 17-4801-82); Ly6G PE (BD Bioscience 551461); CD3 FITC (eBioscience 11-0031-82)
- Flow cytometer

Tissue harvesting

1. Deeply anaesthetize the animal with an intraperitoneal overdose of sodium pentobarbital (Dolethal).
2. Transcardially perfuse the mouse with 60 mL of saline (NaCl 0.9%) to remove circulating red blood cells and leukocytes from the tissue. To do this, place the animal on its back and, using tweezers and dissecting scissors, open the skin and expose the chest cavity. Then, cut the diaphragm (without piercing the heart), grab at the base of the sternum and cut through the ribcage to expose the heart. Finally, insert an 18-gauge needle (from the 50 mL syringe with NaCl 0.9%) into the apex of the ventricle and, immediately after, cut twice the liver. Perfuse the animal slowly.
3. Place the animal in prone position on a plate and soak the animal back with 70 % alcohol to prevent hair dispersion.
4. Remove 1 cm of the spinal cord tissue containing the lesion site and placed it in a 1.5 mL Eppendorf with cold 1mL HBSS without Ca^{2+}/Mg^{2+}. From this point, keep always the samples on ice.

Breaking-up the sample

5. Incubate the samples for 30 minutes at 37ºC in a 1.5mL Eppendorf tube containing 1 mL of 10 % collagenase and 10% DNase in HBSS without Ca^{2+}/Mg^{2+}. Vortex the sample vigorously after 15 minutes of incubation.
6. Mix the samples with DMEM-10% FBS and pass them through a 70 µm cell strainer on a 60 mm Petri dish. Use the embolus of a syringe to facilitate this step.
7. From the Petri dish, collect the spinal cord cell suspension into a 15 mL Falcon. Fill up the tube with DMEM+10% FBS to a final volume of 10 mL.
8. Centrifuge the sample at 500 *x g* for 10 minutes at 4°C.
9. Discard the supernatant and reconstitute the pellet in 1 mL of DMEM+10% FBS.

Extracellular labelling

10. Vortex the cells vigorously for 15s and split the cell suspension into different 1.5 mL Eppendorf tube according to the number of antibodies combinations (for example, if 4 different antibody combinations is planned, the cell suspension will be split in 4 tubes).

11. Fill up the 1.5 Eppendorf tubes containing the cell suspension with DMEM-10% FBS to a final volume of 1 mL and centrifuge the sample at 600 *x g* for 6 minutes at 4°C.

12. Use the time of centrifuge to prepare the master mix of antibodies in DMEM-10% FBS. The working concentration of each antibody should be previously established in the laboratory. In this case, we will use the following antibody combination: anti mouse CD45, CD11b, F4/80, Ly6G, and CD3. Another combination with IgG isotype controls must be done (See "Understanding results". Figure 2). Cell permeabilization is not required for extracellular labelling. It is important to ensure that appropriate combination of fluorochromes is chosen based on the lasers and detectors of the flow cytometer.

13. Discard the supernatant and reconstitute the pellet with 200 µL of master mix of extracellular antibodies.

14. Incubate the cell suspension with the antibodies for 1 hour at 4°C in the dark with continuous shaking.

15. Fill up with DMEM+10% FBS to a final volume of 1 mL and centrifuge the sample at 600 *x g* for 6 minutes at 4°C.

16. Discard the supernatant and reconstitute the pellet with 300 µl of 1% paraformaldehyde in phosphate buffer. Keep the samples at 4°C in the dark with continuous shaking until reading.

17. Read the samples on a cytometer and analyze the data using an appropriate software (i.e. FlowJo®, LLC). Flow cytometric gates will be set up using control IgG isotype to set baseline.

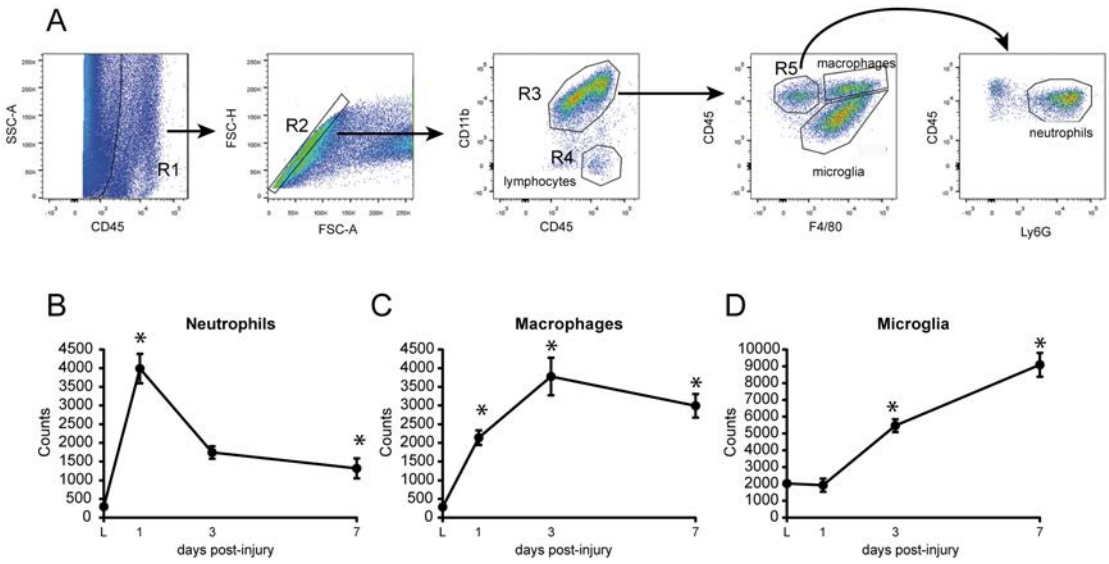

Figure 2: Dynamic changes in myeloid cells in the injured spinal cord. (A) Representative FACS plots showing how the different myeloid cells were gated. (B-D) Quantification of neutrophils, macrophages and microglia in the contused spinal cord of mice. Mean ± SEM. (n =4 per time point). *p < 0.05 against naïve. One-way ANOVA with Dunnett's post hoc correction.

Basic protocol 3: Measurement of mouse cytokines protein levels by Luminex

Introduction

LUMINEX® assay is a bead-based multiplex technique that allows to simultaneously detect and quantify up to 32 cytokines of a single sample in a single 96-well microplate. The assay consists of incubating a protein lysate, extracted from tissue or cell cultures, in wells of a microtiter plate, along with purchased color beads pre-coated with cytokine specific capture antibodies, biotinylated detection antibodies, and phycoerythrin (PE)-conjugated streptavidin (SA). Once the selected analytes have bound to their specific beads, the beads are further read in a specific analyzer (e.g. Luminex™, MAGPIX®, Bio-Rad® or Bio-Plex®) that uses a dual-laser flow cytometry-based technology. While one laser sorts out the analyte-bead, the second one quantifies the amount of analyte that has bound to the selected bead. Finally, xPONENT® software gives you a robust analysis of your assay with highly specific regression analysis. Here we will use commercially available antibodies precoated beads from Millipore to measure various cytokines protein levels.

Materials

- Sodium Pentobarbital (Dolethal) (Vetoquinol, 07400060)
- 60 mL Syringe (BD Biosciences, BD 309653)
- 23G needle (BD Biosciences, BD 300800)
- HEPES: 4-(2-Hydroxyethyl)piperazine-1-ethanesulfonic acid, N-(2-Hydroxyethyl piperazine-N'-(2-ethanesulfonic acid) (Sigma, H3375)
- IGEPAL® CA-630: Octylphenoxy poly(ethyleneoxy)ethanol (Sigma, I8896)
- $MgCl_2$ (Sigma, 208337)
- NaCl (Sigma, 71376)
- EDTA: Ethylenediaminetetraacetic acid. (Sigma, 03609)
- EGTA: Ethylene glycol-bis(2-aminoethylether)-N,N,N',N'-tetraacetic acid. (Sigma, E3889)
- PMSF: Phenylmethanesulfonyl fluoride. (Sigma, P7626)
- PhosStop phoshatase inhibitor cocktail tablet (Roche, 4906837001)
- Protease Inhibitor Cocktail (Sigma, P8340)
- Microcon-10kDa Centrifugal Filter Unit with Ultracel-10 membrane (Millipore, MRCPRT010)
- Protein extraction buffer (lately explained)
- Tissue homogenizer (Qiagen, 900127)
- Ultrasonic Homogenizer (Biologics Inc. Model 3000)
- Centrifuge
- BCA protein assay kit (Pierce, 23225)
- 23G needle (BD Biosciences, BD 300800)
- Hand-Held Magnetic Plate Washer (ThermoFishser Scientific, EPX-555555-000)
- Rpm-controlled shaker

- MAGPIX (Luminex analyzer)
- Cytokine mouse multiplex kit for Luminex Platform (ThermoFishser Scientific) containing:
    - 1x wash buffer
    - Magnetic beads
    - Beads diluent
    - PE-streptavidin

Reagents and solutions

For a total amount of 20 mL extraction buffer, add the following solutions in a 50 mL tube:

- 5000 µl of HEPES 25mM
- 40 µl of IGEPAL 10%
- 1000 µl of MgCl2 0.1 M
- 260 µl of EDTA 1.3mM pH=8
- 200 µl of EGTA 0.1M pH=8
- 200 µl of PMSF 0.1M
- 200 µl of Protease Inhibitor Cocktail (Roche, 11697498001)
- 1 PhosStop phosphatase inhibitor cocktail pills (Roche, 04906845001)
- Fill up the reagent mixture with distilled H_2O up to 20 mL
- Keep on ice while using.
- Store up to 24h at 4 ºC.

Protein extraction

1. Deeply anaesthetize the animal with an intraperitoneal overdose of sodium pentobarbital (Dolethal).

2. Transcardially perfuse the mouse with 60 mL of saline (NaCl 0.9%) in order to remove circulating red blood cells and leukocytes from the tissue.

3. Remove 1 cm of spinal cord tissue sample containing the lesion site and place it to a 2 mL Eppendorf tube or similar polypropylene round-bottom microcentrifuge tube. From this moment to the end of the protocol, keep the samples on ice.

4. Add 300 µl of protein extraction buffer to each sample.

5. Place the tip of an electric tissue homogenizer into the polypropylene microcentrifuge tube and operate at full speed until the lysate is homogenous (around 30 seconds per sample).

6. Place your sample into an ultrasonic homogenizer for around 15 seconds at 40 kHz.

7. Centrifuge the sample at 12000 x *g* for 5 minutes at 4ºC.

8. Transfer the supernatant to a new 1.5 mL Eppendorf tube. Discard the pellet.

9. Remove a small amount of sample and proceed to protein quantification according to manufacturers' kit.

10. Protein concentration must be 4 µg/µl in a suitable volume of 30 µl of overall lysate. If your protein concentration is higher, dilute your sample into a new tube up to 4 µg/µl with a final volume of 30 µl using the protein extraction buffer. If your protein concentration does not reach the desirable threshold, then use micron centrifugal filters to concentrate until the needed concentration is reached.

11. Store your samples up to 1 month at -80°C for later use or keep on ice for the LUMINEX assay.

Luminex Assay

12. Prior to start the assay, design your template and determine the number of dedicated wells.

13. Prepare 200 to 300 mL of 1x wash buffer (supplied with the multiplex kit) in deionized water.

14. Reconstitute the antigen standards and prepare serial dilutions in protein extraction buffer (supplied with the multiplex kit) in 0.2 ml polypropylene tubes according to manufacturers' kit. Keep on ice.

15. Prepare 1x magnetic beads in beads diluent (supplied with the multiplex kit) and mix them according to manufacturers' kit. Once prepared, sonicate each vial for 30 seconds and vortex for 1 minute before use. Keep at room temperature.

    Option 1: if the beads are already premixed, adjust the necessary volume using beads diluent.

    Option 2: if the beads are not already premixed, mix and match each vial and add a remaining volume of beads diluent.

16. Add 150 to 200 µl of 1x wash buffer into each well using a multichannel pipette. Shake the plate for 10 minutes RT at 500 rpm. Pour the washing buffer over a sink and ensure that not remaining liquid is in the well by tapping the plate onto paper towels.

17. Add an appropriate volume of mixture of antibody magnetic beads to the dedicated wells into the 96-well plate (supplied with the multiple kit).

18. Securely rest the 96-well plate containing your magnetic beads into a hand-held magnetic place washer. Wait for at least 1 minute to let the beads attach to the bottom of the plate.

19. Remove the liquid inside the wells by inverting the hand-held magnetic place washer over a sink. Ensure that not remaining liquid is placed inside the wells.

20. Wash the wells by adding 150 to 200 µl of 1x wash buffer into each well using a multichannel pipette. Wait at least 30 seconds to completely wash the beads and repeat step 19.

21. Once having pulled out the liquid, remove the 96-well plate from the hand-held magnetic place.

22. Add 25 µl of assay buffer to each used well.

23. Add 25 µl of prepared standards, positive and negative controls or samples at desired concentration into dedicated wells.

24. Seal the 96-well plate using plate seals and cover the plate using a black microplate lid or using aluminium foil.

25. Place your 96-well-covered plate into a shaker with a specific speed of 500 rpm overnight at 4°C.

26. Place your 96-well-covered plate at room temperature for 30 minutes and shaking at 500 rpm.

27. Prepare 1x detection antibody according to manufacturers' kit.

28. Wash the wells three times, each time with 1x wash buffer as explained in steps 18 to 21.

29. Add an appropriate volume of 1x detection antibody cocktails to each well using a multichannel pipette according to manufacturers' kit. Repeat step 24.

30. Place your 96-well-covered plate at room temperature for 30 minutes and shaking at 500 rpm.

31. Wash wells three times with 1x wash buffer as explained in steps 18 to 21.

32. Once having pulled out the liquid, remove the 96-well plate from the hand-held magnetic place.

33. Add an appropriate volume of PE-streptavidin (supplied with the multiplex kit) to each well using a multichannel pipette according to manufacturers' kit. Repeat step 24.

34. Place your 96-well-covered plate at RT for 30 minutes and shaking at 500 rpm.

35. Wash wells three times with 1x wash buffer as explained in steps 18 to 21.

36. Add an appropriate volume of detection antibody diluent to each well using a multichannel pipette according to manufacturers' kit. Repeat step 24.

37. Place your 96-well-covered plate at room temperature for 5 minutes and shaking at 500 rpm.

38. Remove your seal plate and read the plate on a LUMINEX analyzer.

39. Set up the LUMINEX analyzer by indicating the type of magnetic bead used in the assay and the number of samples being run in the plate using the certificate of analysis.

40. Run your plate into the LUMINEX instrument. By using the specific Luminex software, calculate the Median Fluorescent Intensity (MFI) and extrapolate the amount of protein of each analyte based on its standard curve and dilutions.

41. Analyze the exported data using an appropriate statistics program.

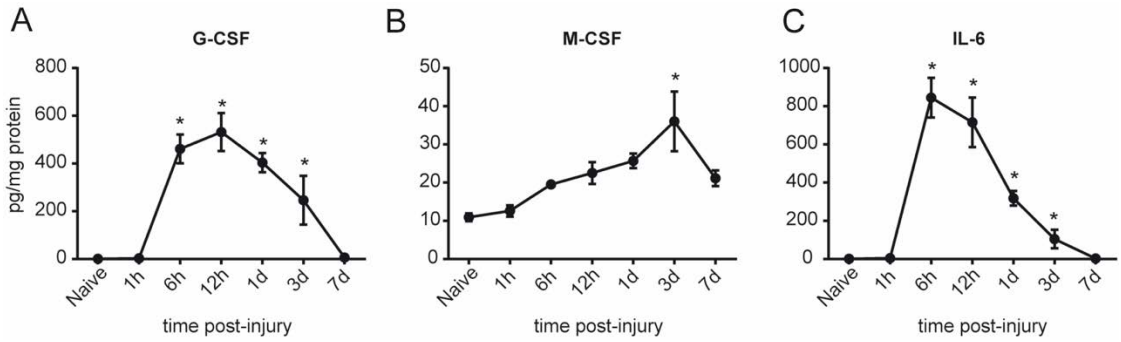

Figure 3: Characterization of G-CSF (A), M-CSF (B), and IL-6 (C) protein level in the spinal cord after injury. Mean ± SEM. * p < 0,05 against naïve. One-way ANOVA with Dunnett's post hoc correction.

Commentary

Background Information

SCI is one of the most prevalent and disabling conditions in the world. The most common cause of SCI is traffic accidents (47%) followed by falls (31%), which are typically the second most common etiology in elderly population, sport accidents (10%), and violence injury (4.6%) (Chen et al., 2013). Although there are many differences between the nervous system of human and animals, several different injury models (specially models developed in rodents) have been developed to study SCI. This has allowed to explore different physiological mechanisms and properties of specific molecular pathways after SCI, as well as to study the efficacy of potential therapies.

Nowadays, there is wide range of models that are used to induce SCI. They include contusion, compression, and transection-based models (Sharif-Alhoseini et al., 2017; Steward and Willenberg, 2017). The contusion model is the oldest and the most widely used. It produces lesions similar to those seen in human patients with SCI. Thoracic contusion models are more common than cervical models, which is rarely reported because of life-threatening adverse effects can occur. Thoracic contusion models facilitate the assessment of locomotor recovery and postural activities and are induced with an impactor device or a weight-drop from specific height (Sharif-Alhoseini et al., 2017; Steward and Willenberg, 2017).

In the last decade, some computer-controlled contusion devices, such as the Infinite Horizon, have been developed to create contusion injuries in a controlled way to limit the variation between animals and to allow the comparison of results obtained in different laboratories (Ghasemlou et al., 2005; Scheff et al., 2003). This device is controlled by a computer to produce a specific force with high precision to the spinal cord. Once the force is reached, the impactor

tip is immediately withdrawn from the exposed spinal cord. Software displays the actual force applied, the amount of displacement, velocity of the impounder peak force measurement, and plots graphs of changes in displacement and force as a function of time from sequence initiation. This device leads to reproducible functional deficits and tissue damage in mice and rats, and thus, allows researchers to minimize the number of animals used in the experiments.

Independently of the model, the inflammatory response that occurs after SCI is an important contributor to secondary tissue damage and functional impairments (David et al., 2012a, 2012b; Popovich, 2014). The detrimental effects of inflammation in the central nervous system (CNS) are more pronounced than in other tissues due to its limited capacity for axon regeneration and replacement of damaged neurons, and consequently, leads to irreversible functional deficits (Cao and Whittemore, 2012; Fawcett, 2015; He and Jin, 2016). The most abundant immune cells in the injured spinal cord are myeloid cells, which encompass neutrophils, microglia and macrophages (Francos-Quijorna et al., 2017; Kroner et al., 2014). It is difficult to distinguish fully activated microglia from macrophages of peripheral origin in the damaged CNS tissue because they display similar morphology and antigenic markers, such as CD11b, Iba1, F4/80 and CD68 (Kroner et al., 2014; Santos-Nogueira et al., 2015). Similarly, macrophages and neutrophils share different markers such as CD11b, Gr1, 7/4 and myeloperoxidase. This complicates the use of histological methodologies to properly distinguish the different myeloid cell populations in the CNS. It is therefore needed to simultaneously combine 3-4 cell markers to properly distinguish the different leukocytes subsets in the lesioned spinal cord, which can be only done by FACS analysis, as we show in this chapter.

Cytokines are key molecules that trigger the influx and activation of immune cells into the injured spinal cord (Coll-Miro et al., 2016). Cytokines are rapidly expressed by endogenous immune cells (Shamash et al., 2002; Vallières et al., 2006) during the first 24 hours after injury, although neutrophils and macrophages that enter the injured spinal cord also contribute to cytokine expression. Several methodologies have been used to assess cytokines in the spinal cord following injury at the RNA and protein levels, such as real time PCR, immunohistochemistry, western blot and ELISA. These methodologies, however, only allow to study one cytokine at the time, and thus, it is required to have large sample amounts to analyze several cytokines, as well as, to invest a lot of time. Multiplex assays are more sensitive, show broader analytical and dynamic range, are highly specific, rapid, require smaller sample volumes and allow the simultaneous measurement of up to 500 different proteins. There are currently different multiplex-cytokine panels for mice, rats and humans that are commercially available that allow the measurement of up to 32 cytokines in the same sample at the time.

In the present chapter, we have combined the use of FACS analysis and Luminex assays to characterize some of the main components of the inflammatory response after SCI. We show that the different myeloid cells can be easily identified and quantified in the contused spinal cord. Similarly, we also confirm that cytokines can be accurately and rapidly measured at the protein level in the injured spinal cord parenchyma using Multiplex Assays. The combination of these methodologies is therefore a useful tool to study neuroinflammation after SCI, as well as in other neurological conditions.

Critical Parameters and Troubleshooting

Spinal cord Injury

1. Animals should be of similar age and same sex. These two factors interfere with the physiopathological events that occurs after SCI.
2. Take care not to damage the spinal cord when doing the laminectomy. Remove carefully the vertebra using fine tweezers.
3. Make sure that the laminectomy is bigger than the impactor tip, otherwise the impactor will hit on the vertebra, leading to milder lesions.
4. When clamped, the vertebral column should be also straight and not curved, otherwise, the injury will be lateralized in the spinal cord

Fluorescent activated Cell Sorting

1. Use fluorophore-conjugated antibodies whenever possible.
2. Use IgG isotype control for each fluorophore.
3. Some proteins can change their epitopes after enzymatic digestion. In this case, it is recommended to perform only mechanical digestion of the sample.
4. Some antibodies can change their specificity after fixation. It is recommended to use specific kits for each problematic antibody.
5. The cytometer must be compensated for each fluorophore before running the experiment.
6. Samples should be read on a cytometer as soon as possible (the same day of labelling or the next morning at most).

Troubleshooting

Statistical Analyses

All results should be expressed as mean ± standard error of the mean (SEM). To determine significant differences in the dynamics of immune cells recruitment and cytokine levels in the spinal cord after injury, One-way ANOVA with Dunnett's post hoc test should be used. Differences are considered significant at $p<0.05$.

Understanding Results

Assessment of microglia and leukocyte infiltration after SCI

We induced severe SCI (60 kdynes) in adult female mice and characterized the changes in immune cells at day 1, 3 and 7 post-injury. The gating and cell identification strategy for our basic staining protocol is shown in Fig 2. Since leukocytes are the only cells expressing CD45, these cells were identified from the whole cell suspension based on expression of CD45 (R1; Fig. 2A). After gating this population, immune cell doublets were eliminated by cell linearity using FSC-H versus FCS-H to ensure that only single cells are counted (R2; Fig. 2A). Leukocytes

include two main immune cell subsets: lymphocytes and myeloid cells. Although both immune cell types express CD45, lymphocytes lack CD11b expression. Therefore, myeloid cells (R3; Fig. 2A) were distinguished from lymphocytes (R4; Fig. 2A) based on the presence of CD11b. Myeloid cells (R3; Fig. 2A) include different immune cells subsets, mainly microglia, macrophages and neutrophils. These immune cells express CD45, CD11b, and F4/80; however, microglial cells express low levels of CD45 and low/absent levels of F4/80 (Fig. 2A) whereas macrophages show high levels of CD45 and express F4/80 (Fig. 2A). Therefore, by gating myeloid cells using these two markers, microglia were clearly differentiated from macrophages (Fig. 2A). After doing this gating, another cell subset expressing high levels of CD45 and lack of F4/80 was also evident (R5; Fig. 2A). This immune cell subset is mainly composed by neutrophils. However, to ensure that only neutrophils were counted, we gated this cell population based on the expression of Ly6G, a specific marker found on neutrophils (Fig. 2A).

Our results show that neutrophils are the earliest inflammatory cells to invade the injured spinal cord. They peak at 24 hours post-injury and decline progressively up to day 7 (Fig. 2B). The infiltration of monocytes peaks in the contused spinal cord at day 3 and decreases in numbers at day 7 (Fig. 2C). Microglial cell counts, however, increased progressively from day 1 to day 7 post-injury, the latest point evaluated (Fig. 2D). The data show that there is an orchestrated recruitment of myeloid cells in the spinal cord injury, being, microglia the most numerous at day 7.

Changes of cytokines protein levels in the spinal cord after contusion injury

We also assessed the protein levels of IL-6, G-CSF and M-CSF in the spinal cord parenchyma at 6, 12, 24 hours post-injury, as well as, at day 3 and 7 days. Our results reveal that IL-6, G-CSF are up-regulated as early as 6 hours, peaking at 6 and 12 hours after injury, respectively (Fig. 3A, B). IL-6 and G-CSF are more highly expressed at this early phase as compared to M-CSF. They could play a key role in triggering the activation of glial cells and the recruitment of granulocytes. Beyond 12 hours, IL-6 and G-CSF protein levels drop progressively and reached basal levels by day 7. M-CSF, however, has a different expression pattern. Its protein levels increase progressively after injury up to day 3, time point when it peaks. (Fig. 3C). Interestingly, the maximum expression of M-CSF coincides with the peak accumulation of macrophages and the increased count of microglia in the injured spinal cord parenchyma, suggesting that M-CSF could play a key role in monocyte recruitment and microglia expansion after SCI.

Time Considerations

For experienced researchers, the total time needed from the anesthesia induction to the placement of the SCI animal into the warmed recovery cage is 30 minutes per mice. An extra 120 minutes after the termination of the surgical protocol must be considered for animal full recovery before returning to their home cages.

The total time need for the FACS analysis is about 6 hours, but it can vary depending on the number of samples, and the different staining combinations done in each sample.

For assessing cytokine levels, about 3 hours are necessary to obtain the concentrated spinal cord protein samples. To perform the Luminex bead-based Multiplex assay, 24 hours more are required.

References

Ahuja, C.S., Wilson, J.R., Nori, S., Kotter, M.R.N., Druschel, C., Curt, A., and Fehlings, M.G. (2017). Traumatic spinal cord injury. Nat. Rev. Dis. Prim.

Brown, M., and Wittwer, C. (2000). Flow cytometry: principles and clinical applications in hematology. Clin. Chem.

Cao, Q., and Whittemore, S.R. (2012). Cell transplantation. stem cells and precursor cells. In Handbook of Clinical Neurology, p.

Chen, Y., Tang, Y., Vogel, L.C., and Devivo, M.J. (2013). Causes of spinal cord injury. Top. Spinal Cord Inj. Rehabil.

Cheriyan, T., Ryan, D.J., Weinreb, J.H., Cheriyan, J., Paul, J.C., Lafage, V., Kirsch, T., and Errico, T.J. (2014). Spinal cord injury models: a review. Spinal Cord *52*, 588–595.

Coll-Miro, M., Francos-Quijorna, I., Santos-Nogueira, E., Torres-Espin, A., Bufler, P., Dinarello, C.A., and Lopez-Vales, R. (2016). Beneficial effects of IL-37 after spinal cord injury in mice. Proc. Natl. Acad. Sci. U. S. A. *113*, 1411–1416.

David, S., Lopez-Vales, R., and Wee Yong, V. (2012a). Harmful and beneficial effects of inflammation after spinal cord injury. potential therapeutic implications. Handb. Clin. Neurol. *109*, 485–502.

David, S., Zarruk, J.G., and Ghasemlou, N. (2012b). Inflammatory Pathways in Spinal Cord Injury. Int. Rev. Neurobiol. *106*, 127–152.

Fawcett, J.W. (2015). The extracellular matrix in plasticity and regeneration after CNS injury and neurodegenerative disease. In Progress in Brain Research, p.

Francos-Quijorna, I., Santos-Nogueira, E., Gronert, K., Sullivan, A.B., Kopp, M.A., Brommer, B., David, S., Schwab, J.M., López-Vales, R., and Lopez-Vales, R. (2017). Maresin 1 Promotes Inflammatory Resolution, Neuroprotection, and Functional Neurological Recovery After Spinal Cord Injury. J. Neurosci.

Ghasemlou, N., Kerr, B.J., and David, S. (2005). Tissue displacement and impact force are important contributors to outcome after spinal cord contusion injury. Exp. Neurol.

He, Z., and Jin, Y. (2016). Intrinsic Control of Axon Regeneration. Neuron.

Kroner, A., Greenhalgh, A.D., Zarruk, J.G., PassosdosSantos, R., Gaestel, M., and David, S. (2014). TNF and Increased Intracellular Iron Alter Macrophage Polarization to a Detrimental M1 Phenotype in the Injured Spinal Cord. Neuron *83*, 1098–1116.

Popovich, P.G. (2014). Neuroimmunology of traumatic spinal cord injury: A brief history and overview. Exp. Neurol.

Roederer, M. (2004). Multiparameter FACS Analysis. In Current Protocols in Immunology, p.

Santos-Nogueira, E., Lopez-Serrano, C., Hernandez, J., Lago, N., Astudillo, A.M., Balsinde, J., Estivill-Torrus, G., de Fonseca, F.R., Chun, J., and Lopez-Vales, R. (2015). Activation of Lysophosphatidic Acid Receptor Type 1 Contributes to Pathophysiology of Spinal Cord Injury.

J. Neurosci.

Scheff, S.W., Rabchevsky, A.G., Fugaccia, I., Main, J.A., and Lumpp, J.E. (2003). Experimental Modeling of Spinal Cord Injury: Characterization of a Force-Defined Injury Device. J. Neurotrauma.

Shamash, S., Reichert, F., and Rotshenker, S. (2002). The cytokine network of Wallerian degeneration: tumor necrosis factor-alpha, interleukin-1alpha, and interleukin-1beta. J. Neurosci.

Sharif-Alhoseini, M., Khormali, M., Rezaei, M., Safdarian, M., Hajighadery, A., Khalatbari, M.M., Safdarian, M., Meknatkhah, S., Rezvan, M., Chalangari, M., et al. (2017). Animal models of spinal cord injury: A systematic review. Spinal Cord.

Steward, O., and Willenberg, R. (2017). Rodent spinal cord injury models for studies of axon regeneration. Exp. Neurol.

Vallières, N., Berard, J.L., David, S., and Lacroix, S. (2006). Systemic injections of lipopolysaccharide accelerates myelin phagocytosis during wallerian degeneration in the injured mouse spinal cord. Glia.

Chapter 2

Modulation of the inflammatory response after spinal cord injury by MABp1 and OLT1177

Jesus Amo-Aparicio[1], Isaac Francos-Quijorna[1], Damaris B. Skouras [2], Charles A. Dinarello[3-4] and Ruben Lopez-Vales[1]

[1]Departament de Biologia Cel·lular, Fisiologia i Immunologia, Institut de Neurociències, Centro de Investigación Biomédica en Red sobre Enfermedades Neurodegenerativas (CIBERNED), Universitat Autònoma de Barcelona, Bellaterra, Catalonia 08193, Spain

[2]Olatec Therapeutics LLC, NewYork, NY 10065, USA

[3]Department of Medicine, University of Colorado Denver, Aurora, CO 80045, USA

[4]Department of Medicine, Radboud University Medical Center, 6500 Nijmegen, The Netherlands

Abstract

Spinal cord injury (SCI) leads to irreversible functional deficits due to the disruption of axons and the death of neurons and glial cells. One of the main factors that contribute to tissue damage is the inflammatory response that occurs in the spinal cord parenchyma following injury. Targeting inflammation after SCI is therefore expected to ameliorate histopathological outcomes and, consequently, minimize neurological impairments. Cytokines of the interleukin 1 (IL-1) family are known to play a crucial role in the initiation of inflammation. Here, we characterized the expression of three members of the IL-1 family with potent pro-inflammatory activity: IL-1α, IL-1β, and IL-18. We found that protein levels for these three cytokines were increased in spinal cord parenchyma after contusion injury although they did not show the same expression profile. While levels of IL-1α and IL-1β were rapidly increased after lesion, peaking at 6 and 12 hours, respectively, levels of IL-18 were not increased up to day 7. We also studied the contribution of these cytokines to the physiopathology of SCI by using MABp1, an IL-1α blocking antibody, and OLT1177, an inhibitor of the NLRP3 inflammasome required for the processing and release of IL-1β and IL-18. We found that administration of MABp1 did not promote functional recovery after SCI mice. Importantly, administration of OLT1177 protected against neurological deficits and demyelination after contusion injury. These results suggest that OLT1177 could be a good candidate to manage neuroinflammation and promote functional recovery after acute SCI in humans.

Keywords: interleukin 1 alpha, interleukin 1 beta, interleukin 18, inflammasome, spinal cord injury

Introduction

Acute inflammation is a rapid physiological response of the immune system aimed to combat infections and clear cell debris (Libby, 2007). This response has to be tightly regulated, otherwise, it can lead to excessive or chronic inflammation and cause tissue damage, as it occurs after spinal cord injury (Fleming et al., 2006; Francos-Quijorna et al., 2016). Among the multiple mediators that participates in the initiation and control of the inflammatory response, members of the interleukin 1 (IL-1) family, such as, interleukin 1 alpha (L-1α), interleukin 1 beta (IL-β), and interleukin-18 (IL-18) are known to play a key role (Dinarello, 2011).

IL-1α is constitutively present as a precursor at the cell nucleus since it contains a nuclear localization signal (NLS) that drives its translocation into the nucleus. In the central nervous system (CNS), IL-1α is expressed by endothelial cells and astrocytes (Dinarello, 2011). However, after SCI, the vast majority of cells expressing IL-1α are microglial cells (Bastien et al., 2015). Upon a signal to initiate necrosis, the IL-1α precursor moves from the nucleus to the cytosol and, when membranes are finally disintegrated, it is released to the extracellular space. There, IL-1α acts as an "alarmin" binding to interleukin 1 receptors 1 and 2 (IL-1R1 and IL-1R2, respectively) at specific cells and initiating a rapid cascade of inflammatory mediators, cytokines and chemokines (Chen et al., 2007). When cells die by apoptosis, IL-1α remains bound to chromatin and is unable to initiate inflammation (White et al., 2010).

IL-1β and IL-18 are also key regulators of the inflammatory response (Dinarello, 2011). IL-1β mediates its actions on inflammation by signaling via the same receptors than IL-1α, IL-1R1 and IL-1R2. Contrarywise, IL-18 binds to the receptors IL-18Rα and IL-18Rβ. IL-1β and IL-18 are detected at very low levels in the CNS at physiological conditions, however, after insult, they are highly expressed by microglia, infiltrated macrophages and neurons (Gustin et al., 2015; de Rivero Vaccari et al., 2008). In contrast to IL-1α, IL-1β and IL-18 are synthesized as inactive precursors and, in order to be fully activated and secreted, they require to be processed by caspase-1. Activation of caspase-1 is mediated by inflammasomes (Franchi et al., 2009).

Inflammasomes are macromolecular complexes in the cytoplasm of stimulates cell that mediates the activation of inflammatory caspase-1, required for the intracellular processing of IL-1β and IL-18 (Franchi et al., 2009; Martinon et al., 2002). Inflammasomes are composed by three elements: a pathogen recognition receptor (PRR), an adaptor protein known as ASC with PYD and CARD domains, and a procaspase-1 protein. To date, five different inflammasomes have been identified, each of them being dictated by its unique PRR. They include the nucleotide-binding oligomerization domain (NOD), leucine-rich repeat (LRR)-containing protein family members NLRP1, NLRP3 and NLRC4; as well as the proteins absent in melanoma 2 (AIM2) and pyrin (Broz and Dixit, 2016). From all of them, the NOD-like receptor pyrin domain-containing protein 3 (NLRP3) inflammasome is one of the best characterized.

NLRP3 respond to a wide variety of stimuli including bacterial toxins, particulate matter or extracellular ATP. All these stimuli share a reduction in intracellular potassium levels as common denominator (Muñoz-Planillo et al., 2013; Yang et al., 2019). Assembly of NLRP3 inflammasome requires the recognition of inflammatory ligands by NLRP3 sensor protein. This results in interaction with ASC via PYD and the recruitment of procaspase-1 via CARD forming a NLRP3-ASC-procaspase-1 complex, also named NLRP3 inflammasome. Proximity-induced auto-processing results in the formation of the catalytically active caspase-1, which initiates downstream responses, including the processing and release of IL-1β and IL-18 but also the

induction pyroptosis, which is a lytic form of cell death by forming pores in the plasma membrane (Broz and Dixit, 2016; Yang et al., 2019). This classic way of maturation and release of IL-1β and IL-18 is known as canonical pathway. However, occasionally both cytokines can mature following a non-canonical pathway**.** Non-canonical pathway is produced in response to LPS from Gram-negative bacteria. LPS is directly recognized by the CARD domain of caspase-11 in mice and caspase 4 and/or caspase 5 in human leading to its oligomerization. Active caspases cleavage gasdermin D, a pore-forming protein that induce pyroptotic cell death. Pyroptosis leads to potassium efflux and, therefore, to the activation of NLRP3 inflammasome and processing of IL-1β and IL-18 (Yang et al., 2019).

In this chapter, we will study the efficacy of two human-safe treatments for the suppression of the inflammatory response elicited by SCI by targeting various members of the IL-1 family. These treatments are a monoclonal antibody against IL-1α, known as MABp1, and an NLRP3 inflammasome inhibitor known as OLT1177. MABp1 (do not confuse with mammalian acting-binding protein 1, mAbp1) is a monoclonal antibody developed by Xbiotech recently approved for clinical use. This monoclonal antibody neutralizes the soluble form of IL-1α inhibiting the binding to its receptors IL-1R1 and IL-1R2. Since this interleukin works as an "alarmin" in the first stages after injury amplifying the production of pro-inflammatory cytokines, blockade by MABp1 may have an important therapeutic potential for SCI. OLT1177 is a beta-sulfonyl nitrile compound, developed by OLATEC LLC that has been described to selectively inhibit the NLRP3 inflammasome (Jiang et al., 2017). OLT1177 prevents NLRP3 oligomerization leading to a reduction in the secretion of IL-1β and IL-18 (Marchetti et al., 2018a).

Materials and Methods

Approvals

All the experiments were approved by the Ethics Committee on Animal and Human Experimentation from the Universitat Autonoma de Barcelona (CEEAH: 4057) and followed the European Communities Council Directive 2010/63/EU. Methods from each procedure were carried out in accordance with approved guidelines.

Spinal cord injury surgical procedure

Spinal cord injury was performed as described in Chapter 1 (Amo-Aparicio et al., 2018). Briefly, adult (8–10 weeks old) female C57BL/6J mice (Charles River) were anesthetized by intramuscular injection with a mixture of ketamine (90 mg/kg) and xylazine (10 mg/kg). After performing laminectomy at 11th thoracic vertebrae, the exposed spinal cord was contused using the Infinite Horizon Impactor device (Precision Scientific Instrumentation). A force of 60 kdynes and a tissue displacement of 450 – 550 μm were applied.

Treatments after SCI

Administration of MABp1 (Xbiotech) were performed by intraperitoneal (i.p.) or intraspinal (i.s.) injections. Intraperitoneally, MABp1 was injected at 0.5 mg/kg or 5 mg/kg in saline solution. Injections were performed 1 hour after injury and repeated at 2 and 4 days after injury. Doses were extracted from previous studies (Hong et al., 2014). Instraspinally, MABp1 was injected at 1 μg/μl in saline solution. 1 μl of solution containing 1 μg of MABp1 was injected into the lesion site 5 minutes after injury. Injections were performed using a glass needle (30 μm internal diameter, Eppendorf) coupled to a 10 ml Hamilton syringe (Hamilton

#701, Hamilton). Injections were controlled by an automatic injector (KDS 310 Plus, KD Scientific) with a 2 µL/min rate. The tip of the needle was maintained inside the cord tissue 3 min after each injection to avoid liquid reflux.

OLT1177 (OLATEC LLC) was injected intraperitoneally at 60 mg/kg based on previous publications (Marchetti et al., 2018a). Injections were performed twice a day, starting 1 hour after the surgery until day 7.

In all cases, control mice were treated with sterile saline solution using the same administration protocol than treated mice.

Functional Assessment

Locomotor recovery after SCI was evaluated at 1, 3, 5,7, 10, 14, 21, and 28 days post-injury (dpi) in an open-field using the nine-point Basso Mouse Scale (BMS) (Basso et al., 2006). BMS evaluation was performed researchers who were blinded to the experimental groups. Consensus score between two researchers was taken. At least 6 mice per group were used unless otherwise stated.

Histology

At 28 dpi, mice were perfused with 4% paraformaldehyde (Sigma-Aldrich) in 0.1 M phosphate buffer. A 6 mm-length sample of spinal cord centered into the lesion site was removed and cryoprotected with 30 % sucrose in 0.1 M phosphate buffer saline (PBS) at 4°C. Samples with 10 - 15 µm thick were cut in the cryostat and picked up with a glass slide. Samples were arranged following a serial distribution. Adjacent sections in the same slide were 100 - 150 µm apart. After graded dehydration, sections were placed in a 1 mg/ml Luxol Fast Blue (LFB) (Sigma-Aldrich) solution in 95% ethanol and 0.05% acetic acid and left overnight at 37°C. Sections were then washed in 95% ethanol and distilled water before clearing with 0.5 mg/ml of Li_2CO_3 in distilled water for 1.5 min. After several washes, sections were dehydrated and mounted in DPX mounting media (Sigma-Aldrich). After fixation, the epicenter of the contusion was localized by determining the tissue section with the lowest LFB stained area. NIH ImageJ software was used to perform the quantifications.

Luminex (bead-based multiplex assay)

Luminex assay was performed according to described protocol (Amo-Aparicio et al., 2018). At different time points after injury, mice received an intraperitoneal injection of sodium pentobarbital (Dolethal). Blood was removed by perfusion with 60 mL of 0.9% NaCl in distillated water. 0.6 cm of the spinal cord centered into the injury site were taken from each mouse. Samples were frozen in liquid nitrogen and homogenized in an extraction buffer using a TissueRuptor (Qiagen) and an Ultrasonic Homogenizer (Biologics Inc.). Buffer was prepared following previous publication (Amo-Aparicio et al., 2018). Protein was quantified and diluted to 2 mg/µl. Beads and samples were added to the Luminex plate following specific commercial protocols (Invitrogen). After washing, 50 µl of samples were added and incubated overnight at 4°C. Finally, secondary antibodies were added, and cytokine concentrations were calculated using a MAGPIX Luminex reader (ThermoFisher). Final values were normalized by the amount of protein added in each well. 4 mice per time-point were used.

Statistics

All analyses were conducted through GraphPad Prism v7. BMS scores were analyzed using two-way repeated measure (RM) ANOVA with Bonferroni's post hoc correction. Luminex results were analyzed using one-way ANOVA with Dunnett's post hoc correction. Luxol Fast Blue measures were analyzed using multiple t-test comparisons with Holm-Sidak's post hoc correction. Results were expressed as mean ± SEM and differences were considered significant at $p < 0.05$.

Results

Protein levels of IL-1α, IL-1β and IL-18 increase after SCI

Since contusion to the spinal cord leads to the immediately increase in the production of pro-inflammatory cytokines, we first evaluated the dynamics of IL-1α, IL-1β, and IL-18 at protein level in the injury environment from 1h to 28 days after lesion.

Luminex analysis revealed that the protein levels for these cytokines were very low, even below the detection limit, in the spinal cord at physiological conditions. However, levels of these three cytokines increased significantly after contusion injury (Fig. 1). IL-1α expression in the injured spinal cord preceded IL-1β and IL-18. IL-1α protein levels were significant increased from 6 to 24h post-injury, reaching peak levels at 6h (Fig. 1A). Protein levels for IL-1β in the spinal cord parenchyma peaked at 12 hours post-lesion and remained at significant high levels up to 24 hours post-injury (Fig. 1B). Comparatively, protein levels for IL-1β were ~3 fold lower than IL-1α at their peaks. The expression of IL-18, however, was produced at later time points after SCI. IL-18 showed maximal levels at day 7 and remained at significant greater levels up to day 21 (Fig. 1C).

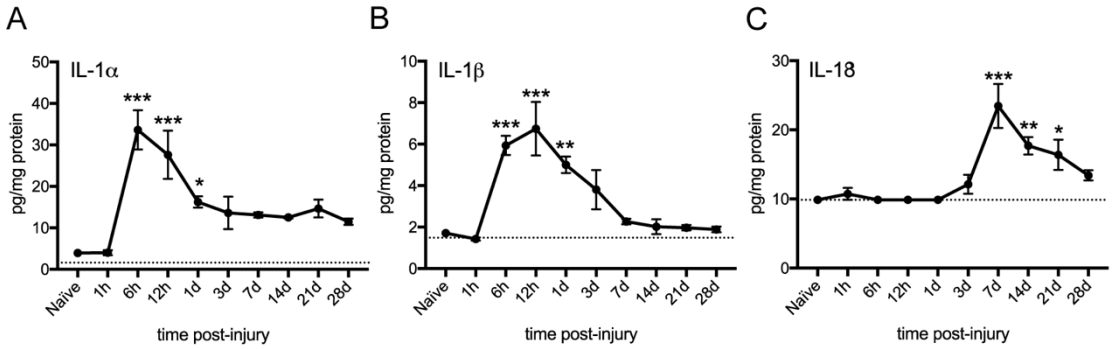

Figure 1: Levels of IL-1α (A), IL-1β (B), and IL-18 (C) in the spinal cord at different time points after injury. Spinal cords without injury were used as naïve condition. Dashed line marks the detection limit of each cytokine. Data are represented as mean ± SEM. N = 4 per time point. * p < 0.05, ** p < 0.01, *** p < 0.001 against naïve. Standard one-way ANOVA with Dunnett's post hoc correction.

Blockade of IL-1α has no therapeutic actions after SCI

IL-1α works as an alarm signal activating the production of pro-inflammatory cytokines in target cells (Chen et al., 2007). Since protein levels for this cytokine rapidly increase during the first 24 hours after injury, we assessed whether administration of an IL-1α blocking antibody (MABp1) exerted therapeutic effects after SCI.

For this purpose, mice were intraperitonially injected with 0.5 mg/kg of MABp1. Injections started 1 hour after SCI and were repeated at 2 and 4 dpi. Locomotor evaluation on an open field revealed that mice receiving MABp1 did not show enhanced neurological recovery as compared to control mice (Fig. 2A). At 28 dpi, around 67% of mice treated with MABp1 showed plantar placement (3 points) and 33% of them showed extensive ankle movement (2 points). In the same line, around 40% of the mice treated with saline showed occasional stepping (4 points). Rest of the mice of the control group were divided equally between plantar placement (3 points) and extensive ankle movement (2 points) (Fig. 2B). Similarly, histological assessment of the lesion area revealed that IL-1α blockade did not protect against myelin loss following SCI (Fig. 2 C,D). We then studied whether increasing the dose of MABp1 could lead to beneficial effects. We therefore injected 5 mg/kg of MABp1 at the same time points. As previously, increasing dose of MABp1 did not enhance locomotor recovery after SCI (Fig. 2E).

Finally, we hypothesized that the failure of the IL-1α blocking therapy to improve neurological outcomes after SCI could be due to the inability of the antibody to reach the injury site. Therefore, we tested in a small cohort of mice whether the administration of MABp1 directly into the lesion site ameliorated functional deficits. Again, this experiment revealed that intraspinal delivery of the IL-1α blocking antibody did not protect against functional disabilities after spinal cord contusion injury (Fig 2F). All together, these data suggest that IL-1α does not contribute to the physiopathology of SCI.

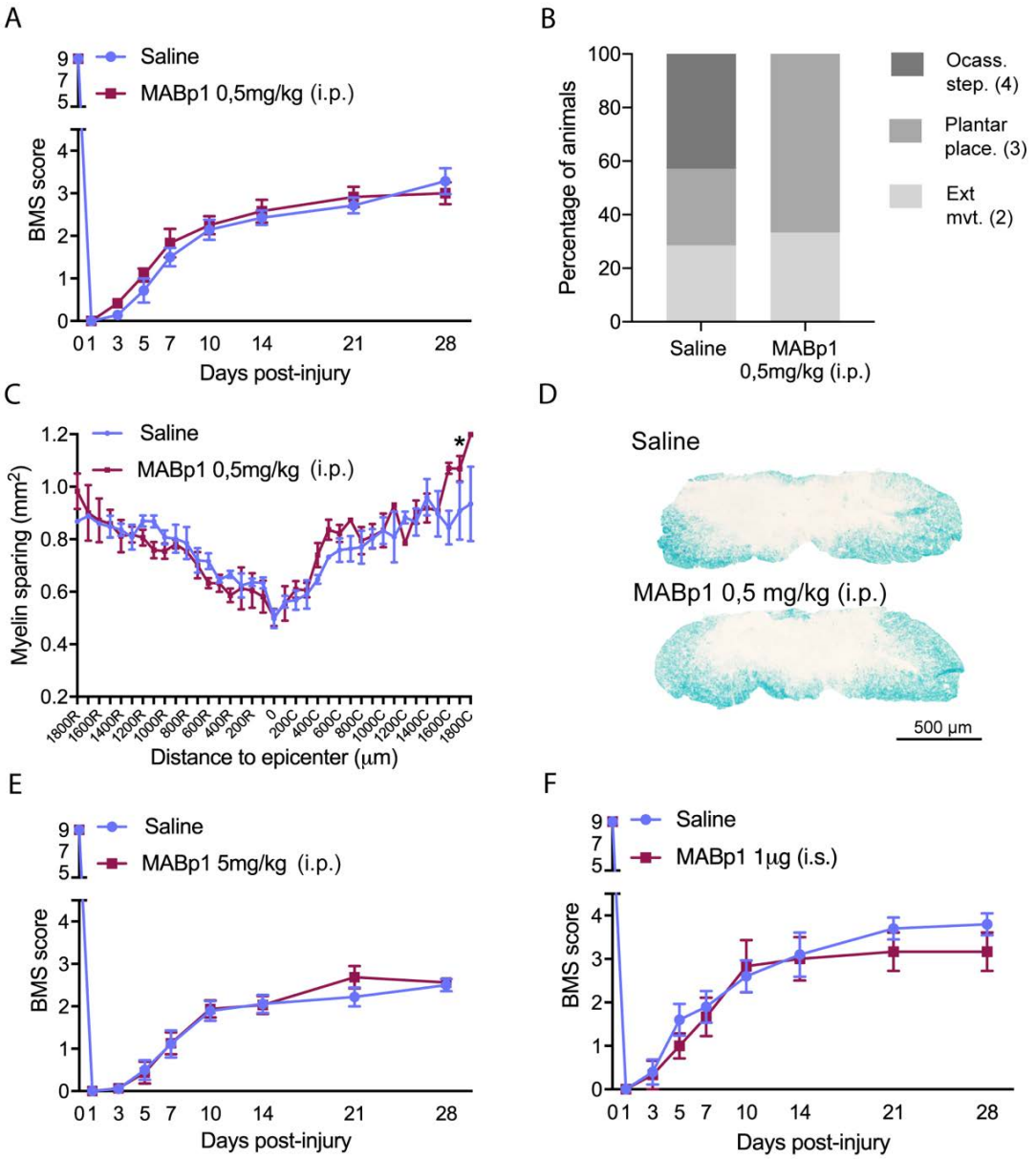

Figure 2: Functional and histological effects of MABp1 after SCI. (A-D) Effect of 0.5 mg/kg doses of MABp1 intraperitoneally. (A) BMS score showing the locomotor progression. (B) Functional distribution of mice at 28 dpi. BMS values of each type of movement are indicated in parenthesis. (C) Myelin preservation in the lesion area obtained by LFB staining. (D) Representative micrographs showing myelin sparing at the injury epicenter. (E) Locomotor recovery of mice receiving 5 mg/kg doses of MABp1 intraperitoneally. (F) Locomotor recovery of mice receiving 1 µg of MABp1 instraspinally. Data are represented as mean ± SEM. N ≤ 6 for (A, B, C, and E). N = 3 for (F). * p < 0.05. Two-way RM-ANOVA with Bonferroni's post hoc correction for (A, E, and F) and multiple t-test comparisons with Holm-Sidak's post hoc correction for (C).

OLT1177 has beneficial effects after SCI

NLRP3 inflammasome plays a key role in the maturation and release of the pro-inflammatory cytokines IL-1β and IL-18 (Marchetti et al., 2018a). Since we reported above that these two cytokines are markedly produced after SCI, we tested whether administration of OLT1177, a

specific NLRP3 inhibitor that it is safe in humans, exerted beneficial actions after spinal cord contusion injury in mice.

We found that animals treated with OLT11177 displayed enhanced locomotor skills as compared to those treated with saline from day 14 post-injury (Fig. 3A). At the end of the follow up, 25% of the mice treated with saline showed extensive ankle movement, 62.5% of them showed plantar placement (3 points), and only 12.5% of them showed occasional plantar stepping (4 points). Contrariwise, all mice treated with OLT1177 displayed at least plantar placement (3 points), 33.3% of them showed occasional plantar stepping (4 points), and 16.7% of them showed frequent plantar stepping (5 points) (Fig. 5B). Importantly, histological outcomes also revealed that OLT1177 led to significant enhancement in myelin preservation at the injury epicenter and at some rostral and caudal regions (Fig. 3 C,D).

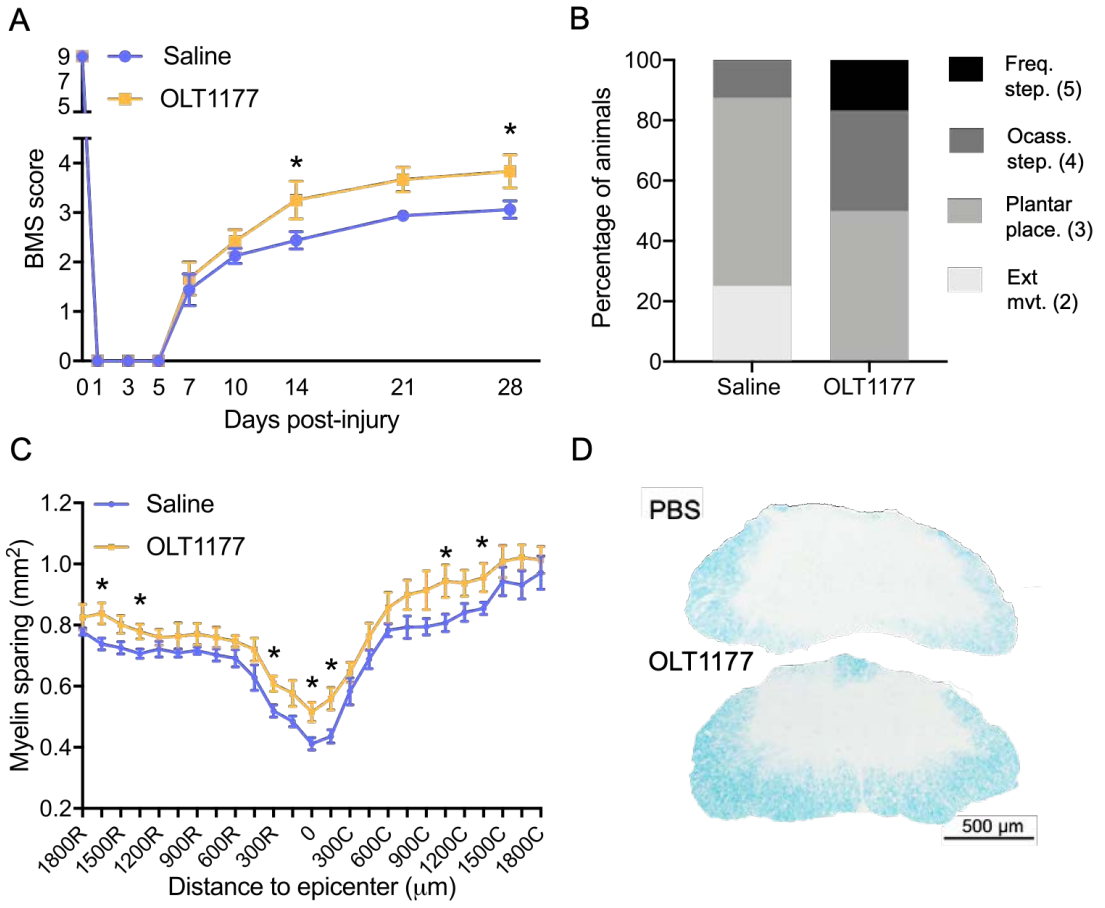

Figure 3: Functional and histological effects of OLT1177 after SCI. (A) BMS score showing the locomotor progression of mice receiving 60 mg/kg of OLT1177 twice a day for 7 days after SCI. (B) Functional distribution of mice at 28 dpi. BMS values of each type of movement are indicated in parenthesis. (C) Myelin preservation in the lesion area obtained by LFB staining. (D) Representative micrographs showing myelin sparing at the injury epicenter. Data are represented as mean ± SEM. N ≤ 6. * p < 0.05. Two-way RM-ANOVA with Bonferroni's post hoc correction for (A) and multiple t-test comparison with Holm-Sidak's post hoc correction for (C).

Discussion

Traumatic SCI leads to the loss of motor, sensory, and autonomic functions below the injury site (Burns et al., 2012). This is due to the immediate damage followed by a secondary phase

of tissue degeneration, known as secondary damage, that ocurrs over a period of several weeks after initial trauma (Muldoon et al., 2013). There are several mechanisms that trigger secondary injury following SCI, however, the exacerbated inflammatory response elicited after neurotrauma is one of the main contributors (David et al., 2012). Despite SCI is one of the main causes of death and disability (Ahuja et al., 2017), there is currently no effective treatment. Therefore, supressing inflammation could be a useful approach to reduce secondary damage, and consequently, to improve functional impairments.

When talking about immunosuppressive therapies, it is important to have into consideration the potential side effects. Chronic use of immunosuppressive drugs for the treatment of inflammatory diseases increase the risk of opportunistic infections (Dinarello et al., 2012). For example, reactivation of *Mycobacterium tuberculosis* in patients receiving anti-TNF therapies can be 25 times higher than in untreated individuals (Solovic et al., 2010). Due to the dangerous nature of opportunistic infections, they become a major concern in all the anti-cytokine therapies. What distinguishes IL-1-based therapies from other agents is the lack of opportunistic infections. Although they increase the risk of routine bacterial infection easily treatable, opportunistic infections are rare (Fleischmann et al., 2003). In the present chapter of this thesis, we focused our interest in testing two different strategies aimed to target various members of the IL-1 family that have potent pro-inflammatory actions. This strategies are a blocking antibody to prevent IL-1α signaling and a NLRP3 selective inhibitor to suppress processing of IL-1β and IL-18.

Previous publications revealed that deletion of *Il1a* gene protected against oligodendrocyte cell death and functional deficits after SCI in mice (Bastien et al., 2015). However, the detrimental actions of IL-1α in SCI were only observed at 24 hours post-injury and not at later stages. Indeed, IL-1α knockout mice did not show greater locomotor skills neither oligodendrocyte survival than their wild-type littermates at 5 weeks following lesion (Bastien et al., 2015). These findings suggest that the absence of IL-1α may delay, but not minimize, secondary damage events after SCI. However, it cannot be dismissed that the lack of IL-1α in the knockout mouse could be compensated by the expression of any other inflammatory cytokine that may have counteracted its effects at long term.

The neutralizing monoclonal IL-1α antibody named MABp1 has proved efficacy in a wide variety of diseases such as diabetes mellitus (Timper et al., 2015), acne vulgaris (Carrasco et al., 2015), and psoriasis (Coleman et al., 2015). This antibody is currently being tested in phase III clinical trial as immunotherapy for metastatic colorectal cancer and in phase II clinical trial for the treatment of atopic dermatitis. This therapy has demonstrated to be safe in humans, and the results from the colorectal cancer trial revealed that MABp1 improved the cancer-associated symptoms such as muscle loss, fatigue, anorexia, and pain (Kanni et al., 2018). However, the effects of the MABp1 therapy after SCI has not been studied yet.

Here, we administrated 0.5 mg/kg or 5mg/kg of MABp1 starting 1 hour after SCI. Injections were repeated at 2 and 4 days after lesion since half-life of MABp1 is 3.25 days (Timper et al., 2015) and levels of IL-1α are still $\sim$3 fold higher at day 3 post-lesion, although this was not statistically significant. Despite the beneficial actions of this blocking antibody in other animal models of disease, MABp1 did not show any beneficial effect on functional recovery or myelin preservation after SCI. These observations support that the previous protective actions observed in the IL-1α knockout mouse after SCI (Bastien et al., 2015) might be due to the

involvement of this cytokine in accelerating rather than contributing to secondary tissue damage.

The lack of efficacy of MABp1 in neurotrauma is unlikely due to the inability of the blocking antibody to reach the lesion environment since the administration of MABp1 directly into the lesion site also failed to exert therapeutic effects. However, we do not discard the possibility that failure of MABp1 therapy in SCI could be produced, in part, by certain levels of IL-1α that remained unattached to this antibody. Consequently, IL-1α signaling could be only blocked partially.

We found that the expression of IL-1β followed IL-1α after SCI. IL-1β controls very important homeostatic functions such as body temperature, sleep, and cell metabolism among others Dinarello 2011). This cytokine is thought to be one of the most important regulators of inflammation, including CNS conditions (Garlanda et al., 2013). However, the contribution of IL-1β to secondary tissue damage after SCI is controversial. An early study using knockout mice for this cytokine revealed that the lack of IL-1β attenuated inflammation and protected against functional deficits and tissue damage (Boato et al., 2013). Nevertheless, a more recent report did not observe any protection on functional or histopathological outcomes in mice lacking *Il1b* gene after SCI, despite they showed reduced neuroinflammation (Bastien et al., 2015).

IL-18 is another member of the IL-1 family with potent proinflammatory actions. The contribution of IL-18 to CNS pathologies has been less studied than IL-1α and IL-1β. However, since previous findings revealed that *Il18* gene deletion resulted in impaired microglia activation after influenza A virus infection (Mori et al., 2001), it was suggested that IL-18 may regulate microglial cell functions during neuroinflammation, and possibly immune cells infiltration. In contrast to IL-1α and IL-1β, we found that the protein levels of IL-18 were not increased at early stages after SCI but at later time points. Indeed, the peak expression for IL-18 in the injured spinal cord was found at 7 days post-lesion, coinciding with the maximal accumulation of microglial cells (Francos-Quijorna et al., 2017). The exact contribution of IL-18 to SCI has not been investigated yet. However, a previous report revealed that IL-18 contributes to the pathogenesis of experimental autoimmune encephalomyelitis (Schif-Zuck et al., 2014), suggesting that this cytokine may be involved in SCI physiopathology. In this line, a recent study revealed that the microRNA MiR-92b-5p increased the levels of IL-18 binding protein (IL-18BP), a soluble IL-18 inhibitor, and ameliorated tissue damage and neurological deficits after SCI (Lin et al., 2019).

Both, IL-18 and IL-1β, are synthesized as inactive cytoplasmic precursors that are proteolytically processed to biologically active forms in response to proinflammatory stimuli by caspase-1, which in turn, is activated by inflammasomes such as NLRP3. It is therefore expected than blocking NLRP3 may have potent anti-inflammatory actions after SCI, since it may impede the signaling of these two pro-inflammatory cytokines. A previous study has demonstrated that administration of the inhibitor BAY 11-7082 mediated therapeutic actions after SCI (Jiang et al., 2017). Although the authors claimed that BAY 11-7082 is an inhibitor of NLRP3, this compound is a broad-spectrum inhibitor with anti-inflammatory activity against multiple targets (Lee et al., 2012). OLT1177, in contrast, is a selective NLRP3 inhibitor that proved value in a murine models of acute arthritis (Marchetti et al., 2018b) and ischemia reperfusion injury (Toldo et al., 2019). Importantly, OLT1177 is safe for humans, crosses the blood-brain barrier, and it has proved efficacy even when given orally (Marchetti et al., 2018b, 2018a). Here, we observed that treatment with OLT1177 after SCI protected against

locomotor deficits and demyelination being revealed as a potent candidate for the treatment of SCI. These results suggest a reduction in the levels of IL-1β and IL-18. Full impact of OLT1177 on the levels of IL-1β and IL-18 after SCI will be studied in the following months.

It is necessary to highlight that IL-1β and IL-18 can also be processed by inflammasome-independent mechanisms (Fantuzzi et al., 1997). This alternative activation is mediated by neutrophil- and macrophage-derived neutral serine proteases such as proteinase 3, elastase, or cathepsin-G that can process pro-IL-1β into a 17 kDa bioactive fragment (Coeshott et al., 2002; Sugawara et al., 2014). Similar to IL-1β, pro-IL-18 can also be processed by metalloproteinase Meprin β or proteinase 3 (Bae et al., 2012; Banerjee and Bond, 2008). This inflammasome-independent processing occurs mainly in inflammatory circumstances when neutrophils are the major cell population (Mencacci et al., 2000).

Overall, the results shown here demonstrate that OLT1177, but not MABp1, is a promising therapy for the treatment of SCI. Aspects such as doses, administration routes, and further details on the mechanisms of action after SCI need to be optimized. Since inflammation is involved in most neurological conditions, the use of OLT1177 may open a new avenue for the treatment of a wide range of CNS disorders.

References

Ahuja, C.S., Wilson, J.R., Nori, S., Kotter, M.R.N., Druschel, C., Curt, A., and Fehlings, M.G. (2017). Traumatic spinal cord injury. Nat. Rev. Dis. Prim.

Amo-Aparicio, J., Martínez-Muriana, A., Sánchez-Fernández, A., and López-Vales, R. (2018). Neuroinflammation Quantification for Spinal Cord Injury. Curr. Protoc. Immunol.

Bae, S., Kang, T., Hong, J., Lee, S., Choi, J., Jhun, H., Kwak, A., Hong, K., Kim, E., Jo, S., et al. (2012). Contradictory functions (activation/termination) of neutrophil proteinase 3 enzyme (PR3) in interleukin-33 biological activity. J. Biol. Chem.

Banerjee, S., and Bond, J.S. (2008). Prointerleukin-18 is activated by meprin β in vitro and in vivo in intestinal inflammation. J. Biol. Chem.

Basso, D.M., Fisher, L.C., Anderson, A.J., Jakeman, L.B.Y.N.B., Tigue, D.M.M.C., Popovich, P.G., McTigue, D.M., and Popovich, P.G. (2006). Basso Mouse Scale for locomotion detects differences in recovery after spinal cord injury in five common mouse strains. J. Neurotrauma *23*, 635–659.

Bastien, D., Bellver Landete, V., Lessard, M., Vallieres, N., Champagne, M., Takashima, A., Tremblay, M.-E., Doyon, Y., and Lacroix, S. (2015). IL-1 Gene Deletion Protects Oligodendrocytes after Spinal Cord Injury through Upregulation of the Survival Factor Tox3. J. Neurosci.

Boato, F., Rosenberger, K., Nelissen, S., Geboes, L., Peters, E.M., Nitsch, R., and Hendrix, S. (2013). Absence of IL-1β positively affects neurological outcome, lesion development and axonal plasticity after spinal cord injury. J. Neuroinflammation.

Broz, P., and Dixit, V.M. (2016). Inflammasomes: Mechanism of assembly, regulation and signalling. Nat. Rev. Immunol.

Burns, S., Biering-Sørensen, F., Donovan, W., Graves, D., Jha, A., Johansen, M., Jones, L.,

Krassioukov, A., Kirshblum, S., Mulcahey, M.J., et al. (2012). International Standards for Neurological Classification of Spinal Cord Injury, Revised 2011. Top. Spinal Cord Inj. Rehabil.

Carrasco, D., Stecher, M., Lefebvre, G.C., Logan, A.C., and Moy, R. (2015). An Open Label, Phase 2 Study of MABp1 Monotherapy for the Treatment of Acne Vulgaris and Psychiatric Comorbidity. J. Drugs Dermatology JDD.

Chen, C.J., Kono, H., Golenbock, D., Reed, G., Akira, S., and Rock, K.L. (2007). Identification of a key pathway required for the sterile inflammatory response triggered by dying cells. Nat. Med.

Coeshott, C., Ohnemus, C., Pilyavskaya, A., Ross, S., Wieczorek, M., Kroona, H., Leimer, A.H., and Cheronis, J. (2002). Converting enzyme-independent release of tumor necrosis factor and IL-1 from a stimulated human monocytic cell line in the presence of activated neutrophils or purified proteinase 3. Proc. Natl. Acad. Sci.

Coleman, K.M., Gudjonsson, J.E., and Stecher, M. (2015). Open-Label Trial of MABp1, a True Human Monoclonal Antibody Targeting Interleukin 1α, for the Treatment of Psoriasis. JAMA Dermatology.

David, S., Lopez-Vales, R., and Wee Yong, V. (2012). Harmful and beneficial effects of inflammation after spinal cord injury. potential therapeutic implications. Handb. Clin. Neurol. *109*, 485–502.

Dinarello, C.A. (2011). Interleukin-1 in the pathogenesis and treatment of inflammatory diseases. Blood.

Dinarello, C.A., Simon, A., and Van Der Meer, J.W.M. (2012). Treating inflammation by blocking interleukin-1 in a broad spectrum of diseases. Nat. Rev. Drug Discov.

Fantuzzi, G., Ku, G., Harding, M.W., Livingston, D.J., Sipe, J.D., Kuida, K., Flavell, R.A., and Dinarello, C.A. (1997). Response to local inflammation of IL-1 beta-converting enzyme-deficient mice. J. Immunol.

Fleischmann, R.M., Schechtman, J., Bennett, R., Handel, M.L., Burmester, G.R., Tesser, J., Modafferi, D., Poulakos, J., and Sun, G. (2003). Anakinra, a recombinant human interleukin-1 receptor antagonist (r-metHuIL-1ra), in patients with rheumatoid arthritis: A large, international, multicenter, placebo-controlled trial. Arthritis Rheum.

Fleming, J.C., Norenberg, M.D., Ramsay, D.A., Dekaban, G.A., Marcillo, A.E., Saenz, A.D., Pasquale-Styles, M., Dietrich, W.D., and Weaver, L.C. (2006). The cellular inflammatory response in human spinal cords after injury. Brain.

Franchi, L., Eigenbrod, T., Muñoz-Planillo, R., and Nuñez, G. (2009). The inflammasome: A caspase-1-activation platform that regulates immune responses and disease pathogenesis. Nat. Immunol.

Francos-Quijorna, I., Amo-Aparicio, J., Martinez-Muriana, A., and Lopez-Vales, R. (2016). IL-4 drives microglia and macrophages toward a phenotype conducive for tissue repair and functional recovery after spinal cord injury. Glia *64*, 2079–2092.

Francos-Quijorna, I., Santos-Nogueira, E., Gronert, K., Sullivan, A.B., Kopp, M.A., Brommer, B., David, S., Schwab, J.M., López-Vales, R., and Lopez-Vales, R. (2017). Maresin 1 Promotes Inflammatory Resolution, Neuroprotection, and Functional Neurological Recovery After Spinal Cord Injury. J. Neurosci.

Garlanda, C., Dinarello, C.A., and Mantovani, A. (2013). The Interleukin-1 Family: Back to the

Future. Immunity.

Gustin, A., Kirchmeyer, M., Koncina, E., Felten, P., Losciuto, S., Heurtaux, T., Tardivel, A., Heuschling, P., and Dostert, C. (2015). NLRP3 inflammasome is expressed and functional in mouse brain microglia but not in astrocytes. PLoS One.

Hong, D.S., Hui, D., Bruera, E., Janku, F., Naing, A., Falchook, G.S., Piha-Paul, S., Wheler, J.J., Fu, S., Tsimberidou, A.M., et al. (2014). MABp1, a first-in-class true human antibody targeting interleukin-1α in refractory cancers: An open-label, phase 1 dose-escalation and expansion study. Lancet Oncol.

Jiang, W., Li, M., He, F., Zhou, S., and Zhu, L. (2017). Targeting the NLRP3 inflammasome to attenuate spinal cord injury in mice. J. Neuroinflammation.

Kanni, T., Argyropoulou, M., Spyridopoulos, T., Pistiki, A., Stecher, M., Dinarello, C.A., Simard, J., and Giamarellos-Bourboulis, E.J. (2018). MABp1 Targeting IL-1α for Moderate to Severe Hidradenitis Suppurativa Not Eligible for Adalimumab: A Randomized Study. J. Invest. Dermatol.

Lee, J., Rhee, M.H., Kim, E., and Cho, J.Y. (2012). BAY 11-7082 is a broad-spectrum inhibitor with anti-inflammatory activity against multiple targets. Mediators Inflamm.

Libby, P. (2007). Inflammatory Mechanisms: The Molecular Basis of Inflammation and Disease. Nutr. Rev.

Lin, X.-L., Zhu, J., Wang, L.-M., Yan, F., Sha, W.-P., and Yang, H.-L. (2019). MiR-92b-5p inhibitor suppresses IL-18 mediated inflammatory amplification after spinal cord injury via IL-18BP up-regulation. Eur. Rev. Med. Pharmacol. Sci. *23*, 1891–1898.

Marchetti, C., Swartzwelter, B., Gamboni, F., Neff, C.P., Richter, K., Azam, T., Carta, S., Tengesdal, I., Nemkov, T., D'Alessandro, A., et al. (2018a). OLT1177, a β-sulfonyl nitrile compound, safe in humans, inhibits the NLRP3 inflammasome and reverses the metabolic cost of inflammation. Proc. Natl. Acad. Sci.

Marchetti, C., Swartzwelter, B., Koenders, M.I., Azam, T., Tengesdal, I.W., Powers, N., de Graaf, D.M., Dinarello, C.A., and Joosten, L.A.B. (2018b). NLRP3 inflammasome inhibitor OLT1177 suppresses joint inflammation in murine models of acute arthritis. Arthritis Res. Ther.

Martinon, F., Burns, K., and Tschopp, J. (2002). The Inflammasome: A molecular platform triggering activation of inflammatory caspases and processing of proIL-β. Mol. Cell.

Mencacci, A., Bacci, A., Cenci, E., Montagnoli, C., Fiorucci, S., Casagrande, A., Flavell, R.A., Bistoni, F., and Romani, L. (2000). Interleukin 18 restores defective Th1 immunity to Candida albicans in caspase 1-deficient mice. Infect. Immun.

Mori, I., Hossain, M.J., Takeda, K., Okamura, H., Imai, Y., Kohsaka, S., and Kimura, Y. (2001). Impaired microglial activation in the brain of IL-18-gene-disrupted mice after neurovirulent influenza A virus infection. Virology.

Muldoon, L.L., Alvarez, J.I., Begley, D.J., Boado, R.J., Del Zoppo, G.J., Doolittle, N.D., Engelhardt, B., Hallenbeck, J.M., Lonser, R.R., Ohlfest, J.R., et al. (2013). Immunologic privilege in the central nervous system and the blood-brain barrier. J. Cereb. Blood Flow Metab.

Muñoz-Planillo, R., Kuffa, P., Martínez-Colón, G., Smith, B., Rajendiran, T., and Núñez, G. (2013). K+ Efflux Is the Common Trigger of NLRP3 Inflammasome Activation by Bacterial Toxins and Particulate Matter. Immunity.

de Rivero Vaccari, J.P., Lotocki, G., Marcillo, A.E., Dietrich, W.D., and Keane, R.W. (2008). A Molecular Platform in Neurons Regulates Inflammation after Spinal Cord Injury. J. Neurosci.

Schif-Zuck, S., Westermann, J., Netzer, N., Zohar, Y., Meiron, M., Wildbaum, G., and Karin, N. (2014). Targeted Overexpression of IL-18 Binding Protein at the Central Nervous System Overrides Flexibility in Functional Polarization of Antigen-Specific Th2 Cells. J. Immunol.

Solovic, I., Sester, M., Gomez-Reino, J.J., Rieder, H.L., Ehlers, S., Milburn, H.J., Kampmann, B., Hellmich, B., Groves, R., Schreiber, S., et al. (2010). The risk of tuberculosis related to tumour necrosis factor antagonist therapies: a TBNET consensus statement. Eur. Respir. J.

Sugawara, S., Uehara, A., Nochi, T., Yamaguchi, T., Ueda, H., Sugiyama, A., Hanzawa, K., Kumagai, K., Okamura, H., and Takada, H. (2014). Neutrophil Proteinase 3-Mediated Induction of Bioactive IL-18 Secretion by Human Oral Epithelial Cells. J. Immunol.

Timper, K., Seelig, E., Tsakiris, D.A., and Donath, M.Y. (2015). Safety, pharmacokinetics, and preliminary efficacy of a specific anti-IL-1alpha therapeutic antibody (MABp1) in patients with type 2 diabetes mellitus. J. Diabetes Complications.

Toldo, S., Mauro, A.G., Cutter, Z., Van Tassell, B.W., Mezzaroma, E., Del Buono, M.G., Prestamburgo, A., Potere, N., and Abbate, A. (2019). The NLRP3 Inflammasome Inhibitor, OLT1177 (Dapansutrile), Reduces Infarct Size and Preserves Contractile Function After Ischemia Reperfusion Injury in the Mouse. J. Cardiovasc. Pharmacol.

White, M.R., Carmi, Y., Rider, P., Apte, R.N., Cohen, I., Martin, M.U., Braiman, A., Voronov, E., Dotan, S., and Dinarello, C.A. (2010). Differential release of chromatin-bound IL-1 discriminates between necrotic and apoptotic cell death by the ability to induce sterile inflammation. Proc. Natl. Acad. Sci.

Yang, Y., Wang, H., Kouadir, M., Song, H., and Shi, F. (2019). Recent advances in the mechanisms of NLRP3 inflammasome activation and its inhibitors. Cell Death Dis.

Chapter 3

Extracellular and nuclear roles of IL-37 after spinal cord injury

Jesus Amo-Aparicio[1], Alba Sanchez-Fernandez[1], Anna Martinez-Muriana[1], Elan Z. Eisenmesser[2], Suzhao LI[3], Charles Dinarello[3,4], and Ruben Lopez-Vales[1]

[1]Departament de Biologia Cel·lular, Fisiologia i Immunologia, Institut de Neurociències, Centro de Investigación Biomédica en Red sobre Enfermedades Neurodegenerativas (CIBERNED), Universitat Autònoma de Barcelona, Bellaterra, Catalonia 08193, Spain

[2]Department of Biochemistry and Molecular Genetics, University of Colorado Denver, Aurora, CO 80238

[3]Department of Medicine, University of Colorado Denver, Aurora, CO 80045, USA

[4]Department of Medicine, Radboud University Medical Center, 6500 Nijmegen, The Netherlands

Abstract

The inability of the central nervous system to resolve the inflammatory response induced after injury is one of the main process that contribute to secondary tissue damage and neurological impairments. Interleukin 37 (IL-37) in an anti-inflammatory cytokine of the IL-1 family for which its mouse homolog has not been found yet. However, transgenic mice expressing the human form of the *IL37* gene (hIL-37Tg) display protective effects in several animal models of disease. Previous results from our group revealed that IL-37 limits inflammation after spinal cord injury (SCI) and ameliorates tissue damage and functional deficits. IL-37 may exert its beneficial effects by acting as a nuclear and an extracellular cytokine. Although the importance of extracellular IL-37 to suppress inflammation is well known, the role of the nuclear function has not been fully elucidated. Moreover, it remains unknown the contribution of the extracellular and nuclear IL-37 to SCI. In the present chapter, we used a wide range of transgenic animals and recombinant proteins to answer these key questions. We found that nuclear IL-37 mediates anti-inflammatory effects during the first hours after LPS stimulation. However, IL-37 was able to contain inflammation in the lack of nuclear IL-37 at later stages. This suggests that extracellular functions of this cytokine are likely to have a major contribution to limit inflammation. In the case of SCI, we found that IL-37 also mediates beneficial effects on functional recovery and myelin sparing in the lack of nuclear route, but not when extracellular route is abolished. Moreover, we also demonstrated that the protective actions of IL-37 after SCI are mediated in the central nervous system (CNS) cells but not peripherally. This work reveals for the first time the contribution of nuclear IL-37 to suppress inflammation and highlights the importance of the extracellular function of IL-37 to mediate beneficial actions after SCI.

Keywords: interleukin 37, inflammation, neuroprotection, spinal cord injury, treatment

Introduction

Interleukin 37 (IL-37 or IL1F7) is an anti-inflammatory cytokine of the IL-1 family (Dunn et al., 2001). Surprisingly, IL-37 is the only member of the IL-1 family for which mouse homolog has not been found yet. Human *IL37* gene is 3617 base pair (bp) long and has three different cleavage sites that generates five different isoforms (IL-37a to IL-37e) (Boraschi et al., 2011; Dinarello and Bufler, 2013; Taylor et al., 2002). From all of the isoforms, IL-37b (isoform 1) is the best characterized and largest isoform containing five of the six available exons (Boraschi et al., 2011). IL-37 has been found in a variety of normal cells and tissues including natural killer cells, stimulated B cells, monocytes, skin keratinocytes, epithelial cells, thymus, lung, colon, uterus, and bone marrow (Wang et al., 2018). However, some isoforms seem to be enriched in some tissues against others (Boraschi et al., 2011).

Since IL-37 is not present in mice, transgenic mice expressing the full-length of the human *IL37b* cDNA were generated (hIL-37Tg) (Nold et al., 2010). In these transgenic mice, the expression of the human *IL37* gene is driven by a constitute cytomegalovirus (CMV) promoter. However, due to untranslated region-independent control elements, levels of IL-37 mRNA are very low in physiological conditions. These instability elements seem to be present in exon 5, as exon 5 deletion significantly increases mRNA stability (Bufler et al., 2004). Only upon stimulation with an inflammatory challenge, the *IL37* mRNA stability increases and the protein is finally synthetized (Boraschi et al., 2011).

Increasing levels of IL-37 by genetic knock-in or injection of recombinant proteins have been demonstrated to produce a beneficial effect on a wide range of diseases such as sepsis (Bulau et al., 2011), hepatitis (Bulau et al., 2011), colitis (McNamee et al., 2011), myocardial infarction (Wu et al., 2014), and metabolic syndrome (Ballak et al., 2014). As common feature in all these studies, IL-37 protection is associates with decreased concentrations of inflammatory cytokines and chemokines. Previous results from our group revealed for the first time that IL-37 has a beneficial effect after SCI (Coll-Miro et al., 2016). In this case, transgenic expression of the human *IL37* gene in mice decreased levels of pro-inflammatory cytokines and attenuated accumulation of immune cells in the injured spinal cord. These effects on inflammatory response after injury led to increased tissue preservation and improved locomotor recovery (Coll-Miro et al., 2016). Not only knock-in mice showed a beneficial effect after SCI, administration of recombinant IL-37 (rIL-37) into the lesion site of wild-type (WT) mice also conferred protection against functional disabilities (Coll-Miro et al., 2016).

To perform its beneficial effects, extracellular IL-37 binds to the interleukin 18 receptor alpha (IL-18Rα) and recruits the co-receptor interleukin 1 receptor 8 (IL-1R8, also known as SIGGIR) forming a tripartite complex. This complex triggers a signaling cascade that concludes with an anti-inflammatory effect, mainly by inhibition of Fyn and TAK1 kinases (Nold-Petry et al., 2015). Although it is assumed that IL-37 acts primarily as a secreted mediator by binding to extracellular receptors, as other cytokines of the IL-1 family, IL-37 can also be translocated to the nucleus. For that purpose, IL-37 needs to be processed by caspase-1, which allows its binding to Smad3 (Sharma et al., 2008). IL-37-Smad3 complex translocates to the nucleus through the nuclear pore. Once in the nucleus, IL-37 may modulate gene expression to produce anti-inflammatory effects (Sharma et al., 2008). Therefore, extracellular and nuclear

pathways of IL-37 lead to reduction of the inflammatory response by down-regulation of pro-inflammatory cytokines and/or up-regulation of anti-inflammatory cytokines. However, since experiments to determine the nuclear function of IL-37 were done inhibiting capase-1, which is also involved in the maturation and release of other pro-inflammatory cytokines such as IL-1β and IL-18 (see chapter 2), the specific contribution of the nuclear function of IL-37 remains to be elucidated (Bulau et al., 2014).

In the present chapter, we assessed for the first time the importance of nuclear IL-37 in reducing cytokine levels. These results were included in a recent publication (Li et al., 2019). Moreover, we also studied to what degree the beneficial actions of IL-37 in SCI are mediated by its extracellular and nuclear functions.

Materials and Methods

Approvals

All the experiments were approved by the Ethics Committee on Animal and Human Experimentation from the Universitat Autonoma de Barcelona (CEEAH: 4057) and followed the European Communities Council Directive 2010/63/EU. Methods from each procedure were carried out in accordance with approved guidelines.

Transgenic mice

hIL-37Tg and hIL-37D20ATg mice were kindly provided by Dr. Charles Dinarello from the University of Colorado (USA) and were generated as previously described (Nold et al., 2010). IL-1R8KO mice were kingly provided by Dr. Cecilia Garlanda from the Humanitas Clinical and Research Center (Italy) and were generated as previously described (Garlanda et al., 2004). hIL-37Tg and IL-1R8KO mice were breed in our animal facilities to produce the double transgenic hIL-37TgxIL-1R8KO mice in homozygosis.

Genotyping

DNA was obtained from the mice tails at 3-4 weeks after birth. Protocol and chemicals were obtained from DANAGEN. Genotyping of *Il1r8* gene was performed by PCR using the following primers: 25/10N 5'- ATC TTT CAG CCA CTG CAC TGA -3'; 5mAcp 5'- GTC TGT GAC ATG GCC CCT AAT -3'; PGK 5'- CTG CTC TTT ACT GAA GGC TC -3'. Genotyping of human *IL37* gene mice was performed by qPCR using the following primers: IL-37f 5'- CTT AGA CCC GGC TGG AAG -3'; IL-37r 5'- TGT GAT CCT GGT CAT GAA TGC T-3'. *Il2* was used as a loading control.

Spinal cord injury surgery

Spinal cord injury procedure was performed according to described protocols (Amo-Aparicio et al., 2018). Adult (8 – 10 weeks old) female mice were anesthetized by intramuscular injection with a mixture of ketamine (90 mg/kg) and xylazine (10 mg/kg). After performing laminectomy at 11^{th} thoracic vertebrae, the exposed spinal cord was contused using the Infinite Horizon Impactor device (Precision Scientific Instrumentation). A force of 60 kdynes and a tissue displacement of 450 – 550 µm were applied. For those experiment in which rIL-37 was injected directly into the spinal cord, a 50 kdynes contusion and a tissue displacement of 400 – 500 µm were applied.

Gene expression (qPCR)

At different time points after SCI, mice receive an intraperitoneal injection of sodium pentobarbital (Dolethal). Blood was removed by perfusion with 60 mL of 0.9 % NaCl in distillated water. A segment of 0.6 cm-length of the spinal cord centered into the injury site was taken from each mouse and frozen in liquid nitrogen. Samples were homogenized with QIAzol lysis reagent and TissueRuptor (Qiagen). RNA was purified using a RNeasy Lipid Tissue kit (Qiagen) following user's guide protocol. Quantitative PCR (qPCR) was performed using a MyiQ Single-color Real-time PCR Detection System (BIO-RAD). Taqman primers for mouse *Il-18ra, Il-1r8, Gapdh* were pursched from ThermoFisher Scientific. *Gapdh* was used as a housekeeping gene. Expression levels of targets mRNAs were normalized to the relative ratio of expression of the *Gapdh* gene and naïve condition following the ΔΔCT method. 4 mice per group were used.

Administration of recombinant IL-37

Recombinant IL-37 proteins (rIL-37) were administered after spinal cord injury either instraspinally (i.s.) or intraperitoneally (ip). For intraspinal injection, 1 µL containing 100 ng of recombinant IL-37 (rIL-$37_{46\text{-}218}$) was injected in the injured spinal cord at 5 minutes after contusion injury. rIL-$37_{46\text{-}218}$ was provided by Dr. Charles Dinarello. Intraspinal injections were performed using a glass micropipette (Fisher Scientific) coupled to a 10 µL Hamilton syringe (Hamilton Co). Injections were controlled by a 310 Plus automatic injection (KD Scientific) with a 2 µL/min rate. After injection, the tip of the micropipette was maintained inside the cord tissue for 3 min to avoid liquid reflux. Sterile saline solution was injected as control using the same protocol.

Intraperitoneal injections of 1µg of IL-$37_{46\text{-}218}$ were performed at 1 hour after injury as a single dose or repeated daily for 3 or 7 days. Moreover, two mutated forms of rIL-37 that cannot dimerize (IL-37D73K and IL-37Y85A) (Eisenmesser et al., 2019) were tested at single dose 1 hour post-injury. Saline solution was injected as control using the same protocol.

Cell culture

Bone marrow cells were obtained from femurs and tibia of mice after euthanasia. Cells were flushed out using a 21G needle-syringe with 5 ml of RPMI medium (ThermoFisher Scientific) supplemented with Penicillin/Streptomycin (P/S) (Sigma-Aldrich). Cells were passed through a 70 µm-cell strainer and quantified. 4 millions of cells in 2 ml of RPMI + P/S were seeded in each well of a 24-well plate. After 2 hours, the medium was aspirated, and non-adherent cells were removed. Adherent cells were cultured with RPMI + P/S and 10 % of FBS (Sigma-Aldrich) in a humidified atmosphere with 5 % CO_2 and 37 °C. Cells were stimulated with LPS (Sigma-Aldrich) at 1 µg/ml. Supernatants were removed at 6 and 24 hours after the stimulation and stored at -80°C. 5 mice per group were used.

ELISA

ELISA DuoSet kits for TNFa, IL-6, and KC (R&D Systems) were used following the manufacturer's protocol. 96-well plates were coated with respective capture antibodies the day before. Samples were incubated for 2 hours at room temperatue. Detection antibodies and

streptavidin-HRP were added. TMB ELISA (eBioscience) was used as substrate solution. Results were measured in a microplate reader (Bio-Tek).

Cytokine array

At 6 hours after LPS stimulation, RNA from bone marrow adherent cells in culture was extracted RNeasy Lipid Tissue kit (Qiagen) as reported above. Reverse transcription was performed using the RT2 first strand kit (Qiagen) following the recommended protocol. Samples from 5 mice were polled and added to the RT2 Profiler PCR cytokine array (Qiagen). At least 1500 ng of cDNA were added to each plate. Results were analyzed using the software tools provided by the manufacturer. Only genes significantly up or down regulated 2-fold, or more, were selected.

Functional Assessment

Locomotor recovery after SCI was evaluated at 1, 3, 5,7, 10, 14, 21, and 28 days post-injury (dpi) in an open-field using the nine-point Basso Mouse Scale (BMS) (Basso et al., 2006). BMS evaluation was performed researchers who were blinded to the experimental groups. Consensus score between two researchers was taken. At least 6 mice per group were used.

Histology

At 28 dpi mice were perfused with 4 % paraformaldehyde in 0.1M phosphate buffer. 0.6 cm of spinal cord centered into the lesion site were removed from each mouse and cryoprotected with 30% sucrose in 0.1 M phosphate buffer saline (PBS) at 4°C. Samples with 15 µm thick were cut in the cryostat and picked up with a glass slide. Samples were arranged following a serial distribution. Adjacent sections in the same slide were 150 µm apart. After graded dehydration, sections were placed in a 1 mg/ml Luxol Fast Blue (LFB) (Sigma-Aldrich) solution in 95% ethanol and 0.05% acetic acid and left overnight at 37°C. Section were then washed in 95% ethanol and distilled water before clearing with 0.5 mg/ml of Li_2CO_3 in distilled water for 1.5 min. After several washes, sections were dehydrated and mounted in DPX mounting media (Sigma-Aldrich). After fixation, the epicenter of the contusion was localized by determining the tissue section with the lowest LFB stained area. NIH ImageJ software was used to perform the quantifications.

Statistics

All analyses were conducted through GraphPad Prism v7. Functional follow-ups for BMS score were analyzed using two-way ANOVA with repeated measures (RM) with Bonferroni's post hoc correction. Cytokine *in vitro* production was analyzed using two-way ANOVA with Tukey's post hoc correction. Receptors expression after SCI was analyzed using one-way ANOVA with Dunnett's post hoc correction. Luxol Fast Blue measures were analyzed using multiple t-test comparisons with Holm-Sidak's post hoc correction. Results were expressed as mean ± SEM and differences were considered significant at $p < 0.05$.

Results

Nuclear IL-37 limits the cytokine production after LPS stimulation

Similar to IL-1α and IL-33, IL-37 is able to interact with selective extracellular receptors but also to translocate to the nucleus upon its cleavage by capase-1. However, it remains unknown to what extend the nuclear function of IL-37 limits inflammation. To address this aim, we used a transgenic mouse expressing a mutation on the capase-1 cleavage site (D20A) of the human *IL37* gene (hIL-37D20ATg). In these transgenic mice, IL-37 cannot translocate to the nucleus, and therefore, it can only act through the extracellular pathway.

We first stimulated bone marrow adherent cells from WT, hIL-37Tg, and hIL-37D20ATg mice with LPS for 6 and 24h. We measured the cytokine concentration of TNFα (Fig. 1A), IL-6 (Fig. 1B), and KC (Fig. 1C) at the supernatant. We found that levels of all these three cytokines progressively increased over time in the supernatants from WT bone morrow cells (Fig. 1). As expected, cytokine levels in the bone-marrow supernatants from hIL-37Tg mice were significantly reduced in comparison with WT mice at these two time points, confirming the anti-inflammatory effects of IL-37 (Fig. 1). However, the supernatants from bone-marrow cells isolated from hIL-37D20ATg mice showed a different pattern. We found that hIL-37D20ATg cells failed to reduce the production of cytokines at 6 hours post-injury, indicating that the nuclear function of IL-37 is critical for this early anti-inflammatory effect. However, at 24 hours upon LPS stimulation, hIL-37D20ATg cells markedly reduced the levels of pro-inflammatory cytokines, being comparable to the anti-inflammatory effect mediated by the natural hIL-37Tg cells. These results demonstrate that the nuclear function of IL-37 is important to limit cytokine levels at early stages after the inflammatory challenge. However, they also shown that IL-37 can suppress cytokine production even in the absence of nuclear IL-37 at later stages. This suggests that the extracellular function of IL-37 is likely the main mechanisms of this cytokine to alleviate inflammation at long term.

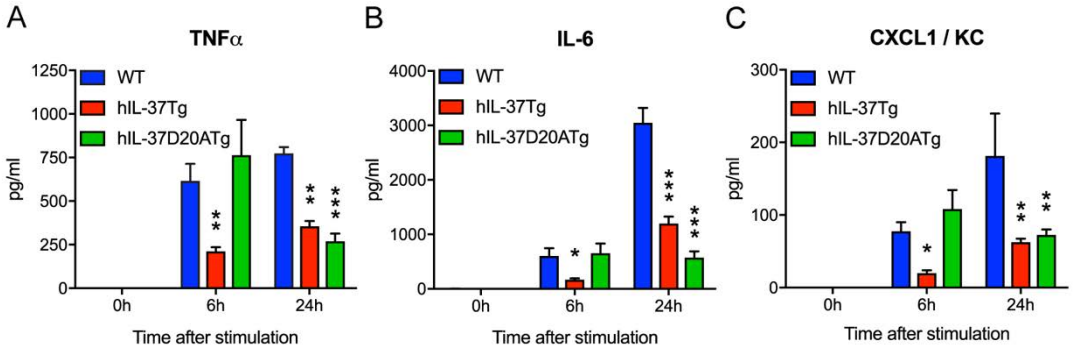

Figure 1: Cytokine production of bone-marrow macrophages from WT, hIL-37Tg and hIL-37D20ATg mice in culture. Levels of TFNα (A), IL-6 (B), and KC (C) were measured by ELISA at different time points after LPS stimulation. Data are represented as mean ± SEM. N = 5. * p < 0.05, ** p < 0.01, *** p < 0.001 against WT from each point. Two-way ANOVA with Tukey's post hoc correction.

Nuclear IL-37 produces changes in gene expression

Since the extracellular pathway of IL-37 seems to be inactive in the first hours after injury, we sought to determine which mechanisms are activated by IL-37 after translocation to the nucleus. For this purpose, we cultured bone marrow adherent cells from hIL-37Tg and hIL-37D20ATg mice and stimulated them with LPS for 6 hours. Afterwards, we collected the RNA and performed a cytokine and chemokine PCR array.

We found that, from the 84 gene evaluated, only 8 were differentially expressed between hIL-37Tg and hIL-37D20ATg bone marrow cells (Fig. 2). Indeed, these 8 genes were downregulated in hIL-37D20ATg as compared to hIL-37Tg bone morrow cells, suggesting that they were induced by nuclear translocation of IL-37. These 8 genes were *Tnfsf11* (tumor necrosis factor ligand superfamily member 11), *Tnfrsf11b* (tumor necrosis factor receptor superfamily member 11b), *Cxcl5* (CXC motif chemokine 5), *Cxcl12* (stromal cell-derived factor 1), *Lif* (leukemia inhibitory factor), *Cxcl7* (CXC motif chemokine ligand 7), *Cxcl9* (CXC chemokine 9), and *Il4* (interleukin 4). Although the contribution of many of these molecules to inflammation is not clear yet, some factors such as LIF, CXCL12, and IL-4 have been proved to limit inflammation in several conditions, including SCI (Francos-Quijorna et al., 2016; Kerr and Patterson, 2004, 2005; Stewart et al., 2017).

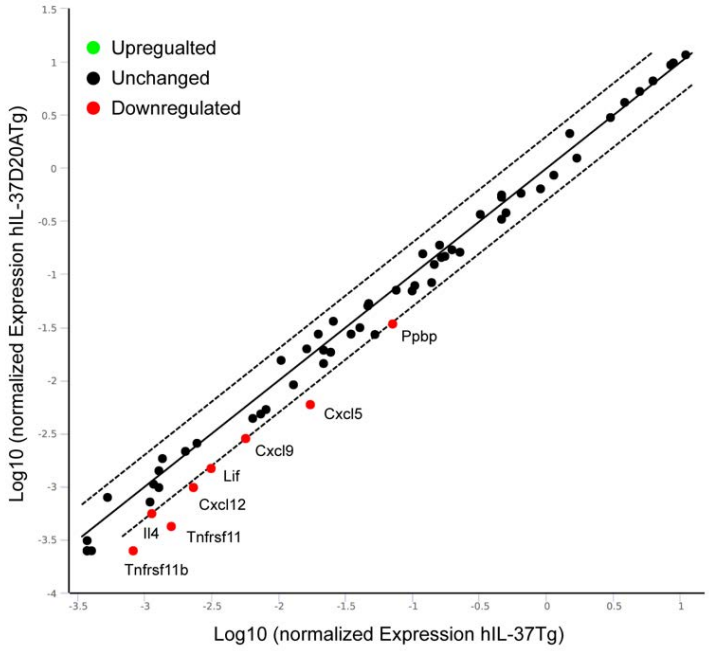

Figure 2: Differential gene expression between hIL-37Tg and hIL-37D20ATg. The expression of 84 genes were measured in bone-marrow macrophages from hIL-37Tg and hIL-37D20ATg mice at 6 hours after LPS stimulation. Central line indicates unchanged gene expression. N = 5 pooled. Genes with normalized relative expression bigger than 2 (dotted lines) were selected as differentially expressed between both conditions.

IL-37 can mediate beneficial effects after SCI in absence of nuclear translocation

To assess to what degree the nuclear function of IL-37 is important to mediate beneficial actions after SCI, we performed contusion injury in hIL-37D20ATg and WT mice and evaluated the recovery of the locomotor task on an open field for 28 days. We found that hIL-37D20ATg

mice showed significant improvement in locomotor performance after SCI from day 10 post-injury (Fig. 3A). At the end of the follow up, almost all of the hIL-37D20ATg mice showed plantar placement of the paw. Moreover, 50% of them were able to perform occasional or frequent stepping (final BMS score 3,6). In contrast, WT mice showed slight or extensive movement of the hindlimbs and only ~20% of them reached plantar placement of the paw without stepping (final BMS score 2,3) (Fig. 3B). Histological evaluation of the spinal cords harvested at 28 days post-injury also revealed that hIL-37D20ATg mice were protected against myelin loss at the injury epicenter and at rostral and caudal regions (Fig. 3C,D). These results demonstrate that, similar to what we found *in vitro*, IL-37 can mediate beneficial actions in SCI even in the absence of its nuclear translocation.

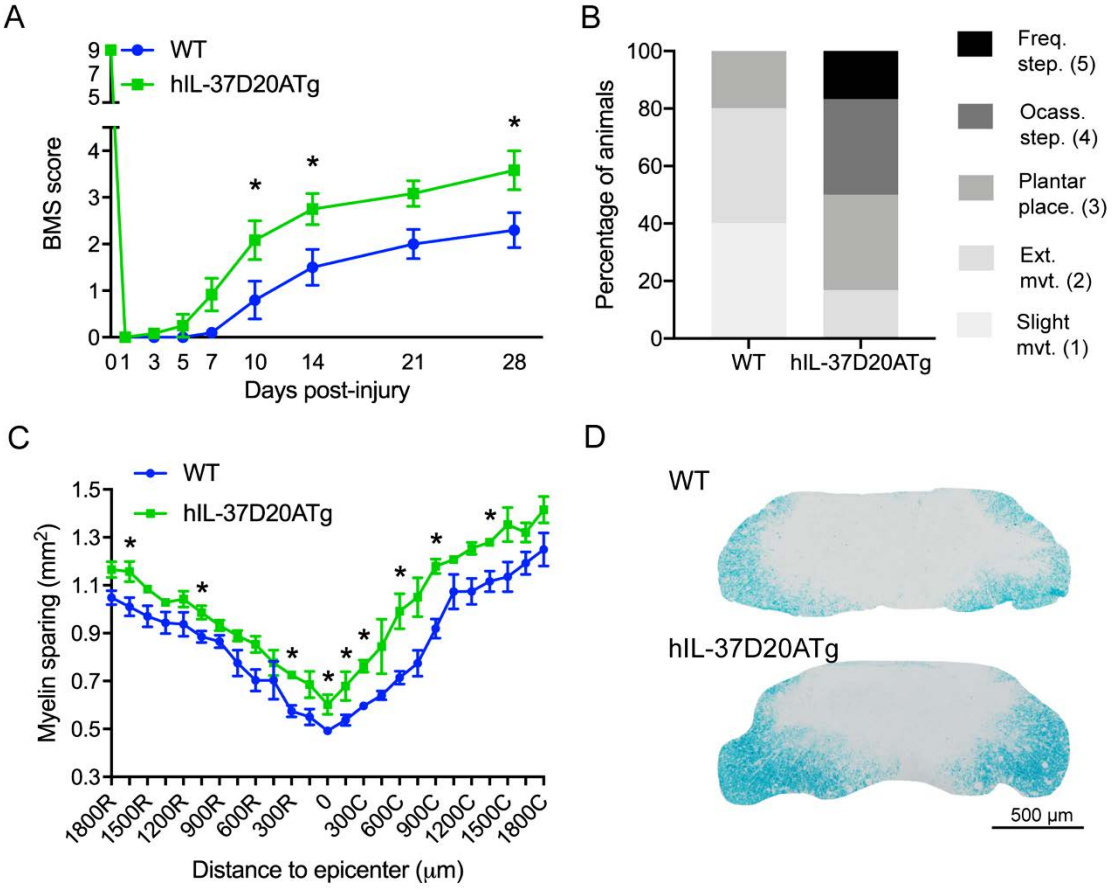

Figure 3: Effect of avoiding nuclear translocation on the protective effect of IL-37 after SCI. (A) BMS score of hIL-37D20ATg mice after SCI. WT mice were used as control. (B) Functional distribution of mice at 28 dpi. BMS values of each type of movement are indicated in parenthesis. (C) Myelin preservation in the lesion area obtained by LFB staining. (D) Representative micrographs showing myelin sparing at the injury epicenter. Data are represented as mean ± SEM. N ≤ 6. * p < 0.05. Two-way RM-ANOVA with Bonferroni's post hoc correction for (A) and multiple t-test comparisons with Holm-Sidak's post hoc correction for (C).

Components of the extracellular pathway are expressed after SCI

Since the experiments reported above suggested that the extracellular function of IL-37 is likely to be critical to confer protection against functional deficits and myelin loss after SCI, we

characterized the dynamics of gene expression of the IL-37 surface receptor components (IL-18Rα and IL-1R8) in the spinal cord from WT mice.

qPCR analysis revealed that the transcripts for *Il18ra* are found at very low levels in the spinal cord in physiological conditions. Levels increased progressively following injury, reaching maximal levels at 14 days post-injury, the latest time point evaluated (Fig. 4A). The expression of *Il1r8* was also found at low levels in physiological conditions. Transcript for *Il1r8* increased ~2 fold at 3 days after lesion but returned to basal levels at later time points. (Fig. 4B).

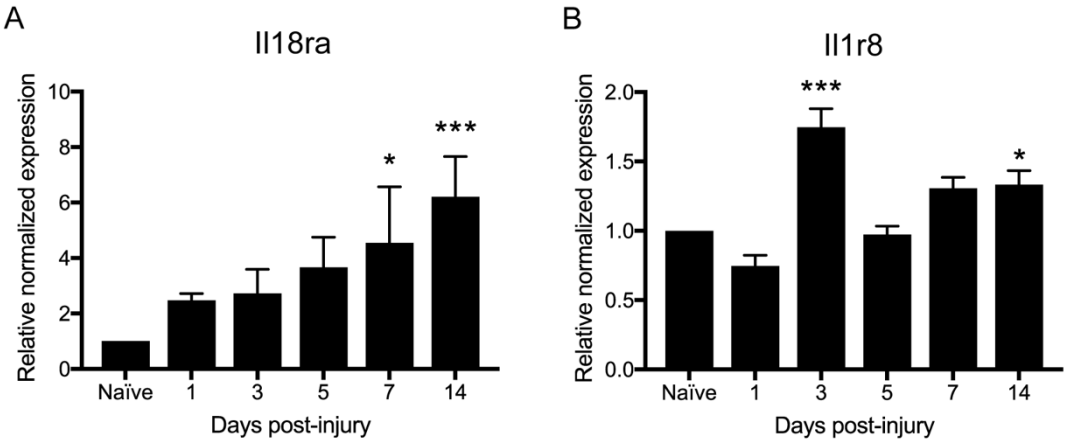

Figure 4: Relative gene expression of IL-18Rα (A) and IL-1R8 (B) at different times points after SCI. Data are represented as mean ± SEM. N = 4. * p < 0.05, *** p < 0.001 against naïve. One-way ANOVA with Dunnett's post hoc correction.

Blocking IL-37 extracellular function reduces the protective effects of IL-37 after SCI

We next assessed the contribution of extracellular IL-37 after spinal cord contusion injury. For this purpose, we crossed hIL-37Tg mice with mice lacking IL-1R8 co-receptor (IL-1R8KO). This double transgenic mouse (hIL-37TgxIL-1R8KO) expresses IL-37 in homozygosis but this cytokine can only act at the nuclear level since IL-1R8, key component of the surface receptor, is genetically delated. Gene deletion of IL-1R8 but not IL-18Rα was chosen to assess the importance of the extracellular IL-37 function in mice since IL-18Rα is also the receptor for IL-18, and thus, mice lacking IL-18Rα would also have affected IL-18 signaling.

We first induced SCI in IL-1R8KO mice and WT littermates. Results revealed that the lack of IL-1R8 did not translate into any change at functional (Fig. 5A,B) neither histological (Fig. 5C,D) levels after SCI.

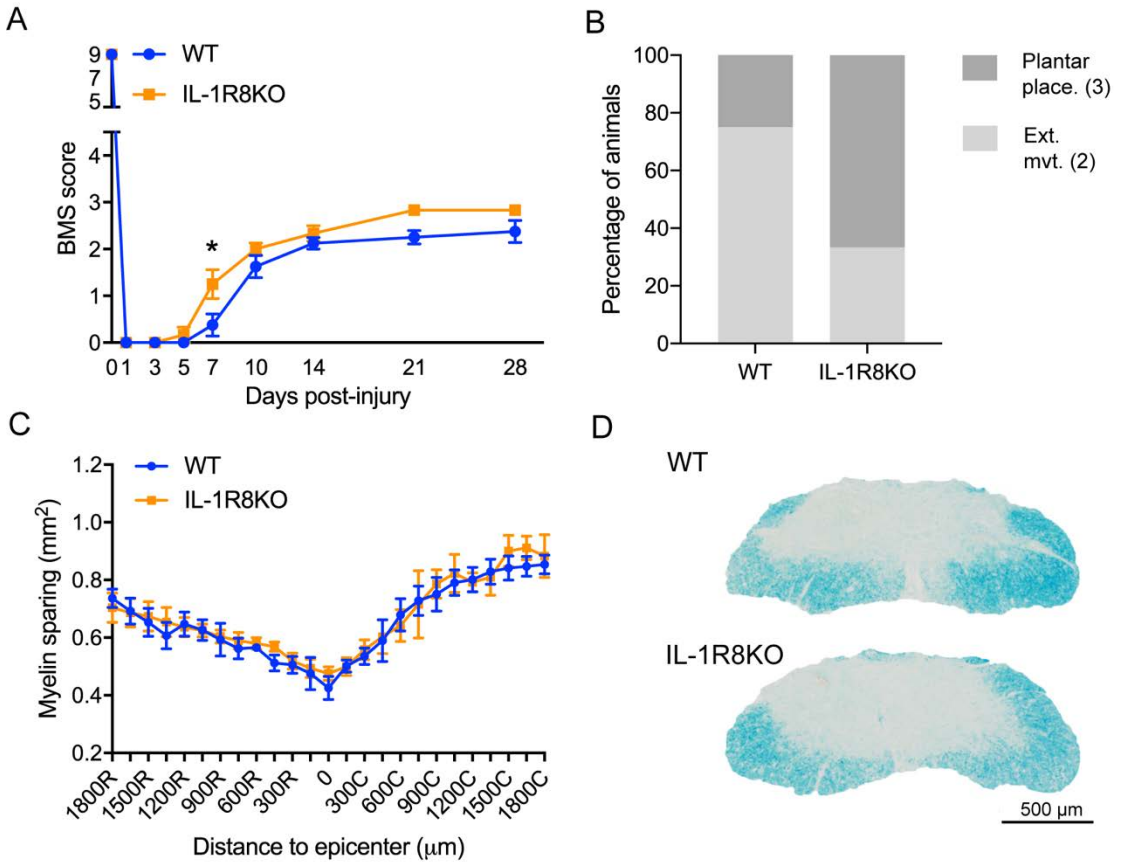

Figure 5: Characterization of IL-1R8KO mice response to SCI. (A) BMS evaluation of locomotor function for 28 days. WT mice were used as control. (B) Functional distribution of mice at 28 dpi. BMS values of each type of movement are indicated in parenthesis. (C) Myelin preservation in the lesion area obtained by LFB staining. (D) Representative micrographs showing myelin sparing at the injury epicenter. Data are represented as mean ± SEM. N ≤ 6. * p < 0.05. Two-way RM-ANOVA with Bonferroni's post hoc correction for (A) and multiple t-test comparison with Holm-Sidak's post hoc correction for (C).

Knowing that IL-1R8 is not involved in the physiopathology of SCI in C57BL/6J mice, we then performed spinal cord contusion injuries in hIL-37Tg, hIL-37TgxIL-1R8KO, and WT littermates. In agreement with our previous reports (Coll-Miro et al., 2016), hIL-37Tg mice showed significant improvement in the BMS score in comparison with WT littermates (Fig 6A). Bonferroni's post-hoc test revealed significant differences in the BMS score starting at day 14 post-injury and remaining enhanced until the end of the follow up (Fig. 6A). At this time point, all hIL-37TG mice showed plantar placement of the paw with weigh support and ~50% of them displayed occasional plantar stepping (final BMS score 3.5) (Fig. 6B)

Interestingly, we found that the beneficial actions of IL-37 on functional recovery after SCI were completely lost in the lack of IL-1R8 co-receptor. This indicates that the extracellular function of IL-37 is critical for mediating helpful effects on neurological recovery. Indeed, hIL-37TgxIL-1R8KO mice showed the same progression than WT littermates on locomotor skill (Fig. 6A). These mice were able to do extensive movement of the hindlimbs and ~50% of them displayed plantar placement of the paw, but not stepping (final BMS score of 2.5 and 2.8, respectively) (Fig. 6B). Importantly, in comparison with respective WT controls, BMS score achieved by hIL-37Tg mice after SCI was very similar to that observed in IL-37D20ATg mice (Fig.

3A). These results suggest the extracellular, but not nuclear IL-37 function is critical to limit functional deficits after SCI.

In line with functional outcomes, spinal cord tissue sections from hIL-37Tg mice also revealed significant greater myelin sparing at the core of the lesion and in some rostral and caudal areas (Fig. 6C,D). Again, the protective effects of IL-37 on myelin preservation were completely lost in the lack of IL-1R8 (Fig. 6C,D). Overall, these results evidence that extracellular function of IL-37 is crucial for mediating the beneficial actions of this cytokine in SCI.

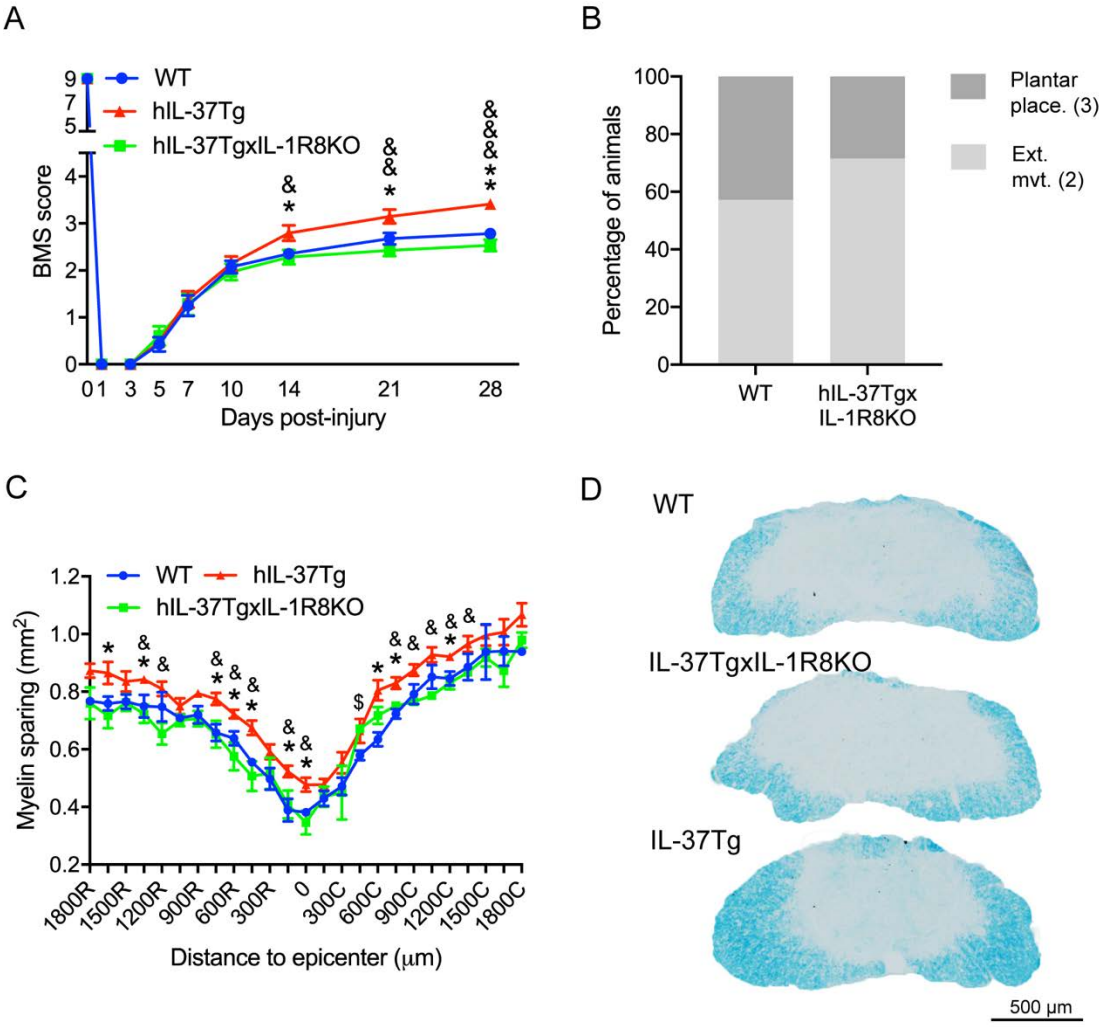

Figure 6: Effect of IL-1R8 gene deletion on the protective effect of IL-37. (A) BMS score of hIL-37TgxIL-1R8KO mice after SCI. WT mice were used as control. (B) Functional distribution of mice at 28 dpi. BMS values of each type of movement are indicated in parenthesis. (C) Myelin preservation in the lesion area. (D) representative micrographs showing the epicenter. Data are represented as mean ± SEM. N = 10. * p < 0.05, ** p < 0.01 hIL-37Tg against WT. & p < 0.05, && p < 0.01, &&& p < 0.001 hIL-37TgxIL-1R8KO against WT. $ p < 0.05 WT against hIL-37TgxIL-1R8KO. Two-way RM-ANOVA with Bonferroni's post hoc correction for (A) and multiple t-test comparison with Holm-Sidak's post hoc correction for (C).

The protective actions of extracellular IL-37 are mediated centrally but not peripherally

Finally, we assessed whether extracellular IL-37 mediates beneficial action after SCI by acting locally in the lesion site or peripherally. For this purpose, we injected recombinant human IL-37 protein (rIL-37) either directly into the core of the lesion or intraperitoneally since IL-37 is unlikely to reach the lesion site at sufficient therapeutic amounts when infected systemically. The rIL-37 used form lacks the first 45 aminoacids of the IL-37 sequence (rIL-$37_{46\text{-}218}$) which are crucial for the caspase-1 processing and its subsequent interaction with Smad3. Therefore, rIL-$37_{46\text{-}218}$ is unable to translocate to the nucleus and can only signal extracellularly.

Similar to our previous report (Coll-Miro et al., 2016), we found that intraspinal administration of rIL-$37_{46\text{-}218}$ into the lesion site after SCI promoted significant improvement in locomotor skills, as compared to those mice treated with saline (Fig. 7A). Importantly, rIL-$37_{46\text{-}218}$ did not resulted in functional recovery when injected into the injury site of IL-1R8KO mice (Fig. 7B), further highlighting the importance of the extracellular route to mediate neurological improvement.

We then studied the effects of rIL-$37_{46\text{-}218}$ when injected intraperitoneally. We found that single administration of rIL-$37_{46\text{-}218}$ 1h post-injury did not enhance motor skills (Fig. 7C). Similarly, daily administration of rIL-$37_{46\text{-}218}$ for 3 or 7 days after injury also failed to improve locomotor outcomes (Fig. 7C). Since it has been recently reported that IL-37 dimerization is able to compromise the anti-inflammatory properties of this cytokine (Ellisdon et al., 2017), we wanted to elucidate whether the lack of therapeutic actions of IL-37 when injected systemically was due to dimers formation. For this purpose, we tested the effects of two mutant monomeric forms of IL-37 (rIL-37D73K and rIL-37Y85A) that cannot dimerize (Eisenmesser et al., 2019). We observed that the mutant monomeric forms of IL-37 did not improve functional recovery when injected 1 hour after SCI (Fig 7D). Altogether, results here presented evidence that beneficial effects of extracellular IL-37 are mediated by acting in the central nervous system but not peripherally.

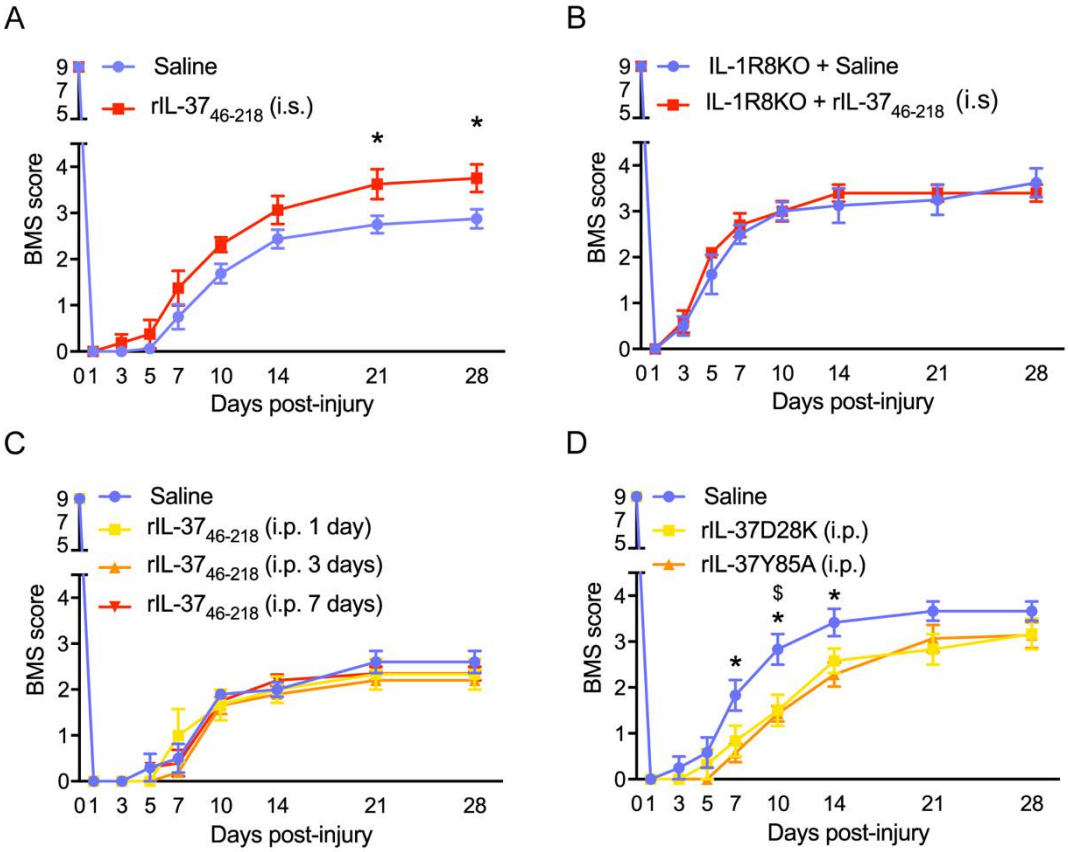

Figure 7: Effect of central and peripheral administration of rIL-7 after SCI. Representative BMS evaluation of WT mice receiving a single intraspinal (A), a single intraperitoneal or repeated (C) injections of rIL-37$_{46-218}$. (B) Representative BMS evaluation of IIL-1R8KO mice receiving a single intraspinal injection of rIL-37$_{46-218}$. (D) Representative BMS evaluation of mice receiving a single intraperitoneal injection of truncated rIL-37D73K and rIL-37Y85A. Data are represented as mean ± SEM. N ≤ 6. * p < 0.05. Two-way RM-ANOVA with Bonferroni's post hoc correction.

Discussion

Spinal cord injury is a devastating neurological disease with consequences for the physical and social well-being of patients. Final impairments are due to tissue damage caused by the initial trauma to the spinal cord, but also, to a cascade of inflammation-mediated degenerative changes, known as secondary damage, that occur in the lesioned spinal cord days after the insult (Oyinbo, 2011). This is especially detrimental in the central nervous system due to its limited ability for spontaneous self-repair. Unfortunately, there are no effective therapies to treat acute SCI in humans. Since inflammation has a key contribution to secondary damage, targeting inflammation could be a useful approach to prevent tissue and functional loss after acute SCI (David et al., 2012).

IL-37 has emerged as a beneficial agent for the treatment of inflammatory-mediated diseases. The first *in vivo* study showing the functional effects of IL-37 was done in transgenic mice exposed to systemic injection of LPS (Nold et al., 2010). This study revealed that hIL-37Tg mice had decreased circulating cytokines, as well as, attenuated acidosis, hyperkalemia, hepatitis, dehydration and hypothermia upon systemic LPS injection compared to WT mice (Nold et al.,

2010). Since then, IL-37 was postulated as a cytokine with a potent function on the suppression of the inflammatory response. The anti-inflammatory function of IL-37 have been observed in other animal models of disease such as colitis (McNamee et al., 2011), hepatitis (Bulau et al., 2011), metabolic syndrome (Ballak et al., 2014), and myocardial infarction (Wu et al., 2014). A previous report from our group demonstrated that transgenic expression of human IL-37 in mice limited inflammation after SCI and protected against secondary tissue damage, highlighting the protective actions of this cytokine in neurotrauma (Coll-Miro et al., 2016).

IL-37 mediates its biological effects by acting as a dual-function cytokine since IL-37 signals via the extracellular receptor complex IL-18Rα/IL-1R8, but it also translocates to the nucleus. Recent studies revealed that extracellular IL-37 has a pivotal role for limiting inflammation in cell culture conditions and after *in vivo* injection of LPS (Nold-Petry et al., 2015). Although previous studies using capase-1 inhibitors suggested that nuclear IL-37 also exerted anti-inflammatory actions (Bulau et al., 2014), it is important to remark that capase-1 is also needed for the processing and maturation of other molecules, such as the pro-inflammatory cytokines IL-1β and IL-18.

In the present chapter, we took advantage of the hIL-37D20ATg mice generated by Charles Dinarello (Li et al., 2019). This mouse expresses of a mutated form of human IL-37 that has resistance to capase-1 cleavage. Since the activity of capase-1 is not altered in the cells of the hIL-37D20ATg mouse this is an ideal tool to dissect out the role for nuclear IL-37 in inflammation without changing other cytokines related with capase-1. We found that IL-37D20, but not the natural IL-37, failed to reduce the concentration of KC, IL-6, and TNFα in bone marrow cell supernatants at 6 hours after LPS stimulation, indicating that nuclear internalization of IL-37 was critical for limiting this early cytokine production. This is likely due to the ability of IL-37 to modulate gene expression after nuclear translocation since we found that at least 8 genes were significantly induced by nuclear IL-37 at 6h after LPS challenge. Among them IL-4, CXCL12, and LIF are known to exert potent immunomodulatory effects and to mediate beneficial actions after SCI (Francos-Quijorna et al., 2016; Kerr and Patterson, 2004, 2005; Stewart et al., 2017). The transcripts for KC, IL-6, and TNFα were not altered by nuclear IL-37 despite protein levels were markedly reduced. Since both RNA and protein levels were assessed at 6 hours after LPS stimulation, and RNA synthesis proceeds protein production, it is possible that the changes in RNA levels for these cytokines could have occurred at earlier time points.

It is noteworthy to mention that the importance for nuclear IL-37 to suppress inflammation seems to be only specific for the first hours after the inflammatory challenge. IL-37D20A was able to reduce the levels of pro-inflammatory cytokines at 24 hours after LPS stimulation, in the lack of nuclear translocation. This may indicate that action of IL-37 in the extracellular compartment is crucial to mitigate inflammation at later stages of the inflammatory stimuli. Indeed, the effects of IL-37 and IL-37D20A on limiting cytokine production at 24h after LPS challenge were very similar, despite IL-37D20A did not affect cytokine levels during the first 6 hours. This rebound anti-inflammatory effect observed in hIL-37D20ATg cells at 24h after LPS exposure could be due to the greater release of IL-37 to the extracellular milieu when nuclear translocation is prevented. These results were included in a recent publication demonstrating the role for nuclear IL-37 on inflammation (Li et al., 2019).

In the present chapter, we also deciphered the contribution of nuclear and extracellular IL-37 to SCI. We found that hIL-37D20ATg mice were protected against neurological impairments and myelin loss after SCI. Indeed, in comparison with their respective WT controls, functional recovery of hIL-37D20ATg mice after SCI was very similar to hIL-37Tg mice. Since IL-37D20A cannot translocate to the nucleus, this suggest that the beneficial effects of IL-37 are mediated extracellularly. Indeed, we found that the components of the IL-37 receptor are expressed in the spinal cord of WT mice at physiological conditions, and increased after SCI. We were unable to study the cell source of IL-1R8 since the commercial antibodies for this receptor does not work properly in mouse tissue. However, this co-receptor is likely to be expressed in immune cells and/or astrocytes since its transcripts are increased after injury, coinciding with the infiltration of macrophages and proliferation of microglia. Indeed, our RNA-seq analysis performed from microglia and macrophages isolated from the injured spinal cord (see chapter 4), revealed that IL-1R8 levels in microglia are ~5 fold higher than in macrophages, suggesting that extracellular IL-37 preferably acts on microglia cells in SCI.

The key importance of extracellular IL-37 to protect against functional and myelin loss after SCI was further confirmed by using hIL-37TgxIL-1R8KO mice and recombinant IL-37 proteins. We found that the beneficial effects of IL-37 in neurotrauma were completely abolished in the lack of IL-1R8 co-receptor. Contrarywise, intraspinal administration of an rIL-37 form that can only act extracellularly (rIL-$37_{46\text{-}218}$) promoted functional recovery in WT mice but not in IL-1R8KO mice. We discard that the failure of IL-37 to promote beneficial actions after SCI in the lack of IL-1R8 was due to some contribution of this receptor to SCI physiopathology because IL-1R8KO mice did not display any alteration in functional and histological outcomes after contusion injury. Therefore, in contrast to cell culture conditions in which nuclear and extracellular IL-37 limits inflammation, after SCI only the extracellular function of this cytokine seems to be important to mediate protection.

Another important issue we addressed in this chapter is whether the beneficial actions of IL-37 are mediated by modulating the activity of the CNS cells directly at the lesion site, or by regulating the activity of immune cells in the periphery before entering into the injured spinal cord. Since rIL-37 is unlikely to reach into the lesioned CNS, or at least at therapeutic amounts, despite the disruption of the blood-brain barrier, we injected rIL-37 systemically to address the peripheral contribution of this cytokine. Results obtained revealed that intraperitoneal administration of IL-37 did not lead to beneficial effects after SCI. We discard that the lack of effectivity of systemic delivery was due to the formation of dimers, which are known to limit the anti-inflammatory features of IL-37 (Ellisdon et al., 2017), because administration of two monomeric rIL-37 forms that cannot dimerize also failed to protect against neurological deficits. We also discard that the lack of efficacy of systemic administration of IL-37 was due to insufficient amounts of this cytokine since we have data showing the effectivity of this IL-37 dose regimen in a mouse model of multiple sclerosis. Together with our findings demonstrating the effectivity of intraspinal delivery of IL-37 after SCI, our results suggest that IL-37 mediates therapeutic actions by acting as an extracellular cytokine at the lesion site. These results are crucial since they indicate that IL-37 should be delivered intrathecally in acute SCI patients in order to mediate therapeutic actions. Apparently, this is not a limitation for the potential translation of IL-37 to treat acute neurotrauma because this delivery route is

currently being used to administrate NOGO-A blocking antibodies in a SCI clinical trial (Kucher et al., 2018).

In summary, the experiments of the present chapter demonstrate that nuclear IL-37 limits inflammation during first hours after LPS stimulation in cell culture conditions. In contrast to other members of the IL-1 family such as IL-1α, which is also able to translocate to the nucleus, translocation of IL-37 to the nucleus is not performed as a mechanism to contain its action. IL-37 performs its anti-inflammatory effects through the nucleus and the extracellular compartment. Nevertheless, in animal models of SCI, in which the inflammatory response is much more complex and persistent than in cell culture conditions, the extracellular function of IL-37 is critical for protecting against functional and myelin loss by acting as a local mediator on CNS cells.

References

Amo-Aparicio, J., Martínez-Muriana, A., Sánchez-Fernández, A., and López-Vales, R. (2018). Neuroinflammation Quantification for Spinal Cord Injury. Curr. Protoc. Immunol.

Ballak, D.B., van Diepen, J.A., Moschen, A.R., Jansen, H.J., Hijmans, A., Groenhof, G.-J., Leenders, F., Bufler, P., Boekschoten, M. V., Müller, M., et al. (2014). IL-37 protects against obesity-induced inflammation and insulin resistance. Nat. Commun. *5*, 4711.

Basso, D.M., Fisher, L.C., Anderson, A.J., Jakeman, L.B.Y.N.B., Tigue, D.M.M.C., Popovich, P.G., McTigue, D.M., and Popovich, P.G. (2006). Basso Mouse Scale for locomotion detects differences in recovery after spinal cord injury in five common mouse strains. J. Neurotrauma *23*, 635–659.

Boraschi, D., Lucchesi, D., Hainzl, S., Leitner, M., Maier, E., Mangelberger, D., Oostingh, G.J., Pfaller, T., Pixner, C., Posselt, G., et al. (2011). IL-37: A new anti-inflammatory cytokine of the IL-1 family. Eur. Cytokine Netw.

Bufler, P., Gamboni-Robertson, F., Azam, T., Kim, S.-H., and Dinarello, C. a (2004). Interleukin-1 homologues IL-1F7b and IL-18 contain functional mRNA instability elements within the coding region responsive to lipopolysaccharide. Biochem. J. *381*, 503–510.

Bulau, A.-M., Nold, M.F., Li, S., Nold-Petry, C.A., Fink, M., Mansell, A., Schwerd, T., Hong, J., Rubartelli, A., Dinarello, C.A., et al. (2014). Role of caspase-1 in nuclear translocation of IL-37, release of the cytokine, and IL-37 inhibition of innate immune responses. Proc. Natl. Acad. Sci.

Bulau, A.M., Fink, M., Maucksch, C., Kappler, R., Mayr, D., Wagner, K., and Bufler, P. (2011). In vivo expression of interleukin-37 reduces local and systemic inflammation in concanavalin A-induced hepatitis. ScientificWorldJournal.

Coll-Miro, M., Francos-Quijorna, I., Santos-Nogueira, E., Torres-Espin, A., Bufler, P., Dinarello, C.A., and Lopez-Vales, R. (2016). Beneficial effects of IL-37 after spinal cord injury in mice. Proc. Natl. Acad. Sci. U. S. A. *113*, 1411–1416.

David, S., Lopez-Vales, R., and Wee Yong, V. (2012). Harmful and beneficial effects of inflammation after spinal cord injury. potential therapeutic implications. Handb. Clin. Neurol. *109*, 485–502.

Dinarello, C.A., and Bufler, P. (2013). Interleukin-37. Semin. Immunol. *25*, 466–468.

Dunn, E., Sims, J.E., Nicklin, M.J.H., and O'Neill, L.A.J. (2001). Annotating genes with potential roles in the immune system: Six new members of the IL-1 family. Trends Immunol.

Eisenmesser, E.Z., Gottschlich, A., Redzic, J.S., Paukovich, N., Nix, J.C., Azam, T., Zhang, L., Zhao, R., Kieft, J.S., The, E., et al. (2019). Interleukin-37 monomer is the active form for reducing innate immunity. Proc. Natl. Acad. Sci.

Ellisdon, A.M., Nold-Petry, C.A., D'Andrea, L., Cho, S.X., Lao, J.C., Rudloff, I., Ngo, D., Lo, C.Y., Soares da Costa, T.P., Perugini, M.A., et al. (2017). Homodimerization attenuates the anti-inflammatory activity of interleukin-37. Sci. Immunol.

Francos-Quijorna, I., Amo-Aparicio, J., Martinez-Muriana, A., and Lopez-Vales, R. (2016). IL-4 drives microglia and macrophages toward a phenotype conducive for tissue repair and functional recovery after spinal cord injury. Glia *64*, 2079–2092.

Garlanda, C., Riva, F., Polentarutti, N., Buracchi, C., Sironi, M., De Bortoli, M., Muzio, M., Bergottini, R., Scanziani, E., Vecchi, A., et al. (2004). Intestinal inflammation in mice deficient in Tir8, an inhibitory member of the IL-1 receptor family. Proc. Natl. Acad. Sci.

Kerr, B.J., and Patterson, P.H. (2004). Potent pro-inflammatory actions of leukemia inhibitory factor in the spinal cord of the adult mouse. Exp. Neurol.

Kerr, B.J., and Patterson, P.H. (2005). Leukemia inhibitory factor promotes oligodendrocyte survival after spinal cord injury. Glia.

Kucher, K., Johns, D., Maier, D., Abel, R., Badke, A., Baron, H., Thietje, R., Casha, S., Meindl, R., Gomez-Mancilla, B., et al. (2018). First-in-man intrathecal application of neurite growth-promoting anti-nogo- a antibodies in acute spinal cord injury. Neurorehabil. Neural Repair.

Li, S., Amo-Aparicio, J., Neff, C.P., Tengesdal, I.W., Azam, T., Palmer, B.E., López-Vales, R., Bufler, P., and Dinarello, C.A. (2019). Role for nuclear interleukin-37 in the suppression of innate immunity. Proc. Natl. Acad. Sci.

McNamee, E.N., Masterson, J.C., Jedlicka, P., McManus, M., Grenz, A., Collins, C.B., Nold, M.F., Nold-Petry, C., Bufler, P., Dinarello, C.A., et al. (2011). Interleukin 37 expression protects mice from colitis. Proc. Natl. Acad. Sci.

Nold-Petry, C.A., Lo, C.Y., Rudloff, I., Elgass, K.D., Li, S., Gantier, M.P., Lotz-Havla, A.S., Gersting, S.W., Cho, S.X., Lao, J.C., et al. (2015). IL-37 requires the receptors IL-18Rα and IL-1R8 (SIGIRR) to carry out its multifaceted anti-inflammatory program upon innate signal transduction. Nat. Immunol. *16*, 354–365.

Nold, M.F., Nold-Petry, C.A., Zepp, J.A., Palmer, B.E., Bufler, P., and Dinarello, C.A. (2010). IL-37 is a fundamental inhibitor of innate immunity. Nat. Immunol. *11*, 1014–1022.

Oyinbo, C.A. (2011). Secondary injury mechanisms in traumatic spinal cord injury: A nugget of this multiply cascade. Acta Neurobiol. Exp. (Wars).

Sharma, S., Kulk, N., Nold, M.F., Graf, R., Kim, S.-H., Reinhardt, D., Dinarello, C.A., and Bufler, P. (2008). The IL-1 Family Member 7b Translocates to the Nucleus and Down-Regulates Proinflammatory Cytokines. J. Immunol.

Stewart, A.N., Matyas, J.J., Welchko, R.M., Goldsmith, A.D., Zeiler, S.E., Hochgeschwender, U., Lu, M., Nan, Z., Rossignol, J., and Dunbar, G.L. (2017). SDF-1 overexpression by mesenchymal stem cells enhances GAP-43-positive axonal growth following spinal cord injury. Restor.

Neurol. Neurosci.

Taylor, S.L., Renshaw, B.R., Garka, K.E., Smith, D.E., and Sims, J.E. (2002). Genomic organization of the interleukin-1 locus. Genomics.

Wang, L., Quan, Y., Yue, Y., Heng, X., and Che, F. (2018). Interleukin-37: A crucial cytokine with multiple roles in disease and potentially clinical therapy (Review). Oncol. Lett.

Wu, B., Meng, K., Ji, Q., Cheng, M., Yu, K., Zhao, X., Tony, H., Liu, Y., Zhou, Y., Chang, C., et al. (2014). Interleukin-37 ameliorates myocardial ischaemia/reperfusion injury in mice. Clin. Exp. Immunol.

Chapter 4

Modulation of the inflammatory response after spinal cord injury by IL-13

Jesus Amo-Aparicio[1], Isaac Francos-Quijorna[1], Anna Esteve-Codina[2,3], Marta Gut[2,3], and Ruben Lopez-Vales[1]

[1]Departament de Biologia Cel·lular, Fisiologia i Immunologia, Institut de Neurociències, Centro de Investigación Biomédica en Red sobre Enfermedades Neurodegenerativas (CIBERNED), Universitat Autònoma de Barcelona, Bellaterra, Catalonia 08193, Spain
[2]CNAG-CRG, Centre for Genomic Regulation (CRG), Barcelona Institute of Science and Technology (BIST), Baldiri i Reixac 4, 08028 Barcelona, Spain
[3]Universitat Pompeu Fabra (UPF), Barcelona, Spain

Abstract

Macrophages and microglia play a key role in spinal cord injury (SCI) since they clear cell and myelin debris and synthesize several molecules that are important for tissue healing. However, these cells also release some cytotoxic factors that can damage healthy neighboring tissue and, consequently, contribute to secondary degeneration and functional impairments. Elucidating the mechanisms that underlie this dual function of macrophages and microglia after SCI may be a critical step to minimize secondary damage and functional deficits. As previously reported by our group, administration of recombinant interleukin 4 (rIL-4) into the injured spinal cord drove macrophages and microglia to adopt a phenotype more conducive for tissue repair. This correlated with improved myelin preservation and locomotor activity. In the present chapter, we evaluated the role of interleukin 13 (IL-13) in the modulation of macrophages and microglia phenotype after SCI. Similar to rIL-4, we found that the administration of recombinant IL-13 (rIL-13) into the contused spinal cord favored a more anti-inflammatory phenotype of macrophages and microglia. However, in contrast to rIL-4, rIL-13 failed to promote functional recovery and myelin preservation after SCI. To understand the differential effects exerted by these two cytokines, we performed a cell-specific RNA sequencing (RNA-seq) of macrophages and microglia sorted from the injured spinal cord after rIL-4 and rIL-13 administration. Analysis revealed that rIL-4 and rIL-13 promoted different transcription profiles. One of the most striking differences found between rIL-4 and rIL-13 treatments was related to cell metabolism. In line with RNA-seq analysis, experiments on cell energy production performed in myeloid cells isolated from injured spinal cords revealed that rIL-4 significantly increased mitochondrial oxidative metabolism as compared to rIL-13. Overall, the results presented in this chapter suggest that the functional effects of macrophages and microglia after SCI should not be predicted based exclusively on the expression of pro-inflammatory and anti-inflammatory markers and that other factors, such as cell metabolism, should also be taken into consideration.

Keywords: macrophages, microglia, polarization, interleukin 4, interleukin 13, cell metabolism, spinal cord injury

Introduction

Spinal cord injury (SCI) is one of the main causes of death and disability (Kang et al., 2017). SCI leads to the disconnection between the brain and the parts of the body below the lesion site. This results in the loss of motor, sensory, and autonomic functions. Final magnitude of SCI is defined by the level, severity, and type of injury (Burns et al., 2012). However, the post-injury events that occur after damage lead to secondary tissue degeneration worsening final neurological impairments. (Oyinbo, 2011). Among the different processes that participate in the secondary injury, inflammatory response is likely to be one of the main contributors to tissue damage.

The inflammatory response elicited after SCI is mainly orchestrated by and macrophages and microglia (Muldoon et al., 2013). Microglia are the tissue-resident macrophages and, therefore, the first cells in responding after injury. Monocytes, in contrast, infiltrate from the peripheral blood some hours later and reach maximal counts after 3-7 days (Donnelly and Popovich, 2008; Francos-Quijorna et al., 2017). These two types of cells participate in the clearance of the cellular debris from the injury site, which is an essential step for tissue healing and repair. However, the clearance response, as it occurs with most of the functions elicited by the innate immunity, is quite unspecific (Charles A Janeway et al., 2001). This is due to secreted cytotoxic factors such as free radical species, complement proteins, and proteases, that remove cell detritus at the extracellular compartment (David et al., 2012). These factors can also act on healthy neighboring tissue promoting cell death and increasing the lesion size (David and Kroner, 2011).

This dual contribution of macrophages and microglia after injury has been extensively discussed. Traditionally, detrimental effects of macrophages and microglia have been associated with M1 (*classic*) phenotype of these cells whereas beneficial effects have been related to M2 (*alternative*) phenotype (Gordon and Martinez, 2010). M1 macrophages/microglia release pro-inflammatory cytokines and some cytotoxic mediators that may cause tissue damage. In contrast, M2 macrophages/microglia release anti-inflammatory cytokines and some tissue factors that mediate repair (David and Kroner, 2011). Although this binary classification of microglia and macrophages can be useful when performing *in vitro* studies, it is quite far from the situation found *in vivo*. *In vivo*, macrophages and microglia are exposed to multiple factors leading to a wide spectrum of intermediate phenotypes (Murray et al., 2014). In the present chapter, the terms detrimental/pro-inflammatory and beneficial/anti-inflammatory will be used to refer the polarization states of macrophages and microglia bearing in mind that they are just an experimental construct.

Interleukin 13 (IL-13) is one of the cytokines that participates in the control of the inflammatory response (May and Fung, 2015). IL-13 is secrete from T cells, but it can also be produced by granulocytes and macrophages (Aoki et al., 2015). This cytokine is closely related to IL-4, and for a long time, they were considered to have a redundant function (Paul, 2015). Both cytokines are expressed by the same cells and share the same receptors composed by IL-13Rα1 and IL-4Rα subunits (Suzuki et al., 2015). However, IL-4 can also signal via IL-4Rα/IL-2Rγc and IL-13 can also signal via IL-13Rα2. There is controversy around IL-13Rα2 receptor and some authors consider it a decoy receptor (Chandriani et al., 2014). Activation of IL-

13Rα1/IL-4Rα receptor complex initiates a signal transduction through JAK/STAT pathways that leads to activation of anti-inflammatory response (Suzuki et al., 2015). In fact, both cytokines drive macrophages towards an anti-inflammatory state *in vitro* (Gordon and Martinez, 2010).

In this chapter, we aimed to modulate the inflammatory response after SCI by targeting the phenotype of macrophages and microglia. Previous results from our group demonstrated that the administration of recombinant IL-4 (rIL-4) after SCI induced an anti-inflammatory phenotype of macrophages and microglia that correlates with tissue protection and functional improvement (Francos-Quijorna et al., 2016). Here we studied whether administration of recombinant IL-13 (rIL-13) induces similar beneficial effects.

Materials and Methods

Approvals

All the experiments were approved by the Ethics Committee on Animal and Human Experimentation from the Universitat Autonoma de Barcelona (CEEAH: 4057) and followed the European Communities Council Directive 2010/63/EU. Methods from each procedure were carried out in accordance with approved guidelines.

Spinal cord injury surgery

Spinal cord injury procedure was performed according to described protocol (Amo-Aparicio et al., 2018). Adult (8 – 10 weeks old) female C57BL/6J mice from Charles River were anesthetized by intramuscular injection with a mixture of ketamine (90 mg/kg) and xylazine (10 mg/kg). After performing laminectomy at 11th thoracic vertebrae, the exposed spinal cord was contused using the Infinite Horizon Impactor device (Precision Scientific Instrumentation). For the experiments here described, a force of 50 kdynes and a tissue displacement of 400-500 μm was applied.

Luminex (bead-based multiplex assay)

Luminex assay was performed according to described protocol (Amo-Aparicio et al., 2018). At different time points after injury, mice received an intraperitoneal injection of sodium pentobarbital (Dolethal). Blood was removed by perfusion with 60 mL of 0.9% NaCl in distillated water. 0.6 cm of the spinal cord centered into the injury site were taken from each mouse. Samples were frozen in liquid nitrogen and homogenized in an extraction buffer using a TissueRuptor (Qiagen) and an Ultrasonic Homogenizer (Biologics Inc.). Buffer was prepared following previous publication (Amo-Aparicio et al., 2018). Protein was quantified and diluted to 2 mg/μl. Beads and samples were added to the Luminex plate following specific commercial protocols (Invitrogen). After washing, 50 μl of samples were added and incubated overnight at 4°C. Finally, secondary antibodies were added, and IL-13 concentrations were calculated using a MAGPIX Luminex reader (ThermoFisher Scientific). Final values were normalized by the amount of protein added in each well. 4 mice per each time-point were used.

Interleukins treatment

At 18 or 48 hours after SCI, 1 µL containing 100 ng of rIL-13 (BD Bioscience) or rIL-4 (eBioscience) were injected into the spinal cord at the injury center. PBS (ThermoFisher Scientific) was used as vehicle. Single injections were performed using a 30 µm-diameter glass micropipette (Fisher Scientific) coupled to a 10 µL Hamilton syringe (Hamilton Co). Injections were controlled by a 310 Plus automatic injection (KD Scientific) with a 2 µL/min rate. After injection, the tip of the micropipette was maintained inside the cord tissue for 3 min to avoid liquid reflux.

Flow cytometry

Flow cytometry from spinal cord was performed according to described protocol (Amo-Aparicio et al., 2018). 24 hours after intraspinal injection of PBS, rIL-13 or rIL-4, mice received an intraperitoneal injection of sodium pentobarbital (Dolethal). Blood was removed by perfusion with 60 mL of 0.9% NaCl in distillated water. 0.6 cm of the spinal cord centered into the injury site were taken from each mouse. After enzymatic and mechanic disaggregation, cells in suspension were stained with the following antibodies: CD45-PerCP (eBioscience), CD11b-PE-Cy7 (eBioscience), F4/80-APC (eBioscience), F4/8-PE (eBioscience), F4/80-FITC (MACS Miltenyi), CD16/32-PE (eBioscience), CD206-FITC (eBioscience), Arg1-unconjugated (Santa Cruz), and iNOS-unconjugated (Abcam). 1:200 dilutions were used for all these antibodies. For unconjugated antibodies, Alexa 488 (ThermoFisher Scientific) or Alexa 647 (Abcam) secondary antibodies at 1:500 dilutions were used. For receptors, IL-13Rα1-PE (eBioscience) and IL-4Rα-APC (MACS Miltenyi) at 1:200 dilutions were used. Proper isotypes for each antibody were selected. Cells were analyzed using the FACSCanto flow cytometer (BD Bioscience). Data was quantified using FlowJo® software. Microglia cells were defined as $CD45^{low}$, $CD11b^{+}$, and $F4/80^{+}$ whereas macrophages were defined as $CD45^{high}$, $CD11b^{+}$, and $F4/80^{+}$ according to previous publications (Amo-Aparicio et al., 2018; Francos-Quijorna et al., 2016). Granulocytes, mainly neutrophils, were defined as $CD45^{high}$, $CD11b^{+}$ and $F4/80^{-}$. Expression level of each marker was represented as percentage. 4 mice per groups were used.

Functional Assessment

Locomotor recovery was evaluated at 1, 3, 5,7, 10, 14, 21, and 28 days post-injury (dpi) on an open-field using the nine-point Basso Mouse Scale (BMS) (Basso et al., 2006). BMS evaluation was performed by two researchers who were blinded to the experimental groups. Consensus score between two researchers was taken. At least 6 mice per group were used.

Histology

At the end of the functional evaluation, mice were perfused with 4% paraformaldehyde (Sigma-Aldrich) in 0.1M phosphate buffer. 0.6 cm of spinal cord centered into the lesion site were removed from each mouse and cryoprotected with 30% sucrose in 0.1M phosphate buffer saline (PBS) at 4°C. Samples with 10 µm thick were cut in the cryostat and picked up with a glass slide. Samples were arranged following a serial distribution. Adjacent sections in the same slide were 100 µm apart. After graded dehydration, sections were placed in a 1 mg/ml Luxol Fast Blue (LFB) (Sigma-Aldrich) solution in 95% ethanol and 0.05% acetic acid and left overnight at 37°C. Sections were then washed in 95% ethanol and distilled water before

clearing with 0.5 mg/ml of Li_2CO_3 in distilled water for 1.5 min. After several washes, sections were dehydrated and mounted in DPX mounting media (Sigma-Aldrich). After fixation, the epicenter of the contusion was localized by determining the tissue section with the lowest LFB stained area. NIH ImageJ software was used to perform the quantifications.

Cell sorting and RNA extraction

The flow cytometry protocol, with slight modifications, was used for cell sorting. Myelin was removed from the spinal cord cell suspension using myelin removal beads (MACS Miltenyi) and LS MACS columns (MACS Miltenyi) following manufacture's recommendations. Afterwards, cells were stained with CD45-PerCP, CD11b-PE-Cy7, and F4/80-PE antibodies and then sorted using the FACSJazz (BD Bioscience). 1 drop pure method was used. A drop frequency of 39.05 kHz and a sheath pressure of 27 psi were established. Sort rate varied between 100-150 cells/sec depending on the sample since treatments can alter cells distribution. Population were gated as previously described using basis of FSC and SSC and CD45-PerCP, CD11b-PE-Cy7, and F4/80-PE antibodies. From 9000 to 73000 events of macrophages or microglia were obtained from each mouse. The purity after sorting was of 99%. Cells from sorting were collected in Eppendorf tubes with 350 µL of ice-cold RLT buffer. RNA extraction was performed using the RNeasy Micro Kit (Qiagen) following the manufacturer's recommendations. RNA was stored at -80°C until processing. 3 mice per group were used.

Low-input RNA-seq

RNA sequencing libraries were prepared following the SMARTseq2 protocol (Picelli et al., 2013) with some modifications. Briefly, RNA was quantified using the Qubit RNA HS Assay Kit (ThermoFisher Scientific) and the input material used for the initial cDNA synthesis varied in function of the available sample concentration (0.12ng-10ng). Reverse transcription was performed using SuperScrpit II (Invitrogen) in the presence of oligo-dT30VN, template-switching oligonucleotides (1µM) and betaine (1M). The cDNA was amplified using the KAPA Hifi Hotstart ReadyMix (Kappa Biosystems), 100 nM ISPCR primer, and 15 cycles of amplification. The amplified cDNA (200 ng) was fragmented using Nextera® XT (Illumina) and amplified for 10-12 cycles with indexed Nextera® PCR primers. The Nextera® library was purified twice with Agencourt Ampure XP beads (0.8:1 ratio). The libraries were sequenced on HiSeq2500 (Illumina, Inc) in paired-end mode with a read length of 2x76bp using TruSeq SBS Kit v4 and Nextera XT Index Kit of 8bp+8bp. Image analysis, base calling and quality scoring of the run were processed using the manufacturer's software Real Time Analysis (RTA 1.18.66.3) and followed by generation of FASTQ sequence files by CASAVA.

RNA-seq processing and data analysis

RNA-seq paired-end reads were mapped against the mouse reference genome (GRCm38) using STAR version 2.5.3a (Dobin et al., 2013) with ENCODE parameters for long RNA. Annotated genes were quantified using RSEM version 1.3.0 with default parameters (Li and Dewey, 2014). Differential expression analysis was performed with DESeq2 version 1.18.1 (Love et al., 2014) for the microglia and macrophages experiments separately. Principal component analysis was done using the top 500 most variable genes with the 'prcomp' R function and 'ggplot2' R library. Heatmap with the top 50 differentially expressed genes for

each comparison was performed with the 'pheatmap' R package with the 'rlog' transformed counts from DESeq2 and scaling by row. KEGG pathway representation was performed with the DAVID db version 6 (Huang et al., 2009b, 2009a).

Cell metabolism

24 hours after intraspinal injection of PBS, rIL-13 or rIL-4, mice were deeply anesthetized with sodium pentobarbital and spinal cord cell suspensions were generated as previously described (Amo-Aparicio et al., 2018). Cells were incubated with CD11b magnetic microbeads (MACS Miltenyi) and then loaded into LS MACS columns (MACS Miltenyi) following the manufacturer's guidelines. Myeloid cells were purified and quantified in the Neubauer Chamber. 200000 cells per mice and well were plated in a XFp cell culture miniplate (Agilent) following the specific manufacturer's protocol for cell suspensions. Seahorse XF Base Medium (Agilent) supplemented with 1 mM pyruvate (Sigma-Aldrich), 2 mM glutamine (Sigma-Aldrich), and 25 mM glucose (Sigma-Aldrich) was used as measurement medium. A Mixture of oligomycin (1 µM) and FCCP (1.5 µM) were loaded into the proper cartridge (Agilent). Measurements of extracellular acidification rate (ECR) and oxygen consumption rate (OCR) from live cells were performed using the Seahorse XFp Cell Energy Phenotype protocol in a XFp Analyzer (Agilent). 3 measures were taken under basal conditions and 5 measures after exposition to oligomycin and FCCP stressors. 3 mice per group were used.

Statistics

All the analyses were conducted by GraphPad Prism 7 software. BMS, ECAR, and OCR scores were analyzed using two-way repeated measure (RM) ANOVA with Bonferroni's post hoc correction. Luminex and flow cytometry were analyzed using one-way ANOVA with Dunnett's and Tukey's post hoc corrections, respectively. Luxol Fast Blue results were analyzed using multiple t-test comparisons with Holm-Sidak's post hoc correction. Results were expressed as mean ± SEM and differences were considered significant at $p < 0.05$.

Results

IL-13 appears at low levels in the injured spinal cord but receptors are available

We first measured the dynamic changes of IL-13 protein levels in the spinal cord at different time points after injury by Luminex technology. We found that IL-13 was detected at very low levels at physiological conditions (Fig. 1). However, after contusion, levels of IL-13 in the spinal cord increased progressively, but not significantly, for first the 12 hours. IL-13 returned to basal conditions at 1 day and remained at the same level until day 28 post-lesion, the last time-point evaluated.

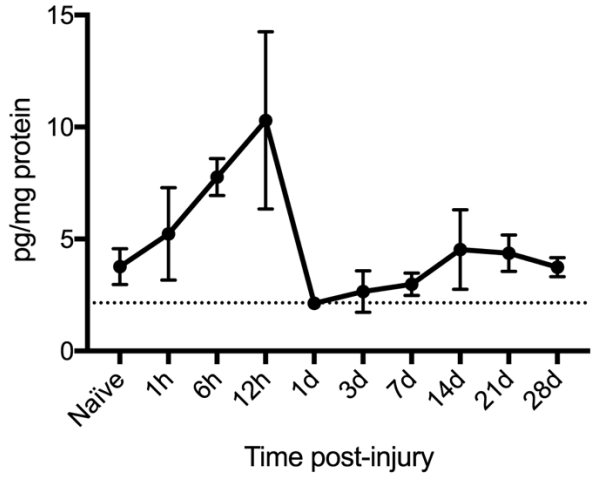

Figure 1: Changes in IL-13 protein levels in the mouse spinal cord at different time points after SCI. Dashed line marks the detection limit. Data are represented as mean ± SEM. N = 4. One-way ANOVA with Dunnett's post hoc correction.

We then analyzed by flow cytometry the expression of IL-13Rα1 and IL-4Rα subunits in microglia and macrophages for the first 48 hours after SCI. This experiment revealed that microglia do not express any of the receptor subunits at physiological conditions (Fig. 2A-F). However, these receptors were found in microglia and infiltrated macrophages at 18 hours after lesion (Fig. 2A-F). At this time-point, IL-4Rα was expressed in ~70% of macrophages and ~55% of microglia (Fig. 2A,B,E) whereas IL-13Rα1 was found in ~30% of macrophages and ~60% of microglia (Fig. 2C,D,F). At 24 and 48 hours after injury, the presence of IL-4Rα was observed in ~50% of both myeloid cell subsets (Fig. 2A,B,E). In contrast, the expression of IL-13Rα1 was markedly reduced in microglia and macrophages at 24 hours after injury. Finally, at 48 hours, only 5% and 15% of macrophages and microglia, respectively, expressed this receptor subunit (Fig. 2C,D,F).

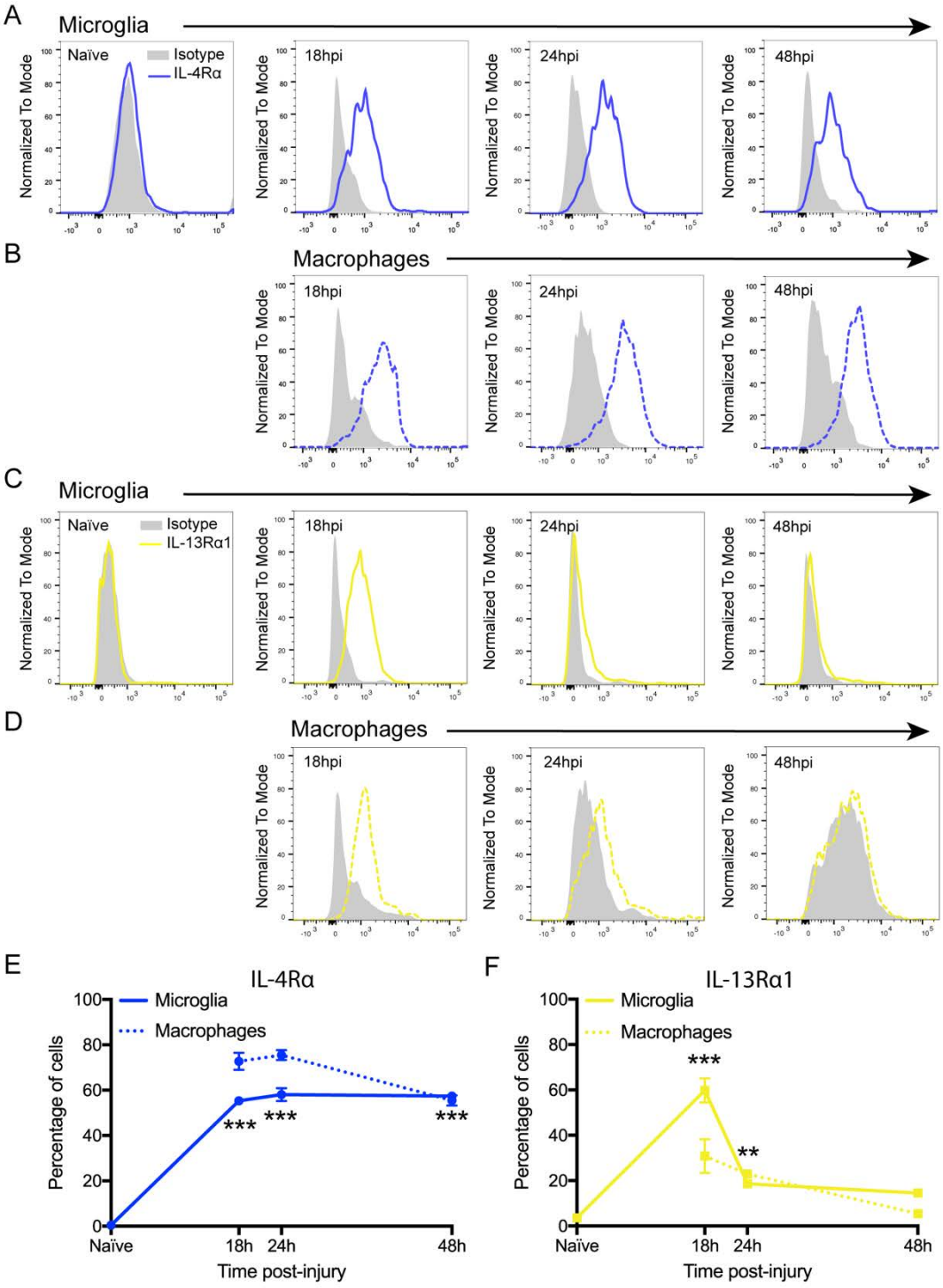

Figure 2: Expression of IL-4Rα and IL-13Rα1 in microglia and macrophages from the spinal cord after contusion injury. (A – D) Representative flow cytometry histogram plots of IL-4Rα (A and B) and IL-13Rα1 (C and D) in the populations of microglia and macrophages after SCI. (E and F) Percentage of microglia (solid line) and macrophages (dashed line) expressing IL-4Rα (E) and IL-13Rα1 (F). Data are represented as Mean ± SEM. N = 4 per time point. ** p < 0.01, *** p < 0.001 against naïve for microglia. One-way ANOVA with Dunnett's post hoc correction.

rIL-13 induces changes on macrophages and microglia after SCI

Since protein levels of IL-13 were very low in the spinal cord after lesion, we hypothesized that increasing the bioavailability of IL-13 at the lesion site may skew microglia and macrophages towards an anti-inflammatory phenotype, as previously reported by rIL-4 (Francos-Quijorna et al., 2016). Based on our previous work with rIL-4 (Francos-Quijorna et al., 2016), we administered rIL-13 at the injury site at 48 hours after SCI and evaluated the changes on the populations of macrophages and microglia after 24 hours by flow cytometry. A group of mice treated with rIL-4 was used as positive control for effective induction of the anti-inflammatory programs. PBS was used as vehicle.

We found that both, rIL-13 and rIL-4, led to similar effects on macrophages and microglia after SCI (Fig. 3A). Both recombinant proteins increased significantly the number of infiltrated macrophages into the spinal cord at day 3 after injury without affecting the number of microglia or neutrophils (Fig. 3B). They also induced the appearance of a new population of cells which are $CD45^{high}$ and $CD11b^{low}$ (Fig. 3A,C), being more pronounced with rIL-4. We previously reported that these cells are macrophages and their phenotype is compatible with resolution-phase macrophages (Bystrom et al., 2008) since they expressed lipoxygenase (LOX) and cyclooxygenase (COX-2), key enzymes in the synthesis of specialized pro-resolving lipid mediators, and anti-inflammatory cytokines such as IL-10 and TGFβ (Francos-Quijorna et al., 2016).

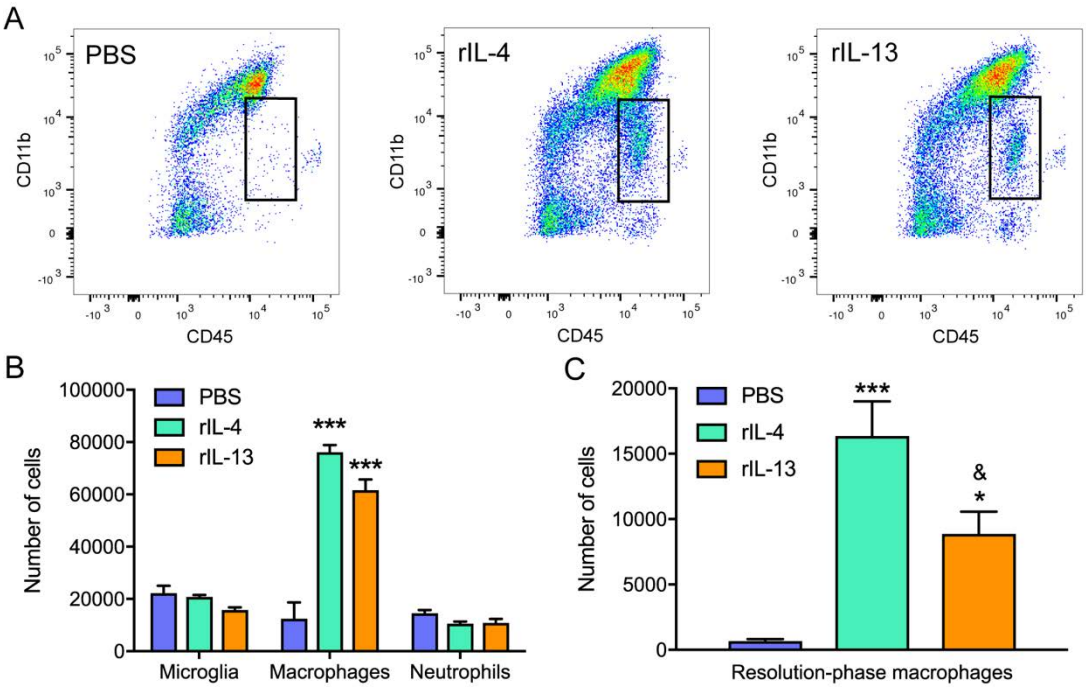

Figure 3: Effect of rIL-13 and rIL-4 on myeloid cells counts in the spinal cord at 3 days after SCI. (A) Representative flow cytometry density plots showing $CD45^{+}$ and $CD11b^{+}$ cells in the spinal cord after treatment with PBS, rIL-4, and rIL-13. Note that rIL-4 and rIL-13 led to the appearance of resolution-phase macrophages (see square). (B) Plot showing the counts of microglia, macrophages and neutrophils. (C) Plot showing the counts of resolution phase-macrophages. Data are presented as mean ± SEM. N = 4. * p < 0.05, *** p < 0.001 against PBS. & p < 0.05 against rIL-4. One-way ANOVA with Tukey's post hoc tests were used.

We then investigated whether rIL-13 altered the polarization of macrophages and microglia in the injured spinal cord evaluating the expression of pro-inflammatory (iNOS and CD16/32) and anti-inflammatory (Arg1 and CD206) markers. In agreement with previous works (Francos-Quijorna et al., 2016; Kigerl et al., 2009), we found that only a small subpopulation of macrophages (Fig. 4A,C) and microglia (Fig. 4B,D) displayed anti-inflammatory markers after PBS treatment. In contrast, pro-inflammatory markers were highly expressed in both myeloid cell subsets. Treatment with rIL-13 increased the levels of the anti-inflammatory markers Arg1 and CD206 in macrophages and microglia as rIL-4 did. Besides that, levels of Arg1 were higher with rIL-14, being significant in the population of macrophages (Fig. 4C,D). rIL-13 significantly decreased the levels of the pro-inflammatory marker iNOS in both macrophages and microglia in contrast to rIL-4 (Fig. 4C,D). Finally, the expression of CD16/32 was increased with both recombinant proteins in the population of macrophages. These results suggested that, similar to rIL-4, intraspinal injection of rIL-13 after SCI favors the anti-inflammatory activation of macrophages and microglia.

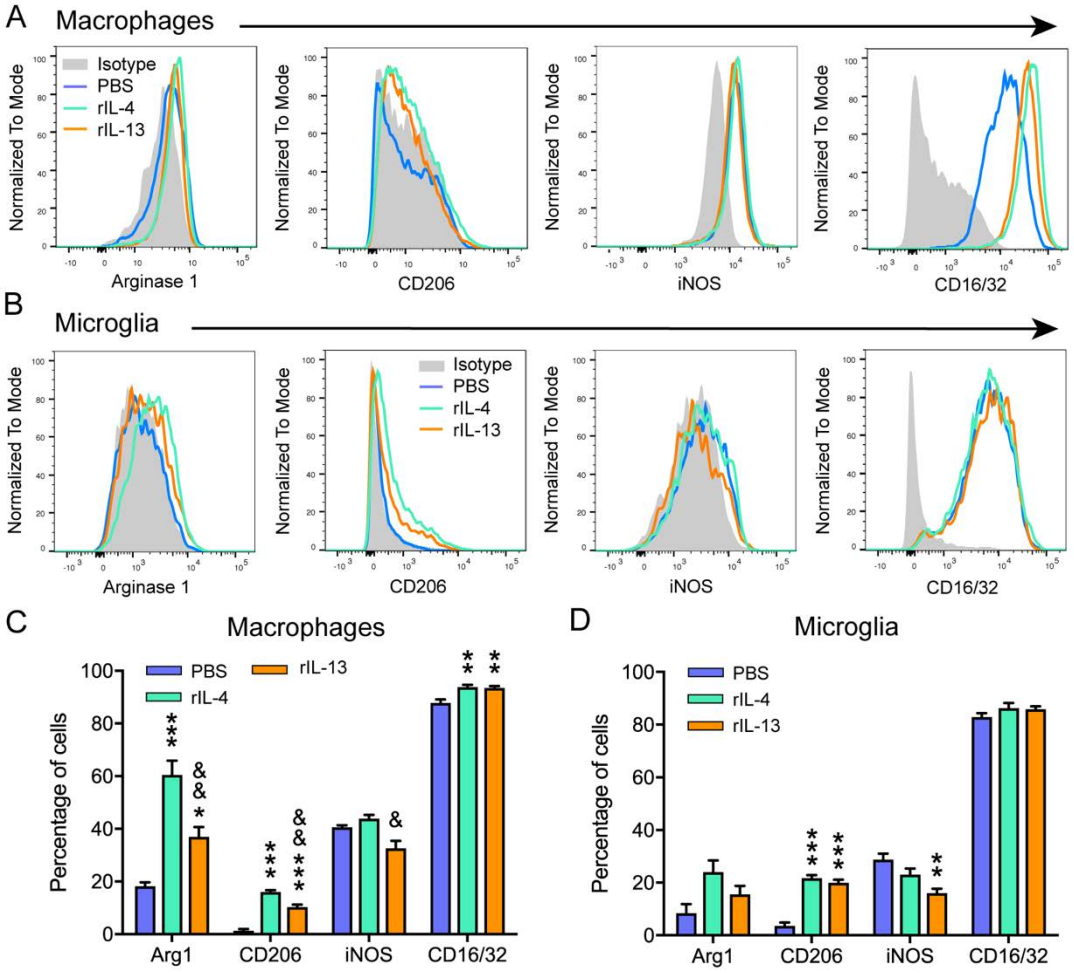

Figure 4: Effect of rIL-13 and rIL-14 on the polarization state of macrophages and microglia after SCI. (A and B) Representative flow cytometry histogram plots of the principal markers used to define the polarization state of macrophages (A) and microglia (B) at 3dpi. (C and D) Graphs showing the quantification of macrophages (C) and microglia (D) expressing polarization markers at 3 dpi. Data are represented as Mean ± SEM. N = 4. * p < 0.05, ** p < 0.01, and *** p < 0.001 against PBS. & p < 0.05 against rIL-4. One-way ANOVA with Tukey's post hoc correction.

rIL-13 does not enhance functional or histological outcomes after SCI

We then studied whether intraspinal administration of rIL-13 improved functional performance when injected at 48 hours following contusion injury. Unexpectedly, we found that rIL-13 did not lead to any improvement in the locomotor activity (Fig. 5A). At the end of the evaluation, around 80% of the mice from both groups showed extensive ankle movement and only few of them reached plantar placement (final BMS score ~2.4) (Fig. 5B). Similarly, histological analysis of the spinal cord from mice injected with rIL-13 did not reveal any enhancement in myelin sparing at 28 days post-injury (Fig. 5C,D). Contrarywise, and in line with our previous report (Francos-Quijorna et al., 2016), rIL-4 resulted in significant improvement of functional recovery (Fig. 5E).

We thought that the failure of rIL-13 to improve functional and histological outcomes after SCI may be attributed, in part, to the low levels of IL-13Rα1 found in myeloid cells at 48 hours after SCI, when rIL-13 was administered. We therefore evaluated the effects of rIL-13 on locomotor recovery when this recombinant protein was injected at 18 hours post-injury, coinciding with the peak of IL-13Rα1 in macrophages and microglia (Fig. 2F). Similarly, this protocol did not improve locomotor function (Fig. 5F). These results revealed that, although the effects of rIL-13 and rIL-4 on the populations of macrophages and microglia were very similar, both recombinant proteins differ at functional levels since only rIL-4 was able to promote recovery after SCI.

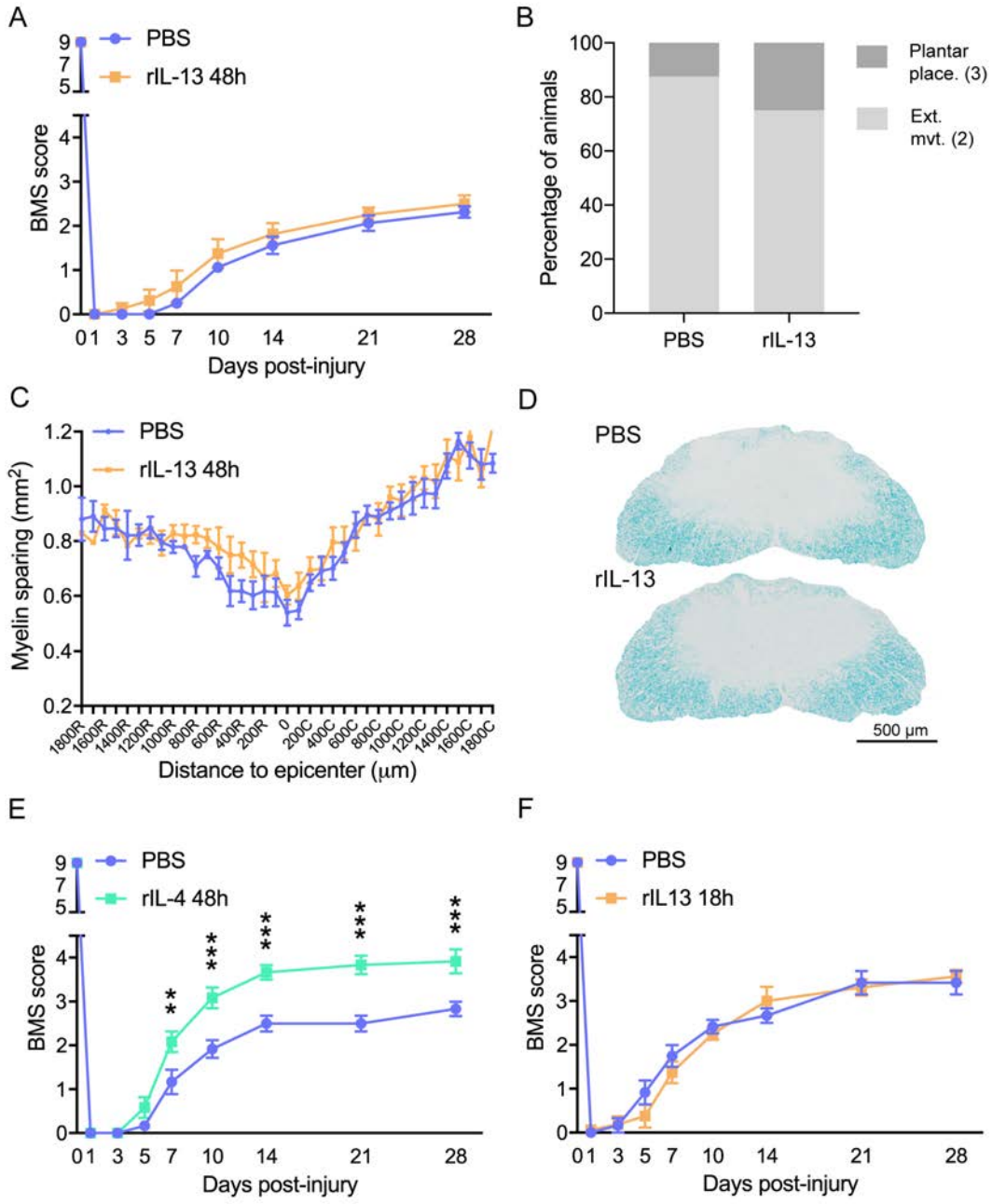

Figure 5: Effect of rIL-13 and rIL-4 on functional and histological outcomes after SCI. (A – D) Results from rIL-13 injection 48 hours after SCI. intraperitoneally. (A) BMS score showing the locomotor progression of mice. (B) Functional distribution of mice at 28 dpi. BMS values of each type of movement are indicated in parenthesis. (C) Myelin preservation in the lesion area obtained by LFB staining. (D) Representative micrographs showing myelin sparing at the injury epicenter. (E) Graph showing locomotor recovery of mice injected with rIL-4 at 48 hours after injury. (F) Plot showing locomotor recovery of mice injected with rIL-13 at 18 hours after injury. Data are represented as mean ± SEM. ** $p < 0.05$, *** $p < 0.001$. Two-way RM-ANOVA with Bonferroni's post hoc correction for (A, E, and F) and multiple t-test comparison with Holm-Sidak's post hoc correction for (C).

rIL-13 and rIL-4 induce different transcriptomic profiles after SCI

We then sought to investigate the mechanisms modulated by rIL-4 and rIL-13 in macrophages and microglia that could be related to SCI repair. For this purpose, we administered intraspinally PBS, rIL-13 or rIL-4 at 48 hours post-injury. 24 hours later, microglia and macrophages from the lesion spinal cord were sorted and RNA-seq analysis was performed.

Principal Component Analysis (PCA) showed samples clustered in 6 groups based on the cell type and the treatment. This indicated that rIL-13 and rIL-4 mediated distinct responses on the populations of macrophages and microglia. To identify differential changes caused by rIL-4 and rIL-13, we focused on genes that were differentially expressed (DE) (adjusted p-value < 0.05) between both recombinant proteins. We found 12688 annotated genes in macrophages, being 415 DE between rIL-13 and rIL-4. From these DE genes in the population of macrophages, 251 genes were up-regulated and 164 genes were down-regulated with rIL-13 relative to rIL-4. In the population of microglia, 13962 annotated genes were detected, being 477 DE between both recombinant proteins. From these genes, 352 genes were up-regulated and 125 genes were down-regulated with rIL-13 relative to rIL-4. The list of the top 50 DE genes in macrophages (Fig. 6B,S1) and microglia (Fig. 6C,S2) also revealed that most of these genes were upregulated by rIL-13 in comparison with rIL-4. However, among the few genes upregulated by rIL-14 from the top 50, most of them were related to elements of the mitochondria respiratory chain, especially in microglia (Fig. S2).

Gene ontology (GO) analysis revealed multiple biological processes, molecular functions, and cellular components that were differentially altered between both recombinant proteins in microglia and macrophages (Fig. S3,S4). GO also highlighted that both recombinant proteins differentially alter events related to metabolism in microglia and macrophages (Fig. S3 and S4). In this line, oxidative phosphorylation appeared as one of the KEGG (Kytoto Encyclopedia of Genes and Genomes) defined pathways differentially enriched with rIL-4 in the population of microglia (Fig. S4D,S5). These data suggest that rIL-4, in contrast to rIL-13, induces the expression of genes related to oxidative metabolism in microglia and macrophages.

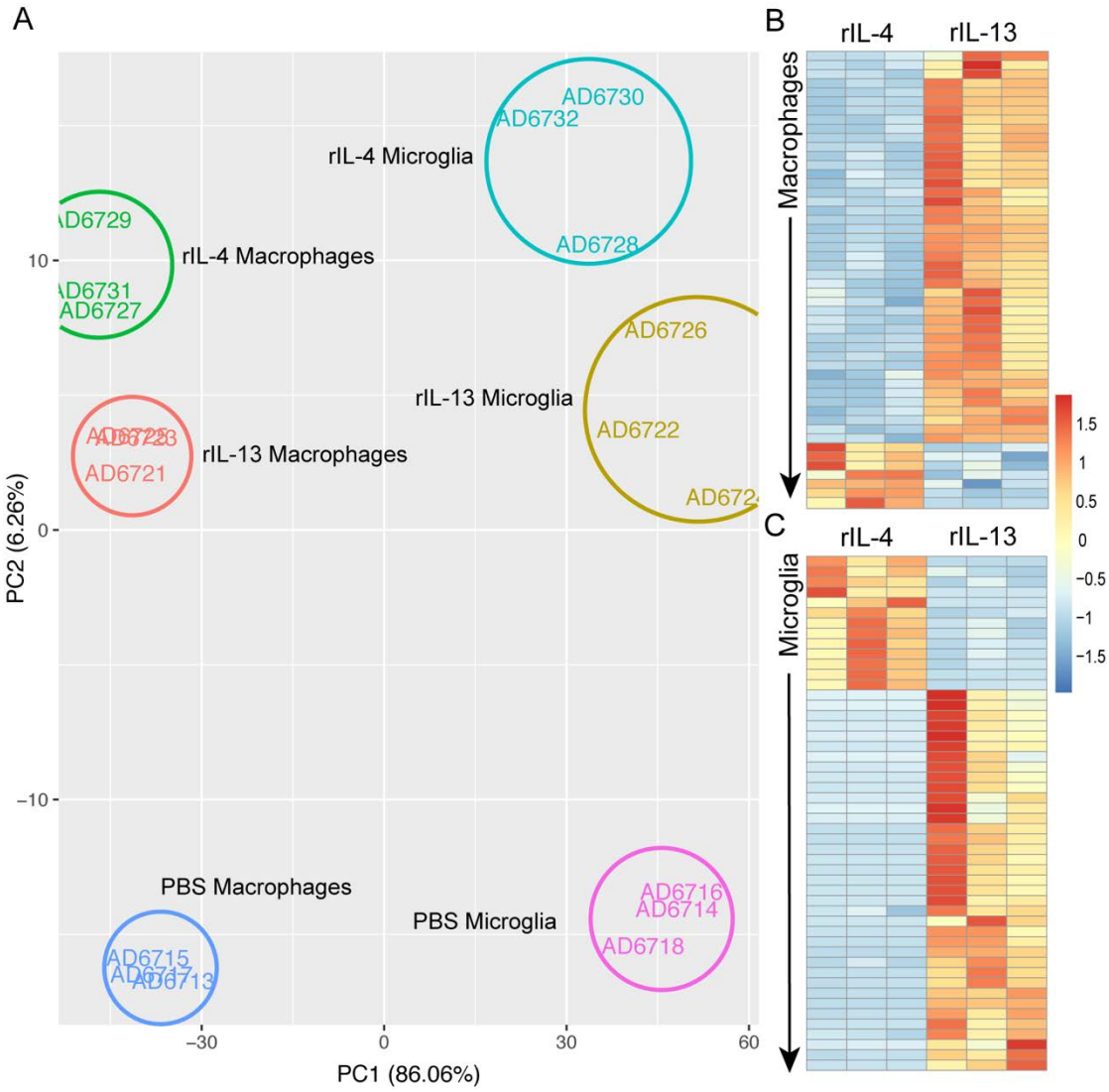

Figure 6: Transcriptomic results of macrophages and microglia from the injured spinal cord after treatment with rIL-13 and rIL-4. (A) Principal component analysis (PCA) of total 18 samples analyzed. PCA1 and PC2 explained the 86,06 and 6,26%, respectively, of the total variance. Microglia and macrophages sorted from the injured spinal cord injected with PBS were used as reference for the control conditions. (B and C) Heatmap of top 50 differentially expressed genes (adjusted p-value < 0.05) between rIL-13 and rIL-4 in macrophages (B) and microglia (C). Genes upregulated are marked in warm colors whereas genes downregulated are marked in cold colors.

rIL-13 and rIL-4 induce different metabolic states in macrophages and microglia

Cell metabolism plays an important role in regulating immune cell activity (Sack, 2018). Since our RNA-seq analysis suggested that one of the main differences between rIL-13 and rIL-4 in microglia and macrophages was related to cell metabolism, we assessed the energetic phenotype induced by rIL-4 and rIL-13 on these immune cells by Seahorse technology (Agilent). With this aim, we intraspinally injected PBS, rIL-13, and rIL-4 at 48 hours post-injury. 24 hours later, we magnetically isolated $CD11b^{+}$ cells (myeloid cells) and assessed the oxygen consumption rate (OCR) and extracellular acidification rate (ECAR) of these cells in suspension.

We found that myeloid cells isolated from PBS treated mice showed low basal levels of OCR and ECAR. Upon exposition to oligomycin and FCCP stressors simultaneously, myeloid cells

increased both glycolytic and oxidative metabolisms, as indicated by the ECAR and OCR values, respectively. Myeloid cells isolated from the injured spinal cord treated with rIL-13 showed ECAR and OCR values similar to those from PBS-treated mice (Fig. 7A,B). Although OCR values tended to be slightly higher, differences were not significant. As observed in myeloid cells from PBS-treated mice, oligomycin and FCCP also boosted glycolytic and oxidative metabolisms (Fig. 7A,B). Myeloid cells from rIL-4-treated spinal cord showed similar ECAR values than those from PBS and rIL-13 groups (Fig. 7A). However, OCR values were significantly increased. These ORC values revealed that myeloid cells from the mice treated with rIL-4 showed significant greater oxidative metabolism as compared to mice treated with PBS and rIL-13 (Fig. 7B). After stressing the cells with oligomycin and FCCP, both anaerobic and aerobic metabolisms were boosted, although the OCR values remained at significant higher level. These results confirm the observations predicted by our RNA-seq analysis, and demonstrate that rIL-4, in contrast to rIL-13, shifts energy production in myeloid cells from glycolytic towards oxidative metabolism.

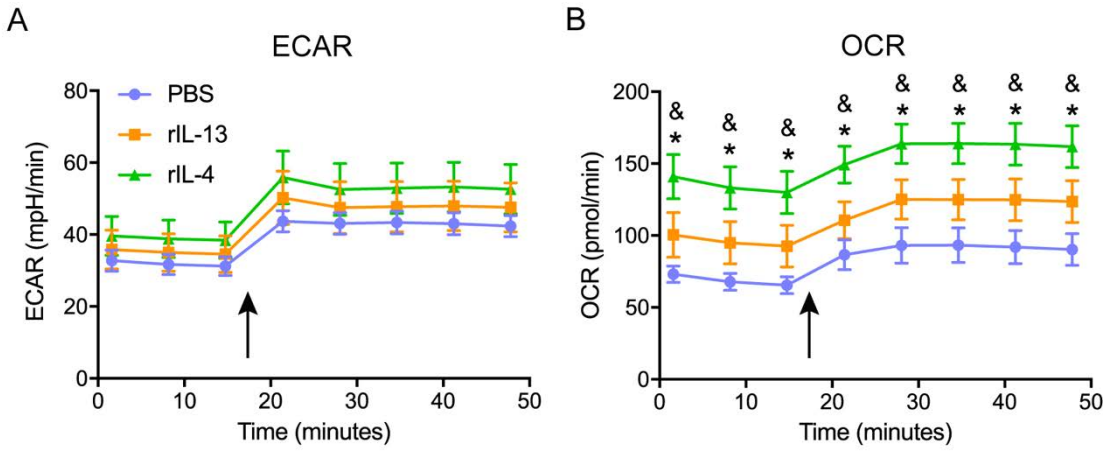

Figure 7: Energetic phenotype of myeloid cells isolated from the spinal cord after intraspinal injection of PBS, rIL-13, and rIL-4. (A) Plot showing the changes in ECAR values, a hallmark of glycolysis based on the rate of increase in proton concentration (or decrease in pH), in the assay medium over 50 minutes. (B) Plot showing OCR values, a hallmark of mitochondrial respiration based on the rate of oxygen concentration in the assay medium over 50 times. A simultaneous injection of oligomycin and FCCP was added after 15 minutes (arrow) to induce stressed phenotype and determine metabolic potential. Data are represented as mean ± SEM. N = 3. * $p < 0.05$ against PBS. & $p < 0.05$ against rIL-13. Two-way RM ANOVA with Bonferroni's post hoc correction.

Dicussion

Spinal cord injury elicits an inflammatory response produced mainly by macrophages and microglia. These cells can polarize along a continuum from pro-inflammatory (*classic*, M1) to anti-inflammatory (*alternative*, M2) phenotype. Pro-inflammatory macrophages and microglia release pro-inflammatory cytokines, cytotoxic mediators, and express phagocytic receptors that exacerbate the inflammatory response and enhance the clearance of the cell detritus (David and Kroner, 2011). Anti-inflammatory macrophages and microglia, in contrast, release anti-inflammatory cytokines and mediators to promote tissue healing and repair (David and Kroner, 2011). Although both phenotypes seem to play a beneficial contribution to tissue homeostasis, cytotoxic factors released by pro-inflammatory macrophages and microglia to

clear cell debris have low specificity (Charles A Janeway et al., 2001). Therefore, they may produce damage to healthy neighboring cells and contribute to secondary damage and neurological deficits (David et al., 2012).

Unfortunately, the first four weeks after spinal cord injury, macrophages and microglia develop a predominant pro-inflammatory phenotype (Francos-Quijorna et al., 2016; Kigerl et al., 2009; Kroner et al., 2014). Anti-inflammatory macrophages and microglia also appear in the contused spinal cord but at low levels. In fact, anti-inflammatory macrophages switch to pro-inflammatory state after transplantation into an injured spinal cord suggesting that the injury environment favors a pro-inflammatory polarization (Kigerl et al., 2009). Understanding the mechanisms that drive macrophages and microglia towards pro-inflammatory and anti-inflammatory phenotypes may be of high relevance for the development of novel therapeutics approached to treat SCI.

Here we observed that macrophages and microglia displayed high levels of pro-inflammatory markers (iNOS and CD16/32) at 3 days post-injury whereas the expression of anti-inflammatory markers (Arg1 and CD206) was restricted to a small population. Since levels of IL-13 were poorly detected in the spinal cord after contusion injury, and this cytokine has been used *in vitro* to induce anti-inflammatory polarity to macrophages (Gordon and Martinez, 2010), we hypothesized that increasing IL-13 could favor an anti-inflammatory phenotype. As we recently demonstrated with rIL-4 (Francos-Quijorna et al., 2016), promotion of this anti-inflammatory state may lead to improved functional and histological outcomes.

We found that single intraspinal injection of rIL-13 two days after SCI increased the infiltration of macrophages into the spinal cord but did not altered microglia or neutrophils count. Microglia and macrophages showed high levels of the anti-inflammatory markers Arg1 and CD206 after increasing IL-13 bioavailability in the lesion site. Indeed, the effects of rIL-13 on myeloid cell count and polarity were very similar to those induced with rIL-4. Therefore, these results demonstrated that rIL-13 is effective for promoting a beneficial state of macrophages and microglia after SCI. Moreover, rIL-13 also led to the appearance of a new subset of macrophages. This new population of macrophages showed high levels of CD45, but lower levels of CD11b than standard macrophages. These cells were found at extremely low numbers in mice treated with PBS. In a previous report from our lab, we found that this macrophage population was also found after intraspinal injection of rIL-4 into the lesioned spinal cord (Francos-Quijorna et al., 2016). These macrophages expressed LOX and COX-2, key enzymes in the synthesis of pro-resolving lipid mediators (Francos-Quijorna et al., 2016). They also expressed anti-inflammatory cytokines such as IL-10 and TGFβ, and high levels of both pro-inflammatory and anti-inflammatory markers (Francos-Quijorna et al., 2016). According to these characteristics, this population was proposed as resolution-phase macrophages (Bystrom et al., 2008). Resolution-phase macrophages promote clearance of apoptotic cells and triggers the resolution of the inflammatory response leading to tissue homeostasis. Indeed, we previously observed that administration of rIL-4 into the lesioned spinal cord accelerated the clearance of granulocytes, which is a cardinal feature of enhanced inflammatory resolution (Francos-Quijorna et al., 2016).

Despite rIL-4 and rIL-13 led to similar effects on macrophages and microglia, rIL-13, contrary to rIL-4, failed to improve locomotor recovery and myelin preservation after SCI. This fact is

unlikely to be related to the decreased levels of IL-13Rα1 in the lesioned spinal cord at 48 hours after injury since rIL-13 successfully promoted anti-inflammatory polarity at that time. This is further supported by the fact that administration of rIL-13 at 18 hours, when levels of 13Rα1 in macrophages and microglia were higher, also failed to show therapeutic efficacy. This highlights that the presence of anti-inflammatory markers in macrophages and microglia is not necessarily related to restorative actions of these immune cells in the challenged tissue. Moreover, it also indicates that IL-4 and IL-13 differentially modulate microglia and macrophage cell responses and these differences could be related to the final outcomes.

To determine such differences, we performed a cell-specific RNA-seq of macrophages and microglia sorted from the injured spinal cord at 24 hours after treatment with PBS, rIL-4 or rIL-13. To our knowledge, this is the first time that the transcriptomic profiles of macrophages and microglia has been studied separately in the context of SCI. We found that, from all the active genes detected in macrophages and microglia, around 3.3% were differentially expressed between rIL-4 and rIL-13. GO analysis revealed several cell responses altered in macrophages and microglia after treatment with rIL-13 and rIL-4. One of the biological events more differentially altered between treatments was the cell metabolism. Processes related with cell division and adhesion were also significantly altered between rIL-13 and rIL-4 in the population of macrophages. This correlates with previous publications showing that treatment of *in vitro* macrophages with rIL-4 improved its migratory properties by rearrangement of their cytoskeleton. However, these changes were not translated into improved adhesion capacity (Vogel et al., 2014). A deeper analysis of these processes in the context of SCI will be performed in the following months.

To verify results from RNA-seq, we conducted a metabolic analysis with myeloid cells magnetically isolated from the contused spinal cord. These populations were comprised mainly by macrophages and microglia, although there was ~12% of neutrophilic contamination. Magnetic isolation of these cells was chosen instead of cell sorting because, when the metabolic analysis of sorted cells was performed, we achieved very low reproducibility. This was likely attributed to alterations in the cells due to divergent waiting times during the sorting procedure. We observed that myeloid cells from injured spinal cord injected with PBS showed a predominant glycolytic phenotype. This correlates with previous publications demonstrating that macrophages undergo glycolytic metabolism after inflammatory challenge (Van den Bossche et al., 2015; Holland et al., 2017). However, myeloid cells isolated from spinal cord after treatment with rIL-4 showed enhanced oxidative metabolism. These findings were in agreement with a previous report demonstrating that bone morrow derived macrophages stimulated with rIL-4 *in vitro* showed enhanced mitochondrial oxidative metabolism (Van den Bossche et al., 2015). However, this shift from glycolytic to oxidative metabolism exerted by rIL-4 was not observed after treatment with rIL-13, although this cytokine tented to increase OCR. According to our results, this differential effect between rIL-13 and rIL-4 on myeloid cell metabolism may be crucial for explaining the protective effects exerted by rIL-4 after SCI.

How cell metabolism affects the immune cells responses has been emphasized in the recent years leading to the creation of the term immunometabolism (Van den Bossche et al., 2017). This field, which has been mostly explored in macrophages, started in 1970 by G. C. Hard (Hard,

1970). Hard showed that transition from quiescent to activated cells is an energy-demanding event and that activated murine peritoneal macrophages has lower levels of oxygen consumption than resting ones (Hard, 1970). This elucidated for the first time a metabolic change as a consequence of activation.

The discovery of different polarization states of macrophages gave rise to new metabolic studies. These studies revealed that pro-inflammatory macrophages, which are key players of the first line of defense, obtain energy through glycolysis (Galvan-Peña and O'Neill, 2014). In glycolytic metabolism, glucose uptake and conversion of pyruvate to lactate is increased, and parallelly, respiratory chain activity is depressed leading to ROS production. Moreover, the pentose phosphate pathway is also induced generating NADPH oxidase which is important for nitric oxide synthesis (Aktan, 2004). All these metabolic events provide rapid energy for the cells to effort the switch from quiescent to activated (Galvan-Peña and O'Neill, 2014). In contrast, anti-inflammatory macrophages, which are involved in longer-term functions such as tissue repair and wound healing use oxidative metabolism, as we observed in the present chapter (Galvan-Peña and O'Neill, 2014). Energy from these processes is obtained from the fatty acid oxidation to longer sustain oxidative metabolism. After adopting anti-inflammatory polarization, macrophages induce the expression of constituents of the electron transport chain for the oxidative phosphorylation, as well as, drives pyruvate into the Krebs cycle. The pentose phosphate pathway is also more limited in anti-inflammatory macrophages (Galvan-Peña and O'Neill, 2014). Importantly, blocking oxidative metabolism drives macrophages into an pro-inflammatory state and forcing oxidative metabolism in pro-inflammatory macrophages potentiates anti-inflammatory phenotype (Rodriguez-Prados et al., 2010; Vats et al., 2006). Surprisingly, our results with rIL-13 and rIL-4 demonstrated that anti-inflammatory macrophages and microglia can also differ on their metabolic state.

This link between metabolism and polarization is especially evident with the metabolic intermediates. Metabolic intermediates are not just a source of energy, they can be used as agents to develop the immune responses of a particular phenotype (Galvan-Peña and O'Neill, 2014). The metabolism of arginine is a good example. Pro-inflammatory macrophages show high levels of iNOS resulting in the catabolism of arginine to citrulline and nitric oxide (Knowles and Moncada, 1994). This nitric oxide is used by macrophages for the intracellular killing of pathogens (Munder et al., 1998). In contrast, when macrophages are polarized towards an anti-inflammatory phenotype, Arg1 is highly expressed transforming arginine to ornithine and urea (Wu and Morris, 1998), which are important for wound healing (Munder et al., 1998)..

Trophic modulation of the injury environment is a fundamental step to prevent tissue degeneration. The results showed in the present chapter elucidate some mechanisms underlying the protective phenotype of macrophages and microglia after SCI. As first statement, these results suggest that the polarity of macrophages and microglia according to pro-inflammatory and anti-inflammatory markers cannot be used to predict beneficial or detrimental effects of these cells after lesion. This classification is useful when performing *in vitro* studies, but *in vivo* the complexity of the injury environment makes it not-relevant. Our results also demonstrate that other capacities such as cell adhesion, division and, especially, metabolism should be also studied when evaluating macrophage and microglia phenotypes. For this case, wide-analysis tools such as RNA sequencing are fundamental.

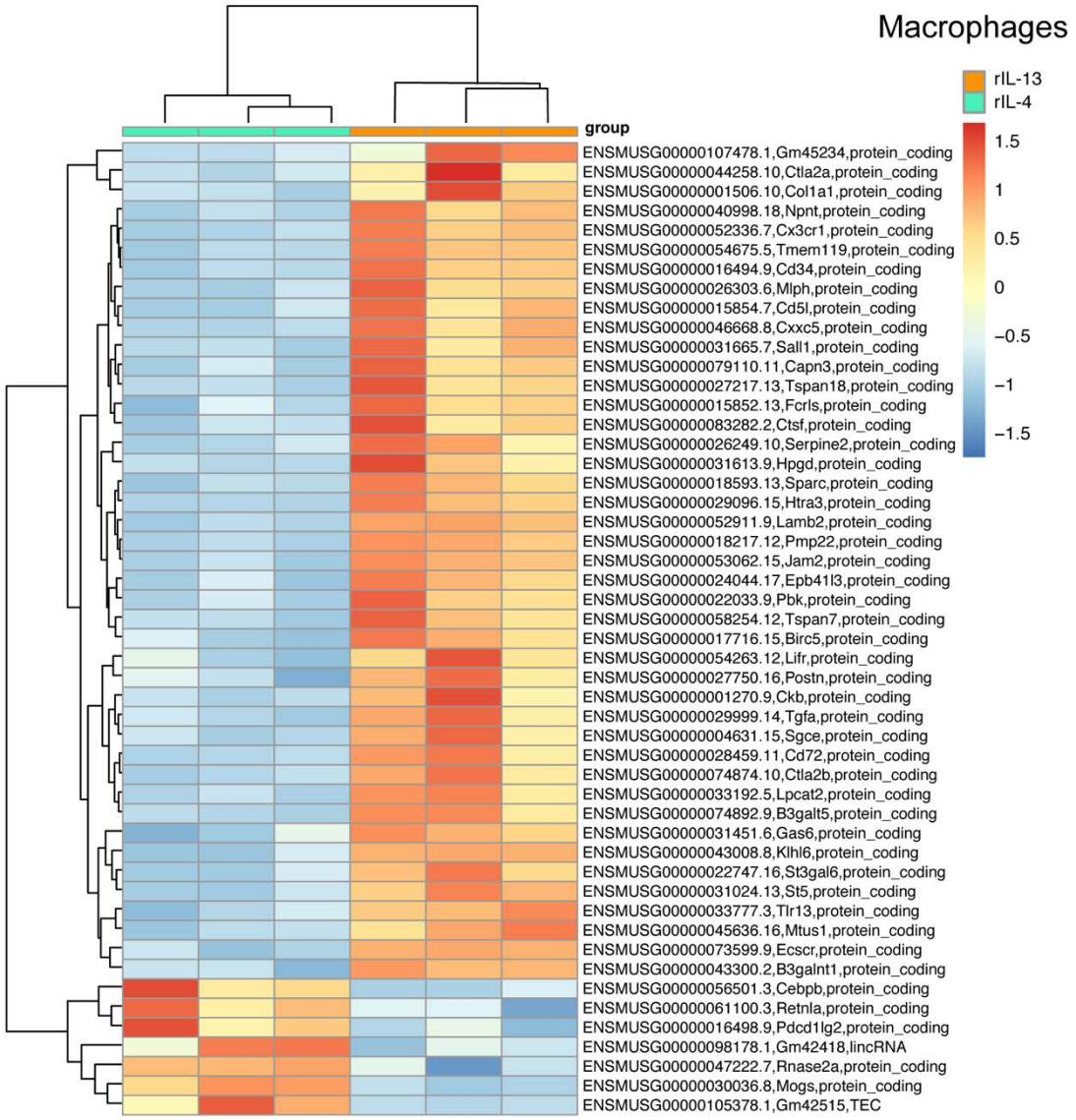

Figure Supplemental 1: Heatmap showing the top 50 DE (adjusted p-value < 0.05) genes between rIL-13 and rIL-4 in macrophages sorted from the injured spinal cord. Genes upregulated are marked in warm colors whereas genes downregulated are marked in cold colors.

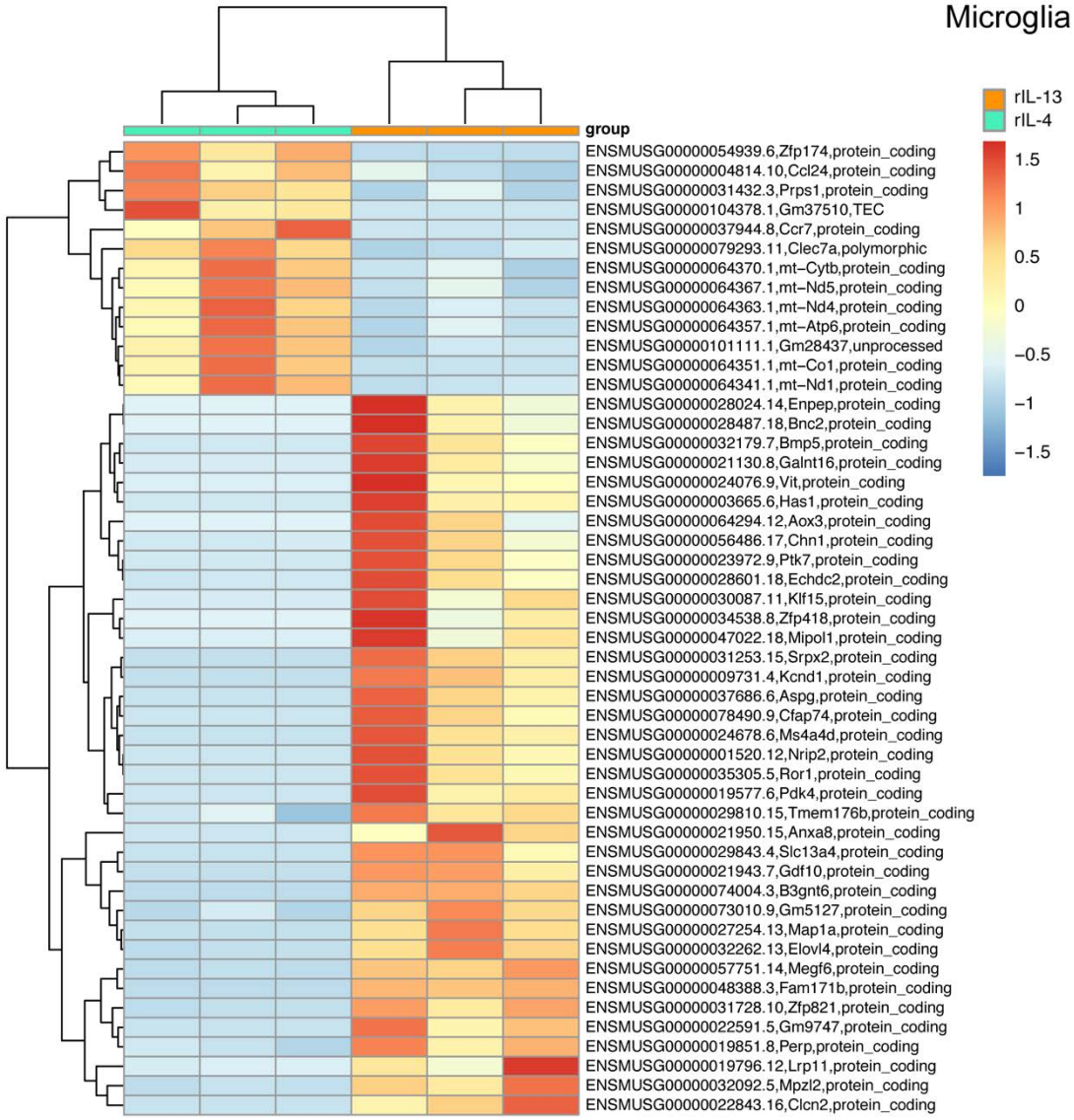

Figure Supplemental 2: Heatmap showing the top 50 DE (adjusted p-value < 0.05) genes between rIL-13 and rIL-4 in microglia sorted from the injured spinal cord. Genes upregulated are marked in warm colors whereas genes downregulated are marked in cold colors.

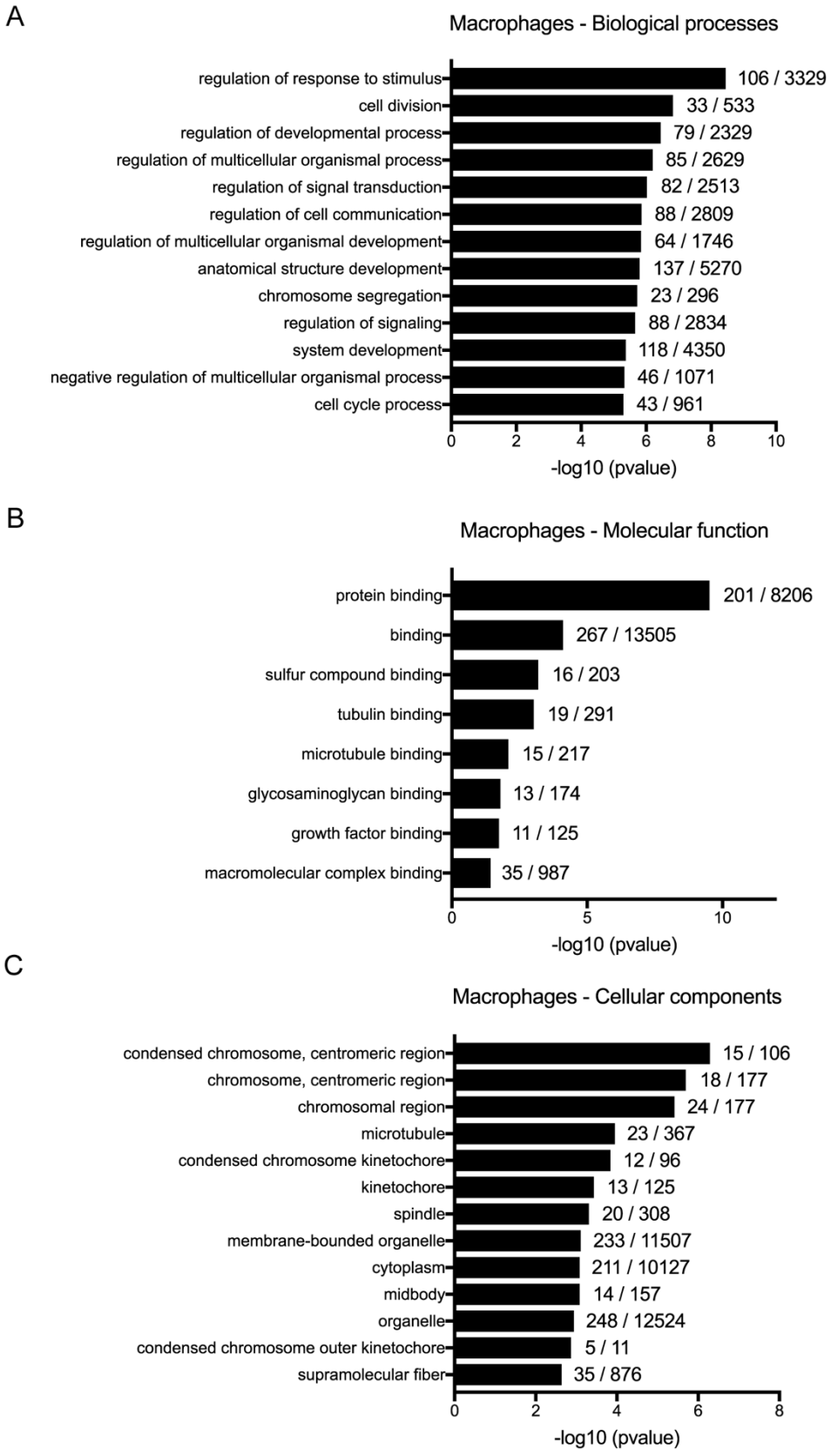

Figure Supplemental 3: Significantly pathways altered between rIL-13 and rIL-4 in spinal cord injury sorted macrophages. Note −log10 (0.05) = 1.3. Main Biological processes (A), molecular function (B), and cellular components (C) expressed as −log10 (p-value). Number of DE genes respect to the total number of genes assigned to each pathway are indicated.

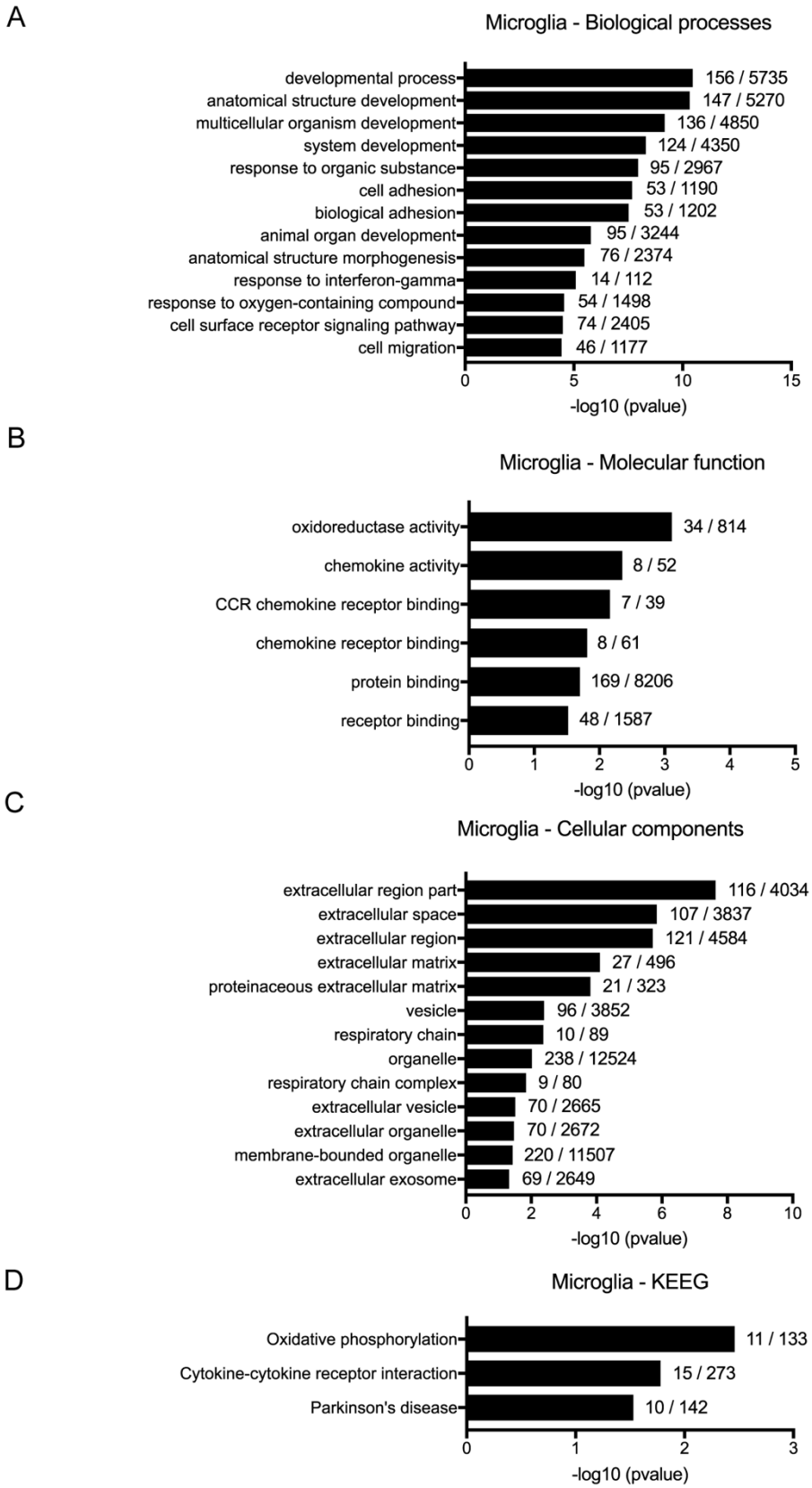

Figure Supplemental 3: Significantly pathways altered between rIL-13 and rIL-4 in spinal cord injury sorted microglia. Note −log10 (0.05) = 1.3. Main Biological processes (A), molecular function (B), cellular components (C), and KEGG expressed as −log10 (p-value). Number of DE genes respect to the total number of genes assigned to each pathway are indicated.

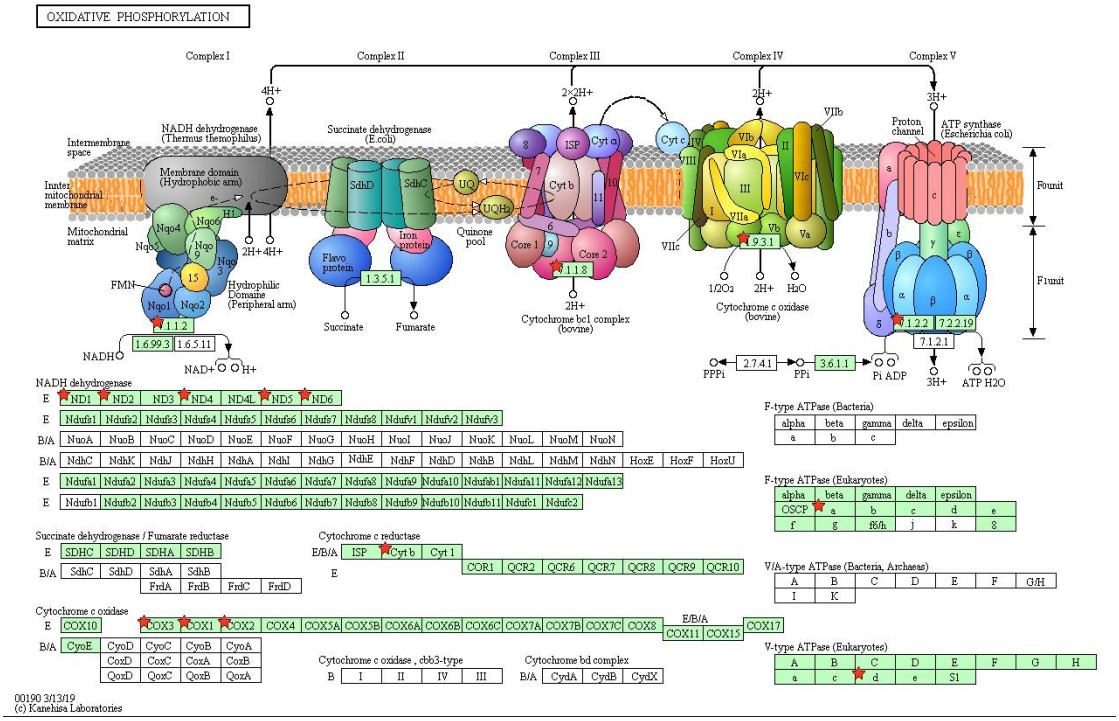

Figure Supplemental 4: Oxidative phosphorylation KEEG pathway. Genes differentially expressed in spinal cord injury microglia after rIL-4 and rIL-13 treatment are marked with a red star.

References

Aktan, F. (2004). iNOS-mediated nitric oxide production and its regulation. Life Sci.

Amo-Aparicio, J., Martínez-Muriana, A., Sánchez-Fernández, A., and López-Vales, R. (2018). Neuroinflammation Quantification for Spinal Cord Injury. Curr. Protoc. Immunol.

Aoki, M., Yamaguchi, R., Yamamoto, T., Ishimaru, Y., Ono, T., Sakamoto, A., Narahara, S., Sugiuchi, H., Hirose, E., and Yamaguchi, Y. (2015). Granulocyte–macrophage colony-stimulating factor primes interleukin-13 production by macrophages via protease-activated receptor-2. Blood Cells, Mol. Dis. *54*, 353–359.

Basso, D.M., Fisher, L.C., Anderson, A.J., Jakeman, L.B.Y.N.B., Tigue, D.M.M.C., Popovich, P.G., McTigue, D.M., and Popovich, P.G. (2006). Basso Mouse Scale for locomotion detects differences in recovery after spinal cord injury in five common mouse strains. J. Neurotrauma *23*, 635–659.

Van den Bossche, J., Baardman, J., and de Winther, M.P.J. (2015). Metabolic Characterization of Polarized M1 and M2 Bone Marrow-derived Macrophages Using Real-time Extracellular Flux Analysis. J. Vis. Exp.

Van den Bossche, J., O'Neill, L.A., and Menon, D. (2017). Macrophage Immunometabolism: Where Are We (Going)? Trends Immunol.

Burns, S., Biering-Sørensen, F., Donovan, W., Graves, D., Jha, A., Johansen, M., Jones, L., Krassioukov, A., Kirshblum, S., Mulcahey, M.J., et al. (2012). International Standards for Neurological Classification of Spinal Cord Injury, Revised 2011. Top. Spinal Cord Inj. Rehabil.

Bystrom, J., Evans, I., Newson, J., Stables, M., Toor, I., Van Rooijen, N., Crawford, M., Colville-Nash, P., Farrow, S., and Gilroy, D.W. (2008). Resolution-phase macrophages possess a unique inflammatory phenotype that is controlled by cAMP. Blood.

Chandriani, S., DePianto, D.J., N'Diaye, E.N., Abbas, A.R., Jackman, J., Bevers, J., Ramirez-Carrozzi, V., Pappu, R., Kauder, S.E., Toy, K., et al. (2014). Endogenously Expressed IL-13R 2 Attenuates IL-13-Mediated Responses but Does Not Activate Signaling in Human Lung Fibroblasts. J. Immunol.

Charles A Janeway, J., Travers, P., Walport, M., and Shlomchik, M.J. (2001). Immunobiology: The Immune System in Health and Disease. 5th edition.

David, S., and Kroner, A. (2011). Repertoire of microglial and macrophage responses after spinal cord injury. Nat. Rev. Neurosci. *12*, 388–399.

David, S., Lopez-Vales, R., and Wee Yong, V. (2012). Harmful and beneficial effects of inflammation after spinal cord injury. potential therapeutic implications. Handb. Clin. Neurol. *109*, 485–502.

Dobin, A., Davis, C.A., Schlesinger, F., Drenkow, J., Zaleski, C., Jha, S., Batut, P., Chaisson, M., and Gingeras, T.R. (2013). STAR: Ultrafast universal RNA-seq aligner. Bioinformatics.

Donnelly, D.J., and Popovich, P.G. (2008). Inflammation and its role in neuroprotection, axonal regeneration and functional recovery after spinal cord injury. Exp. Neurol.

Francos-Quijorna, I., Amo-Aparicio, J., Martinez-Muriana, A., and Lopez-Vales, R. (2016). IL-4 drives microglia and macrophages toward a phenotype conducive for tissue repair and functional recovery after spinal cord injury. Glia *64*, 2079–2092.

Francos-Quijorna, I., Santos-Nogueira, E., Gronert, K., Sullivan, A.B., Kopp, M.A., Brommer, B., David, S., Schwab, J.M., López-Vales, R., and Lopez-Vales, R. (2017). Maresin 1 Promotes Inflammatory Resolution, Neuroprotection, and Functional Neurological Recovery After Spinal Cord Injury. J. Neurosci.

Galvan-Peña, S., and O'Neill, L.A.J. (2014). Metabolic reprogramming in macrophage polarization. Front. Immunol.

Gordon, S., and Martinez, F.O. (2010). Alternative activation of macrophages: Mechanism and functions. Immunity *32*, 593–604.

Hard, G.C. (1970). Some biochemical aspects of the immune macrophage. Br. J. Exp. Pathol.

Holland, R., McIntosh, A.L., Finucane, O.M., Mela, V., Rubio-Araiz, A., Timmons, G., McCarthy, S.A., Gun'ko, Y.K., and Lynch, M.A. (2017). Inflammatory microglia are glycolytic and iron retentive and typify the microglia in APP/PS1 mice. Brain. Behav. Immun.

Huang, D.W., Sherman, B.T., and Lempicki, R.A. (2009a). Systematic and integrative analysis of large gene lists using DAVID bioinformatics resources. Nat. Protoc.

Huang, D.W., Sherman, B.T., and Lempicki, R.A. (2009b). Bioinformatics enrichment tools: Paths toward the comprehensive functional analysis of large gene lists. Nucleic Acids Res.

Kang, Y., Ding, H., Zhou, H., Wei, Z., Liu, L., Pan, D., and Feng, S. (2017). Epidemiology of worldwide spinal cord injury: a literature review. J. Neurorestoratology.

Kigerl, K.A., Gensel, J.C., Ankeny, D.P., Alexander, J.K., Donnelly, D.J., and Popovich, P.G. (2009). Identification of two distinct macrophage subsets with divergent effects causing either neurotoxicity or regeneration in the injured mouse spinal cord. J. Neurosci. *29*, 13435–13444.

Knowles, R.G., and Moncada, S. (1994). Nitric oxide synthases in mammals. Biochem. J.

Kroner, A., Greenhalgh, A.D., Zarruk, J.G., PassosdosSantos, R., Gaestel, M., and David, S. (2014). TNF and Increased Intracellular Iron Alter Macrophage Polarization to a Detrimental M1 Phenotype in the Injured Spinal Cord. Neuron *83*, 1098–1116.

Li, B., and Dewey, C.N. (2014). RSEM: Accurate transcript quantification from RNA-seq data with or without a reference genome. In Bioinformatics: The Impact of Accurate Quantification on Proteomic and Genetic Analysis and Research, p.

Love, M.I., Huber, W., and Anders, S. (2014). Moderated estimation of fold change and dispersion for RNA-seq data with DESeq2. Genome Biol.

May, R.D., and Fung, M. (2015). Strategies targeting the IL-4/IL-13 axes in disease. Cytokine.

Muldoon, L.L., Alvarez, J.I., Begley, D.J., Boado, R.J., Del Zoppo, G.J., Doolittle, N.D., Engelhardt, B., Hallenbeck, J.M., Lonser, R.R., Ohlfest, J.R., et al. (2013). Immunologic privilege in the central nervous system and the blood-brain barrier. J. Cereb. Blood Flow Metab.

Munder, M., Eichmann, K., and Modolell, M. (1998). Alternative metabolic states in murine macrophages reflected by the nitric oxide synthase/arginase balance: competitive regulation by CD4+ T cells correlates with Th1/Th2 phenotype. J. Immunol.

Murray, P.J., Allen, J.E., Biswas, S.K., Fisher, E.A., Gilroy, D.W., Goerdt, S., Gordon, S., Hamilton, J.A., Ivashkiv, L.B., Lawrence, T., et al. (2014). Macrophage Activation and Polarization: Nomenclature and Experimental Guidelines. Immunity.

Oyinbo, C.A. (2011). Secondary injury mechanisms in traumatic spinal cord injury: A nugget of

this multiply cascade. Acta Neurobiol. Exp. (Wars).

Paul, W.E. (2015). History of interleukin-4. Cytokine.

Picelli, S., Björklund, Å.K., Faridani, O.R., Sagasser, S., Winberg, G., and Sandberg, R. (2013). Smart-seq2 for sensitive full-length transcriptome profiling in single cells. Nat. Methods.

Rodriguez-Prados, J.-C., Traves, P.G., Cuenca, J., Rico, D., Aragones, J., Martin-Sanz, P., Cascante, M., and Bosca, L. (2010). Substrate Fate in Activated Macrophages: A Comparison between Innate, Classic, and Alternative Activation. J. Immunol.

Sack, M.N. (2018). Mitochondrial fidelity and metabolic agility control immune cell fate and function. J. Clin. Invest.

Suzuki, A., Leland, P., Joshi, B.H., and Puri, R.K. (2015). Targeting of IL-4 and IL-13 receptors for cancer therapy. Cytokine *75*, 79–88.

Vats, D., Mukundan, L., Odegaard, J.I., Zhang, L., Smith, K.L., Morel, C.R., Greaves, D.R., Murray, P.J., and Chawla, A. (2006). Oxidative metabolism and PGC-1β attenuate macrophage-mediated inflammation. Cell Metab.

Vogel, D.Y.S., Heijnen, P.D.A.M., Breur, M., de Vries, H.E., Tool, A.T.J., Amor, S., and Dijkstra, C.D. (2014). Macrophages migrate in an activation-dependent manner to chemokines involved in neuroinflammation. J. Neuroinflammation.

Wu, G., and Morris, S.M. (1998). Arginine metabolism: nitric oxide and beyond. Biochem. J.

GENERAL DISCUSSION

Spinal cord injury (SCI) is one of the main causes of death and disability. When the spinal cord is damaged, there is a permanent loss of communication between the brain and the areas of the body below the lesion site. This results in loss of motor and sensory functions, but also, in many autonomic alterations that favor bladder and kidney infections, cardiac, respiratory, and bowel insufficiency, as well as, sexual dysfunction. All these events have consequences for the physical, social, and vocational well-being of patients. Final magnitude of these dysfunctions is defined by the level, severity and type of injury (Burns et al. 2012). In Europe, the number of people suffering from SCI is approximately 15 cases per million individuals (Kang et al. 2017). Automobile accident are the main cause, especially in the young population. Their care costs are staggering at 1 - 4 millions of euros per patient over their lifetime (Ahuja et al. 2017; Chen et al. 2013). Since there is not effective cure for SCI, prevention is for the moment the most important intervention that can be delivered.

The degenerative processes induced by traumatic injury to the spinal cord can be divided in two phases: primary and secondary damage. Primary damage refers to the immediate changes after trauma that cause tissue degeneration (Oyinbo 2011). Secondary damage includes the extension of many of the processes of the primary damage but also novel ones such as vascular dysfunction, glutamate excitotoxicity, free radical production, glial reactivity or inflammation (Oyinbo 2011). All these processes induce progressive degeneration of the neurological tissue that expands through healthy neighboring areas and makes the lesion larger. Unlike primary injury, secondary degenerating processes last from minutes to weeks after SCI, providing a clinically feasible therapeutic window for the administration of pharmacological strategies. Although restoration of neural connectivity and replacement of cell lost are important goals to recover the neurological function after SCI, here we studied strategies based on the reduction of the secondary damage as an approach more easily applicable. More precisely, we focused our efforts on modulating the inflammatory response since it is one of the main contributors to secondary damage after SCI.

Inflammatory response involves a wide variety of immune cells and mediators. In the case of SCI, microglia and myeloid cells that migrate from the peripheral circulation, are among the main contributors (David and Kroner 2011; López-Vales and David 2019). For many years, the contribution of these immune cells to the progression of the pathology was not clearly understood. Literature is full of examples of the detrimental effects of extensive neuroinflammation in the central nervous system (CNS). In this line, many groups showed that inhibition of macrophages infiltration and/or activation after SCI leads to tissue preservation and functional recovery (Letellier et al. 2010; López-Vales et al. 2005; Popovich et al. 1999; Stirling 2004). In contrast, there are also multiple evidences about the significant benefits of inflammatory response to CNS injuries. For example, it has been described that macrophages and microglia are necessary for proper remyelination and neurogenesis after SCI (Hines et al. 2009; Kotter et al. 2005). This beneficial effect of neuroinflammation should not be surprising since inflammatory response in other tissues contributes to healing of damaged areas and recovery of homeostasis. However, what differences the inflammatory response in the CNS from other tissues, even the PNS, is its failure to be properly resolved (David et al. 2018; Libby 2007).

Dual contribution of inflammatory response after CNS injury was resolved by the introduction of the term polarization. Macrophages and microglia have a remarkable plasticity and they can present different phenotypes. The term polarization was used to refer the process by through macrophages and microglia acquire different, and even opposite, phenotypes

attending to signals from the environment. Traditionally, two opposite polarization states of macrophages and microglia have been described. These states were termed as M1 and M2, based on the Th1 and Th2 polarization of T lymphocytes. According to this classification, stimulation of macrophages and microglia with the prototypical Th1 cytokines (IFNγ or LPS) induces M1 (*classic*) polarization whereas stimulation of macrophages and microglia with the prototypical Th2 cytokines (IL-4 or IL-13) induces M2 (*alternative*) polarization (Martinez, Helming, and Gordon 2009). M1 macrophages and microglia are pro-inflammatory. They secrete a wide cohort of pro-inflammatory cytokines, free radicals, lipid mediators, proteases, and glutamate to potentiate the inflammatory response after SCI. Through these mediators, they promote the clearance of cellular debris and potentially toxic products. Moreover, they remove inhibitory molecules for axon regeneration such as CSPGs (David and Kroner 2011; Martinez, Helming, and Gordon 2009). In contrast, M2 macrophages and microglia are anti-inflammatory and release mediators to resolve inflammation and recover tissue homeostasis (David and Kroner 2011; Martinez, Helming, and Gordon 2009). Although all these functions of neuroinflammation seem to have a beneficial effect after insult, excessive and uncontrolled neuroinflammation leads to unspecific damage to healthy tissue. This produces extension of the lesion size and worsening of the neurological outcomes. It is important to remark that M1/M2 classification of macrophages and microglia is an experimental construct since polarity is a continuum spectrum of phenotypes with M1 and M2 at the opposite edges.

Previous result from our group showed that although both phenotypes are found in the spinal cord after injury, most of the macrophages and microglia display a predominant M1 phenotype (Francos-Quijorna et al. 2016). Preferential M1 phenotype has also been observed in other CNS injuries such as ischemic stroke (Hu et al. 2012). This exacerbated pro-inflammatory environment of the injured CNS may be responsible of secondary tissue degeneration. In 2009, Kigler observed that M2 polarized BMDM switched to M1 when they were transplanted into an injured spinal cord (Kigerl et al. 2009). In contrast, when they were transplanted into an intact spinal cord, they remained as M2. This finding revealed for first time that the polarization of macrophages and microglia depends on the injury environment opening a new line of research. It also demonstrated that not only permanence, but also phenotype of macrophages and microglia, need to be considered. Therefore, modulating rather than suppressing macrophages and microglia activity may be a promising therapeutic approach for the treatment of SCI.

In this thesis, we firstly assessed whether the use of different cutting-edge technologies could be applied to characterize the inflammatory response after SCI (chapter 1). Techniques, such as, flow cytometry or Luminex assay allow us to determine the degree of inflammation (Amo-Aparicio et al. 2018). Through flow cytometry, we can count the number of macrophages, microglia, and granulocytes at different time points after SCI. Since these cells are considered the main contributors to the inflammatory response after SCI, they can be used as a hallmark for the course of inflammation. Moreover, flow cytometry, in contrast to histological procedures, allows to measure multiple markers simultaneously. This is essential when studying inflammatory cells since they share many markers that only differ on their expression intensity. Besides, the number of cells is not the only factor needed for the characterization of the immune response; cytokines dynamic is also important. Multiplex-based techniques such as Luminex can be used to measure the levels of a large extent of pro-inflammatory and anti-inflammatory cytokines at the same time. We showed that both techniques are useful tools to analyze inflammation after CNS injury in a rapid, reproducible, and more reliable way (Amo-Aparicio et al. 2018).

In the following chapters, by using those techniques, we studied different therapeutic approaches for the modulation of the injury environment after SCI. As it has been previously demonstrated, reduction of the secondary damage results in improved locomotor recovery (Francos-Quijorna et al. 2016; Kroner et al. 2014). The question now is how to modulate the injury environment maintaining the obvious necessity of a properly directed immune response but avoiding the dangers of exacerbated immunity. In this line, we decided to target the bioavailability of both pro-inflammatory and anti-inflammatory cytokines. In chapter 2 we assessed the effects of reducing pro-inflammatory agents at early points after injury. Contrariwise, in chapter 3, we potentiated anti-inflammatory agents at early points after injury. Finally, in chapter 4, we potentiated anti-inflammatory agents at more delayed points after injury.

In chapter 2, were aimed to reduce some molecules involved in the first stages of the inflammatory response. We focused on IL-1α and IL-1β/IL-18 since these cytokines controls the very early stages of inflammation. We observed that IL-1α production is induced after SCI showing a peak at 6 hours. This cytokine is secreted after cell death and works as an "alarmin" acting on other immune cells that become rapidly activated (Dinarello 2011). IL-1β is also expressed at early time points after SCI, but later than IL-1α. IL-18, however, was expressed from 1 to 3 weeks post-injury. In contrast to IL-1α, IL-1β and IL-18 are produced as precursor inactive forms and require processing by inflammasomes, such as NLRP3, in order to be fully activated (Dinarello 2011). To reduce the effects of IL-1α and IL-1β on the first stages of the inflammatory response, we used two pharmacological approaches that have demonstrated to be safe in humans and to induce protective effects in a variety of inflammatory-dependent diseases. These approaches were MABp1 and OLT1177.

MABp1 is a monoclonal antibody targeting IL-1α. In our case, treatment with MABp1 failed to produce protective effect when injected after SCI. Although we tested different doses of MABp1, they failed to promote recovery. We cannot exclude that the lack of efficacy of MAPp1 may be due to insufficient neutralization of IL-1α. Maybe certain levels of IL-1α remained unattached to the antibody and, thus, they were enough to activate the inflammatory response on target cells. This lack of efficacy was not attributable to incapacity of MABp1 to reach the target tissue since we tested peripheral and central injections and same results were obtained. Our findings correlate with previous publications showing that knocking out *Il1a* gene in mouse does not improve functional outcomes after SCI (Bastien et al. 2015). Although these mice presented locomotor improvement at the early stages of the evaluation, differences with control mice were not maintained during the follow up. Altogether, our data suggest that blocking IL-1α is not a good therapeutic strategy for acute SCI.

OLT1177 is an inhibitor of the NLRP3 inflammasome. Selectively, OLT1177 binds to NLRP3 inflammasome and inhibits its ATPase activity needed for its oligomerization (Marchetti, Swartzwelter, Gamboni, et al. 2018). Without oligomerization, NLRP3 cannot mediate the maturation of caspase-1 involved in the processing and releasing of IL-1β and IL-18. Both cytokines were observed at the spinal cord after injury although the expression pattern was quite opposite. IL-1β showed a peak at 12 hours whereas IL-18 showed a peak at 7 days coinciding with the maximum levels of microglia (Francos-Quijorna et al. 2017). We observed that inhibition of NLRP3 inflammasome by OLT1177 improves functional outcomes and tissue preservation after SCI. We assumed that beneficial effects of OLT1177 were mediated mainly by reducing levels of IL-1β rather than IL-18, since treatment was applied only for the first 7 days, when levels of IL-18 peaked in the contused spinal cord. However, proper

characterization on the effect of OLT1177 on cytokine levels and immune cell counts will be performed in the following months.

Currently, there are clinical treatments targeting IL-1β using antibodies and receptor antagonists such as canakinumab and anakinra, respectively (Dinarello, Simon, and Van Der Meer 2012). Anakinra has reported no beneficial effect after SCI in mice (Bastien et al. 2015). Some histological improvement has been reported in rats but only at early stages (Hasturk et al. 2015). In the case of canakinumab, its effect after SCI has not been studied as far as we know. Targeting upstream phases of IL-1β seems to be the best choice, since it can block simultaneously this cytokine together with other inflammatory factors that share their mechanism of activation and/or release. Involvement of NLRP3 inflammasome in different kinds of diseases provides a new avenue for designing novel drugs to target inflammation. Many compounds have shown efficacy in preventing NLRP3 inflammasome activation including MCC950, β-hydroxybutyrate, dimethyl sulfoxide, and type I interferon (Yang et al. 2019). However, most of these inhibitors are relatively nonspecific and have low efficacy. OLT1177 was postulated as one of the best inhibitors of NLRP3 since it does not produce changes of AIM2 and NLRC4 inflammasomes. However, whether OLT1177 has some effects on NLRP1, NLRP12, or pyrin inflammasomes needs to be fully elucidated (Yang et al. 2019).

Results obtained using OLT1177 administration demonstrate that the modulation of the injury environment by the reduction of the pro-inflammatory phase is a promising target for the treatment of SCI. Main limitation of the treatment of acute SCI is the timing. Since IL-1β showed a strong production peak at early stages, therapies aimed to reduce its action need to be applied at the very beginning. This may suppose an inconvenient for the applicability of this therapy since usually patients do not receive medical assistance immediately. Moreover, diagnosis requires a thorough patient history, standardized neurological physical examination and radiographic imaging of the spinal cord. However, what makes OLT1177 special, is the lack of biochemical and hematological adverse effects in humans (Marchetti, Swartzwelter, Gamboni, et al. 2018; Marchetti, Swartzwelter, Koenders, et al. 2018). This reveals OLT1177 as a promising candidate for the treatment of acute traumatic SCI.

As reported above, exacerbated neuroinflammation after SCI can also be explained by an inefficient activation of resolution programs (Yong et al. 2019). Since elevated pro-inflammatory mediators were detected at the spinal cord even at late stages following injury (Francos-Quijorna et al. 2016), in chapters 3 and 4 of this thesis, we modulated the inflammatory response by promoting anti-inflammatory programs. In chapter 3, we used IL-37 as a promising agent to turn on anti-inflammatory programs. Surprisingly, this cytokine has not been found in the mouse genome yet, although its receptors are available. To solve this limitation, transgenic mice expressing the human *IL37* gene were developed (Nold et al. 2010). Previous results from our group showed that the transgenic expression of human *IL37* in mice induced beneficial effect after SCI (Coll-Miro et al. 2016).

As many other members of the IL-1 family, such as IL-1α and IL-33, IL-37 can be observed at extracellular and nuclear compartments (Nold-Petry et al. 2015; Sharma et al. 2008). Extracellular IL-37 binds to IL-18Rα and IL-1R8 triggering a signaling cascade where inhibition of Fyn and TAK1 kinases may represent the main effects. These two kinases promote the inflammation and skews macrophages polarization to the pro-inflammatory phenotype (Li et al. 2015; Nold-Petry et al. 2015). Extracellular signaling also triggers the inhibition of the insulin receptor-mTOR-kinase S6K pathway and increases the activity of the AMP-activated kinase

(AMPK), STAT6, and transcription factors of the Foxo family (Li et al. 2015; Nold-Petry et al. 2015). How IL-37 is released from the cells in absence of cell death, as there is no increase in LDH levels (Li et al. 2019), remains still unknown.

In the case of the nuclear signaling, IL-37 is processed by caspase-1 at the cytoplasm. Then, IL-37 binds to Smad3 subunit allowing its internalization to the nucleus. Although recent reports demonstrate the contribution of the extracellular pathway to the beneficial effect of IL-37 (Nold-Petry et al. 2015), the contribution of the nuclear pathway is not fully elucidated since studies to address this issue have been done using caspase-1 inhibitors (Bulau et al. 2014). As previously explained, caspase-1 mediates the processing of other pro-inflammatory cytokines such as IL-1β and IL-18. Therefore, inhibiting caspase-1 produces many changes, not only at nuclear IL-37 level.

To solve this limitation, we used hIL-37D20Tg mice. These mice express a mutated version of IL-37 at D20 position, the caspase-1 cleavage site of IL-37, and thus, this cytokine cannot be translocated to the nucleus. We observed that nuclear translocation of IL-37 is required to mediate the anti-inflammatory effects of this cytokine at early time points after LPS challenge *in vitro*. Moreover, we provided a set of genes that were downregulated in hIL-37D20ATg cells in comparison with hIL-37Tg cells being attributed to the nuclear signaling. Although the exact contribution of these genes needs to be analyzed, some of them are known to promote immunomodulatory effects after SCI (Francos-Quijorna et al., 2016; Kerr and Patterson, 2004, 2005; Stewart et al., 2017). Therefore, we demonstrated for the first time that nuclear IL-37 seems to be required to mediate anti-inflammatory actions at the first hours of the inflammatory challenge. This is in contrast to other cytokines such as IL-1α for which nuclear translocation is used to retains its pro-inflammatory effects on the extracellular compartment. In the case of IL-37, this cytokine can mediate anti-inflammatory actions by both nuclear and extracellular signaling. Nevertheless, we observed that, at later time points after LPS stimulation, protective effects of hIL-37D20ATg cells were comparable to hIL-37Tg cells, despite not having nuclear function (Li et al. 2019). We hypothesize that the strong anti-inflammatory effect observed in hIL-37D20ATg cells at late time points, may be produced by a greater release of IL-37 since its nuclear translocation is blocked. However, attempts to measure the release of IL-37 from mouse cells failed since human IL-37 antibodies are very unspecific and recognize IL-1RA.

By using IL-37D20A mice after SCI, we found that IL-37 can mediate protective effects even in the absence of nuclear signaling. This suggested that the beneficial effects of IL-37 in neurotrauma are mediate by acting as an extracellular cytokine. These findings were further confirmed by experiments in which the extracellular function of IL-37 was impeded by gene deletion of the IL-1R8 co-receptor. In this case, beneficial effects of IL-37 were completely abolished in the lack of extracellular function. We discard that lack of efficacy of IL-37 in hIL-37TgxIL-1R8KO mice was due to any protective effect of IL-1R8 after SCI since characterization of IL-1R8KO mice showed no involvement of this co-receptor in the SCI pathophysiology. Therefore, the combination of hIL-37Tg, hIL-37TgxIL1-R8KO and hIL-37D20ATg mice demonstrated that extracellular signaling is the major contributor to the beneficial effects of IL-37 after SCI.

Since the processing of IL-37 requires caspase-1, it may suppose a conflict between the IL-37 and OLT1177 therapies. Treatment with caspase-1 inhibitors prevents nearly all the nuclear translocation of mature IL-37 in transfected macrophages (Bulau et al. 2014). However, in

contrast to IL-1β and IL-18, the extracellular release of IL-37 is independent of caspase-1 activation (Bulau et al. 2014). This is of particular interest in the case of IL-37 since immature form is also functional and is able to activate target cells (Coll-Miro et al. 2016), as observed with the D20A mutation. Indeed, the maturation of IL-37 can be produced extracellularly by unknown proteases, probably, elastases (Dinarello et al. 2016). Since we have demonstrated that extracellular pathway of IL-37 is responsible for the protective effects of this cytokine after SCI, the combination of IL-37 with OLT1177, or any other inflammasome inhibitor, should not suppose an impairment for the beneficial effect of IL-37. Moreover, in a murine model of invasive pulmonary aspergillosis, intraperitoneal injection of rIL-37 greatly reduced *Nlrp3* mRNA levels in the lungs. This correlated with a reduction in the levels of IL-1β and mitigation of the lung damage (Moretti et al. 2014). Although the inflammatory response that occurs after SCI and invasive pulmonary aspergillosis is very different, previous results from our laboratory demonstrated that hIL-37Tg mice had reduced levels of IL-1β at 24 hours after injury (Coll-Miro et al. 2016). This may suggest that IL-37 also attenuates NLRP3 action in the context of SCI. However, whether the combination of IL-37 and OLT1177 therapies leads to beneficial effects after SCI needs to be assessed.

Results reported here about the function of nuclear IL-37 are in contrast to previous publications showing that *Nlrp3* or *Asc* deletion fully abrogated the anti-inflammatory properties of IL-37. In particular, authors found that bone marrow-derived macrophages from NLRP3 or ASC deficient mice transfected with an IL-37-expressing plasmid failed to reduce the levels of pro-inflammatory cytokines after LPS challenge (Bulau et al. 2014). In these experiments, levels of IL-6 and IL-1β were measured at 24 hours after stimuli, the same time point when we observed the anti-inflammatory actions of macrophages from hIL-37D20ATg mice (Li et al. 2019). It is necessary to remark that in our experiments, we used cells from IL-37D20ATg mice, in which only the nuclear translocation of IL-37 is interfered. However, in the work from Bulau and colleagues, the full inflammasome function was impaired. Since inflammasome is involved in many biological functions, including processing of IL-1β and IL-18 among other, the discrepancy between both works may be due to the lack of specificity of the inflammasome function on nuclear translocation of IL-37.

Since the use of transgenics is quite far away from the clinical application, demonstrating that recombinant IL-37 (rIL-37) is able to promote beneficial effects is crucial for the future of IL-37 therapy. Accumulating evidence has shown that administration of rIL-37 has anti-inflammatory properties. Exogenous administration of rIL-37 ameliorated the progression of atherosclerosis by inhibiting macrophage infiltration (Ji et al. 2017). In the case of SCI, previous results from our group showed that administration of rIL-37 into the injured spinal cord improved locomotor progression (Coll-Miro et al. 2016). Since rIL-37 is unlikely to reach the lesioned spinal cord when injected systemically, we assessed whether its effect at peripheral level could be beneficial after SCI. No changes in the locomotor progression were observed after peripheral administration of rIL-37, demonstrating that effects of IL-37 are mediated centrally, but not peripherally. Therefore, therapies aimed to reduce secondary damage after SCI based on IL-37 should be applied intrathecally.

In chapter 4, we assessed the effect of another interleukin, IL-13, as an inductor of anti-inflammatory programs in macrophages and microglia. Since experimental modulation of macrophages and microglia phenotype can be easily achieved *in vitro* through rIL-13, as well as by IL-4, we sought to determine their effects *in vivo*. In 2016, results from our group showed that increasing levels of IL-4 by recombinant proteins favored the anti-inflammatory activation

of macrophages and microglia and reduced tissue damage and neurological deficits after SCI (Francos-Quijorna et al. 2016). Since natural levels of IL-4 were very low after SCI, these results remarked that injury environment can be modulated in order to limit inflammation. Similar to IL-4, IL-13 appeared at low levels in the spinal cord parenchyma after injury. However, IL-13Rα1 and IL-4Rα subunits were found in macrophages and microglia after SCI, but not at physiological conditions, suggesting rIL-13 could lead to similar therapeutic effects than rIL-4. Single injection of rIL-13 into the lesioned spinal cord at 2 days after contusion injury promoted changes in the counts and phenotype of macrophages and microglia. The number of infiltrated macrophages, but not microglia, was significantly increased after intraspinal injection of rIL-13. Moreover, rIL-13 drove microglia and macrophages to adopt a more anti-inflammatory phenotype, based on Arg1 and CD206 expression. Results obtained by intraspinal injection of rIL-13 were quite similar to those observed by rIL-4 in this thesis and in a previous publication from our group (Francos-Quijorna et al. 2016). Moreover, both rIL-13 and rIL-4 promoted the appearance of a new population of macrophages that expressed low levels of CD11b. These macrophages were phenotypically compatible with resolution-phase macrophages (Francos-Quijorna et al. 2016) since they expressed LOX and COX2, key enzymes in the synthesis of pro-resolving lipid mediators that turn on inflammatory resolution programs (Bystrom et al. 2008). Despite the similarities observed between rIL-4 and rIL-13 after SCI, therapy with rIL-13 failed to promote functional recovery or tissue preservation. Contrarywise, and in agreement with our previous publication (Francos-Quijorna et al. 2016), administration of rIL-4 led to improvement in locomotor skills. This was unexpected since IL-13 has demonstrated beneficial actions in other CNS conditions. For example, in a demyelinating model by cuprizone, lentiviral mediates expression of IL-13 forced macrophages and microglia towards an anti-inflammatory phenotype during the course of the disease. This was correlated with protective effects on oligodendrocyte survival and, consequently, with less severe demyelination due to cuprizone (Guglielmetti et al. 2016). Although no improvements at locomotor neither histological level were observed in the context of SCI, rIL-13 was effective promoting alternative polarization of macrophages and microglia *in vivo*. To elucidate the divergent effects of rIL-13 and rIL-4 on macrophages and microglia that could explain differences on functional recovery, we performed an RNA sequencing analysis.

We selectively separated macrophages and microglia from the contused spinal cord at 24 hours after treatment with rIL-13 and rIL-4 and compared their transcriptome. According to our knowledge, this is the first time that RNA profile of both populations is studied separately in the context of SCI, since previous publications have focused only in macrophages (Zhu et al. 2017). PCA revealed that both treatments induced different gene expression patterns since samples from the same group were clustered together and separately from the other groups. Moreover, we observed that the transcriptomic profile of macrophages and microglia treated with rIL-13 was more resemblance to PBS than rIL-4. Deep analysis of differentially expressed genes and processes between rIL-13 and rIL-4 revealed cell metabolism as one of the main processes altered between rIL-4 and rIL-13, in both cell populations. Indeed, many genes related to the mitochondrial respiratory chain were upregulated by rIL-4. To confirm these results, we measured the metabolic state of myeloid cells from the spinal cord after *in vivo* treatment with rIL-13 and rIL-4. Measurement of the metabolic state of cells treated with rIL-13 and rIL-4 showed no differences in the ECAR, a hallmark of glycolysis. Levels of ECAR were also comparable to the PBS group. However, rIL-4 significantly increased basal levels of OCR, a hallmark of oxidative phosphorylation. Differences were statistically significant not only at basal conditions but also after stressing the cells with simultaneous exposure to FCCP and

oligomycin. Although myeloid cells from rIL-13-treated group also tended to have increased basal levels OCR than those isolated from the PBS-treated group, differences were not statistically significant. Therefore, these experiments provide a clear evidence that rIL-4, in contrast to rIL-13, successfully shifts the cell metabolism of microglia and macrophages from glycolytic towards mitochondrial oxidative metabolism.

Many works have studied the relation between metabolism and immunity (Van den Bossche, O'Neill, and Menon 2017). Since transition from quiescent to activation is an energy-demanding event, how cells obtain that energy may be crucial for the development of a robust immune response (Hard 1970). The field of immunometabolism has advanced our understanding about in what extend immune response is supported by metabolic processes. Whether cells obtain its energy through glycolysis or trough oxidative metabolism can give rise to different immune cells responses. Trough oxidative metabolism, cells have an efficient supply of energy that can be maintained for longer. Moreover, metabolic intermediates can also be used in tissue repair and wound healing (Galvan-Peña and O'Neill 2014).

A lot of evidences suggest a complex interplay between metabolism and inflammation, that must be precisely regulated to support biological functions. It has been demonstrated that polarization of *in vitro* BMDM and microglia towards an M1 phenotype through IFNγ increases the expression of TNFα and 6-phosphofructo-2-kinase/fructose-2,6-biphosphatase 3 (PFKFB3), a key metabolic enzyme. These cells showed increased levels of ECAR, a hallmark of glycolysis (Holland et al. 2017). In microglia, IFNγ stimulation increased expression of ferritin and retention of iron, a driver to M1 phenotype as previously observed (Kroner et al. 2014). In contrast, polarization with IL-4 increased OCR, a hallmark of oxidative metabolism (Holland et al. 2017). Upon LPS stimulation, macrophages lacking IL-10, an anti-inflammatory cytokine, had further reduced oxidative phosphorylation (Ip et al. 2017). In this case, IL-10 was demonstrated to inhibit mTORC1 activation via STAT3. Since mTORC1 acts as a central regulator of cellular metabolism (Sengupta, Peterson, and Sabatini 2010), inhibition mediates the switch from oxidative phosphorylation to glycolysis after LPS stimulation (Ip et al. 2017). Treatment with rIL-37 also resulted in a promotion of OCR in skeletal muscle (Cavalli et al. 2017). Surprisingly, here we found for the first time that although IL-4 and IL-13 are anti-inflammatory cytokines and led to the same effect on immune cell polarization based on Arg1 and CD206, they showed divergent effects on cell metabolism. The exact mechanisms by which these cytokines produce different effects on the metabolisms need to be elucidated. Moreover, it is important to remark that our RNA-seq revealed many other processes altered between both cytokines, and thus, the metabolism is just one of the potential explanations.

The tight link between metabolism and immune response is also evident through NLRP3 and mitochondria (Sack 2018). As previously described, NLRP3 activation requires two steps: priming and activation (Broz and Dixit 2016; Yang et al. 2019). Priming step involved the *Nlrp3* expression after TLR4 stimulation, however, this stimulation can also be mediated by mitochondrial products such as ROS (Traba et al. 2017), mitochondrial DNA (mtDNA) (West, Koblansky, and Ghosh 2006), and cardiolipin (Iyer et al. 2013). Furthermore, after stimulation, mitochondria functions as a structural platform upon proteins of the NLRP3 inflammasome can assemble (Zhou et al. 2011). Therefore, it seems quite obvious that mitochondrial dysfunction can mediate NLRP3 inflammasome activation through the release of different products. However, whether mitochondrial metabolism is also able to activates NLRP3 is less characterized. Previous works demonstrated that impairment of mitochondrial electron transport chain trough rotenone induces NLRP3 inflammasome activation only with ATP co-

stimulation (Won et al. 2015). More recently, it has been described that that pharmacological inhibition of pyruvate kinase isozyme M2 (PKM2), a key modulator of the glycolytic pathway, impairs NLRP3 inflammasome activation in BMDMs after inflammatory challenge (Xie et al. 2016). Therefore, inhibition of mitochondrial respiration and/or promotion of anaerobic glycolysis facilitates inflammasome activation and can be also targeted for the modulation of the inflammatory response after SCI as the rest of the approaches here studied.

Future of SCI is multidisciplinary and trophic modulation of the injury environment to reduce secondary degeneration is a fundamental step. Immune cells can be found in the spinal cord for several months after injury. This aberrant resolution of inflammation is one of the main contributors to secondary tissue damage and neurological impairments. Therefore, modulation of the inflammatory response is a promising field for the treatment of SCI. Since several factors are involved in this process, inflammation can be targeted at different points. Here, we evaluated the efficacy of different compounds to minimize the detrimental and/or promote the beneficial aspects of the inflammatory response. Although further characterization of these compounds needs to be done, they may lead to novel approaches for acute SCI in humans for which there is no effective therapy.

CONCLUSIONS

Chapter 1: Neuroinflammation quantification for spinal cord injury

- Infinite Horizon Impactor Devices allows the performance of reproducible spinal cord contusion injuries in mice.
- Flow cytometry is a useful technique for the quantification of specific immune cell populations in the spinal cord after injury.
- Luminex assay is valuable technique for measuring simultaneously the protein levels of different cytokines in the spinal cord after injury.

Chapter 2: Modulation of the inflammatory response after spinal cord injury by MABp1 and OLT1177

- The pro-inflammatory cytokines IL-1α, IL-1β, and IL-18 are significantly produced in the spinal cord after injury. IL-1α, IL-1β are generated in the early stages whereas IL-18 is expressed later.
- Neutralizing IL-1α activity by MABp1 does not protect against functional deficits or demyelination after SCI.
- Blocking IL-1β and IL-18 processing and release by intraperitoneal injections of OLT1177 improves myelin preservation and functional outcomes after SCI.

Chapter 3: Extracellular and nuclear roles of IL-37 after spinal cord injury

- Nuclear IL-37 mediates anti-inflammatory actions at early stages after LPS challenge in cell culture conditions.
- Extracellular, but not nuclear, IL-37 improves functional recovery and myelin sparing after SCI.
- Administration of recombinant IL-37 promotes beneficial effects after SCI injected into the lesion site but not systemically.

Chapter 4: Modulation of the inflammatory response after spinal cord injury by IL-13

- Intraspinal administration of rIL-13 after SCI favors macrophages and microglia to adopt a more anti-inflammatory phenotype.
- The effects of rIL-13 on microglia and macrophage polarity are very similar to those elicited by IL-4.
- Administration of rIL-13, in contrast to rIL-4, does not promote functional recovery or tissue preservation after SCI.

- rIL-13 and rIL-4 induce different transcriptomic profiles in macrophages and microglia in the injured spinal cord.
- rIL-4 leads to metabolic shift from glycolysis towards oxidative phosphorylation in myeloid cells from the injured spinal cord.
- The restorative potential of immune cells cannot be predicted based exclusively on the expression of polarization markers.

REFERENCES

Ahuja, C.S., Wilson, J.R., Nori, S., Kotter, M.R.N., Druschel, C., Curt, A., and Fehlings, M.G. (2017). Traumatic spinal cord injury. Nat. Rev. Dis. Prim.

Aktan, F. (2004). iNOS-mediated nitric oxide production and its regulation. Life Sci.

Allan, S.M., Tyrrell, P.J., and Rothwell, N.J. (2005). Interleukin-1 and neuronal injury. Nat. Rev. Immunol.

Allen, A.R. (1911). Surgery of experimental lesion of spinal cord equivalent to crush injury of fracture dislocation of spinal column: A preliminary report. J. Am. Med. Assoc.

Amo-Aparicio, J., Martínez-Muriana, A., Sánchez-Fernández, A., and López-Vales, R. (2018). Neuroinflammation Quantification for Spinal Cord Injury. Curr. Protoc. Immunol.

Aoki, M., Yamaguchi, R., Yamamoto, T., Ishimaru, Y., Ono, T., Sakamoto, A., Narahara, S., Sugiuchi, H., Hirose, E., and Yamaguchi, Y. (2015). Granulocyte–macrophage colony-stimulating factor primes interleukin-13 production by macrophages via protease-activated receptor-2. Blood Cells, Mol. Dis. *54*, 353–359.

Bae, S., Kang, T., Hong, J., Lee, S., Choi, J., Jhun, H., Kwak, A., Hong, K., Kim, E., Jo, S., et al. (2012). Contradictory functions (activation/termination) of neutrophil proteinase 3 enzyme (PR3) in interleukin-33 biological activity. J. Biol. Chem.

Ballak, D.B., van Diepen, J.A., Moschen, A.R., Jansen, H.J., Hijmans, A., Groenhof, G.-J., Leenders, F., Bufler, P., Boekschoten, M. V., Müller, M., et al. (2014). IL-37 protects against obesity-induced inflammation and insulin resistance. Nat. Commun. *5*, 4711.

Banerjee, S., and Bond, J.S. (2008). Prointerleukin-18 is activated by meprin β in vitro and in vivo in intestinal inflammation. J. Biol. Chem.

Basso, D.M., Fisher, L.C., Anderson, A.J., Jakeman, L.B.Y.N.B., Tigue, D.M.M.C., Popovich, P.G., McTigue, D.M., and Popovich, P.G. (2006). Basso Mouse Scale for locomotion detects differences in recovery after spinal cord injury in five common mouse strains. J. Neurotrauma *23*, 635–659.

Bastien, D., Bellver Landete, V., Lessard, M., Vallieres, N., Champagne, M., Takashima, A., Tremblay, M.-E., Doyon, Y., and Lacroix, S. (2015). IL-1 Gene Deletion Protects Oligodendrocytes after Spinal Cord Injury through Upregulation of the Survival Factor Tox3. J. Neurosci.

Bedard, A., Tremblay, P., Chernomoretz, A., and Vallières, L. (2007). Identification of genes preferentially expressed by microglia and upregulated during cuprizone-induced inflammation. Glia.

Berda-Haddad, Y., Salers, P., Farnarier, C., Dinarello, C.A., Kaplanski, G., Zekraoui, L., Robert, S., and Dignat-George, F. (2011). Sterile inflammation of endothelial cell-derived apoptotic bodies is mediated by interleukin-1 . Proc. Natl. Acad. Sci.

Boato, F., Rosenberger, K., Nelissen, S., Geboes, L., Peters, E.M., Nitsch, R., and Hendrix, S. (2013). Absence of IL-1β positively affects neurological outcome, lesion development and axonal plasticity after spinal cord injury. J. Neuroinflammation.

Boraschi, D., Lucchesi, D., Hainzl, S., Leitner, M., Maier, E., Mangelberger, D., Oostingh, G.J., Pfaller, T., Pixner, C., Posselt, G., et al. (2011). IL-37: A new anti-inflammatory cytokine of the IL-1 family. Eur. Cytokine Netw.

Van den Bossche, J., Baardman, J., and de Winther, M.P.J. (2015). Metabolic Characterization

of Polarized M1 and M2 Bone Marrow-derived Macrophages Using Real-time Extracellular Flux Analysis. J. Vis. Exp.

Van den Bossche, J., O'Neill, L.A., and Menon, D. (2017). Macrophage Immunometabolism: Where Are We (Going)? Trends Immunol.

Brightling, C.E., Chanez, P., Leigh, R., O'Byrne, P.M., Korn, S., She, D., May, R.D., Streicher, K., Ranade, K., and Piper, E. (2015). Efficacy and safety of tralokinumab in patients with severe uncontrolled asthma: A randomised, double-blind, placebo-controlled, phase 2b trial. Lancet Respir. Med.

Brown, M., and Wittwer, C. (2000). Flow cytometry: principles and clinical applications in hematology. Clin. Chem.

Broz, P., and Dixit, V.M. (2016). Inflammasomes: Mechanism of assembly, regulation and signalling. Nat. Rev. Immunol.

Bufler, P., Gamboni-Robertson, F., Azam, T., Kim, S.-H., and Dinarello, C. a (2004). Interleukin-1 homologues IL-1F7b and IL-18 contain functional mRNA instability elements within the coding region responsive to lipopolysaccharide. Biochem. J. *381*, 503–510.

Bulau, A.-M., Nold, M.F., Li, S., Nold-Petry, C.A., Fink, M., Mansell, A., Schwerd, T., Hong, J., Rubartelli, A., Dinarello, C.A., et al. (2014). Role of caspase-1 in nuclear translocation of IL-37, release of the cytokine, and IL-37 inhibition of innate immune responses. Proc. Natl. Acad. Sci.

Bulau, A.M., Fink, M., Maucksch, C., Kappler, R., Mayr, D., Wagner, K., and Bufler, P. (2011). In vivo expression of interleukin-37 reduces local and systemic inflammation in concanavalin A-induced hepatitis. ScientificWorldJournal.

Burns, S., Biering-Sørensen, F., Donovan, W., Graves, D., Jha, A., Johansen, M., Jones, L., Krassioukov, A., Kirshblum, S., Mulcahey, M.J., et al. (2012). International Standards for Neurological Classification of Spinal Cord Injury, Revised 2011. Top. Spinal Cord Inj. Rehabil.

Butovsky, O., Jedrychowski, M.P., Moore, C.S., Cialic, R., Lanser, A.J., Gabriely, G., Koeglsperger, T., Dake, B., Wu, P.M., Doykan, C.E., et al. (2014). Identification of a unique TGF-β-dependent molecular and functional signature in microglia. Nat. Neurosci.

Byrnes, K.R., Fricke, S.T., and Faden, A.I. (2010). Neuropathological differences between rats and mice after spinal cord injury. J. Magn. Reson. Imaging.

Bystrom, J., Evans, I., Newson, J., Stables, M., Toor, I., Van Rooijen, N., Crawford, M., Colville-Nash, P., Farrow, S., and Gilroy, D.W. (2008). Resolution-phase macrophages possess a unique inflammatory phenotype that is controlled by cAMP. Blood.

Campanella, M., Sciorati, C., Tarozzo, G., and Beltramo, M. (2002). Flow cytometric analysis of inflammatory cells in ischemic rat brain. Stroke.

Cao, Q., and Whittemore, S.R. (2012). Cell transplantation. stem cells and precursor cells. In Handbook of Clinical Neurology, p.

Carrasco, D., Stecher, M., Lefebvre, G.C., Logan, A.C., and Moy, R. (2015). An Open Label, Phase 2 Study of MABp1 Monotherapy for the Treatment of Acne Vulgaris and Psychiatric Comorbidity. J. Drugs Dermatology JDD.

Castro, M., Corren, J., Pavord, I.D., Maspero, J., Wenzel, S., Rabe, K.F., Busse, W.W., Ford, L., Sher, L., FitzGerald, J.M., et al. (2018). Dupilumab Efficacy and Safety in Moderate-to-Severe Uncontrolled Asthma. N. Engl. J. Med.

de Castro, E., Sigrist, C.J.A., Gattiker, A., Bulliard, V., Langendijk-Genevaux, P.S., Gasteiger, E., Bairoch, A., and Hulo, N. (2006). ScanProsite: Detection of PROSITE signature matches and ProRule-associated functional and structural residues in proteins. Nucleic Acids Res.

Cavalli, G., Koenders, M., Kalabokis, V., Kim, J., Tan, A.C., Garlanda, C., Mantovani, A., Dagna, L., Joosten, L.A.B., and Dinarello, C.A. (2016). Treating experimental arthritis with the innate immune inhibitor interleukin-37 reduces joint and systemic inflammation. Rheumatol. (United Kingdom).

Cavalli, G., Justice, J.N., Boyle, K.E., D'Alessandro, A., Eisenmesser, E.Z., Herrera, J.J., Hansen, K.C., Nemkov, T., Stienstra, R., Garlanda, C., et al. (2017). Interleukin 37 reverses the metabolic cost of inflammation, increases oxidative respiration, and improves exercise tolerance. Proc. Natl. Acad. Sci.

Chai, M., Ji, Q., Zhang, H., Zhou, Y., Yang, Q., Zhou, Y., Guo, G., Liu, W., Han, W., Yang, L., et al. (2015). The Protective Effect of Interleukin-37 on Vascular Calcification and Atherosclerosis in Apolipoprotein E-Deficient Mice with Diabetes. J. Interf. Cytokine Res.

Chandriani, S., DePianto, D.J., N'Diaye, E.N., Abbas, A.R., Jackman, J., Bevers, J., Ramirez-Carrozzi, V., Pappu, R., Kauder, S.E., Toy, K., et al. (2014). Endogenously Expressed IL-13R 2 Attenuates IL-13-Mediated Responses but Does Not Activate Signaling in Human Lung Fibroblasts. J. Immunol.

Charles A Janeway, J., Travers, P., Walport, M., and Shlomchik, M.J. (2001). Immunobiology: The Immune System in Health and Disease. 5th edition.

Chen, C.J., Kono, H., Golenbock, D., Reed, G., Akira, S., and Rock, K.L. (2007). Identification of a key pathway required for the sterile inflammatory response triggered by dying cells. Nat. Med.

Chen, Y., Tang, Y., Vogel, L.C., and Devivo, M.J. (2013). Causes of spinal cord injury. Top. Spinal Cord Inj. Rehabil.

Cheriyan, T., Ryan, D.J., Weinreb, J.H., Cheriyan, J., Paul, J.C., Lafage, V., Kirsch, T., and Errico, T.J. (2014). Spinal cord injury models: a review. Spinal Cord *52*, 588–595.

Chu, X.P., and Xiong, Z.G. (2013). Acid-sensing ion channels in pathological conditions. In Advances in Experimental Medicine and Biology, p.

Coeshott, C., Ohnemus, C., Pilyavskaya, A., Ross, S., Wieczorek, M., Kroona, H., Leimer, A.H., and Cheronis, J. (2002). Converting enzyme-independent release of tumor necrosis factor and IL-1 from a stimulated human monocytic cell line in the presence of activated neutrophils or purified proteinase 3. Proc. Natl. Acad. Sci.

Coleman, K.M., Gudjonsson, J.E., and Stecher, M. (2015). Open-Label Trial of MABp1, a True Human Monoclonal Antibody Targeting Interleukin 1α, for the Treatment of Psoriasis. JAMA Dermatology.

Coll-Miro, M., Francos-Quijorna, I., Santos-Nogueira, E., Torres-Espin, A., Bufler, P., Dinarello, C.A., and Lopez-Vales, R. (2016). Beneficial effects of IL-37 after spinal cord injury in mice. Proc. Natl. Acad. Sci. U. S. A. *113*, 1411–1416.

Conta, A., and Stelzner, D. (2008). The Spinal Cord: A Christopher and Dana Reeve Foundation Text and Atlas. In The Spinal Cord: A Christopher and Dana Reeve Foundation Text and Atlas, p.

Davalos, D., Grutzendler, J., Yang, G., Kim, J. V., Zuo, Y., Jung, S., Littman, D.R., Dustin, M.L.,

and Gan, W.B. (2005). ATP mediates rapid microglial response to local brain injury in vivo. Nat. Neurosci.

David, S. (2015). Neuroinflammation: New Insights into Beneficial and Detrimental Functions.

David, S., and Kroner, A. (2011). Repertoire of microglial and macrophage responses after spinal cord injury. Nat. Rev. Neurosci. *12*, 388–399.

David, S., Greenhalgh, A.D., and Lopez-Vales, R. (2012a). Role of phospholipase A2s and lipid mediators in secondary damage after spinal cord injury. Cell Tissue Res.

David, S., Lopez-Vales, R., and Wee Yong, V. (2012b). Harmful and beneficial effects of inflammation after spinal cord injury. potential therapeutic implications. Handb. Clin. Neurol. *109*, 485–502.

David, S., Zarruk, J.G., and Ghasemlou, N. (2012c). Inflammatory Pathways in Spinal Cord Injury. Int. Rev. Neurobiol. *106*, 127–152.

David, S., Kroner, A., Greenhalgh, A.D., Zarruk, J.G., and López-Vales, R. (2018). Myeloid cell responses after spinal cord injury. J. Neuroimmunol.

Davies, A.L., Hayes, K.C., and Dekaban, G.A. (2007). Clinical Correlates of Elevated Serum Concentrations of Cytokines and Autoantibodies in Patients With Spinal Cord Injury. Arch. Phys. Med. Rehabil.

Dibaj, P., Nadrigny, F., Steffens, H., Scheller, A., Hirrlinger, J., Schomburg, E.D., Neusch, C., and Kirchhoff, F. (2010). NO mediates microglial response to acute spinal cord injury under ATP control in vivo. Glia.

Dietrich, W.D., Levi, A.D., Wang, M., and Green, B.A. (2011). Hypothermic Treatment for Acute Spinal Cord Injury. Neurotherapeutics.

Dinarello, C.A. (2007). Historical Review of Cytokines. Eur J Immunol.

Dinarello, C.A. (2011). Interleukin-1 in the pathogenesis and treatment of inflammatory diseases. Blood.

Dinarello, C.A. (2015). The history of fever, leukocytic pyrogen and interleukin-1. Temperature.

Dinarello, C.A., and Bufler, P. (2013). Interleukin-37. Semin. Immunol. *25*, 466–468.

Dinarello, C.A., Rider, P., White, M.R., Braiman, A., Carmi, Y., Guttman, O., Apte, R.N., Cohen, I., and Voronov, E. (2011). IL-1 and IL-1 Recruit Different Myeloid Cells and Promote Different Stages of Sterile Inflammation. J. Immunol.

Dinarello, C.A., Simon, A., and Van Der Meer, J.W.M. (2012). Treating inflammation by blocking interleukin-1 in a broad spectrum of diseases. Nat. Rev. Drug Discov.

Dinarello, C.A., Nold-Petry, C., Nold, M., Fujita, M., Li, S., Kim, S., and Bufler, P. (2016). Suppression of innate inflammation and immunity by interleukin-37. Eur. J. Immunol.

Ditunno, J.F., Little, J.W., Tessler, A., and Burns, A.S. (2004). Spinal shock revisited: A four-phase model. Spinal Cord.

Dobin, A., Davis, C.A., Schlesinger, F., Drenkow, J., Zaleski, C., Jha, S., Batut, P., Chaisson, M., and Gingeras, T.R. (2013). STAR: Ultrafast universal RNA-seq aligner. Bioinformatics.

Doble, A. (1999). The role of excitotoxicity in neurodegenerative disease: Implications for therapy. Pharmacol. Ther.

Donnelly, D.J., and Popovich, P.G. (2008). Inflammation and its role in neuroprotection, axonal regeneration and functional recovery after spinal cord injury. Exp. Neurol.

Drake, R.L., Vogl, A.W., and Mitchell, A.W.. (2015). Gray's Anatomy for Students, Third Edition.

Dunn, E., Sims, J.E., Nicklin, M.J.H., and O'Neill, L.A.J. (2001). Annotating genes with potential roles in the immune system: Six new members of the IL-1 family. Trends Immunol.

Eisenmesser, E.Z., Gottschlich, A., Redzic, J.S., Paukovich, N., Nix, J.C., Azam, T., Zhang, L., Zhao, R., Kieft, J.S., The, E., et al. (2019). Interleukin-37 monomer is the active form for reducing innate immunity. Proc. Natl. Acad. Sci.

Ellisdon, A.M., Nold-Petry, C.A., D'Andrea, L., Cho, S.X., Lao, J.C., Rudloff, I., Ngo, D., Lo, C.Y., Soares da Costa, T.P., Perugini, M.A., et al. (2017). Homodimerization attenuates the anti-inflammatory activity of interleukin-37. Sci. Immunol.

Fantuzzi, G., Ku, G., Harding, M.W., Livingston, D.J., Sipe, J.D., Kuida, K., Flavell, R.A., and Dinarello, C.A. (1997). Response to local inflammation of IL-1 beta-converting enzyme-deficient mice. J. Immunol.

Faust, N., Varas, F., Kelly, L.M., Heck, S., and Graf, T. (2000). Insertion of enhanced green fluorescent protein into the lysozyme gene creates mice with green fluorescent granulocytes and macrophages. Blood.

Fawcett, J.W. (2015). The extracellular matrix in plasticity and regeneration after CNS injury and neurodegenerative disease. In Progress in Brain Research, p.

Fawcett, J.W., and Asher, R.A. (1999). The glial scar and central nervous system repair. Brain Res. Bull.

Feldman, R.P., and Goodrich, J.T. (1999). The Edwin Smith Surgical Papyrus. Child's Nerv. Syst.

Fichtner-Feigl, S., Strober, W., Kawakami, K., Puri, R.K., and Kitani, A. (2006). IL-13 signaling through the IL-13α2 receptor is involved in induction of TGF-β1 production and fibrosis. Nat. Med.

Fleischmann, R.M., Schechtman, J., Bennett, R., Handel, M.L., Burmester, G.R., Tesser, J., Modafferi, D., Poulakos, J., and Sun, G. (2003). Anakinra, a recombinant human interleukin-1 receptor antagonist (r-metHuIL-1ra), in patients with rheumatoid arthritis: A large, international, multicenter, placebo-controlled trial. Arthritis Rheum.

Fleming, J.C., Norenberg, M.D., Ramsay, D.A., Dekaban, G.A., Marcillo, A.E., Saenz, A.D., Pasquale-Styles, M., Dietrich, W.D., and Weaver, L.C. (2006). The cellular inflammatory response in human spinal cords after injury. Brain.

Franchi, L., Eigenbrod, T., Muñoz-Planillo, R., and Nuñez, G. (2009). The inflammasome: A caspase-1-activation platform that regulates immune responses and disease pathogenesis. Nat. Immunol.

Francos-Quijorna, I., Amo-Aparicio, J., Martinez-Muriana, A., and Lopez-Vales, R. (2016). IL-4 drives microglia and macrophages toward a phenotype conducive for tissue repair and functional recovery after spinal cord injury. Glia *64*, 2079–2092.

Francos-Quijorna, I., Santos-Nogueira, E., Gronert, K., Sullivan, A.B., Kopp, M.A., Brommer, B., David, S., Schwab, J.M., López-Vales, R., and Lopez-Vales, R. (2017). Maresin 1 Promotes Inflammatory Resolution, Neuroprotection, and Functional Neurological Recovery After Spinal Cord Injury. J. Neurosci.

Frostell, A., Hakim, R., Thelin, E.P., Mattsson, P., and Svensson, M. (2016). A review of the segmental diameter of the healthy human spinal cord. Front. Neurol.

Galvan-Peña, S., and O'Neill, L.A.J. (2014). Metabolic reprogramming in macrophage polarization. Front. Immunol.

Garlanda, C., Riva, F., Polentarutti, N., Buracchi, C., Sironi, M., De Bortoli, M., Muzio, M., Bergottini, R., Scanziani, E., Vecchi, A., et al. (2004). Intestinal inflammation in mice deficient in Tir8, an inhibitory member of the IL-1 receptor family. Proc. Natl. Acad. Sci.

Garlanda, C., Dinarello, C.A., and Mantovani, A. (2013). The Interleukin-1 Family: Back to the Future. Immunity.

Gautiar, E.L., Shay, T., Miller, J., Greter, M., Jakubzick, C., Ivanov, S., Helft, J., Chow, A., Elpek, K.G., Gordonov, S., et al. (2012). Gene-expression profiles and transcriptional regulatory pathways that underlie the identity and diversity of mouse tissue macrophages. Nat. Immunol.

Ghasemlou, N., Kerr, B.J., and David, S. (2005). Tissue displacement and impact force are important contributors to outcome after spinal cord contusion injury. Exp. Neurol.

Ginhoux, F., Greter, M., Leboeuf, M., Nandi, S., See, P., Gokhan, S., Mehler, M.F., Conway, S.J., Ng, L.G., Stanley, E.R., et al. (2010). Fate mapping analysis reveals that adult microglia derive from primitive macrophages. Science (80-.).

Glabinski, A.R., Balasingam, V., Tani, M., Kunkel, S.L., Strieter, R.M., Yong, V.W., and Ransohoff, R.M. (1996). Chemokine monocyte chemoattractant protein-1 is expressed by astrocytes after mechanical injury to the brain. J. Immunol.

Gómez-Nicola, D., Fransen, N.L., Suzzi, S., and Perry, V.H. (2013). Regulation of microglial proliferation during chronic neurodegeneration. J. Neurosci. *33*, 2481–2493.

Gordon, S., and Martinez, F.O. (2010). Alternative activation of macrophages: Mechanism and functions. Immunity *32*, 593–604.

Greenhalgh, A.D., and David, S. (2014). Differences in the Phagocytic Response of Microglia and Peripheral Macrophages after Spinal Cord Injury and Its Effects on Cell Death. J. Neurosci.

Guerrero, A.R., Uchida, K., Nakajima, H., Watanabe, S., Nakamura, M., Johnson, W.E., and Baba, H. (2012). Blockade of interleukin-6 signaling inhibits the classic pathway and promotes an alternative pathway of macrophage activation after spinal cord injury in mice. J. Neuroinflammation *9*, 40.

Guglielmetti, C., Le Blon, D., Santermans, E., Salas-Perdomo, A., Daans, J., De Vocht, N., Shah, D., Hoornaert, C., Praet, J., Peerlings, J., et al. (2016). Interleukin-13 immune gene therapy prevents CNS inflammation and demyelination via alternative activation of microglia and macrophages. Glia.

Guo, Y., Zhang, H., Yang, J., Liu, S., Bing, L., Gao, J., and Hao, A. (2013). Granulocyte colony-stimulating factor improves alternative activation of microglia under microenvironment of spinal cord injury. Neuroscience.

Gustin, A., Kirchmeyer, M., Koncina, E., Felten, P., Losciuto, S., Heurtaux, T., Tardivel, A., Heuschling, P., and Dostert, C. (2015). NLRP3 inflammasome is expressed and functional in mouse brain microglia but not in astrocytes. PLoS One.

Hanania, N.A., Korenblat, P., Chapman, K.R., Bateman, E.D., Kopecky, P., Paggiaro, P., Yokoyama, A., Olsson, J., Gray, S., Holweg, C.T.J., et al. (2016). Efficacy and safety of

lebrikizumab in patients with uncontrolled asthma (LAVOLTA I and LAVOLTA II): replicate, phase 3, randomised, double-blind, placebo-controlled trials. Lancet Respir. Med.

Hard, G.C. (1970). Some biochemical aspects of the immune macrophage. Br. J. Exp. Pathol.

Hasturk, A.E., Yilmaz, E.R., Turkoglu, E., Arikan, M., Togral, G., Hayirli, N., Erguder, B.I., and Evirgen, O. (2015). Potential neuroprotective effect of Anakinra in spinal cord injury in an in vivo experimental animal model. Neurosciences.

Hausmann, O.N. (2003). Post-traumatic inflammation following spinal cord injury. Spinal Cord.

Haynes, S.E., Hollopeter, G., Yang, G., Kurpius, D., Dailey, M.E., Gan, W.B., and Julius, D. (2006). The P2Y12 receptor regulates microglial activation by extracellular nucleotides. Nat. Neurosci.

He, Z., and Jin, Y. (2016). Intrinsic Control of Axon Regeneration. Neuron.

Hickman, S.E., Kingery, N.D., Ohsumi, T.K., Borowsky, M.L., Wang, L.C., Means, T.K., and El Khoury, J. (2013). The microglial sensome revealed by direct RNA sequencing. Nat. Neurosci.

Hines, D.J., Hines, R.M., Mulligan, S.J., and Macvicar, B.A. (2009). Microglia processes block the spread of damage in the brain and require functional chloride channels. Glia.

Holland, R., McIntosh, A.L., Finucane, O.M., Mela, V., Rubio-Araiz, A., Timmons, G., McCarthy, S.A., Gun'ko, Y.K., and Lynch, M.A. (2017). Inflammatory microglia are glycolytic and iron retentive and typify the microglia in APP/PS1 mice. Brain. Behav. Immun.

Hong, D.S., Hui, D., Bruera, E., Janku, F., Naing, A., Falchook, G.S., Piha-Paul, S., Wheler, J.J., Fu, S., Tsimberidou, A.M., et al. (2014). MABp1, a first-in-class true human antibody targeting interleukin-1α in refractory cancers: An open-label, phase 1 dose-escalation and expansion study. Lancet Oncol.

Horie, S., Okubo, Y., Hossain, M., Sato, E., Nomura, H., Koyama, S., Suzuki, J., Isobe, M., and Sekiguchi, M. (1997). Interleukin-13 but not interleukin-4 prolongs eosinophil survival and induces eosinophil chemotaxis. Intern. Med.

Hu, X., Li, P., Guo, Y., Wang, H., Leak, R.K., Chen, S., Gao, Y., and Chen, J. (2012). Microglia/macrophage polarization dynamics reveal novel mechanism of injury expansion after focal cerebral ischemia. Stroke.

Huang, D.W., Sherman, B.T., and Lempicki, R.A. (2009a). Systematic and integrative analysis of large gene lists using DAVID bioinformatics resources. Nat. Protoc.

Huang, D.W., Sherman, B.T., and Lempicki, R.A. (2009b). Bioinformatics enrichment tools: Paths toward the comprehensive functional analysis of large gene lists. Nucleic Acids Res.

Ip, W.K.E., Hoshi, N., Shouval, D.S., Snapper, S., and Medzhitov, R. (2017). Anti-inflammatory effect of IL-10 mediated by metabolic reprogramming of macrophages. Science (80-.).

Iyer, S.S., He, Q., Janczy, J.R., Elliott, E.I., Zhong, Z., Olivier, A.K., Sadler, J.J., Knepper-Adrian, V., Han, R., Qiao, L., et al. (2013). Mitochondrial cardiolipin is required for Nlrp3 inflammasome activation. Immunity.

Jander, S., Schroeter, M., and Stoll, G. (2002). Interleukin-18 expression after focal ischemia of the rat brain: Association with the late-stage inflammatory response. J. Cereb. Blood Flow Metab.

Jazayeri, S.B., Beygi, S., Shokraneh, F., Hagen, E.M., and Rahimi-Movaghar, V. (2015). Incidence of traumatic spinal cord injury worldwide: a systematic review. Eur. Spine J.

Ji, Q., Meng, K., Yu, K., Huang, S., Huang, Y., Min, X., Zhong, Y., Wu, B., Liu, Y., Nie, S., et al. (2017). Exogenous interleukin 37 ameliorates atherosclerosis via inducing the Treg response in ApoE-deficient mice. Sci. Rep.

Jiang, W., Li, M., He, F., Zhou, S., and Zhu, L. (2017). Targeting the NLRP3 inflammasome to attenuate spinal cord injury in mice. J. Neuroinflammation.

Jones, J.W., Antle, J.M., Basso, B., Boote, K.J., Conant, R.T., Foster, I., Godfray, H.C.J., Herrero, M., Howitt, R.E., Janssen, S., et al. (2017). Brief history of agricultural systems modeling. Agric. Syst.

Kang, Y., Ding, H., Zhou, H., Wei, Z., Liu, L., Pan, D., and Feng, S. (2017). Epidemiology of worldwide spinal cord injury: a literature review. J. Neurorestoratology.

Kanni, T., Argyropoulou, M., Spyridopoulos, T., Pistiki, A., Stecher, M., Dinarello, C.A., Simard, J., and Giamarellos-Bourboulis, E.J. (2018). MABp1 Targeting IL-1α for Moderate to Severe Hidradenitis Suppurativa Not Eligible for Adalimumab: A Randomized Study. J. Invest. Dermatol.

Kerr, B.J., and Patterson, P.H. (2004). Potent pro-inflammatory actions of leukemia inhibitory factor in the spinal cord of the adult mouse. Exp. Neurol.

Kerr, B.J., and Patterson, P.H. (2005). Leukemia inhibitory factor promotes oligodendrocyte survival after spinal cord injury. Glia.

Kigerl, K.A., Gensel, J.C., Ankeny, D.P., Alexander, J.K., Donnelly, D.J., and Popovich, P.G. (2009). Identification of two distinct macrophage subsets with divergent effects causing either neurotoxicity or regeneration in the injured mouse spinal cord. J. Neurosci. *29*, 13435–13444.

Knowles, R.G., and Moncada, S. (1994). Nitric oxide synthases in mammals. Biochem. J.

Kotter, M.R., Zhao, C., Van Rooijen, N., and Franklin, R.J.M. (2005). Macrophage-depletion induced impairment of experimental CNS remyelination is associated with a reduced oligodendrocyte progenitor cell response and altered growth factor expression. Neurobiol. Dis.

Kroemer, G., Galluzzi, L., Vandenabeele, P., Abrams, J., Alnemri, E.S., Baehrecke, E.H., Blagosklonny, M. V., El-Deiry, W.S., Golstein, P., Green, D.R., et al. (2009). Classification of cell death: Recommendations of the Nomenclature Committee on Cell Death 2009. Cell Death Differ.

Kroner, A., Greenhalgh, A.D., Zarruk, J.G., PassosdosSantos, R., Gaestel, M., and David, S. (2014). TNF and Increased Intracellular Iron Alter Macrophage Polarization to a Detrimental M1 Phenotype in the Injured Spinal Cord. Neuron *83*, 1098–1116.

Kucher, K., Johns, D., Maier, D., Abel, R., Badke, A., Baron, H., Thietje, R., Casha, S., Meindl, R., Gomez-Mancilla, B., et al. (2018). First-in-man intrathecal application of neurite growth-promoting anti-nogo- a antibodies in acute spinal cord injury. Neurorehabil. Neural Repair.

Laman, J.D., and Weller, R.O. (2013). Drainage of cells and soluble antigen from the CNS to regional lymph nodes. J. Neuroimmune Pharmacol.

Lee, J., Rhee, M.H., Kim, E., and Cho, J.Y. (2012). BAY 11-7082 is a broad-spectrum inhibitor with anti-inflammatory activity against multiple targets. Mediators Inflamm.

Lein, E.S., Hawrylycz, M.J., Ao, N., Ayres, M., Bensinger, A., Bernard, A., Boe, A.F., Boguski, M.S., Brockway, K.S., Byrnes, E.J., et al. (2007). Genome-wide atlas of gene expression in the

adult mouse brain. Nature.

Letellier, E., Kumar, S., Sancho-Martinez, I., Krauth, S., Funke-Kaiser, A., Laudenklos, S., Konecki, K., Klussmann, S., Corsini, N.S., Kleber, S., et al. (2010). CD95-Ligand on Peripheral Myeloid Cells Activates Syk Kinase to Trigger Their Recruitment to the Inflammatory Site. Immunity.

Ley, K., Laudanna, C., Cybulsky, M.I., and Nourshargh, S. (2007). Getting to the site of inflammation: The leukocyte adhesion cascade updated. Nat. Rev. Immunol.

Li, B., and Dewey, C.N. (2014). RSEM: Accurate transcript quantification from RNA-seq data with or without a reference genome. In Bioinformatics: The Impact of Accurate Quantification on Proteomic and Genetic Analysis and Research, p.

Li, J., O, W., Li, W., Jiang, Z.G., and Ghanbari, H. a (2013). Oxidative stress and neurodegenerative disorders. Int J Mol Sci.

Li, S., Neff, C.P., Barber, K., Hong, J., Luo, Y., Azam, T., Palmer, B.E., Fujita, M., Garlanda, C., Mantovani, A., et al. (2015). Extracellular forms of IL-37 inhibit innate inflammation in vitro and in vivo but require the IL-1 family decoy receptor IL-1R8. Proc. Natl. Acad. Sci.

Li, S., Amo-Aparicio, J., Neff, C.P., Tengesdal, I.W., Azam, T., Palmer, B.E., López-Vales, R., Bufler, P., and Dinarello, C.A. (2019). Role for nuclear interleukin-37 in the suppression of innate immunity. Proc. Natl. Acad. Sci.

Libby, P. (2007). Inflammatory Mechanisms: The Molecular Basis of Inflammation and Disease. Nutr. Rev.

Lin, X.-L., Zhu, J., Wang, L.-M., Yan, F., Sha, W.-P., and Yang, H.-L. (2019). MiR-92b-5p inhibitor suppresses IL-18 mediated inflammatory amplification after spinal cord injury via IL-18BP up-regulation. Eur. Rev. Med. Pharmacol. Sci. *23*, 1891–1898.

Liu, D., Xu, G.Y., Pan, E., and McAdoo, D.J. (1999). Neurotoxicity of glutamate at the concentration released upon spinal cord injury. Neuroscience.

Liu, H., Leak, R.K., and Hu, X. (2016). Neurotransmitter receptors on microglia. Stroke Vasc. Neurol.

López-Vales, R., and David, S. (2019). Bioactive Lipids in Inflammation After Central Nervous System Injury. (Springer, Cham), pp. 181–194.

López-Vales, R., García-Alías, G., Forés, J., Udina, E., Gold, B.G., Navarro, X., and Verdú, E. (2005). FK506 reduces tissue damage and prevents functional deficit after spinal cord injury in the rat. J. Neurosci. Res.

Love, M.I., Huber, W., and Anders, S. (2014). Moderated estimation of fold change and dispersion for RNA-seq data with DESeq2. Genome Biol.

Lunding, L., Webering, S., Vock, C., Schröder, A., Raedler, D., Schaub, B., Fehrenbach, H., and Wegmann, M. (2015). IL-37 requires IL-18Rα and SIGIRR/IL-1R8 to diminish allergic airway inflammation in mice. Allergy Eur. J. Allergy Clin. Immunol.

M., A., R., Y., T., Y., Y., I., T., O., A., S., S., N., H., S., E., H., and Y., Y. (2015). Granulocyte-macrophage colony-stimulating factor primes interleukin-13 production by macrophages via protease-activated receptor-2. Blood Cells, Mol. Dis.

Mantovani, A., Sozzani, S., Locati, M., Allavena, P., and Sica, A. (2002). Macrophage polarization: Tumor-associated macrophages as a paradigm for polarized M2 mononuclear

phagocytes. Trends Immunol.

Mao, Y.M., Zhao, C.N., Leng, J., Leng, R.X., Ye, D.Q., Zheng, S.G., and Pan, H.F. (2018). Interleukin-13: A promising therapeutic target for autoimmune disease. Cytokine Growth Factor Rev.

Marchetti, C., Swartzwelter, B., Gamboni, F., Neff, C.P., Richter, K., Azam, T., Carta, S., Tengesdal, I., Nemkov, T., D'Alessandro, A., et al. (2018a). OLT1177, a β-sulfonyl nitrile compound, safe in humans, inhibits the NLRP3 inflammasome and reverses the metabolic cost of inflammation. Proc. Natl. Acad. Sci.

Marchetti, C., Swartzwelter, B., Koenders, M.I., Azam, T., Tengesdal, I.W., Powers, N., de Graaf, D.M., Dinarello, C.A., and Joosten, L.A.B. (2018b). NLRP3 inflammasome inhibitor OLT1177 suppresses joint inflammation in murine models of acute arthritis. Arthritis Res. Ther.

Martinez, F.O., Helming, L., and Gordon, S. (2009). Alternative activation of macrophages: an immunologic functional perspective. Annu. Rev. Immunol. *27*, 451–483.

Martinon, F., Burns, K., and Tschopp, J. (2002). The Inflammasome: A molecular platform triggering activation of inflammatory caspases and processing of proIL-β. Mol. Cell.

May, R.D., and Fung, M. (2015). Strategies targeting the IL-4/IL-13 axes in disease. Cytokine.

McNamee, E.N., Masterson, J.C., Jedlicka, P., McManus, M., Grenz, A., Collins, C.B., Nold, M.F., Nold-Petry, C., Bufler, P., Dinarello, C.A., et al. (2011). Interleukin 37 expression protects mice from colitis. Proc. Natl. Acad. Sci.

Meletis, K., Barnabé-Heider, F., Carlén, M., Evergren, E., Tomilin, N., Shupliakov, O., and Frisén, J. (2008). Spinal cord injury reveals multilineage differentiation of ependymal cells. PLoS Biol.

Mencacci, A., Bacci, A., Cenci, E., Montagnoli, C., Fiorucci, S., Casagrande, A., Flavell, R.A., Bistoni, F., and Romani, L. (2000). Interleukin 18 restores defective Th1 immunity to Candida albicans in caspase 1-deficient mice. Infect. Immun.

Miller, L.E., Zimmermann, A.K., and Herbert, W.G. (2016). Clinical effectiveness and safety of powered exoskeleton-assisted walking in patients with spinal cord injury: Systematic review with meta-analysis. Med. Devices Evid. Res.

Minty, A., Chalon, P., Derocq, J.M., Dumont, X., Guillemot, J.C., Kaghad, M., Labit, C., Leplatois, P., Liauzun, P., Miloux, B., et al. (1993). Interleukin-13 is a new human lymphokine regulating inflammatory and immune responses. Nature.

Mizel, S.B., and Farrar, J.J. (1979). Revised nomenclature for antigen-nonspecific T-cell proliferation and helper factors. Cell. Immunol.

Moretti, S., Bozza, S., Oikonomou, V., Renga, G., Casagrande, A., Iannitti, R.G., Puccetti, M., Garlanda, C., Kim, S., Li, S., et al. (2014). IL-37 Inhibits Inflammasome Activation and Disease Severity in Murine Aspergillosis. PLoS Pathog.

Mori, I., Hossain, M.J., Takeda, K., Okamura, H., Imai, Y., Kohsaka, S., and Kimura, Y. (2001). Impaired microglial activation in the brain of IL-18-gene-disrupted mice after neurovirulent influenza A virus infection. Virology.

Motoya, S., Watanabe, M., Kim, H.J., Kim, Y.H., Han, D.S., Yuasa, H., Tabira, J., Isogawa, N., Arai, S., Kawaguchi, I., et al. (2018). Corrigendum: Tofacitinib induction and maintenance therapy in East Asian patients with active ulcerative colitis: subgroup analyses from three phase 3 multinational studies. Intest. Res.

Muldoon, L.L., Alvarez, J.I., Begley, D.J., Boado, R.J., Del Zoppo, G.J., Doolittle, N.D., Engelhardt, B., Hallenbeck, J.M., Lonser, R.R., Ohlfest, J.R., et al. (2013). Immunologic privilege in the central nervous system and the blood-brain barrier. J. Cereb. Blood Flow Metab.

Munder, M., Eichmann, K., and Modolell, M. (1998). Alternative metabolic states in murine macrophages reflected by the nitric oxide synthase/arginase balance: competitive regulation by CD4+ T cells correlates with Th1/Th2 phenotype. J. Immunol.

Muñoz-Planillo, R., Kuffa, P., Martínez-Colón, G., Smith, B., Rajendiran, T., and Núñez, G. (2013). K+ Efflux Is the Common Trigger of NLRP3 Inflammasome Activation by Bacterial Toxins and Particulate Matter. Immunity.

Murray, P.J., Allen, J.E., Biswas, S.K., Fisher, E.A., Gilroy, D.W., Goerdt, S., Gordon, S., Hamilton, J.A., Ivashkiv, L.B., Lawrence, T., et al. (2014). Macrophage Activation and Polarization: Nomenclature and Experimental Guidelines. Immunity.

Murzin, A.G., Lesk, A.M., and Chothia, C. (1992). β-Trefoil fold. Patterns of structure and sequence in the Kunitz inhibitors interleukins-1β and 1α and fibroblast growth factors. J. Mol. Biol.

Nakamura, K., Okamura, H., Wada, M., Nagata, K., and Tamura, T. (1989). Endotoxin-induced serum factor that stimulates gamma interferon production. Infect. Immun.

Nas, K. (2015). Rehabilitation of spinal cord injuries. World J. Orthop.

Newcomb, D.C., Boswell, M.G., Huckabee, M.M., Goleniewska, K., Dulek, D.E., Reiss, S., Lukacs, N.W., Kolls, J.K., and Peebles, R.S. (2012). IL-13 Regulates Th17 Secretion of IL-17A in an IL-10-Dependent Manner. J. Immunol.

Nhong, M., Wei, T., Boring, L., Charo, I.F., Ransohoff, R.M., and Jakeman, L.B. (2002). Monocyte recruitment and myelin removal are delayed following spinal cord injury in mice with CCR2 chemokine receptor deletion. J. Neurosci. Res.

Noble, L.J., Donovan, F., Igarashi, T., Goussev, S., and Werb, Z. (2002). Matrix metalloproteinases limit functional recovery after spinal cord injury by modulation of early vascular events. J. Neurosci.

Nold-Petry, C.A., Lo, C.Y., Rudloff, I., Elgass, K.D., Li, S., Gantier, M.P., Lotz-Havla, A.S., Gersting, S.W., Cho, S.X., Lao, J.C., et al. (2015). IL-37 requires the receptors IL-18Rα and IL-1R8 (SIGIRR) to carry out its multifaceted anti-inflammatory program upon innate signal transduction. Nat. Immunol. *16*, 354–365.

Nold, M.F., Nold-Petry, C.A., Zepp, J.A., Palmer, B.E., Bufler, P., and Dinarello, C.A. (2010). IL-37 is a fundamental inhibitor of innate immunity. Nat. Immunol. *11*, 1014–1022.

Oudega, M., Bradbury, E.J., and Ramer, M.S. (2012). Combination therapies. Handb. Clin. Neurol.

Oyinbo, C.A. (2011). Secondary injury mechanisms in traumatic spinal cord injury: A nugget of this multiply cascade. Acta Neurobiol. Exp. (Wars).

Parkin, J., and Cohen, B. (2001). An overwiew of the immune system. Immunol. Lancet @Bullet.

Paul, W.E. (2015). History of interleukin-4. Cytokine.

Picelli, S., Björklund, Å.K., Faridani, O.R., Sagasser, S., Winberg, G., and Sandberg, R. (2013). Smart-seq2 for sensitive full-length transcriptome profiling in single cells. Nat. Methods.

Pineau, I., and Lacroix, S. (2007). Proinflammatory cytokine synthesis in the injured mouse spinal cord: Multiphasic expression pattern and identification of the cell types involved. J. Comp. Neurol. *500*, 267–285.

Popovich, P.G. (2014). Neuroimmunology of traumatic spinal cord injury: A brief history and overview. Exp. Neurol.

Popovich, P.G., and Hickey, W.F. (2001). Bone marrow chimeric rats reveal the unique distribution of resident and recruited macrophages in the contused rat spinal cord. J. Neuropathol. Exp. Neurol.

Popovich, P.G., Guan, Z., Wei, P., Huitinga, I., Van Rooijen, N., and Stokes, B.T. (1999). Depletion of hematogenous macrophages promotes partial hindlimb recovery and neuroanatomical repair after experimental spinal cord injury. Exp. Neurol.

Profyris, C., Cheema, S.S., Zang, D.W., Azari, M.F., Boyle, K., and Petratos, S. (2004). Degenerative and regenerative mechanisms governing spinal cord injury. Neurobiol. Dis.

Prüss, H., Kopp, M.A., Brommer, B., Gatzemeier, N., Laginha, I., Dirnagl, U., and Schwab, J.M. (2011). Non-resolving aspects of acute inflammation after spinal cord injury (SCI): Indices and resolution plateau. Brain Pathol.

Puren, A.J., Fantuzzi, G., and Dinarello, C.A. (2002). Gene expression, synthesis, and secretion of interleukin 18 and interleukin 1 are differentially regulated in human blood mononuclear cells and mouse spleen cells. Proc. Natl. Acad. Sci.

Raineteau, O., and Schwab, M.E. (2001). Plasticity of motor systems after incomplete spinal cord injury. Nat. Rev. Neurosci.

Reimand, J., Kull, M., Peterson, H., Hansen, J., and Vilo, J. (2007). G:Profiler-a web-based toolset for functional profiling of gene lists from large-scale experiments. Nucleic Acids Res.

Ren, Y., Stuart, L., Lindberg, F.P., Rosenkranz, A.R., Chen, Y., Mayadas, T.N., and Savill, J. (2001). Nonphlogistic Clearance of Late Apoptotic Neutrophils by Macrophages: Efficient Phagocytosis Independent of 2 Integrins. J. Immunol.

Rexed, B. (1952). The cytoarchitectonic organization of the spinal cord in the cat. J. Comp. Neurol.

Rice, T., Larsen, J., Rivest, S., and Yong, V.W. (2007). Characterization of the early neuroinflammation after spinal cord injury in mice. J. Neuropathol. Exp. Neurol.

de Rivero Vaccari, J.P., Lotocki, G., Marcillo, A.E., Dietrich, W.D., and Keane, R.W. (2008). A Molecular Platform in Neurons Regulates Inflammation after Spinal Cord Injury. J. Neurosci.

Rivers-Auty, J., and Brough, D. (2015). Potassium efflux fires the canon: Potassium efflux as a common trigger for canonical and noncanonical NLRP3 pathways. Eur. J. Immunol.

Rodriguez-Prados, J.-C., Traves, P.G., Cuenca, J., Rico, D., Aragones, J., Martin-Sanz, P., Cascante, M., and Bosca, L. (2010). Substrate Fate in Activated Macrophages: A Comparison between Innate, Classic, and Alternative Activation. J. Immunol.

Roederer, M. (2004). Multiparameter FACS Analysis. In Current Protocols in Immunology, p.

Sack, M.N. (2018). Mitochondrial fidelity and metabolic agility control immune cell fate and function. J. Clin. Invest.

Sadrzadeh, S.M.H., Anderson, D.K., Panter, S.S., Hallaway, P.E., and Eaton, J.W. (1987).

Hemoglobin potentiates central nervous system damage. J. Clin. Invest.

Sakai, N., Van Sweringen, H.L., Belizaire, R.M., Quillin, R.C., Schuster, R., Blanchard, J., Burns, J.M., Tevar, A.D., Edwards, M.J., and Lentsch, A.B. (2012). Interleukin-37 reduces liver inflammatory injury via effects on hepatocytes and non-parenchymal cells. J. Gastroenterol. Hepatol.

Santos-Nogueira, E., Lopez-Serrano, C., Hernandez, J., Lago, N., Astudillo, A.M., Balsinde, J., Estivill-Torrus, G., de Fonseca, F.R., Chun, J., and Lopez-Vales, R. (2015). Activation of Lysophosphatidic Acid Receptor Type 1 Contributes to Pathophysiology of Spinal Cord Injury. J. Neurosci.

Scheff, S.W., Rabchevsky, A.G., Fugaccia, I., Main, J.A., and Lumpp, J.E. (2003). Experimental Modeling of Spinal Cord Injury: Characterization of a Force-Defined Injury Device. J. Neurotrauma.

Schif-Zuck, S., Westermann, J., Netzer, N., Zohar, Y., Meiron, M., Wildbaum, G., and Karin, N. (2014). Targeted Overexpression of IL-18 Binding Protein at the Central Nervous System Overrides Flexibility in Functional Polarization of Antigen-Specific Th2 Cells. J. Immunol.

Sengupta, S., Peterson, T.R., and Sabatini, D.M. (2010). Regulation of the mTOR Complex 1 Pathway by Nutrients, Growth Factors, and Stress. Mol. Cell.

Serhan, C.N., and Savill, J. (2005). Resolution of inflammation: The beginning programs the end. Nat. Immunol.

Shamash, S., Reichert, F., and Rotshenker, S. (2002). The cytokine network of Wallerian degeneration: tumor necrosis factor-alpha, interleukin-1alpha, and interleukin-1beta. J. Neurosci.

Sharif-Alhoseini, M., Khormali, M., Rezaei, M., Safdarian, M., Hajighadery, A., Khalatbari, M.M., Safdarian, M., Meknatkhah, S., Rezvan, M., Chalangari, M., et al. (2017). Animal models of spinal cord injury: A systematic review. Spinal Cord.

Sharma, S., Kulk, N., Nold, M.F., Graf, R., Kim, S.-H., Reinhardt, D., Dinarello, C.A., and Bufler, P. (2008). The IL-1 Family Member 7b Translocates to the Nucleus and Down-Regulates Proinflammatory Cytokines. J. Immunol.

Sheikh, F., Dickensheets, H., Pedras-Vasconcelos, J., Ramalingam, T., Helming, L., Gordon, S., and Donnelly, R.P. (2015). The Interleukin-13 Receptor-α1 Chain Is Essential for Induction of the Alternative Macrophage Activation Pathway by IL-13 but Not IL-4. J. Innate Immun.

Shi, H., Wang, Y., Li, X., Zhan, X., Tang, M., Fina, M., Su, L., Pratt, D., Hui Bu, C., Hildebrand, S., et al. (2016). NLRP3 activation and mitosis are mutually exclusive events coordinated by NEK7, a new inflammasome component. Nat. Immunol.

Shlosberg, D., Benifla, M., Kaufer, D., and Friedman, A. (2010). Blood-brain barrier breakdown as a therapeutic target in traumatic brain injury. Nat. Rev. Neurol.

Solovic, I., Sester, M., Gomez-Reino, J.J., Rieder, H.L., Ehlers, S., Milburn, H.J., Kampmann, B., Hellmich, B., Groves, R., Schreiber, S., et al. (2010). The risk of tuberculosis related to tumour necrosis factor antagonist therapies: a TBNET consensus statement. Eur. Respir. J.

Steward, O., and Willenberg, R. (2017). Rodent spinal cord injury models for studies of axon regeneration. Exp. Neurol.

Stewart, A.N., Matyas, J.J., Welchko, R.M., Goldsmith, A.D., Zeiler, S.E., Hochgeschwender, U.,

Lu, M., Nan, Z., Rossignol, J., and Dunbar, G.L. (2017). SDF-1 overexpression by mesenchymal stem cells enhances GAP-43-positive axonal growth following spinal cord injury. Restor. Neurol. Neurosci.

Stirling, D.P. (2004). Minocycline Treatment Reduces Delayed Oligodendrocyte Death, Attenuates Axonal Dieback, and Improves Functional Outcome after Spinal Cord Injury. J. Neurosci.

Sugawara, S., Uehara, A., Nochi, T., Yamaguchi, T., Ueda, H., Sugiyama, A., Hanzawa, K., Kumagai, K., Okamura, H., and Takada, H. (2014). Neutrophil Proteinase 3-Mediated Induction of Bioactive IL-18 Secretion by Human Oral Epithelial Cells. J. Immunol.

Suzuki, A., Leland, P., Joshi, B.H., and Puri, R.K. (2015). Targeting of IL-4 and IL-13 receptors for cancer therapy. Cytokine *75*, 79–88.

Taylor, S.L., Renshaw, B.R., Garka, K.E., Smith, D.E., and Sims, J.E. (2002). Genomic organization of the interleukin-1 locus. Genomics.

Timper, K., Seelig, E., Tsakiris, D.A., and Donath, M.Y. (2015). Safety, pharmacokinetics, and preliminary efficacy of a specific anti-IL-1alpha therapeutic antibody (MABp1) in patients with type 2 diabetes mellitus. J. Diabetes Complications.

Toldo, S., Mauro, A.G., Cutter, Z., Van Tassell, B.W., Mezzaroma, E., Del Buono, M.G., Prestamburgo, A., Potere, N., and Abbate, A. (2019). The NLRP3 Inflammasome Inhibitor, OLT1177 (Dapansutrile), Reduces Infarct Size and Preserves Contractile Function After Ischemia Reperfusion Injury in the Mouse. J. Cardiovasc. Pharmacol.

Traba, J., Geiger, S.S., Kwarteng-Siaw, M., Han, K., Ra, O.H., Siegel, R.M., Gius, D., and Sack, M.N. (2017). Prolonged fasting suppresses mitochondrial NLRP3 inflammasome assembly and activation via SIRT3-mediated activation of superoxide dismutase 2. J. Biol. Chem.

Tripp, C.S., Cuff, C., Campbell, A.L., Hendrickson, B.A., Voss, J., Melim, T., Wu, C., Cherniack, A.D., and Kim, K. (2017). RPC4046, A Novel Anti-interleukin-13 Antibody, Blocks IL-13 Binding to IL-13 α1 and α2 Receptors: A Randomized, Double-Blind, Placebo-Controlled, Dose-Escalation First-in-Human Study. Adv. Ther.

Vallières, N., Berard, J.L., David, S., and Lacroix, S. (2006). Systemic injections of lipopolysaccharide accelerates myelin phagocytosis during wallerian degeneration in the injured mouse spinal cord. Glia.

Vats, D., Mukundan, L., Odegaard, J.I., Zhang, L., Smith, K.L., Morel, C.R., Greaves, D.R., Murray, P.J., and Chawla, A. (2006). Oxidative metabolism and PGC-1β attenuate macrophage-mediated inflammation. Cell Metab.

Vogel, D.Y.S., Heijnen, P.D.A.M., Breur, M., de Vries, H.E., Tool, A.T.J., Amor, S., and Dijkstra, C.D. (2014). Macrophages migrate in an activation-dependent manner to chemokines involved in neuroinflammation. J. Neuroinflammation.

Wagner, F.B., Mignardot, J.B., Le Goff-Mignardot, C.G., Demesmaeker, R., Komi, S., Capogrosso, M., Rowald, A., Seáñez, I., Caban, M., Pirondini, E., et al. (2018). Targeted neurotechnology restores walking in humans with spinal cord injury. Nature.

Wang, L., Quan, Y., Yue, Y., Heng, X., and Che, F. (2018). Interleukin-37: A crucial cytokine with multiple roles in disease and potentially clinical therapy (Review). Oncol. Lett.

Wells, J.E.A. (2003). Neuroprotection by minocycline facilitates significant recovery from spinal cord injury in mice. Brain.

West, A.P., Koblansky, A.A., and Ghosh, S. (2006). Recognition and Signaling by Toll-Like Receptors. Annu. Rev. Cell Dev. Biol.

Wherry, E.J., and Masopust, D. (2016). Adaptive Immunity: Neutralizing, Eliminating, and Remembering for the Next Time. In Viral Pathogenesis: From Basics to Systems Biology: Third Edition, p.

Whetstone, W.D., Hsu, J.Y.C., Eisenberg, M., Werb, Z., and Noble-Haeusslein, L.J. (2003). Blood-spinal cord barrier after spinal cord injury: Relation to revascularization and wound healing. J. Neurosci. Res.

White, M.R., Carmi, Y., Rider, P., Apte, R.N., Cohen, I., Martin, M.U., Braiman, A., Voronov, E., Dotan, S., and Dinarello, C.A. (2010). Differential release of chromatin-bound IL-1 discriminates between necrotic and apoptotic cell death by the ability to induce sterile inflammation. Proc. Natl. Acad. Sci.

Wilson, J.R., and Fehlings, M.G. (2014). Riluzole for acute traumatic spinal cord injury: A promising neuroprotective treatment strategy. World Neurosurg.

Wilson, M.S., Ramalingam, T.R., Rivollier, A., Shenderov, K., Mentinkkane, M.M., Madala, S.K., Cheever, A.W., Artis, D., Kelsall, B.L., and Wynn, T.A. (2011). Colitis and intestinal inflammation in IL10-/- mice results from IL-13Rα2-mediated attenuation of IL-13 activity. Gastroenterology.

Won, J.H., Park, S., Hong, S., Son, S., and Yu, J.W. (2015). Rotenone-induced Impairment of Mitochondrial Electron Transport Chain Confers a Selective Priming Signal for NLRP3 Inflammasome Activation. J. Biol. Chem.

Wu, G., and Morris, S.M. (1998). Arginine metabolism: nitric oxide and beyond. Biochem. J.

Wu, B., Meng, K., Ji, Q., Cheng, M., Yu, K., Zhao, X., Tony, H., Liu, Y., Zhou, Y., Chang, C., et al. (2014). Interleukin-37 ameliorates myocardial ischaemia/reperfusion injury in mice. Clin. Exp. Immunol.

Xie, M., Yu, Y., Kang, R., Zhu, S., Yang, L., Zeng, L., Sun, X., Yang, M., Billiar, T.R., Wang, H., et al. (2016). PKM2-Dependent glycolysis promotes NLRP3 and AIM2 inflammasome activation. Nat. Commun.

Y., F., C.K., S., L., B., W., Z., S.R., B., S.G., T., A., Z., G., S., W.L., T., A.M., T., et al. (2017). Tofacitinib Ameliorates Murine Lupus and Its Associated Vascular Dysfunction. Arthritis Rheumatol.

Yan, P., Zhang, Y., Wang, C., Lv, F., and Song, L. (2018). Interleukin-37 (IL-37) Suppresses Pertussis Toxin-Induced Inflammatory Myopathy in a Rat Model. Med. Sci. Monit.

Yang, L., Xu, L.Z., Liu, Z.Q., Yang, G., Geng, X.R., Mo, L.H., Liu, Z.G., Zheng, P.Y., and Yang, P.C. (2016). Interleukin-13 interferes with activation-induced t-cell apoptosis by repressing p53 expression. Cell. Mol. Immunol.

Yang, Y., Zhang, Z.X., Lian, D., Haig, A., Bhattacharjee, R.N., and Jevnikar, A.M. (2015). IL-37 inhibits IL-18-induced tubular epithelial cell expression of pro-inflammatory cytokines and renal ischemia-reperfusion injury. Kidney Int.

Yang, Y., Wang, H., Kouadir, M., Song, H., and Shi, F. (2019). Recent advances in the mechanisms of NLRP3 inflammasome activation and its inhibitors. Cell Death Dis.

Yasuda, K., Nakanishi, K., and Tsutsui, H. (2019). Interleukin-18 in Health and Disease. Int. J. Mol. Sci.

Yin, Y., Cui, Q., Li, Y., Irwin, N., Fischer, D., Harvey, A.R., and Benowitz, L.I. (2003). Macrophage-derived factors stimulate optic nerve regeneration. J. Neurosci. *23*, 2284–2293.

Yılmaz, T., Turan, Y., and Keleş, A. (2014). Pathophysiology of the spinal cord injury Omurilik yaralanmaların patofizyolojisi. J. Clin. Exp. Investig. J Clin Exp Invest.

Yona, S., Kim, K.W., Wolf, Y., Mildner, A., Varol, D., Breker, M., Strauss-Ayali, D., Viukov, S., Guilliams, M., Misharin, A., et al. (2013). Fate Mapping Reveals Origins and Dynamics of Monocytes and Tissue Macrophages under Homeostasis. Immunity.

Yong, H.Y.F., Rawji, K.S., Ghorbani, S., Xue, M., and Yong, V.W. (2019). The benefits of neuroinflammation for the repair of the injured central nervous system. Cell. Mol. Immunol.

Zhou, R., Yazdi, A.S., Menu, P., and Tschopp, J. (2011). A role for mitochondria in NLRP3 inflammasome activation. Nature.

Zhou, T., Huang, Z., Sun, X., Zhu, X., Zhou, L., Li, M., Cheng, B., Liu, X., and He, C. (2017). Microglia polarization with M1/M2 phenotype changes in rd1 mouse model of retinal degeneration. Front. Neuroanat.

Zhu, Y., Lyapichev, K., Lee, D.H., Motti, D., Ferraro, N.M., Zhang, Y., Yahn, S., Soderblom, C., Zha, J., Bethea, J.R., et al. (2017a). Macrophage Transcriptional Profile Identifies Lipid Catabolic Pathways That Can Be Therapeutically Targeted after Spinal Cord Injury. J. Neurosci.

Zhu, Y., Lyapichev, K., Lee, D.H., Motti, D., Ferraro, N.M., Zhang, Y., Yahn, S., Soderblom, C., Zha, J., Bethea, J.R., et al. (2017b). Macrophage Transcriptional Profile Identifies Lipid Catabolic Pathways That Can Be Therapeutically Targeted after Spinal Cord Injury. J. Neurosci.

ABBREVIATIONS

AIM2	Absent in Melanoma 2
AIS	ASIA Impairment Scale
APC	Antigen-presenting Cell
Arg1	Arginase 1
ASIA	American Spinal Cord Injury Association
ATP	Adenosine Triphosphate
BMDMS	Bone marrow-derived macrophages
BMS	Basso Mouse Scale
BSCB	Blood-Spinal Cord Barrier
CARD	Caspase recruitment domain
CMV	Cytomegalovirus
CNS	Central Nervous System
COX-2	Cyclooxygenase 2
CSF	Colony-stimulating factor
CSPG	Chondroitin sulfate proteoglycan
Cxcl12	stromal cell-derived factor 1
Cxcl5	CXC motif chemokine 5
Cxcl7	CXC motif chemokine ligand 7
Cxcl9	CXC chemokine 9
DAMP	Damage-associated molecular pattern
ECR	Extracellular Acidification Rate
FBS	Fetal Bovine Serum
FCCP	Carbonyl cyanide-4-(trifluoromethoxy)phenylhydrazone
G-CSF	Granulocyte-Colony Stimulating Factor
i.p.	Intraperitoneal
i.s.	Instraspinal
IFN	Interferon
IL	Interleukin
IL-1F	Interleukin-1 family
IL-1R	IL-1 family receptor
Il4	interleukin 4

iNOS	inducible Nitric Oxide Synthase
JAK	Janus Kinase
KEEG	Kytoto Encyclopedia of genes and Genomes
KO	Knock-out
LFB	Luxol Fast Blue
Lif	leukemia inhibitory factor
LIF	Leukemia Inhibitor Factor
LOX	Lipoxygenase
LPS	Lipopolysaccharide
LRR	Leucine-rich repeat
MAG	Myelin-Associated Glycoprotein
MAPK	Mitogen-activated protein kinase
MCP-1	Monocyte Chemoattractant Protein 1
MHC	Major Histocompatibility Complex
MMP	Matrix Metallopeptidase
NADPH	Nicotinamide adenine dinucleotide phosphate
NEK7	NIMA-related kinase 7
NES	Normalized Enrichement Score
NF-κB	Nuclear factor κ-light-chain-enhancer of activated B cells
NK	Natural Killer
NLRP3	NOD-like receptor pyrin domain-containing-3
NLS	Nuclear Localization Sequence
NO	Nitric Oxide
NOD	Nucleotide-binding oligomerization domain
OCR	Oxygen Consumption Rate
OMgp	Oligodendrocyte Myelin glycoprotein
P/S	Penicillin/Streptomycin
PAMP	Pathogen-associated molecular pattern
PBS	Phosphate Buffer Saline
PCA	Principal Component Analysis
PNS	Peripheral Nervous System

POST	Post-natal microglia
PRR	Pattern Recognition Receptor
PYD	Pyrin domain
qPCR	Quantitative PCR
rIL-4	Recombinant IL-4
rIL-13	Recombinant IL-13
rIL-37	Recombinant IL-37
RNS	Reactive Nitrogen Species
ROS	Reactive Oxygen Species
SAC	Folk sac microglia
SCI	Spinal Cord Injury
STAT	Signal Transducer and Activator of Transcription
Tg	Transgenic
TLR	Toll-like receptor
TNF	Tumor Necrosis Factor
Tnfrsf11b	Tumor necrosis factor receptor superfamily member 11b
Tnfsf11	Tumor necrosis factor ligand superfamily member 11
WT	Wild-type